UNIVERSITY OF NOTTINGHAM

DEPARTMENT OF CIVIL ENGINEERING

REPEATED LOAD TRIAXIAL TESTING OF SOILS

by

A. F. L. HYDE B.Sc.

Thesis submitted to the University of Nottingham for the degree of Doctor of Philosophy.

September, 1974

CONTENTS

Page

CHAPTER SIX: DISCUSSION OF RESULTS FROM TESTS ON KEUPER MARL

ACKNOWLEDGEMENTS

The author would like to thank the following people for their help in completing this thesis:

Professor R.C. Coates, B.Sc.(Eng.), Ph.D., C.Eng., F.I.C.E., F.I.Struct.E., M.I.Mech.E., for making available the full facilities of the Department of Civil Engineering.

The supervisors of the work, Professor P.S. Pell and Dr. S.F. Brown, for their support and advice at all stages of the project.

Koninklijke-Shell Laboratorium, Amsterdam, for their financial aid.

Mr. G. Stokes for his unfailing help and advice in all technical aspects and for his friendly and cheerful demeanour, even when working under pressure in the laboratory.

Mr. F. Brookes and Mr. G. Hanley for designing and assembling the electronic apparatus.

Mr. M. Bettison for his expert strain gauging.

Miss S. Bowering for her excellent photographic skills.

Miss C. Davey for tracing the graphs.

Special thanks to Miss J.L. Clerbaut for her patience, understanding and efficiency while typing this thesis.

Last of all, the author would like to thank Victoria for her love and understanding while the thesis was being written.

ABSTRACT

Samples of an over-consolidated saturated silty clay, Keuper marl, and a partially saturated granular material, Breedon gravel, have been used in a triaxial test programme, with a view to characterising certain aspects of the material behaviour for use in a flexible pavement design procedure.

Samples of over-consolidated Keuper marl were subjected to repeated axial sinusoidal loads. In addition, further samples were tested under creep loads and standard slow rate of strain triaxial tests.

The results from these tests are used to relate the plastic deformation under repeated loads to simple creep tests and to the standard undrained soil strength test. In addition, the resilient behaviour is shown to be a function of the stresses applied to the soil.

The samples of granular material were tested drained and were subjected to cyclic vertical and horizontal stresses. The development of a method of lateral strain measurement allowed a fundamental analysis of the behaviour of this material under a cyclic lateral stress.

The resilient and permanent deformations occurring under a cyclic horizontal stress have been related to those occurring under the simpler situation of a static horizontal stress.

A review of previous work considers research carried out on flexible pavement design with special reference to the role of unbound materials. In addition, an outline is

given of studies carried out on creep of clays and repeated behaviour of clays and granular materials.

The behaviours of the silty clay and the granular material are analysed in the context of a theoretical pavement structure.

The basic testing apparatus is outlined briefly, while developments to the apparatus including an automated computer based data collection system are described in the form of appendices.

A summary of the test results is given in the conclusions together with suggestions for further work.

NOTATION

A	pore water pressure parameter
CBR	California bearing ratio
e	voids ratio
E	Young's modulus
F	equivalence factor
G	shear modulus
G_R	resilient shear modulus
K	bulk modulus
K_R	resilient bulk modulus
L	wheel load
M_R	resilient modulus
OCR	over-consolidation ratio
p	mean principal stress
p_e	equivalent pressure
p_m	mean value of repeated mean principal stress
p_R	repeated mean principal stress
p_{max}	maximum mean principal stress
q	deviator stress
q_f	strain controlled sample strength
q_m	mean deviator stress
q_{max}	maximum deviator stress
q_R	repeated deviator stress
S	standard wheel load
T	time in seconds
u	pore water pressure
Δu	change in pore water pressure

v_R	resilient volumetric strain
α	function for plastic strain rate at unit time
α'	general function for plastic strain rate at unit time
ϵ_p	plastic strain
$\dot{\epsilon}$	strain rate
ϵ_{oct}	octahedral normal strain
ϵ_T	strain after T seconds
ϵ_R	resilient strain
$\dot{\epsilon}_1$	plastic strain rate at unit time
λ	decay constant
ν_R	resilient Poisson's ratio
σ_1	vertical stress
σ_3	cell pressure
σ_{3max}	maximum cell pressure
σ_{3mean}	mean cell pressure
$\sigma_3'_i$	initial effective stress
$(\sigma_1-\sigma_3)$	deviator stress
$(\sigma_1-\sigma_3)_R$	repeated deviator stress
$(\sigma_1-\sigma_3)_{max}$	maximum deviator stress
σ_{oct}	octahedral normal stress
τ_{oct}	octahedral shear stress
φ_{oct}	octahedral shear strain
φ_R	resilient shear strain

Stresses with primes are effective.

The notation used in the review of previous work is that of the original authors and is defined in the text.

AUTHOR'S NOTE

Figures and tables are placed wherever possible, directly after their first mention in the text.

CHAPTER ONE

INTRODUCTION

In many foundations repeated loads can form a large part of the live load on the soil. These loads can be traffic induced in the case of a road pavement, or, for example, they could be naturally imposed vibrations in soil strata due to earth tremors or wave forces on structures currently being constructed for use in the North Sea (Bjerrum, 1973). In the case of the traffic induced stresses, the frequencies expected on the soil would be of the order of 10 Hz; however, for the naturally imposed earth tremors or wave forces, the frequencies are much lower, of the order of 0.1 Hz.

In all of these cases, a greater knowledge of the time dependent behaviour of soil will help in providing engineering solutions to the problems encountered.

The research described in this thesis, although it has wider applications, was carried out in the context of the flexible pavement design problem. A comprehensive review of research related to this problem has, therefore, been presented in Section 2.1.

Current methods of pavement design are largely empirical. In order to improve pavement design, Brown and Pell (1970, 1972) proposed a structural design approach to the problem. The procedure was similar to that accepted by engineers when designing steel or reinforced concrete structures. It involved the consideration of

traffic loading and material characteristics under these loads. This approach has been made possible by the advent of greater access to powerful digital computers which allow the analysis of pavement structures in terms of the applied loads and resultant displacements. Using either layered elastic or finite element techniques providing the resilient characteristics of the components of the structure are known, then it can be designed to limiting stress or strain criteria to prevent fatigue cracking of the bituminous layer. In addition to cracking, many pavements fail due to an unnacceptable build up of irrecoverable deformation, a process commonly known as rutting. This, in particular, is the most common form of failure in the British Isles. It is, therefore, also necessary to design pavements against excessive permanent deformation.

The unbound materials play an important part in the overall behaviour of the pavement structure. However, relatively little is known of the resilient and permanent deformation characteristics of these materials. The resilient modulus of these materials is currently determined from a CBR test which is a static test to failure (Heukelom and Klomp, 1962) while the permanent deformation in the subgrade is limited by a resilient strain criterion without any consideration of the type of soil (Dormon and Metcalf, 1965). An attempt has been made, therefore, in this work to characterise the resilient behaviour in terms

of the applied stresses and to relate the permanent deformation to the plastic properties of the soil.

Much repeated load research on clays has been carried out on remoulded, partially saturated, compacted clays. This did not allow analysis in terms of effective stresses. In addition, many pavement failures occur on saturated subgrades which, if they are undisturbed clays, would generally be over-consolidated. A programme of research has, therefore, been carried out on the effects of repeated loading on the plastic and elastic properties of an over-consolidated silty clay. The measurement of mean values of pore water pressure has allowed a more fundamental stress-strain analysis.

In a pavement structure, the unbound materials are subjected to cyclic horizontal stresses as well as vertical stresses. A partially saturated granular material whose stress-strain characteristics have already been documented by Lashine et al (1971) was tested to determine what effect a cyclic, horizontal stress has on this material's behaviour.

A servo-hydraulic loading rig was used to test samples (Cullingford et al, 1972), which gave flexibility in the types of load applied, allowing a closer approximation to some of the loading conditions under a flexible pavement. In addition, a triaxial apparatus was used which allowed the variation of both the major and minor principal stresses on the soil samples. This was

once again in order to obtain a closer representation of stresses due to vehicle loads.

All of the tests were carried out with a view to relating the material behaviour where possible to a more simple laboratory test which could be incorporated into a design procedure.

The broad objective, therefore, of the work described in this thesis was material characterisation related to the development of design methods for flexible pavements.

CHAPTER TWO

REVIEW OF PREVIOUS WORK

2.1 THE STRUCTURAL DESIGN OF FLEXIBLE PAVEMENTS WITH SPECIAL REFERENCE TO THE ROLE OF UNBOUND MATERIALS

2.1.1 Pavement Design Schema

Current flexible road pavement design in Britain is carried out using the Department of the Environment publication Road Note No. 29 (1971). The design method is largely empirical, being based on criteria established from field performance. Predicted traffic is reduced to equivalent numbers of standard (8200 kg) axles. The subgrade strength is determined from the CBR value (which can be an estimated one). Using this information and a series of charts the thickness of the pavement layers is determined.

In recent years, interest has been shown in developing design methods based on stress analyses of the pavement structure which use the stress-strain characteristics of the constituent materials. The advantages of these methods are that they allow extrapolation to new and unforeseen situations.

Waters and Shenton (1968) and Heath et al (1972) outline a procedure using the stress-strain characteristics of materials for estimating the depth of ballast in conventional rail track foundations. The basic information required is:

(a) The applied loading spectra.

(b) The stress or strain distribution through the structure.

(c) The subsoil material parameters under relevant conditions.

Repeated load tests on samples of London clay show a threshold stress level, above which deformation is continuous. A limiting elastic strain is associated with this level. The depth of ballast is calculated using simple elastic theory such that this level is not exceeded.

The flexible pavement design problem is more complex as Hveem (1955) showed. He proposed that as well as designing a pavement against plastic deformation, consideration should be given to providing a structure with sufficient stiffness to reduce flexing to an acceptable value, to protect against fatigue failure.

Brown and Pell (1970, 1972) propose a structural design approach to the problem. The procedure is similar to that accepted by engineers when designing steel or reinforced concrete structures. This involves the consideration of traffic loading and material characteristics under repeated loads. A structure is assumed, which then allows the computation of stresses and strains and their comparison with the maximum allowable. An iterative process is then commenced to produce a pavement which is satisfactory both structurally and economically.

Finn et al (1972) propose a similar procedure using a series of subsystems. The elastic properties are

considered as part of the traffic associated fatigue subsystem. The plastic deformation is considered inside a distortion subsystem. Each of these subsystems is part of the overall design process.

Many of the parameters used in the design process cannot be estimated with absolute accuracy, but have an inherent variability. Darter et al (1973) have derived theory and concepts for a probabilistic approach to pavement design which allows the designer to design for a specified level of reliability. The variations considered are:

(1) Variations within a project.
(2) Variations between design values and the as-built structure.
(3) The lack of fit of the design models.

2.1.2 Theoretical Analyses of Pavement Structures

The most commonly available analysis in the form of computer programmes is the linear elastic layer theory. This theory was first developed by Burmister (1943). His analysis revealed the controlling influence of two ratios on the load settlement characteristics of the two layer system, namely a/h_1 and E_2/E_1 where:

a = radius of bearing area

h_1 = thickness of pavement layer

E_1 = modulus of subgrade

E_2 = modulus of pavement

The assumptions made using this theory are, infinite extent horizontally of the top layer, infinite extent both vertically and horizontally for the subgrade, and continuity of stresses across the interface. Linear elastic theory has now been incorporated into multi-layer programmes such as BISTRO and CHEVRON.

Barksdale and Hicks (1973) outline the assumptions made in this sort of computer programme. They are:

(1) Each layer is a continuous, isotropic homogeneous linearly elastic medium of infinite horizontal extent.
(2) Surface loading can be represented by uniformly distributed vertical stress acting over a circular area.
(3) Interfaces are either perfectly smooth or perfectly rough.
(4) Each layer is continuously supported by the layer beneath.
(5) Inertial forces are negligible.
(6) Deformations throughout the system are small.
(7) Temperature effects are neglected.

The modulus of both granular and cohesive soils varies with the applied stress. This provides a problem in determing what values to use. This can be overcome by using an iterative elastic layered solution. Havens et al (1973) and Brown and Pell (1972) suggest that the state of knowledge of material characteristics is now at a stage where layered elastic theory can begin to be used with some confidence.

Several studies have been made of pilot scale pavements by Brown and Pell (1967), Brown and Bush (1972) and Thrower et al (1972). All of which showed that provided realistic, measured values of elastic parameters were used for each layer, reasonably accurate predictions of stress and strain levels can be made, using layered elastic theory. Thrower et al, however, found that at higher temperatures higher stresses were imposed on the unbound materials. This resulted in less accurate predictions because of the increased influence of the non-linear behaviour of these materials.

Marek and Dempsey (1972) produced a model for determining stresses and strains incorporating both layered elastic theory and functions for temperature. The data produced by this model was in good agreement with measurements from the AASHO road test.

There are available in addition to elastic layered analyses more sophisticated finite element techniques. The computer programmes using these techniques use a greater amount of computer time, but have the advantage of being able to incorporate the non-linear response of pavement materials.

Dehlen (1969) and Dehlen and Monismith (1970) used both linear and non-linear finite element analyses which led to the conclusion that non-linear material response is not a disqualification for the use of linear elastic theory for the practical design of a flexible pavement over a sandy clay subgrade. Less error was introduced by non-linearity than by other assumptions made.

Taylor (1971) developed a finite element computer programme for a two-dimensional analysis but found that a true three-dimensional analysis used a prohibitive amount of computer storage.

Hicks and Monismith (1972) applied loads to a prototype pavement and also to the San Diego test road. Measured responses were compared with computed responses from a multilayer iterative elastic programme and two finite element programmes. The finite element procedure provided a closer agreement than did the multilayer elastic procedure. Similarly, Richards and Gordon (1972) used a finite element analysis to include moisture and stress dependent material properties. Predicted and observed behaviour were in good agreement.

Although finite element analyses seem to provide good agreement between computed and measured pavement responses their use seems justified only in cases where their increased sophistication brings economic savings.

2.1.3 Design Criteria for Unbound Materials

As already outlined in Section 1.1.1, Heath et al (1972) proposed a limiting elastic strain criterion on the subgrade for railway track foundation design. This limit was the elastic stress or strain below which the plastic deformation determined in repeated load laboratory tests became asymptotic to a limit.

Critical conditions for flexible pavements used by Dormon and Edwards (1967) in their proposed design method are:

(a) The horizontal tensile strain at the bottom of the bituminous bound layer.

(b) The vertical compressive stress or elastic strain in the surface of the subgrade.

The criterion for the compressive strain was based on that strain calculated to have been withstood satisfactorily by existing roads. This was set at 6.5×10^{-4} for 10^6 repetitions of loading.

Dormon and Edwards (1964) and Dormon and Metcalf (1965) explain that this criterion was derived by applying elastic theory to pavements designed by CBR methods, which gave the maximum vertical compressive strain as $8 - 9 \times 10^{-4}$ irrespective of the type of soil. To allow for increased traffic intensity 6.5×10^{-4} was chosen as the limit for 10^6 load applications. Analysis of results from the AASHO road test showed a relationship between the calculated vertical compressive strain in the subgrade and the number of load applications to a given performance level measured by the Present Serviceability Index (P.S.I.).

Brown and Pell (1972) in outlining the structural design approach also list design criteria which should be considered for unbound materials. Granular bases, it is pointed out, are unable to take more than a nominal amount of tensile stress. It is hence suggested that the design criterion for this layer should be the horizontal tensile stress and that this should not exceed 0.5 times the vertical stress plus the horizontal overburden pressure.

The current lack of information prevents the use of the plastic strain accumulated in this layer as a further criterion. For the subgrade it is suggested that the Shell criterion as outlined by Dormon and Edwards (1967) be used, i.e. limiting the vertical strain in the subgrade according to the number of design load applications.

From tests on a model pavement, Lister (1972) indicated that the combination of high temperature and wheel load close to the maximum regularly recorded on British main roads generates stresses on the subgrade which approach the strength of typical clay soils in conventional triaxial testing, Table 2.1.

Location in road	Parameter	Temperature Condition		
		Hottest at 2.8 k/h	Intermediate at 2.8 k/h	Coldest at 2.8 k/h
Soil formation (on load axis)	Vertical stress (kN/m^2)	82.5	60	21.4
	Deviatoric stress (kN/m^2)	75	56.5	18.6
	Vertical compressive strain x 10^6	680	519	170

Table 2.1 Values of stress and strain parameters likely to be associated with failure in an asphalt pavement and its subgrade. After Lister (1972).

It can be seen from this table that the maximum compressive strain coincides with the limiting criterion put forward by Dormon and Edwards.

In Britain, permanent deformation is accepted by

engineers as the principal indication of failure and major reconstruction is undertaken when the rut depth is 20 mm (Croney, 1972). As a large proportion of this occurs in the unbound layers some prediction of rutting in the subgrade should ultimately be a design criterion.

2.1.4 Unbound Material Parameters In Situ

The elastic analysis for design purposes requires a measure of the elastic material parameters. For this reason a great deal of attention has been paid to characterising these for the unbound pavement layers. Robnett and Thompson (1973) report that results from the WASHO and AASHO full scale road tests indicate that the subgrade contributes 60-70% of the pavement deflection at the surface. In addition, Dehlen (1969) showed that pavements tested by plate tests showed stress softening or stiffening characteristics depending on the proportions of the stiffening or softening materials in the pavement.

The elastic parameters are largely governed by the applied stress but in addition the elastic modulus is affected in situ by a number of environmental conditions.

Nash (1958) found that the strength of laboratory samples of clay subjected to repeated loading reduced as the saturation increased. Seed et al (1962) also found that the modulus of a compacted clay varied with the water content and method of compaction. It was also reported that the resilient characteristics of a soil compacted with pneumatic rollers in the field are very similar to those

of laboratory samples prepared by kneading compaction. Heukelom and Klomp (1962) reported that the modulus of the subgrade decreases with increasing moisture content and increases with increasing compactive effort. Croney and Bulman (1972) show that the elastic modulus of a moisture sensitive heavy clay can be six or seven times greater in an arid environment than in a shallow water table. Similarly, Dehlen (1969), testing undisturbed and compacted clay samples, showed that the resilient modulus increased with an increase in soil suction. Richards (1970) and Richards and Gordon (1972) show that the resilient modulus is related to soil suction and that this is related to the moisture content of the soil. Hicks and Monismith (1972) reported a measured 40% decrease in modulus for a granular layer for a change from a partially saturated condition to a saturated one. Bergan and Monismith (1973) reported a significant seasonal change of the modulus in cold regions. Freeze-thaw cycles seeming to reduce the measured moduli.

The elastic modulus is currently often measured in situ using the soil CBR value. This is done using the simple relationship:

$$E = 100 \times CBR \text{ kg/cm}^2$$

Heukelom and Klomp (1962)

It is not considered, however, that this static test is a good measure of the resilient characteristics of the unbound materials. Pell and Brown (1972) suggest that there is a need for the correlation of laboratory and field

work and a need to extend present laboratory techniques to make them more relevant to the design problem.

2.2 REPEATED LOAD BEHAVIOUR OF GRANULAR SOILS

2.2.1 Introduction

Repeated load studies of granular materials have been mainly concerned with the characterisation of both the resilient and plastic material behaviour. The effects of stress configuration, aggregate type and grading, relative densities, and degrees of saturation, have all been documented.

The most widely studied of the above parameters has been the effect of applied stresses. Model functions have been developed to fit the data, which show that the resilient response is non-linearly stress dependent.

2.2.2 Models of Resilient Behaviour

Williams (1963) carried out tests on a sand and a limestone gravel. The elastic modulus was found to be a function of the cell pressure, σ_3, in the form:

$$M_R = F[(\sigma_3)^{\frac{1}{3}}]$$

Moore, Britton and Scrivner (1970) testing a crushed limestone base material, showed that the resilient modulus in the vertical direction could be expressed as a function of the cell pressure in the form:

$$M_R = K_1 + K_2\sigma_3^2$$

where K_1 and K_2 are constants.

Huang (1968) used a similar relationship in his analysis of the stresses and displacements in non-linear soil media, this relates the modulus to the stress invariant, θ, in the form:

$$E = E_o(1+\beta\theta)$$

where E = the elastic modulus

E_o = the modulus when $\theta = 0$

β = constant

$\theta = (\sigma_1+\sigma_2+\sigma_3)$

Kallas and Riley (1967) reported tests on gravel base and sub-base materials which show that the resilient modulus varies according to:

$$M_r = K_1\sigma_3^{K_2}$$

This relationship is the commonly accepted one for defining the resilient behaviour of granular materials and was originally formulated by Biarez (1962).

Hicks (1970) and Hicks and Monismith (1971) showed that the resilient modulus can be related to either σ_3 or θ, the sum of the principal stresses in the form:

$$M_R = K_1\sigma_3^{K_2}$$

and $$M_R = K_1'\theta^{K_2'}$$

Brown and Pell (1967) reported from measurements taken in a model pavement study that the resilient modulus for the granular layer was a function of the first stress invariant (this is the same as θ) and that this function took the same form as that reported by Hicks.

Barksdale (1972) (1), using a repeated load test to evaluate base course materials, found the resilient response followed the relationship put forward by Hicks of:

$$K_R = K_1 \theta^{K_2}$$

Similarly, Allen and Thompson (1973), carrying out a statistical analysis of data collected from their own repeated load tests on three different granular materials, showed that $M_R = K_1 \theta^{K_2}$ was a model with high correlation coefficients.

Lashine et al (1971) showed, however, that the model

$$M_R = K_1 \sigma_3^{K_2}$$

was only applicable to the special case of the mean deviator stress being equal to half the amplitude, otherwise the stress-strain relationship should be written:

$$\epsilon_R = \frac{K_1 (\sigma_1 - \sigma_3)_m^{K_2} (\sigma_1 - \sigma_3)_{p/p}^{K_3}}{\sigma_3^{K_4}}$$

where ϵ_R = resilient strain in vertical direction

$(\sigma_1 - \sigma_3)_m$ = mean deviator stress

$(\sigma_1 - \sigma_3)_{p/p}$ = peak to peak deviator stress

σ_3 = confining pressure

2.2.3 Resilient Poisson's Ratio

On examining integral transform and finite element solutions of flexible pavement stress-strain responses, Hicks (1970) found that reasonable changes in Poisson's ratio could result in changes in fatigue life of the order of 50%. He found that Poisson's ratio increased with decreasing horizontal stress and increasing repeated axial stress, which could be put in the form:

$$\nu = A_o + A_1(\sigma_1/\sigma_3) + A_2(\sigma_1/\sigma_3)^2 + A_3(\sigma_1/\sigma_3)^3$$

Allen and Thompson reported on repeated load tests using both constant and repeated confining pressure. They showed that expressing the resilient Poisson's ratio as a function of (σ_1/σ_3) in a similar manner to Hicks, gave the best fit to the experimental data. Under constant cell pressure the Poisson's ratio increased markedly with the principal stress ratio, values exceeding 0.5. However, under repeated cell pressure the Poisson's ratio was observed to be virtually constant with values in the region of 0.4 to 0.5.

Morgan (1966) found that resilient Poisson's ratio values were in the range 0.2 to 0.4 but that they did not appear to be related to the confining pressure, deviator stress or number of stress applications.

2.2.4 Loading History

As far as the resilient behaviour of granular materials

is concerned it would appear that samples do not have a "memory" of previous sub-failure loading cycles. Hicks (1970), investigating the effect of stress sequence, revealed that as long as the stresses were representative of those found in an actual pavement system, one specimen may be used to measure the resilient response at all stress levels and that these different stress levels could be applied in any sequence.

A preliminary test series carried out by Allen and Thompson (1973) showed that the effects of stress history on resilient response was negligible.

Dehlen (1969) found, however, that the resilient modulus of granular materials did depend somewhat on stress history, but that the resilient response of sands and clays subjected to complex stress histories could be estimated adequately after 50 to 100 load repetitions.

2.2.5 Cyclic Cell Pressure

In order to better simulate the in situ stress conditions, it is possible to cycle the confining stress as well as the deviator stress in the triaxial apparatus.

Preliminary tests carried out by Lashine et al (1971) seemed to show a softening effect on the resilient modulus of cyclic cell pressure. Measurements, however, were only made of vertical deformation of the samples, with the result that the resilient modulus defined as the deviator stress divided by the vertical strain was in no way

analagous to Young's modulus. The definition given above takes no account of the increased cyclic stress in the vertical direction due to the confining pressure component nor of the Poisson's ratio effect.

Allen and Thompson (1973) reported on tests using constant and cyclic cell pressure. The values of resilient modulus computed from the cyclic cell pressure tests were less than those computed from constant cell pressure tests. Also, as already reported in Section 2.2.3, values of Poisson's ratio were much reduced under cyclic cell pressure conditions.

2.2.6 Frequency and Duration of Load Application

Hicks conducted tests at stress durations of 0.1, 0.15 and 0.25 seconds and found no change in the resilient modulus or Poisson's ratio. Similarly, Lashine et al (1971) also showed that the frequency in the range 1 Hz to 10 Hz had little effect on the resilient properties of a granular material. Allen and Thompson (1973), in their preliminary test series, showed that the effects of frequency were negligible.

Williams (1963), testing a sand and a limestone gravel with durations of load application from .03 sec to 300 sec, reported that the duration of load application had little effect on the modulus.

2.2.7 Density, Saturation and Aggregate Type

Hicks (1970) reported that the resilient modulus is

greater for samples compacted to higher relative densities and subjected to identical stresses. The results of Allen and Thompson (1973) indicate a similar trend. They also considered the effect of the density on the parameters K_1 and K_2 in the model:

$$M_R = K_1 \theta^{K_2}$$

K_1 showed a tendency to increase with density while K_2 showed a tendency to decrease.

Haynes and Yoder (1963) found that the resilient moduli of gravels and crushed stone were decreased by an increase in the degree of saturation. This effect was more marked for the gravels. Hicks (1970) also found that an increase in the degree of saturation adversely affected the resilient properties of granular materials.

Hicks reported that the resilient modulus increased with the particle angularity or surface roughness. Allen and Thompson demonstrated from their tests that, in general, a crushed stone yields higher values of resilient modulus than a gravel.

2.2.8 Permanent Deformation Properties of Granular Materials

For the purposes of flexible pavement design it is necessary to be able to quantify the plastic deformation occurring in any granular layer which is present.

Haynes and Yoder (1963) made a study of base course materials used in the AASHO road test using a repeated load triaxial test. As the saturation of the samples increased,

so the permanent deformation for a given number of cycles increased. Permanent deformation was still occurring after 100,000 load repetitions and no equilibrium state was apparent.

Morgan (1966) concluded that for sand permanent deformation continues to accumulate even after two million cycles of load application although the accumulation is considered to become negligible (1% per 10^6 cycles).

Lashine et al (1971), contrary to the findings of others, found that an equilibrium value of permanent strain was reached after 10^5 cycles of load application. The finite strain developed was a function of the ratio of the deviator stress to the confining pressure. Drainage conditions, despite the fact that the samples were partially saturated, were found to have a major influence on the permanent strain properties. There is a marked increase of permanent deformation in undrained tests compared to drained. This is almost certainly due to the development of pore water pressures and hence a reduction of the effective confining stress.

Shackel (1972) related the cumulative permanent strain to the ratio of octahedral shear to normal stresses. This is similar to the findings of Lashine but uses instead two stress invariants.

Barksdale (1972) (1) and (2) found that a hyperbolic relationship derived by Kondner (1963) could be fitted to the permanent stress-strain curves for granular materials.

This function relates the permanent strain to the deviator stress and confining pressure. A rut index (defined as the sum of the permanent strains occurring in the top and bottom halves of the base multiplied by 10^5) which is approximately proportional to rut depth in the base was proposed for evaluating the relative rutting characteristics of base materials.

Note

Further reviews of recent work on granular materials may be found in Allen and Thompson (1973) and Boyce et al (1974).

2.3 REPEATED LOAD BEHAVIOUR OF COHESIVE SOILS

2.3.1 Introduction

The repeated load behaviour of cohesive soils was first studied in the context of the pavement design problem by Seed et al (1955). This study and subsequent ones, Seed and McNeill (1956 and 1957) showed that deformation characteristics determined by normally accepted tests are not necessarily indicative of soil deformation under repeated loading conditions.

Since then repeated load behaviour has been examined in terms of rheological models, Kawakami and Ogawa (1965)(1,2) energy and hysteresis, Taylor and Bacchus (1969) or predictive equations using rate process theories or empirical data, Glynn and Kirwan (1969), Lashine (1971).

2.3.2 Plastic Deformation under Repeated Loading

Cohesive soils under the application of repeated loads suffer an irrecoverable or plastic strain.

Seed and others have made exhaustive investigations of the effects of the various loading parameters on the plastic deformation of partially saturated compacted clay specimens. Seed et al (1955) found the stress required to reach a given strain was lower under repeated loading than under normal unconfined compression. A general relationship was formulated between the strain after one cycle and after any number of applications of the same stress.

Tests were carried out cycling the confining pressure in phase with the deviator stress by Seed and McNeill (1957) and Seed and Fead (1959). Under these conditions the cumulative axial strain was greater than that accruing under a repeated deviator stress and constant radial stress.

The effects of the loading history were examined by Seed and Chan (1958). They found that by applying a series of conditioning stress pulses for 10,000 applications then applying a larger repeated stress, the permanent strain was reduced compared with applying a small number of conditioning stress pulses. It was maintained that this is not due to densification but to some structural rearrangement of the particles. It was also found that the more highly saturated samples exhibited a degree of thixotropy, evidenced by an increased resistance to permanent deformation when long rest periods were allowed.

2.3.3 Yield Stress Concepts

Larew and Leonards (1962), testing partially saturated compacted soils, found a critical level of applied stress above which the strain rate eventually increased, leading to shear failure. A similar concept of the existence of a threshold stress was proposed by Lashine (1971). Glynn and Kirwan (1969) postulate the existence of both a lower yield stress below which no plastic deformation develops and upper yield or threshold stress above which rupture rapidly occurs. Parr (1972), however, found no evidence of the existence of a lower yield stress. Kawakami and Ogawa (1965) (1) and (2), testing a compacted clay, defined the yield stress as the stress at which the strain rate rapidly increased under the influence of increasing stress increments. The estimation of the yield stress was carried out after a given number of applications of repeated load. They found, as did Seed and Chan, that for compacted clay, repeated loading causes a hardening effect, and that the yield stress increases with the number of load applications. Waters and Shenton (1968), testing London clay, discovered a threshold stress below which samples subjected to repeated loads reached a finite plastic strain limit.

2.3.4 Plastic Flow Concepts

Deformation under repeated loading can be considered as plastic flow and hence can be examined in terms of the rate process theory as it has been in the case of behaviour under creep stress conditions (Section 2.4.2).

Murayama (1970) derives an equation using the rate process theory to predict the time to flow failure of clay under repeated loads. The equation, however, includes parameters related to the number of bonds per unit area of clay, the temperature, the structural condition of the clay and the free energy of activation of the absorbed water. These are all difficult to evaluate in practice.

Glynn (1968) and Glynn and Kirwan (1969) developed the work of Murayama and Shibata to derive a relationship to predict the plastic displacement. This relationship assumes the resilient modulus is an index of the non-elastic behaviour. When applied to the results of the AASHO road test, this equation gives a measure of agreement.

Lashine (1971) found that deformation under repeated load at subfailure stresses follows a similar pattern to that experienced under the transient phase of creep.

If it is possible to relate the stress-strain-time behaviour of repeated loading to that of creep, then one would expect to find a continuous function relating behaviour across the whole time spectrum. Konder and Krizek (1964) used a compliance function to formulate the static and dynamic response of a cohesive soil. The compliance is defined as the ratio of the strain at a given time to the applied stress level, normalised with respect to the unconfined compressive strength. Fig. 2.1 shows this function plotted for a single stress level, against the logarithm of the length of time for which the

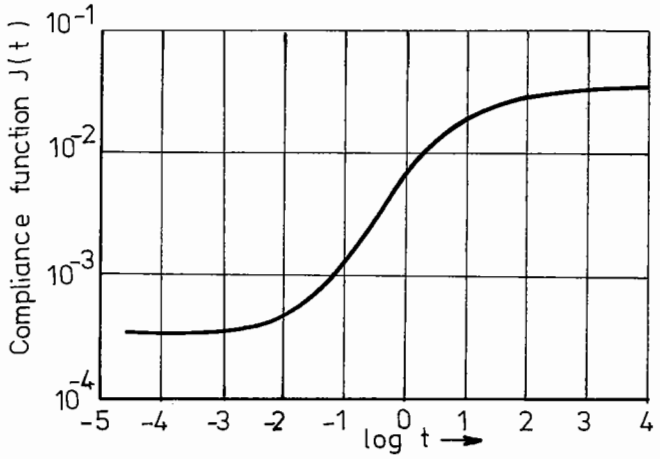

Fig 2.1 Compliance function versus time : total experimental time spectrum. (After Kondner and Krizek (1964))

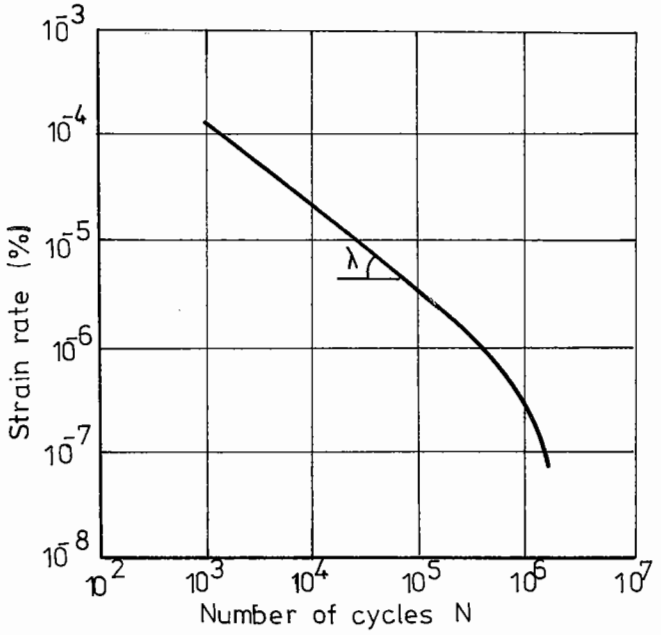

Fig 2.2 Strain rate variation with number of cycles.

load is applied. There exists a family of S-shaped curves each corresponding to a particular stress level.

Following the analysis due to Murayama and Shibata, Parr (1972) showed that the plastic strain rate could be plotted as:

$$\log\left(\frac{\dot{\epsilon}}{\dot{\epsilon}_1}\right) = \log A - \lambda \log N \qquad \text{Fig. 2.2}$$

where $\dot{\epsilon}$ = plastic strain per cycle

$\dot{\epsilon}_1$ = plastic strain after 1 cycle

log A = constant

λ = decay constant (-1 for his tests)

N = number of cycles of load application

Integration of the above equation enables a prediction of the plastic strain after N cycles providing the strain and strain rate after one cycle and the constant λ are known. Lashine (1973), plotting his results, arrives at a similar predictive equation. He also found that the decay constant λ varied with the applied repeated stress to sample strength ratio.

Although the plastic strain can be quantified in the manner shown above there seems to exist instabilities for some soils similar to those found by Bishop and Lovenbury (1969) in their work on creep. Seed et al (1955) found that sample failure could suddenly occur after a large number of load applications. Parr (1972) also found this occurring when testing undisturbed samples of London clay.

2.3.5 Elastic Properties under Repeated Loading

As well as an irrecoverable or plastic strain there exists under conditions of repeated loading an elastic or resilient strain. Seed et al (1955) defined a resilient modulus, analogous to Young's modulus, as the ratio of the repeated deviator stress to the recoverable or resilient strain. This modulus was stress dependent, increasing with increasing deviator stress and it was considerably greater than the static modulus. Later work by Seed et al (1965) at lower stresses, however, showed that the resilient modulus decreased rapidly with increasing deviator stress. This finding is supported by the findings of other researchers whose work on the stress-strain behaviour of soils is outlined below.

Larew and Leonards (1962), working on compacted clay, found that the resilient strain increased with increasing compactive effort. Ahmed and Larew (1962) showed that the resilient modulus decreased with increasing moisture content. Kawakami and Ogawa (1963), also working on compacted clay, found that the resilient modulus decreased with increasing repeated stress.

Converse (1961) carried out tests on San Francisco Bay mud, using an oscillating shear box. Higher strain amplitudes resulted in lower shearing moduli. Taylor and Bacchus (1969) carried out cyclic strain controlled triaxial tests on a clay prepared from a slurry. The moduli obtained from these tests reduced with increasing strain

amplitude. Humphries and Wahls (1968) applied an oscillating torque to cylindrical specimens in a triaxial cell. Tests performed with Kaolin indicated that the dynamic shear modulus decreased with increasing stress amplitude. Lashine (1971), examining the dynamic stress-strain relationship of normally consolidated Keuper marl, showed that a softening effect was found to take place with increasing amplitude of cyclic stress, but that the mean stress had a hardening effect.

There is clearly overwhelming evidence for both saturated and partially saturated cohesive soils, of non-linear stress-strain behaviour under repeated loading.

2.3.6 Repeated Loading Related to Static Soil Strength

A great deal of work has been carried out either attempting to relate the repeated loading behaviour to a static soil strength test or measuring the reduction in soil strength due to repeated loading.

Larew and Leonards (1962) defined a critical level of applied repeated stress above which the slope of the plastic strain against number of cycles curve turns concave upwards. The ratio of this stress level to the static strength is taken as a measure of the reduction in strength due to repeated loading. This ratio was found to be a minimum at or near the optimum moisture content.

Konder and Krizek (1964), in their formulation of a compliance function (see Section 2.3.4), used the unconfined compressive strength as a normalising parameter to allow

for changes in moisture content. Lashine (1971) defined a single loading strength (determined by strain controlled undrained tests) as q_{max}. Under repeated loading there was a critical range of stresses (from $0.75q_{max}$ to $0.80q_{max}$) below which applied stresses did not cause failure, within which the chances of failure and non-failure were even and above which applied cyclic stresses would ultimately lead to failure. Later work by Lashine et al (1971) showed that the above concept was only applicable to normally consolidated specimens and that it does not seem possible to easily relate the repeated load behaviour of over-consolidated specimens to their single load strength.

In order to relate the behaviour of a sample under dynamic loading to its behaviour under single loading, Parr (1972) defined a stress ratio, S, as follows:

$$S = \frac{\text{peak to peak dynamic stress applied to sample}}{\text{predicted single loading strength of the sample}}$$

For S less than 0.55 there was little likelihood of sample failure, for S between 0.55 and 0.85, not all samples failed, for S greater than 0.85 all of the samples failed within 10^5 cycles.

2.3.7 The Effect of Stress History on the Repeated Load Properties of Cohesive Soils

The stress history of cohesive soils can be measured in the form of an over-consolidation ratio. This is defined as the ratio of the preconsolidation pressure to

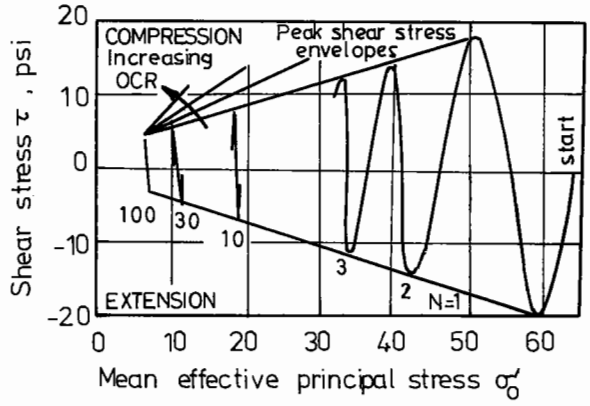

Fig. 2.3 Dynamic stress path

After Taylor and Bacchus (1969)

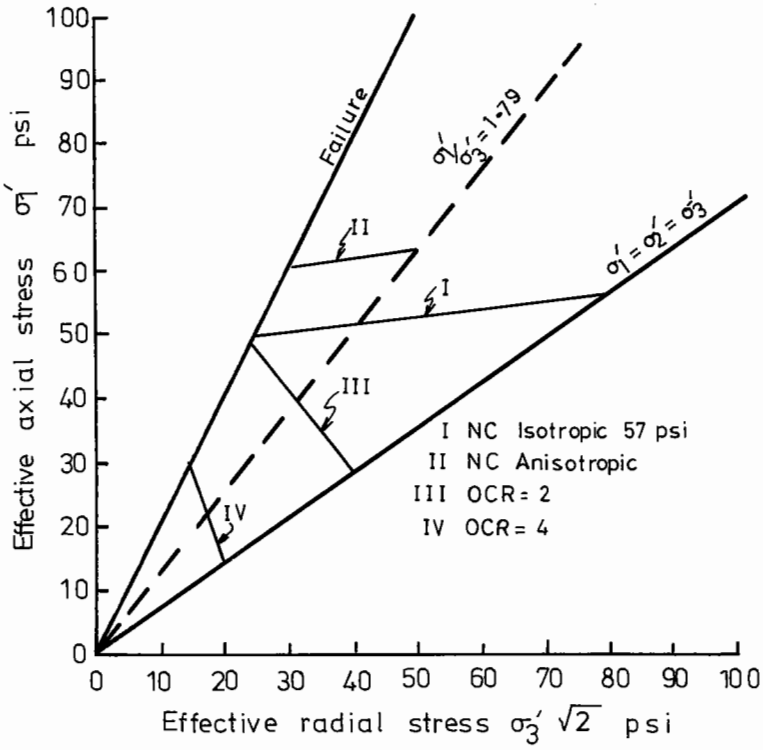

Fig. 2.4 Equilibrium lines for various consolidation histories

After Sangrey et al (1969)

the pressure at which the soil is finally consolidated.

Tests were carried out by Humphries and Wahls (1968) on two idealised materials, kaolinite and bentonite. The effect on the dynamic shear modulus of the effective stress, the void ratio and the over-consolidation ratio was evaluated by linear regression methods. It was found that for the kaolinite the effective pressure was the dominant factor and the over-consolidation ratio was found to be insignificant. In the case of the bentonite which had a much higher liquid limit, the over-consolidation ratio was a little more significant but was still considered to be of little importance. Taylor and Bacchus carried out cyclic strain controlled tests at various amplitudes of strain. Plotting the shear stress against the mean effective principal stress for each test gives an envelope for the peak shear stress (Fig. 2.3). For over-consolidated clay, a series of envelopes is found converging to the normally consolidated case. Sangrey, Henkel and Esrig (1969) carried out cyclic loading tests, each cycle being of ten hours' duration. Under low stresses, an equilibrium position was reached. Plotting these positions in an effective stress space gave a series of lines for different consolidation conditions (Fig. 2.4).

Lashine et al (1971) derived a relationship between the resilient modulus, the applied deviator stress, and the over-consolidation ratio (OCR). However, both

the moisture content and the effective confining stress varied with the OCR and neither was taken into account.

Note

Further comprehensive reviews of repeated load behaviour of cohesive soils may be found in Lashine (1971), Lashine et al (1971), Parr (1972) and Shackel (1973).

2.4 CREEP BEHAVIOUR OF COHESIVE SOILS

2.4.1 Introduction

Several researchers into the repeated load properties of clay (Glynn and Kirwan, 1969, Murayama, 1970, and Lashine, 1971) have established that stress-strain-time behaviour under sustained loads follows a similar pattern to that experienced under cyclic loading. For this reason, a detailed study has been made of work carried out on the creep behaviour of cohesive soils. A typical deformation-time curve of a clay under the application of a constant stress shows two main stages, (1) an instantaneous strain, and (2) a retarded or creep strain. The study of the creep behaviour of cohesive soils has been carried out by various authors using different methods of analysis. The two main approaches can be outlined as follows. Either a model of clay behaviour has been developed, followed by the analysis of empirical data to check the

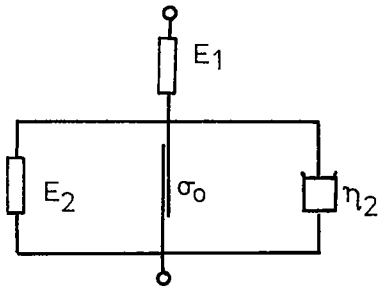

Fig. 2.5 Rheological model for clays.

After Murayama and Shibata (1961)

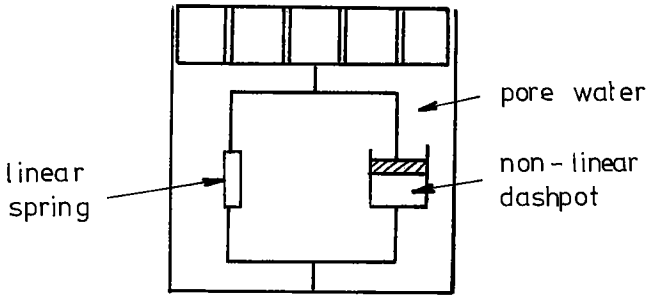

Fig. 2.6 Model of saturated element

After Barden (1969)

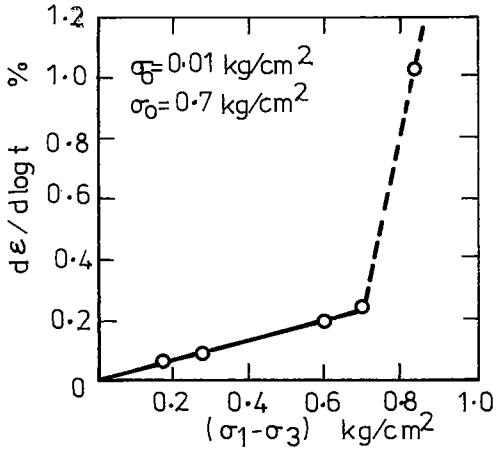

Fig. 2.7 Relation between dε/d log t and stress

After Murayama and Shibata (1961)

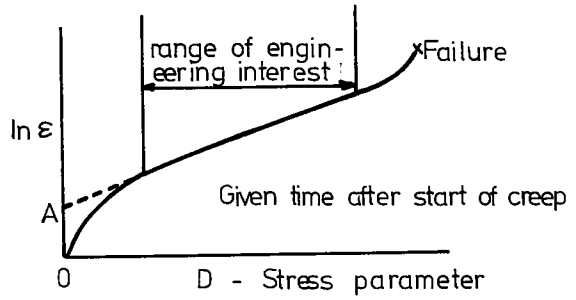

Fig. 2.8 Influence of creep stress intensity on creep rate.

After Singh and Mitchell (1968)

applicability of the model, or experimental data has been analysed on a phenomenological basis to give predictive equations connecting the various measured parameters.

2.4.2 Models of Creep Behaviour

Several researchers have based their proposed mechanisms of clay behaviour on the work of Eyring, who in Glasstone et al (1941), outlines a rate process theory for the viscosity of liquids. Using statistical mechanics, it is postulated that an activation energy is required for the local loosening of particles from their equilibrium positions and displacement to new positions. Sources of this energy are external forces and the thermal energy contained in the material. Developing this theory, Murayama and Shibata (1961, 1964) assumed the viscosity of clay to be a structural viscosity based on the frequency of the mutual exchange of position between each water molecule and its void in a bond material containing soil particles.

A rheological model was developed, Fig. 2.5, containing both elastic and viscous elements, the latter representing the structural viscosity.

The equations developed from this model agreed with experimental data from drained creep tests carried out on Osaka clay.

A similar theory was put forward by Geuze(1963) who postulated that the creep mechanism was due to the

breakage and re-establishment of bonds between clay particles and viscous resistance to particle movement by water in voids.

Mitchell (1964) suggested that the shearing resistance of a soil at a given void ratio should be a function of the frictional and cohesive properties of the soil, effective stress, structure, rate of strain and temperature. By applying the theory of rate processes, an expression was derived which provides a relationship of all the above factors to the deviator stress. This relationship also implies that the number of interparticle contacts is the most significant factor influencing the magnitude of cohesion.

Christensen and Wu (1964) considered strain under shear stress to be the result of slip at particle contacts and that this slip was assumed to obey the rate process theory. The behaviour of this rheological model agrees with experimental results from undrained creep tests. Experiments were also carried out using dry clay specimens which suggested that absorbed water is not the primary source of visco-elastic behaviour.

A different mechanism is proposed by Barden (1969). This mechanism is illustrated in Fig. 2.6. The model is based on a system of micropores and macropores. In this mechanism, the primary stage of creep behaviour is the dissipation of pore pressures in the macropores followed by the secondary compression which is the draining of

the micropores. The behaviour of the dashpot in this system can still be characterised by the rate process theory. Empirical power laws to fit this model were found to agree with experimental findings from tests on clay and peat.

2.4.3 Prediction of Creep Behaviour

Creep strain rates generally decrease with time under sub-failure stress conditions. After a period of time, creep may cease, continue at a decreasing rate, or start increasing. It is desirable to be able to predict future creep movements.

Singh and Mitchell (1968) proposed the following general function for soils which expresses the strain rate, $\dot{\epsilon}$, as a function of time, t, and sustained deviator stress, D:

$$\dot{\epsilon} = Ae^{\alpha D}\left(\frac{t_1}{t}\right)^m$$

where A = strain rate at time t_1 and D = 0 (projected value)

α = value of the slope of the linear portion of a plot of logarithmic strain rate versus deviator stress

t_1 = unit time

m = slope of the logarithmic strain rate versus logarithmic time.

Fig. 2.8 shows the relationship between $\dot{\epsilon}$ and D for a given time after the start of creep. This can be extended to a series of curves for different times (Fig. 2.9, Holzer et al, 1972).

This equation was derived from experimental data and is held to be valid irrespective of whether clays are undisturbed, remoulded, normally consolidated or over-

consolidated, or tested drained or undrained. Similarly, Parr (1972), from experiments on undisturbed samples of London clay, shows that the strain rate is a function of the applied stress and time of the form:

$$\log \dot{\varepsilon} = \log[k.f(\sigma)] - \log t$$

where σ = applied stress.

This type of equation was further developed by Singh and Mitchell (1969). The time to failure or creep rupture of a given soil is given by:

$$\log_e t_f = \frac{1}{1-m}\left(C_2 - \alpha D\right)$$

where $C_2 = f(\dot{\varepsilon}_{tf}, A, t_1, m)$

and t_f = time to failure

However, $\dot{\varepsilon}_{tf}$ was assumed to be a constant for a given soil and must be known in order to evaluate t_f under any conditions.

From undrained creep tests carried out on normally consolidated Keuper marl, Lashine (1971) derived an equation describing the stress-strain-time behaviour under creep conditions. This was:

$$\varepsilon_t = 6 \times 10^{-3}\ e^{3(D-0.40)} + 5.5 \times 10^{-2}\ e^{5.5(D-0.40)}\ t^{0.20}$$

where ε_t = axial strain

D = applied stress/failure stress

t = time (seconds)

This last relationship is only applicable to one material.

Bishop and Lovenbury (1969) found that while the

early part of the strain time plots could be represented by simple logarithmic or power laws, the period over which these laws apply closely is limited, for example, to 100-200 days for London clay. Limited instabilities occurred after this which were considered to be a significant characteristic of some undisturbed clays.

Saito and Uezawa (1961) found that the product of the creep rupture life and the strain rate was constant and equal to 214. This, it was claimed, was independent of the type of soil and method of testing.

2.4.4 Relation of Creep to Pore Water Pressure

During undrained creep, excess pore water pressures are generated. Holzer et al (1972) made a study of how the excess pore water pressure is related to the mechanism for undrained creep. Pore water pressure under the application of a constant stress consists of two components. The first is an instantaneous increase which is a function of the applied stress, the second is a slow steady increase. This second component is a function of the amount of secondary consolidation which has taken place. The shear strains during undrained creep are directly related to the gradual increase in excess pore pressures. Shen et al (1973) showed that pore pressure build up was related to the initial period of consolidation.

Walker (1969) used a theoretical analysis based on the theories of Roscoe et al (1963) to suggest that creep of pore pressure is proportional to mean effective stress

and that creep strain and pore pressure are directly related.

2.4.5 Relation of Creep to Temperature

It is postulated in the rate process theory that the activation energy is derived from both external forces and thermal energy. If this theory is applicable, then undrained creep should be a temperature dependent phenomenon.

Murayama and Shibata (1961) confirmed that the strain rate was directly related to the temperature. An apparatus for creep tests with temperature control was developed by Mitchell and Campanella (1964). Using this apparatus, a study was carried out showing that creep was temperature dependent. A temperature increase leads to a significant decrease in effective stresses and an increase in strain rate.

Considering creep as caused by energy activation, Campanella et al (1968) theorised that:

$$\frac{\partial \log \frac{\dot{\epsilon}}{T}}{\partial \frac{1}{T}} = \frac{-E}{R}$$

where E = the experimental activation energy, $f(R,T,\dot{\epsilon})$

R = gas constant

T = absolute temperature

$\dot{\epsilon}$ strain rate

Experimental data confirmed the above relationship,

lending support to the postulate that creep is a thermally activated process.

2.4.6 Yield Values Associated with Creep

Several researchers have defined yield values delimiting the different types of behaviour of soil under a constant applied stress.

Geuze and Tan (1953) define a lower yield value below which elastic behaviour only is observed. Murayama and Shibata (1961, 1964) define an upper yield value, σ_u, as the turning point on the strain rate versus deviator stress curve (Fig. 2.7). The intercept is defined as the lower yield value, σ_o. Below σ_o no flow deformation occurs and below σ_u no failure occurs.

Lohnes et al (1972) carried out in situ creep tests in bore holes using a vane apparatus. The yield stress was defined as the stress below which no creep occurs and was determined by extrapolation of the strain rate versus shear stress plot back to zero.

2.4.7 Creep Related to Soil Strength and Stress Space

Acceptance of the rate process theory as applied to creep behaviour involves the implication that the application of external forces will affect the rate of creep.

Singh and Mitchell (1968, 1969), who apply the rate process theory to their analysis, have shown experimentally that the strain rate is a function of the applied stress

(Figs. 2.8 and 2.9). This relationship can be generalised by normalising the applied stress with respect to the soil strength.

Roscoe et al (1963) considered creep to be a diffusion process. Equations are derived for the shape of the state paths and it is shown that the effective stress states of the samples at the end of a period of creep correspond with states reached under "slow" stress controlled tests (Fig. 2.10). Arulandan et al (1971) successfully used the equation derived for "slow" tests to predict the values to which the mean normal effective stress falls during creep. It was also shown that the normal strength, failure during creep, and strength after creep all fell on the critical state line when projected onto the same stress plane.

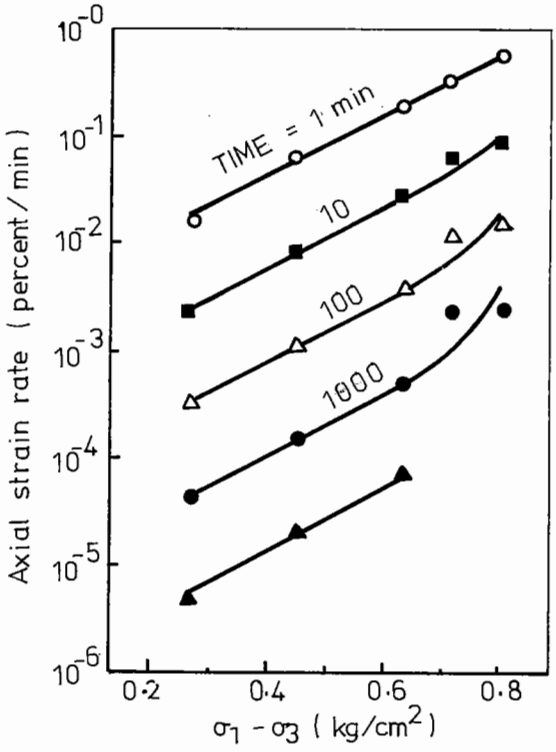

Fig. 2.9 Axial strain rate versus principal stress difference during undrained creep at different times during creep.

After Holzer et al (1972)

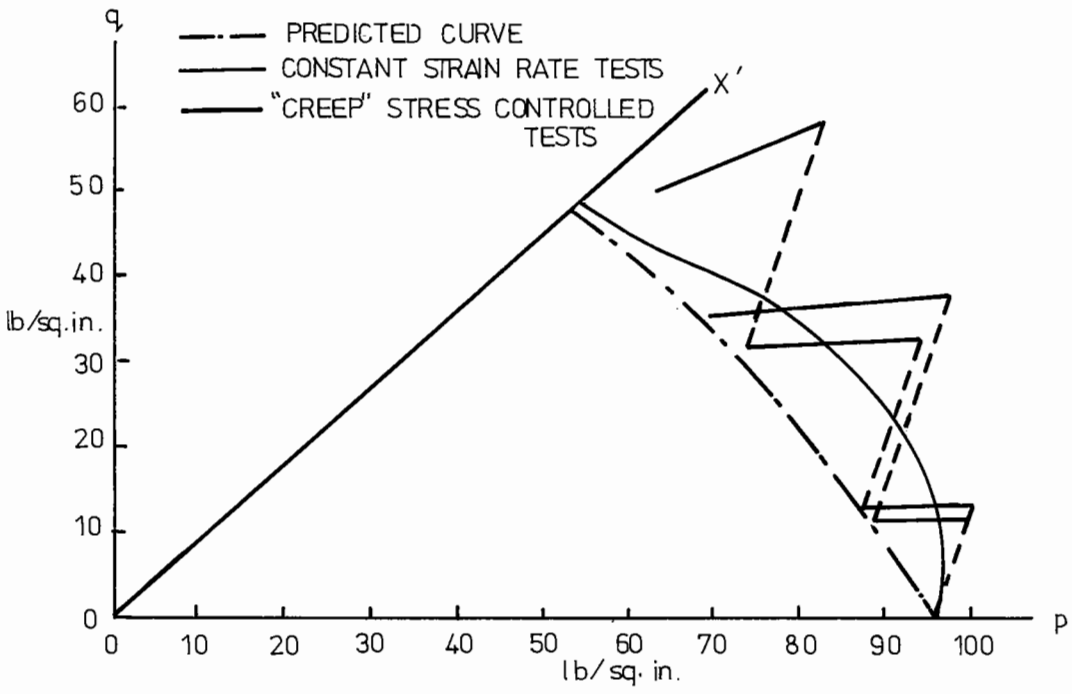

Fig. 2.10 Predicted and observed stress paths for undrained tests on Cambridge Gault Clay (Stress controlled test data, by W. J. Thompson (1962))

After Roscoe et al (1963)

CHAPTER THREE

OUTLINE OF THE TESTING PROGRAMME

3.1 INTRODUCTION

The programme of tests outlined in this chapter was developed largely with reference to the pavement design problem already referred to in Chapter 1 and in the review of previous work.

The work is, however, relevant to other fields where repeated loading of soils occurs. The tests carried out on saturated over-consolidated clay are particularly relevant to problems currently being encountered in the extraction of oil from underneath the North Sea (Bjerrum, 1973).

The author was not concerned in establishing failure criteria as normally understood in the field of soil mechanics. Rather, tests were carried out to assess both the response of the unbound materials under repeated loading and the relation of this wherever possible to a simple laboratory test.

The resilient properties of the unbound materials in a pavement structure are required for incorporation into linear elastic or finite element analyses. In addition, the permanent deformation of these materials needs to be characterised in order to predict rutting in a road pavement.

3.2 KEUPER MARL TESTS

A large part of the testing of cohesive soils under repeated loading conditions has been carried out on partially saturated compacted soil. If, however, a road is being built in a cut situation, then the subgrade may consist of a saturated clay with a geologically imposed stress history. It is admitted by the author that usually the water table in the subgrade varies seasonally, but it has been shown by Lister (1972) that the greatest deformation occurs when the water table is at its highest, and the subgrade, therefore, at its maximum saturation. Gravity structures at present being constructed for use in the North Sea will rest on saturated over-consolidated clays and during heavy storms they will transmit cyclic stresses to these clays.

The consolidation history of an undisturbed clay determines its final moisture content and its behaviour under an applied stress.

The effects, therefore, of three parameters were studied. These parameters were the voids ratio or moisture content, the effective final consolidation pressure and the over-consolidation ratio (OCR). This was carried out with two series of tests, KA and KB. These are shown diagrammatically in Fig. 3.1 and are in addition listed in Table 3.1. A supplementary series of tests (KH) was carried out to extend the range of voids ratios and OCR's considered. At each particular

Test Series	OCR	Effective Preconsolidation Pressure kN/m^2	Final Effective Consolidation Pressure kN/m^2
KA	4	160	40
KA	10	400	40
KA	20	800	40
KB	2	440	220
KB	4	480	120
KB	20	660	33
KH	75	3000	40

Table 3.1 Keuper Marl Repeated Load Tests

consolidation history a series of tests at different repeated deviator stresses was performed.

In order to relate the repeated load behaviour to a simple test, two other types of test were carried out. Strain controlled undrained tests were used to give a measure of the sample single loading strength. Several authors (Parr, 1972, Lashine, 1971) have attempted to relate repeated load behaviour or strength to this form of single loading test. In addition, a series of stress controlled "creep" tests was carried out at the same stress history conditions as the KA and KH series repeated load tests (Table 3.2). The data from these tests was used to relate repeated loading behaviour to this more simple form of test.

It is quite rare in practice for a soil to be subjected

Sample Nos.	OCR	Preconsolidation pressure kN/m^2	Final consolidation pressure kN/m^2
CR 1-6	4	160	40
CR 7-12	10	400	40
CR 13-18	20	800	40
KH 7-9	75	3000	40

Table 3.2 Keuper Marl Creep Tests

to continuous cyclic loading. It was, therefore, decided to assess the effect of imposed rest periods between trains of continuous load cycles (Tables 3.3(a) and (b)). As shown in the tables, both the length of rest period and the number of load pulses between rests were investigated.

For the purposes of establishing the stress history of clay samples, it is necessary to know the relationship between the moisture content and the consolidation pressure for virgin consolidated samples. Six samples were, therefore, normally consolidated and used purely for moisture content determination (Table 3.4).

3.3 BREEDON GRAVEL TESTS

Traffic loads, in addition to imposing repeated vertical stresses, also give rise to repeated horizontal stresses. These can be reproduced under triaxial test conditions by cycling the confining stress.

Lashine et al (1971) carried out extensive tests to determine the stress-strain behaviour of partially saturated

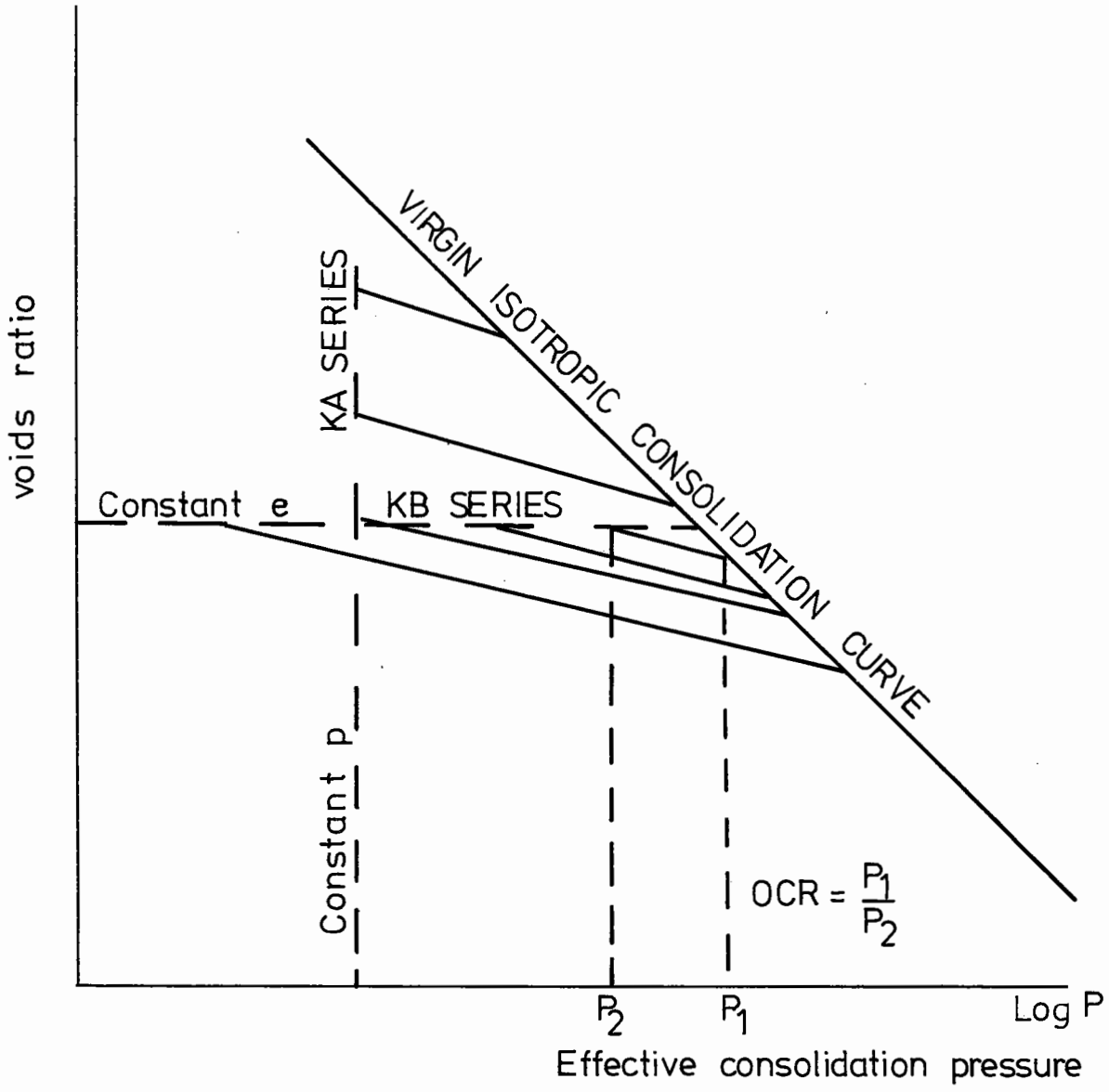

Fig. 3.1 Relation of keuper marl tests to the voids ratio and effective consolidation pressure.

Sample Nos.	No. of cycles	Length of rest period seconds	$(\sigma_1-\sigma_3)_{max}$ kN/m^2
RPK 1-3	8	1	150
RPK 3-6	8	5	150
RPK 7-9	8	10	150
RPK 10-12	4	1	150
RPK 13-15	4	5	150
RPK 16-18	4	10	150
RPK 19-21	1	1	150

OCR = 2

Preconsolidation pressure = 440 kN/m^2

Final consolidation pressure = 220 kN/m^2

Table 3.3(a) Rest Period Tests - Over-consolidated Keuper Marl - Wet Side

Sample Nos.	No. of cycles	Length of rest period seconds	$(\sigma_1-\sigma_3)_{max}$ kN/m^2
RPK 28-30	8	1	75
RPK 31-33	8	5	75
RPK 34-36	8	10	75

OCR = 10

Preconsolidation pressure = 400 kN/m^2

Final consolidation pressure = 40 kN/m^2

Table 3.3(b) Rest Period Tests - Over-consolidated Keuper Marl - Dry Side

Sample Nos.	Effective Consolidation Pressure kN/m^2
NC 1, 2	200
NC 3, 4	400
NC 5, 6	600

Table 3.4 Tests to Determine Virgin Isotropic Consolidation Curve

compacted Breedon gravel under repeated loading. It was considered that the influence of cyclic confining pressure would be more marked on a partially saturated granular material. Tests using a cyclic confining stress were, therefore, confined to this material.

In order to obtain meaningful data under a cyclic confining stress, it was necessary to develop equipment to measure lateral strain. This is described in Appendix B.

A preliminary test series (Table 3.5) was carried out to determine the effects of loading history on both resilient and permanent deformation properties. Information from these tests showed that it was possible to apply sequences of loading to a small number of samples to determine the resilient stress-strain behaviour. This was not possible, however, for the characterisation of permanent deformation. Therefore, the main series of tests was carried out as outlined in Tables 3.6 and 3.7. Data for the study of permanent deformation was obtained from tests both with and without lateral strain measurement.

Cell Pressure σ_3 kN/m^2	Deviator Stress ($\sigma_1 - \sigma_3$) kN/m^2
50-150	50-250
50-150	50-450
50-150	50-650
50-150	50-250, 50-350, 50-450, 50-550, 50-650
50-250	50-250
50-250	50-650
50-250	50-250, 50-350, 50-450, 50-550, 50-650

Table 3.5 Preliminary Breedon Gravel Tests

Test No.	Cell Pressure σ_3 kN/m^2	Deviator Stress ($\sigma_1 - \sigma_3$) kN/m^2
BA 1-3	200-250	0-200
BA 4-6	150-300	"
BA 7-9	50-400	"
BA 10-12	225	"
BA 13-15	250	"
BA 16-18	300	"
BA 18-21	400	"

Table 3.6 Comparison of Constant Cell Pressure and Cyclic Cell Pressure

Cell Pressure σ_3 kN/m^2	Mean σ_3 kN/m^2	Peak to Peak σ_3 R kN/m^2	Deviator Stress ($\sigma_1 - \sigma_3$) kN/m^2
200-250	225	50	0-200, 0-300, 0-400
150-300	225	150	" " "
50-400	225	350	" " "
0-100	50	100	0-200, 0-300, 0-400
50-150	100	100	" " "
100-200	150	100	" " "
50	50	0	0,200, 0-300, 0-400
100	100	0	" " "
225	225	0	" " "
300	300	0	" " "
400	400	0	" " "

Table 3.7 Tests carried out using Lateral Strain Measurement

CHAPTER FOUR

DESCRIPTION OF EQUIPMENT

4.1 INTRODUCTION

A brief description is given in this chapter of the testing apparatus. A large part of the details of modifications and developments in the equipment has been written in the form of Appendices.

The basic equipment consisting of the triaxial cells and loading rigs was not developed by the author. Details of the design of the loading frame, and triaxial cell may be found in Lashine et al (1970) and Lashine (1971). The development of the electrohydraulic servo control equipment is described in Lashine (1971), Cullingford et al (1972) and Parr (1972). Many aspects of the existing apparatus were, however, found to be unsatisfactory and improvements and modifications were carried out to enable the carrying out of the testing programme already outlined. In addition, an automated data recording system was developed which allowed the use of a small computer for analysis of analogue data stored on magnetic tape (Appendix D).

4.2 TESTING RIGS

Two identical testing frames with associated electronic control equipment (Fig. 4.2) were used. Fig. 4.1 shows a triaxial cell in position with the load being applied to a soil sample. The vertical position of the cell was adjusted

at the start of each test using a manual screw jack situated underneath. The deviator stress was applied to the sample using a double acting hydraulic actuator with a 100 mm stroke. The flow to the actuator was controlled by a "Dowty" servo valve. The servo control is described in Section 4.3. The load could be cycled at frequencies up to 30 Hz. The load range depended on the frequency, but at 1 Hz it was possible to apply a peak 8.5 kN to the sample (equivalent to a stress of 700 kN/m^2).

The load was measured using a load cell underneath the triaxial cell. This meant that both friction on the triaxial cell loading ram and the thrust of the confining pressure on the ram were being included in the measured applied load. Corrections were made for both of these.

The static confining pressure was supplied by distilled water from a tank pressurised using regulated air. The air was contained in a rubber bladder inside the tank.

The vertical deformation of the sample was measured using a linear variable differential transformer (LVDT) with a range of 50 mm. The deformation measured included the deformation of the system and corrections were made for this (Appendix C).

In addition to being able to cycle the deviator stress, there was also the facility for cycling the confining stress. This was carried out using a smaller hydraulic actuator which was connected to a bellofram piston. This piston was connected via $\frac{3}{8}$" nylon pressure

tubing to a gate valve on the triaxial cell. Provided that the system including the triaxial cell was carefully de-aired to reduce compliance to a minimum, it was possible to cycle the cell pressure from 0 to 500 kN/m^2 at a frequency of 1 Hz.

4.3 THE ELECTRO-HYDRAULIC SERVO CONTROL EQUIPMENT

The basic electro-hydraulic servo control loop is shown in Fig. 4.3. An input command signal, together with feedback from the load cell or the LVDT is fed into a summing function. The resulting error signal is fed to the servo valve which in turn adjusts the flow to the hydraulic actuator. The valve operates about a null position, no flow occurring into or out of the hydraulic ram to coincide with a zero error signal. In addition to the basic control loop there has been incorporated a stress control. The output from the LVDT is fed to a thermistor which in turn controls the gain of an amplifier in this subsidiary control loop. The result is that as the output from the LVDT increases, a compensation is made in the load to allow for the increased area of the sample.

As can be seen, depending on the type of input, command signal and control feedback, repeated load, constant stress or constant rate of strain tests can be carried out.

A problem encountered during the testing was drift of the null position of the servo valve as the temperature varied. This is a mechanical phenomenon, but it can be

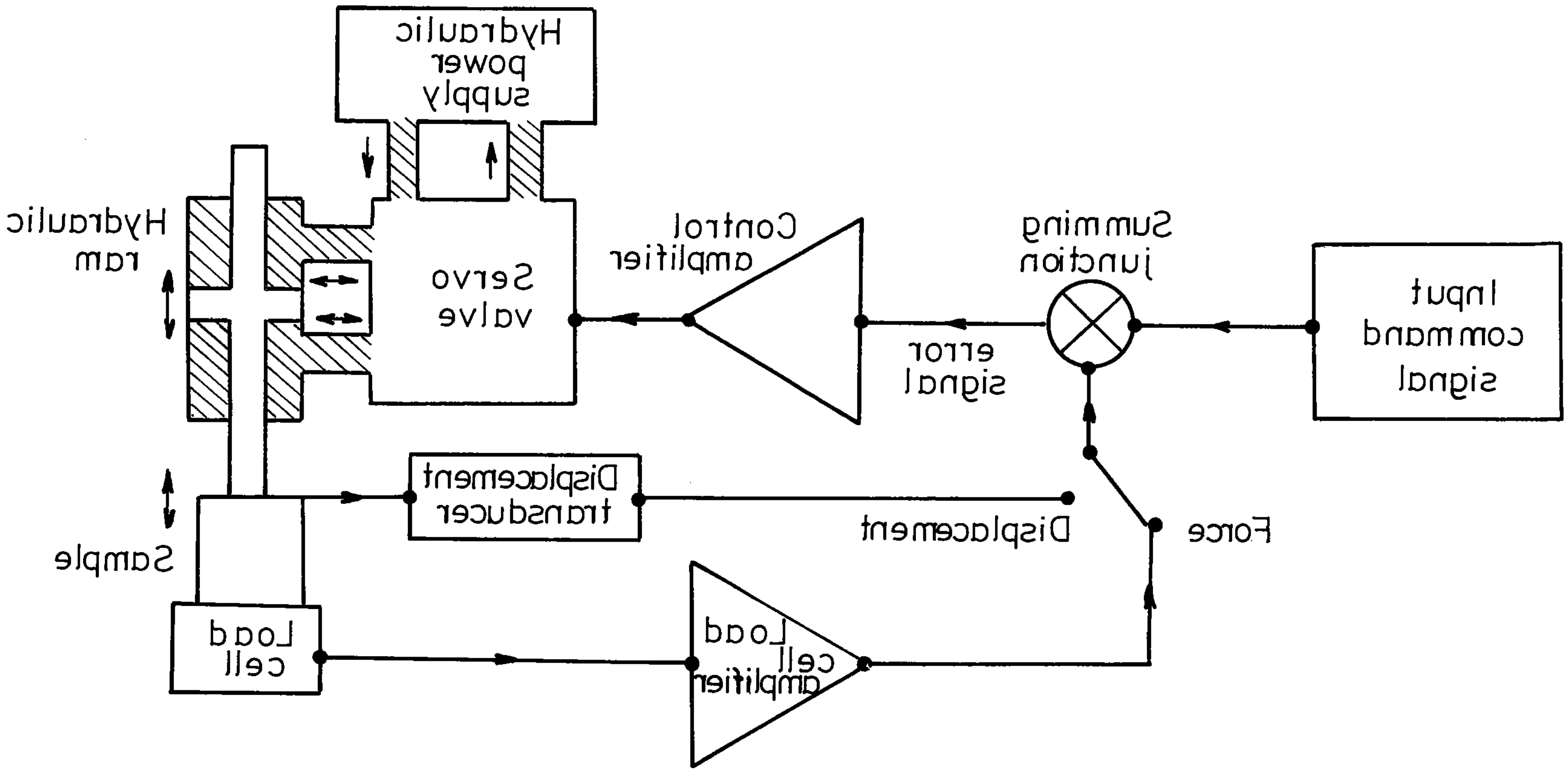

Fig. 4.3 Basic electro hydraulic servo control loop.

After Parr (1972)

controlled electronically by allowing the null position of the signal to the servo valve to drift while keeping the mean of the error signal equal to zero at the summing junction (Stirling and Chadwick, 1973).

A similar servo control loop was used to control the cyclic confining pressure. The phase of this loop could be controlled independently of the vertical stress.

To help overcome friction in both the servo valve and the hydraulic actuator, a very high frequency (700 Hz) dither signal was applied to the summing junction.

4.4 THE TRIAXIAL CELL

Six triaxial cells were used for the clay testing programmes. This gave sufficient time for consolidation of each sample to a particular stress history, while allowing full use to be made of the loading rigs. A typical triaxial cell used for most tests is illustrated in Fig. 4.4. Each cell consisted of a perspex walled lid and a base. The connections on the base were for confining pressure and end drainage from the top and base plattens. The bottom platten was fixed to the cell base while the top platten was loose. Each platten had a polished stainless steel face and drainage of the samples was allowed through porous sintered bronze rings connected to separate drainage lines. Several modifications were made to the cells to allow certain tests to be performed and these are described below.

4.4.1 High Pressure Cell

In order to produce samples of a high over-consolidation ratio (OCR) it was necessary to modify the perspex walled cell to allow pressurisation to 3000 kN/m^2 (Fig. 4.5).

The perspex walls were removed and replaced by anodised aluminium walls 180 mm internal diameter and 12 mm thick. The 12 rods clamping the cell top together were replaced by slightly longer silvered steel ones to allow the use of full $\frac{5}{16}$" BSF nuts instead of the half nuts already fitted. A shear test was carried out of the thread on these rods which gave an adequate factor of safety against failure. In addition, the six clamps attaching the lid to the cell base were redesigned to give a greater load bearing area, and to allow the use of $\frac{3}{8}$" BSF bolts.

4.4.2 Pressure Transducers

The original transducers for monitoring the cell pressure were installed inside each cell lid and were manufactured from aluminium alloy. They were found to be badly corroded and were prone to leakage under pressure. New transducers were, therefore, manufactured from brass and stainless steel and located outside the cell lid as shown in Fig. 4.4. A stainless steel diaphragm was clamped between the two brass halves of the transducer. The transducer body screwed onto a valve located on top of the triaxial cell. (Further details may be found in Appendix A.)

The existing pore water pressure transducers were located beneath the cell base and were found to be unsatisfactory for several reasons. Their sensitivity was very low and there was a large air trap where the klinger cock used for venting the system was screwed into the base. Despite all attempts at de-airing the system, it was difficult to reduce the compliance to a level where pore water pressure measurements were reliable. The position of the gauges also rendered them liable to damage and damp.

The original transducer was replaced by new transducers manufactured from stainless steel placed on the outside of the cell (Fig. 4.4). By careful design of the connectors the compliance of the system was reduced to an acceptable value (see Appendix A).

4.4.3 Elimination of Friction

The triaxial cell as originally designed incorporated a pressure equalisation device intended to eliminate the upward thrust exerted on the ram by the cell pressure. This had been thought necessary because the load cell was located outside the triaxial cell. The device, however, needed three tightly fitting seals on the ram. Although this compensated for the upward thrust of the cell pressure, it created an even larger problem because of the high friction on the ram. The friction force varied according to the surface condition of the ram, the state of deformation of the sample (i.e. position) and also with

frequency of stress application. Values as high as 250 N were measured.

The two top seals were, therefore, removed. When the ram was cleaned well in paraffin and then lubricated with "Vaxiella" oil, it was found to drop under its own weight. This level of friction was considered acceptable.

The problem of upward thrust on the ram due to static and cyclic cell pressure has been solved by applying a compensating factor to the calculations in the data analysis.

4.4.4 Lateral Strain Measurement

In order to satisfactorily characterise the behaviour of partially saturated granular materials under cyclic cell pressure, it is necessary to measure the lateral strain as well as the vertical strain. It was decided to use strain coils for this purpose (Fig. 4.6). A description of their development and method of use may be found in Appendix B.

4.5 DATA MONITORING EQUIPMENT

Monitoring of the tests was carried out using several devices (Fig. 4.2). Repeated load tests were monitored using a digital voltmeter in combination with a dual trace oscilloscope. The digital voltmeter had a facility for holding maximum and minimum voltages. Readings were recorded to four figures on a prepared data sheet. In addition, an ultra-violet oscillograph chart recorder was

used when storage of data was required. This was used for the beginning of repeated load tests, creep tests and for monitoring the whole of the strain controlled tests. Using this facility, it was possible to record six channels simultaneously on photographic paper.

An automated data collection process was developed using a 14-channel F.M. tape recorder. This system incorporated a programmable unit which allowed data to be recorded for any length of time at preset intervals. Data from the tape recorder was then analysed using a small computer. Details of this may be found in Appendix D.

4.6 CONSOLIDATION EQUIPMENT

4.6.1 One-Dimensional Consolidation

The consolidation of Keuper marl was carried out in two stages. The first stage was one-dimensional consolidation from a slurry in a mould. The equipment for this stage is shown in Fig. 4.7, and allows consolidation at two independent pressures. For Keuper marl, the lowest pressure which produced a sample which was easy to extrude and handle was 150 kN/m^2.

4.6.2 Over-consolidation Apparatus

In order to reproduce stress history effects on the clay samples, they were first pre-consolidated at a given pressure under drained conditions in the triaxial cell and then allowed to finally consolidate at a "swell back" pressure.

To carry out this process, it was necessary to have a variable confining pressure in the triaxial cell and a back pressure on the drainage line to maintain full saturation. In addition, it was considered necessary to monitor the flow of moisture into and out of the samples.

The confining pressure was supplied from a pressure tank filled with distilled water and pressurised using a regulated air supply fed to a rubber bladder inside the tank. The back pressure for the drainage line was also supplied from a pressure tank maintained at 150 kN/m^2 for most tests. The pressure for this tank was supplied from a perspex reservoir in which the pressure was maintained by regulated air which was separated from the water by a 50 mm layer of paraffin. This system was necessary to allow for a greater volume changes on the drainage line which a rubber bladder could not cope with.

The flow of moisture on the drainage lines was monitored by a bank of six volume change indicators (Fig. 4.8).

4.6.3 High Pressure Supply

In addition to the pressure lines already outlined, it was also necessary to supply a very high pressure for the KH (high OCR) series of tests. Using air pressure the safest maximum that could be achieved was 900 kN/m^2. In order to be able to pressurise the cells to an effective confining pressure of 3000 kN/m^2, it was necessary to supply an additional high pressure line.

The pressure for this line was supplied by an "Airhydro Power Unit" (Fig. 4.9). This power unit was in effect a pressure amplifier and pump combined. Using a regulated air supply, water was pressurised using two connected pistons whose areas were in the ratio of 10:1. Pressure was maintained on the return stroke by a non-return valve. The pumping action continued until an equilibrium was reached when the water pressure was ten times the air pressure. Using this system, it was possible to maintain the required maximum pressure of 3350 kN/m^2 ± 1%.

The reduction in pressure during the swelling process was limited to increments equal to the back pressure on the drainage line. For this series of tests the back pressure was, therefore, raised to 350 kN/m^2 to speed up the consolidation process.

CHAPTER FIVE

EXPERIMENTAL PROCEDURE

5.1 CLAY SAMPLE PREPARATION

5.1.1 Slurry Preparation

The material used in the test programme was obtained from a local brickworks. It was first oven dried, then crushed in a mill and those particles passing a No. 200 sieve were stored in plastic bins.

A slurry of the clay was prepared by thoroughly mixing the powdered clay with distilled de-aired water to a moisture content of approximately twice the liquid limit (70%). Enough slurry was prepared at each mixing to produce three specimens. The mixing was carried out in a "Hobart" mixer for several hours to produce a uniform slurry.

5.1.2 One-Dimensional Consolidation

The slurry was transferred to the one-dimensional consolidation moulds (Fig. 4.7). Each mould was 101.6 mm in diameter. To ensure sample uniformity and to speed up the consolidation process sample drainage was allowed from each end. The consolidation process took three days. At the end of this period, the samples were extruded from the mould into a 102 x 102 mm cylinder. The ends of the sample were trimmed using a thin wire cheese cutter. The off-cuts were used for moisture content determination.

5.1.3 Cell Base Preparation

A shallow trough 60 mm deep was mounted on the cell

base. This was filled with de-aired distilled water. Then the pore water pressure measuring system was flushed thoroughly with water until all air was removed. A blank was inserted at one end and the null indication equipment (Fig. 4.8) was used to check the compliance of the system. A compliance of 5×10^{-6} cm^3 kN/m^2 (Appendix A) was taken as acceptable. This was equivalent to 0.5 cm movement of the mercury column for a pressure drop of 500 kN/m^2. If this value was not obtained, any remaining air was removed by dissolving it under a pressure of 600 kN/m^2 for five or six hours and then flushing the system under pressure with de-aired water. To prevent the formation of corrosion gases, the system was then flushed through with a buffer solution with a pH value of 7. This solution inhibited corrosion by preventing the formation of acids in the system. A ceramic probe which had been boiled for several minutes to remove any air was screwed into the centre of the bottom platten. Fig. 5.1 shows the probe in position with the trough removed.

The end plattens were cleaned, polished, smeared with silicone grease and a latex disc placed on each one to reduce sample end restraint to a minimum. Both plattens were thoroughly flushed under water to remove any trapped air.

5.1.4 Clay Sample Mounting

The sides of the sample were lightly scraped with a spatula to remove any mould grease which might block the

filter paper drains. The sample was then weighed and placed on the bottom platten forcing the ceramic pore pressure probe (6 mm dia. x 10 mm high) into the base of the sample. The top platten was placed in position and the filter paper drains were attached to the sintered bronze drainage rings by means of two latex bands (Fig. 5.2). A membrane was placed on a vacuum former and slipped over the sample. A small tube was inserted between the top platten and the membrane to allow trapped air and water to escape. When all air had been carefully removed from between the sample and the membrane, the tube was removed, and two sealing rings were placed around the plattens at each end. The top drainage line was connected and the cell was filled with distilled de-aired water.

5.1.5 Consolidation in the Triaxial Cell

A confining pressure supplied as described in Section 4.6.2 was connected to the cell and the pressure adjusted to the required preconsolidation pressure. The drainage connections for the top and bottom plattens were connected to a back pressure of 150 kN/m^2 for the low OCR's or 350 kN/m^2 for the OCR of 75. In the case of the high pressure consolidation, the vent for the pore water pressure transducer had to be left open to prevent damage to the diaphragm. The preconsolidation of the samples was allowed until volume change had reduced to less than 1 cc per day measured by the volume change indicators (Fig. 4.8). This stage usually took from four to six days. The cell pressure

was then reduced in 150 kN/m^2 increments to the appropriate final consolidation pressure. Care was taken that negative pore water pressures did not develop. Swelling of the sample usually took from two to three days.

5.2 GRANULAR SAMPLE PREPARATION

5.2.1 Granular Sample Compaction

The granular material used was a crushed rock passing a $\frac{3}{8}$" sieve. It was carefully sieved and graded to give a grading curve the same as that one used by Lashine et al (1971).

Samples were prepared by compaction in a split mould using a falling hammer. The standard AASHO method of compaction was used, the material being compacted in three layers with 25 blows to each layer. This produced a sample just wet of the optimum moisture content (OMC). The samples when removed from the split mould were stiff enough to be handled.

5.2.2 Granular Sample Mounting

The sample from the mould was placed on the prepared cell base. The top platten was put in position and the filter paper drains put in place. A latex membrane was placed on the sample using a vacuum former. For some of the tests the strain coils were placed on the sample using the techniques outlined in Appendix B. The top platten drainage was connected and the cell filled with distilled water. The samples were allowed to consolidate for several

hours before testing. The drainage cocks were left open to atmospheric pressure.

5.3 TESTING PROCEDURES

5.3.1 Repeated Load Tests on Clay

Samples were placed on the loading machine where the following procedure was carried out. The confining pressure was reconnected and the cell pressure transducer screwed onto the small valve on the cell top. The pore pressure transducer cock was opened and the strain gauge bridge electrically balanced, the klinger cock was then closed again and the response of the transducer observed, and the equilibrium value of the pore water pressure (PWP) noted.

The cell was moved using the screw jack underneath until the output from the LVDT connected to the cell ram was approximately zero. The output was noted for a nominal deviator stress of 2-3 kN/m^2.

The drainage cocks on the cell were kept closed and samples were tested undrained. A constant load equal to the mean value of the repeated load was first applied followed immediately by the increase of the cyclic amplitude to the appropriate value. The initial 10-15 cycles were at 1 Hz, then the frequency was increased to 10 Hz and readings of the deformation, deviator stress, cell pressure, and pore water pressure recorded using the digital volt meter (DVM). The initial stages of the test

were recorded using the ultra-violet recorder. Readings were also taken automatically at fixed intervals on a 14-channel F.M. tape recorder.

5.3.2 Repeated Load Tests on Granular Materials

The setting up procedure for the tests on Breedon gravel was very similar to that followed for the clay.

As the samples were partially saturated, they were tested drained without pore water pressure measurement.

If cyclic cell pressure was required, then the bellofram piston was connected via a nylon tube to the gate valve on the cell base. Care was taken to flush out any air in the line to maintain compliance at a minimum.

In the case of cyclic cell pressure tests, 100 cycles of cell pressure were applied to condition the sample before the application of the vertical deviator stress.

5.4 STRAIN CONTROLLED AND CREEP TESTS

All of the single loading tests were carried out on the saturated Keuper marl samples. The procedure for setting up the creep tests was similar to that used for the repeated load tests. The only difference being that instead of applying a mean stress first, the full stress was applied immediately and maintained at as near a constant level as was possible within the limitations of the equipment.

A series of strain controlled "strength" tests was also carried out. The rate of strain in these tests was 0.075%/min. This was in order to allow pore pressure

equilibrium in the samples throughout the test. The LVDT was used as a feedback on the servo loop and a ramp voltage as the command signal.

CHAPTER SIX

DISCUSSION OF RESULTS FROM TESTS ON KEUPER MARL

6.1 INTRODUCTION

Tests have been carried out on over-consolidated saturated Keuper marl to characterise the plastic and elastic properties. Carefully prepared reconstituted soil was used in order to be able to determine which parameters are the most important in the study of repeated load behaviour of over-consolidated clay. The effects of the stress history, moisture content and consolidation pressures were studied.

With reference to the accumulation of plastic strain a model has been developed relating the phenomenon of creep to repeated loading. In addition, repeated load and creep behaviours of samples prepared to different stress histories have been found to fit general models according to whether the samples are heavily or lightly over-consolidated.

Elastic behaviour has been found to be dependent on the applied stresses and to be independent of stress history or moisture content. Tests using rest periods as opposed to continuous loading show a large delayed elastic component of deformation. For the purposes of pavement design this component should be considered in any estimate made of modulus under repeated non-continuous loading.

6.2 THE MATERIAL

Geologically, Keuper marl consists of a series of red-brown mudstones and silty mudstones of Triassic age (Chandler and Davis, 1973). The Keuper marl outcrop forms two limbs either side of the Pennines which unite in the Midlands and extend southwest to the Bristol Channel. Particle size analyses show a variation in the clay size fraction according to the degree of weathering.

The material used in the test programme was obtained from a local brickworks. In order to produce consistent samples only the portion passing a No. 200 sieve was used. The material was oven dried, crushed in a mill and those particles passing a No. 200 sieve were stored in plastic bins.

Standard classification tests performed on the material yielded the following results:

Specific gravity:	2.74
Liquid limit:	32.0%
Plastic limit:	18.0%
Plasticity index:	14.0%

The particle size distribution, determined by the pipette method for the material passing the 200 sieve was:

Coarse silt:	48.5%
Medium silt:	14.5%
Fine silt:	19.0%
Clay:	18.0%

The liquid limit, plastic limit and specific gravity are the same as those given for a typical marl by Chandler and Davis (1973). The clay size content is, however, lower than their value, which may be due to aggregates of clay particles forming silt sized particles. This is a property of unweathered marl.

6.3 RELATIONSHIP BETWEEN CONSOLIDATION PRESSURE AND MOISTURE CONTENT

Two main series of repeated load tests were carried out on the Keuper marl. Samples in the first series (KA) all had a constant initial effective confining pressure ($\sigma_3' = 40$ kN/m^2). While in the second series (KB) the moisture content was approximately constant. There was some scatter in the final moisture contents for these tests resulting in a range of moisture contents from 18.4 to 20.2%. A supplementary series of samples were produced at an over-consolidation ratio of 75. This was done to extend the range of OCR's and moisture contents being investigated. The idealised equilibrium moisture content versus effective confining pressure relationships for these tests is shown in Figs. 6.1 and 6.2. The virgin isotropic consolidation curve was determined by preparing a series of normally consolidated samples. This curve is in good agreement with those drawn by Cooper (1970) and Lashine (1971) for the same material. The swelling curves were drawn as straight lines since no measurements were taken at intermediate pressures. Cooper (1970),

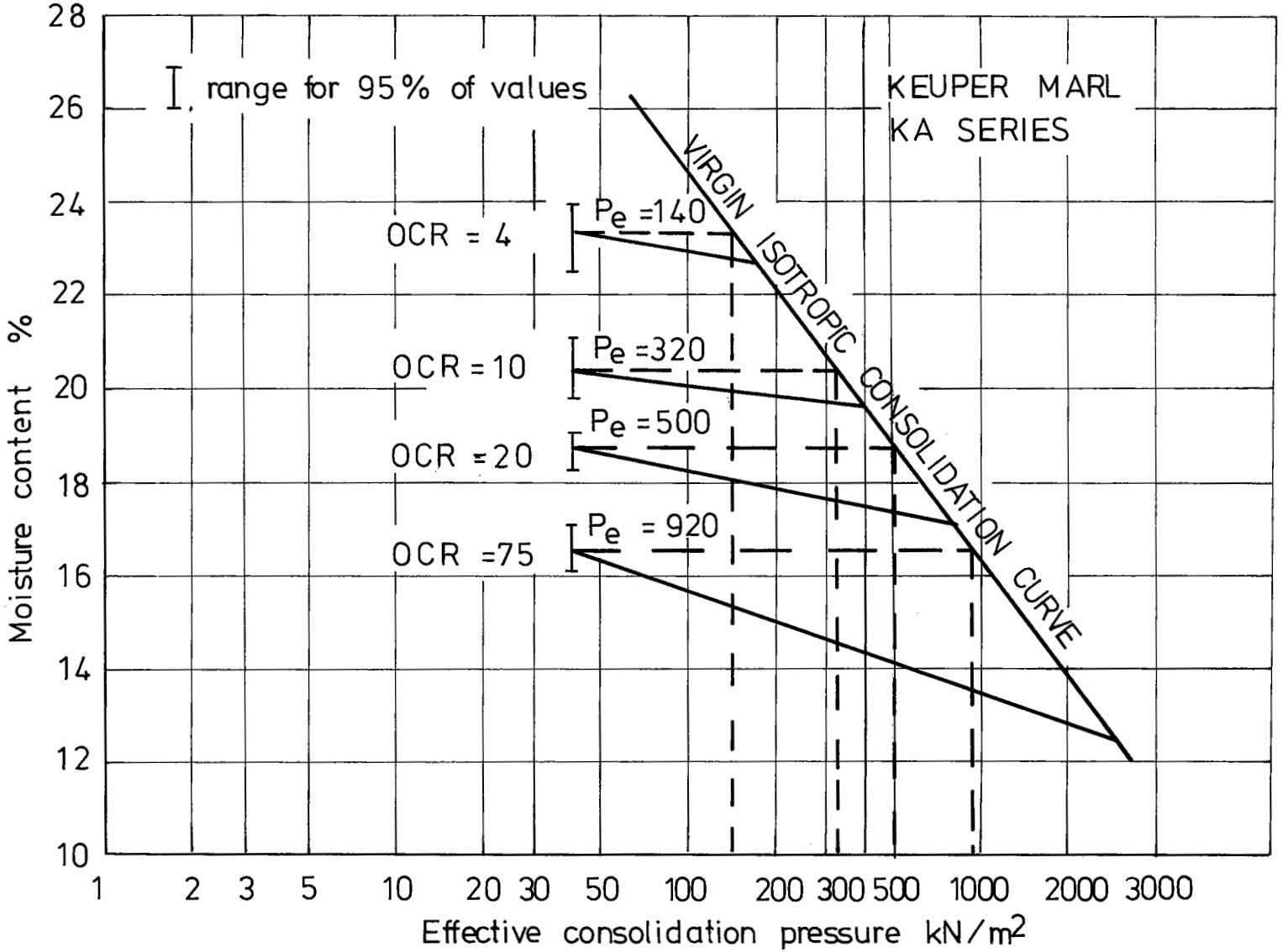

Fig. 6.1 Idealized consolidation curves for keuper marl.

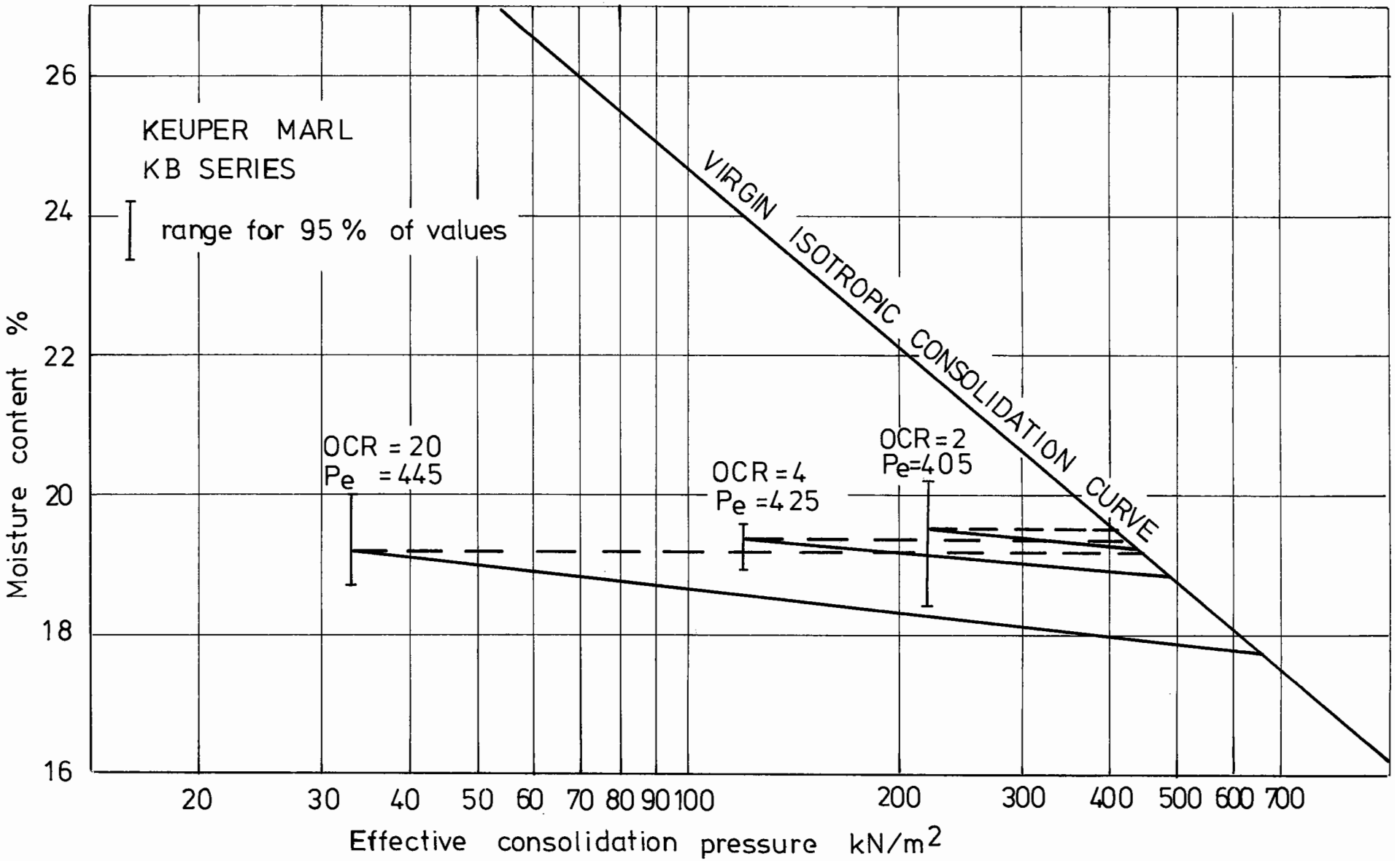

Fig. 6.2 Idealized consolidation curves for keuper marl.

however, found that the swelling lines were in fact non-parallel and curved concave upwards.

From Figs. 6.1 and 6.2 the average values of equivalent pressure p_e were obtained and are shown on the figures. p_e is defined as the pressure of the point on the normal or virgin consolidation line which is at the same specific volume (moisture content) as the sample itself (Roscoe et al, 1958 and Wroth and Loudon, 1967). This parameter can be used in the prediction of sample strength (see Section 6.4.2), and in addition allows samples with different stress histories to be normalised onto a single stress plane.

6.4 SINGLE LOADING STRAIN CONTROLLED TESTS

Samples were tested undrained with pore water pressure measurements. The cell pressure was maintained at the swelling pressure throughout the tests. To allow the pore pressures to reach equilibrium during the test the samples were tested at a "slow" rate of strain of 0.076 mm/min. This value had been used by Lashine (1971) when carrying out similar tests. The object of the single loading tests was to obtain a simple strength criterion to compare with the behaviour under repeated loading. Pore water pressure, deformation and strength characteristics were examined.

6.4.1 Pore Water Pressures

The behaviour of pore water pressure in this type of

test was examined with respect to longitudinal strain in two different ways. Firstly, it was compared with the applied deviator stress by examining the non-dimensional pore water pressure parameter "A" where:

$$A = \frac{\Delta u}{(\sigma_1' - \sigma_3')} \qquad (\Delta u = \text{pore water pressure change})$$

Secondly, the results were presented by dividing the pore water pressure by the equivalent pressure p_e.

The variation in the pore water pressure parameter "A" is shown in Figs. 6.3 and 6.4. All the samples showed a steep rise as the load was initially applied. On further straining the value of "A" tended towards an equilibrium value.

The contrasting ways in which the pore water pressure develops is an illustration of the different soil particle structures. This difference in structure, it will also be shown, is evident also in the creep and repeated load behaviour of the soil. The contrast is best shown in Fig. 6.5 where the pore water pressure is normalised with respect to the equivalent pressure and plotted against the longitudinal strain. As the OCR increases, the equilibrium value of u/p_e decreases.

It is possible to divide the samples into two categories; these are, samples on the "wet" side and samples on the "dry" side of the critical state (Roscoe et al, 1958). Samples on the wet side are those which develop positive pore pressures during shear while those on the dry side develop negative pore pressures.

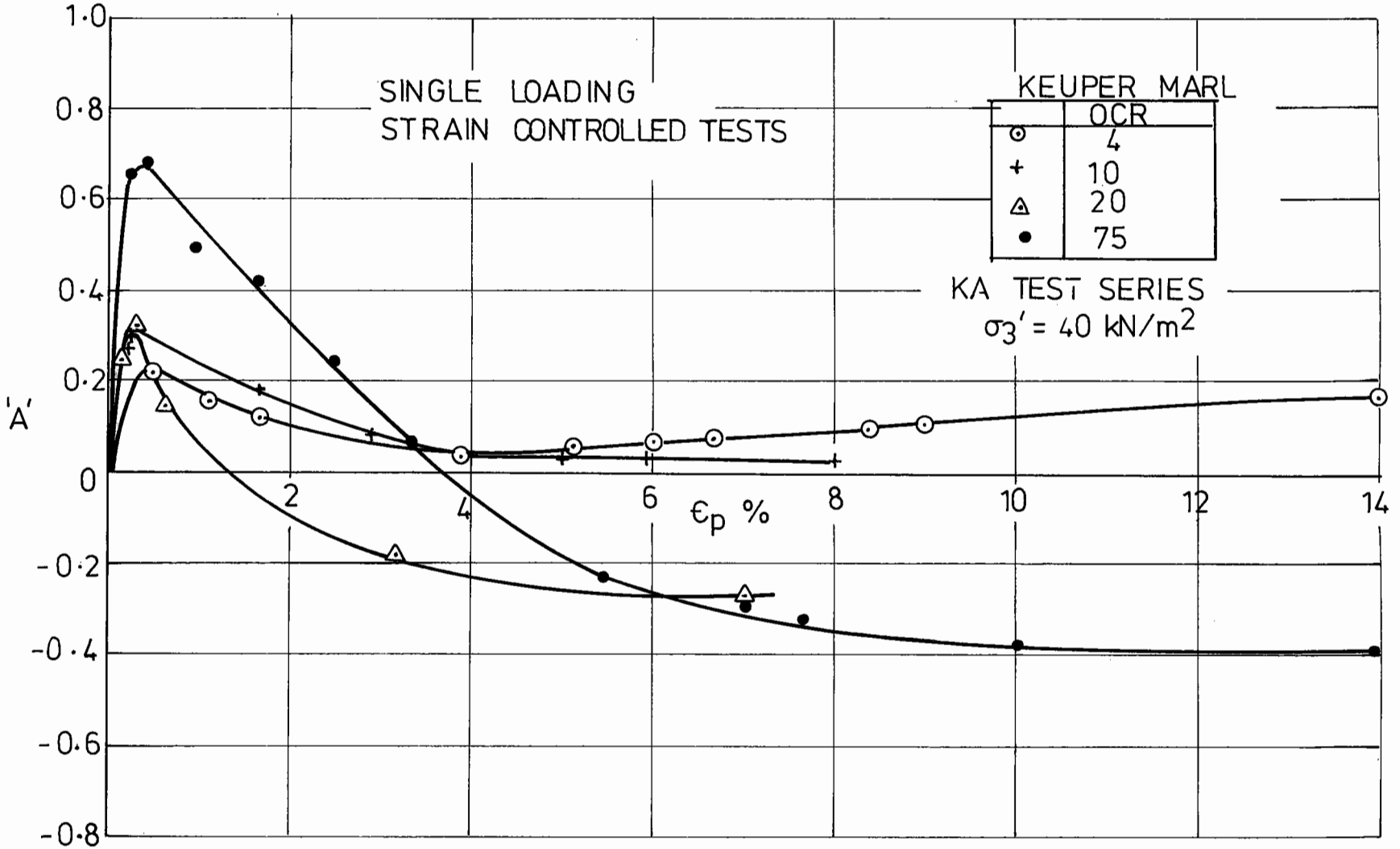

Fig. 6.3 Variation of 'A' values with overconsolidation ratio for a constant swell back pressure.

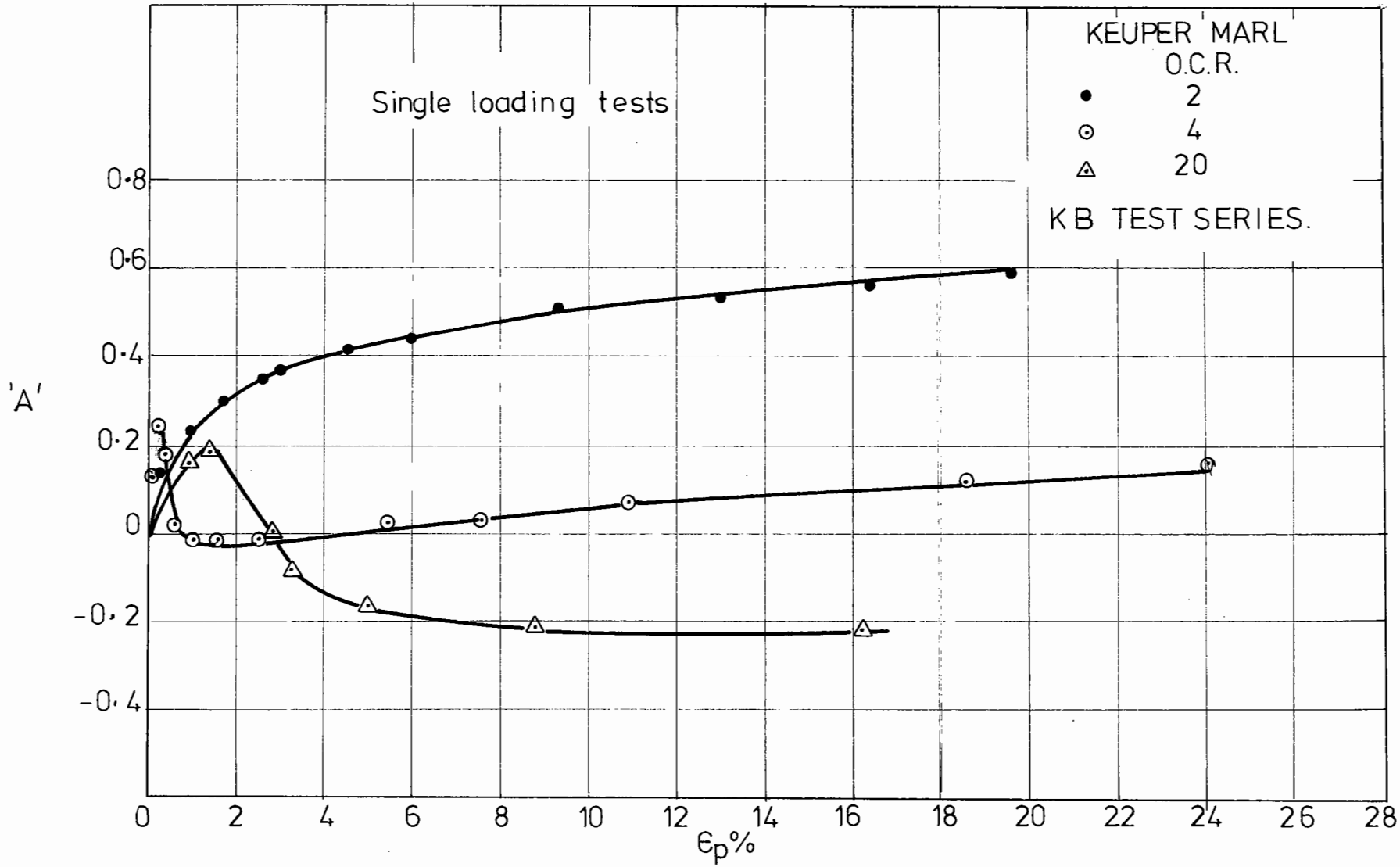

FIG. 6.4 Variation of 'A' values with strain and overconsolidation ratio for constant moisture content

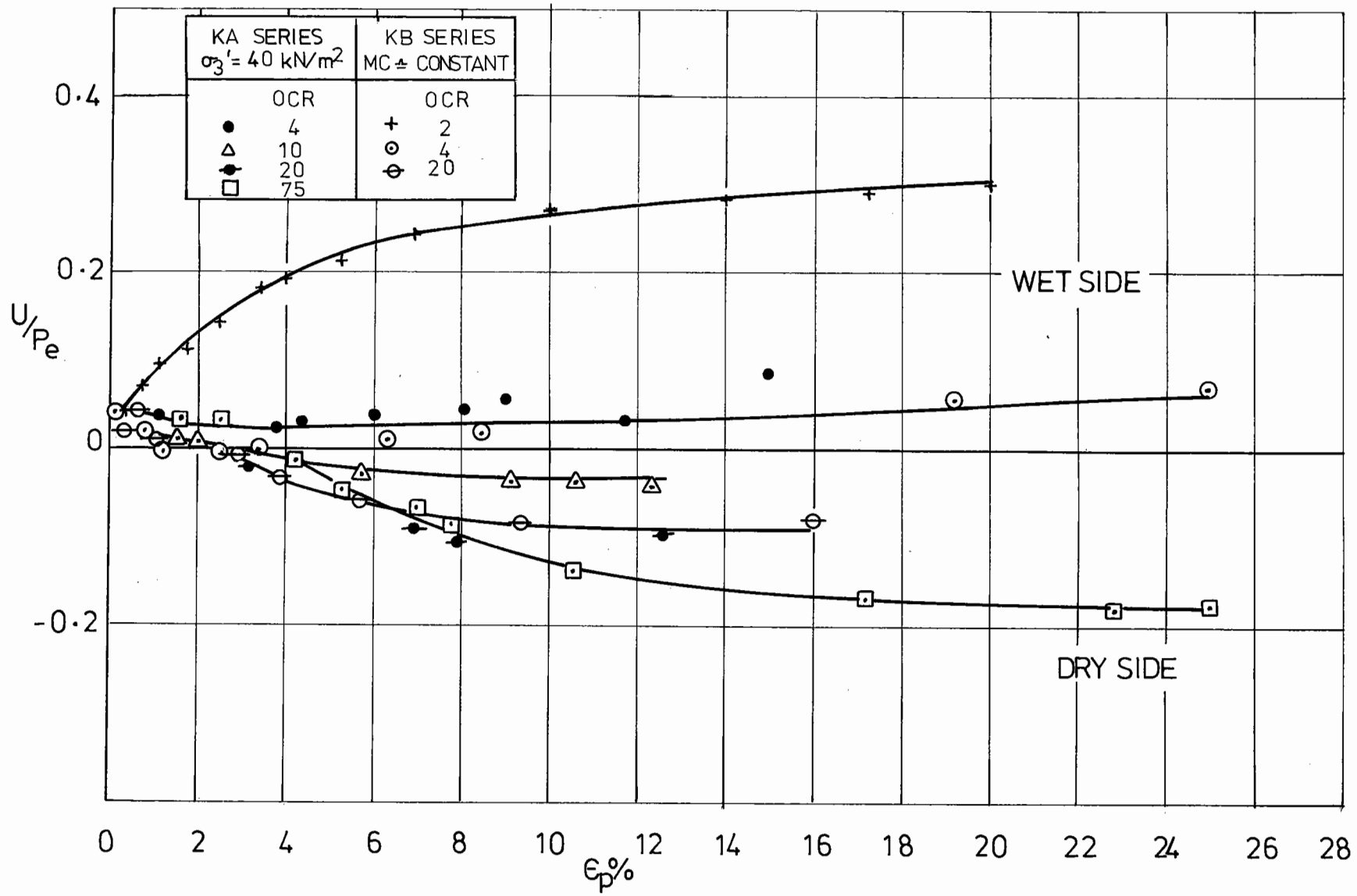

Fig. 6.5 Variation of normalised pore water pressure with axial strain for strain controlled tests.

6.4.2 The Stress Invariants p and q

In order to better examine the single loading strength of samples the following parameters were used:

$$\text{Deviator stress } q = (\sigma_1' - \sigma_3')$$

$$\text{Mean normal effective stress } p = \tfrac{1}{3}(\sigma_1' + 2\sigma_3')$$

By normalising p and q with respect to p_e it is possible to compare tests carried out at different void ratios. Fig. 6.6 shows the non-dimensional parameters q/p_e and p/p_e plotted against each other and is the projection of all the plots of q against p onto a single plane. It can be seen that whatever the starting point all the stress paths converge on one point, the critical state, at which q/p_e is equal to 0.45 and p/p_e equals 0.36 for this particular soil.

Some strain contours have been plotted on Fig. 6.6. These follow a similar pattern to those plotted for kaolin by Wroth and Loudon (1967). It can be seen that those on the dry side of the critical state converge on a point on the p/p_e axis. The contours on the wet side are, however, parallel to the p/p_e axis. In addition, it can be seen that a larger proportion of the sample strength is mobilised to reach a given strain on the wet side than for highly over-consolidated samples on the dry side.

The development of the terminal value of q/p_e is shown in Fig. 6.7. As the OCR increases, the terminal value is reached at a higher strain. This terminal value is defined as q_f/p_e.

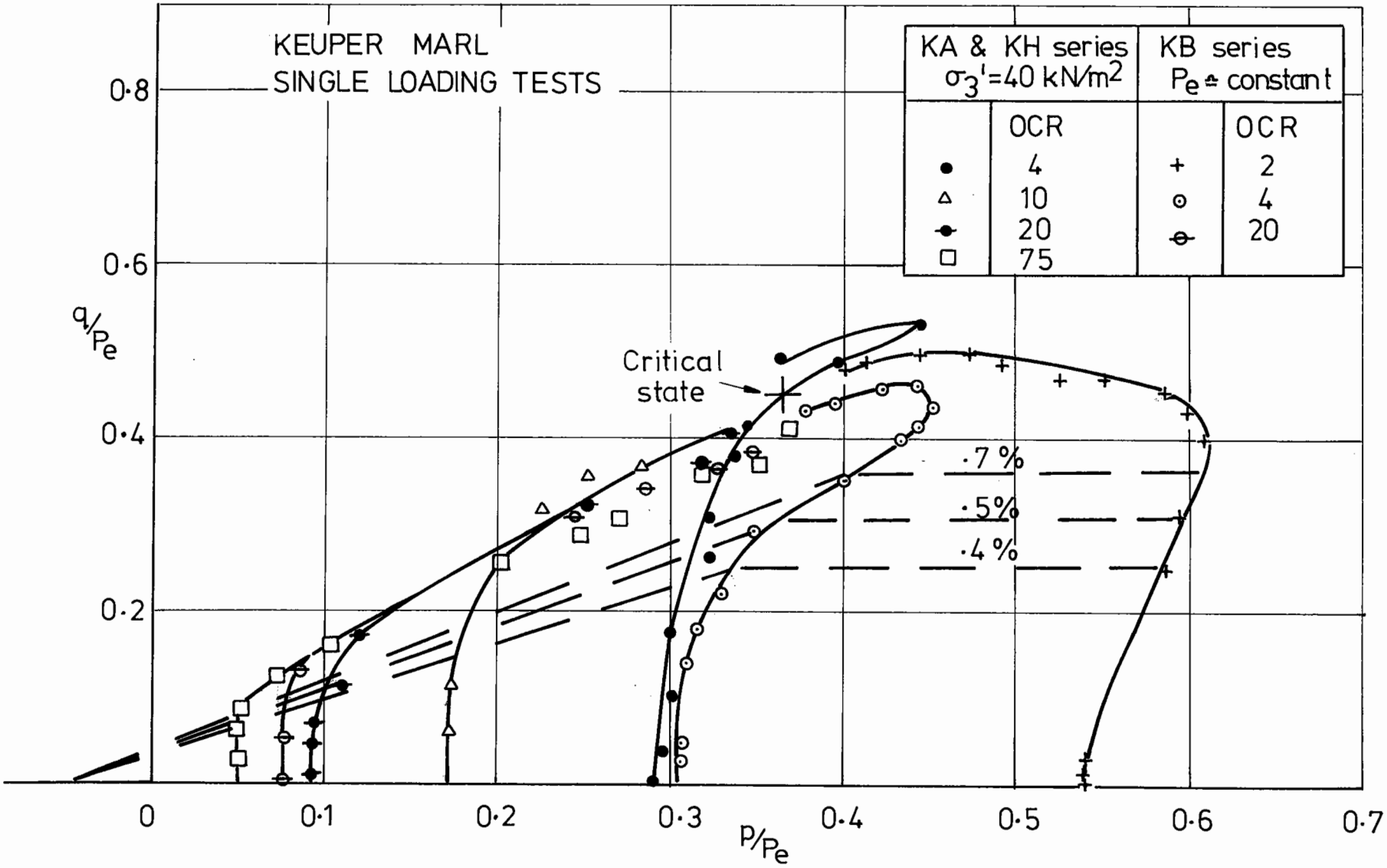

Fig. 6.6 Normalized stress paths for strain controlled tests.

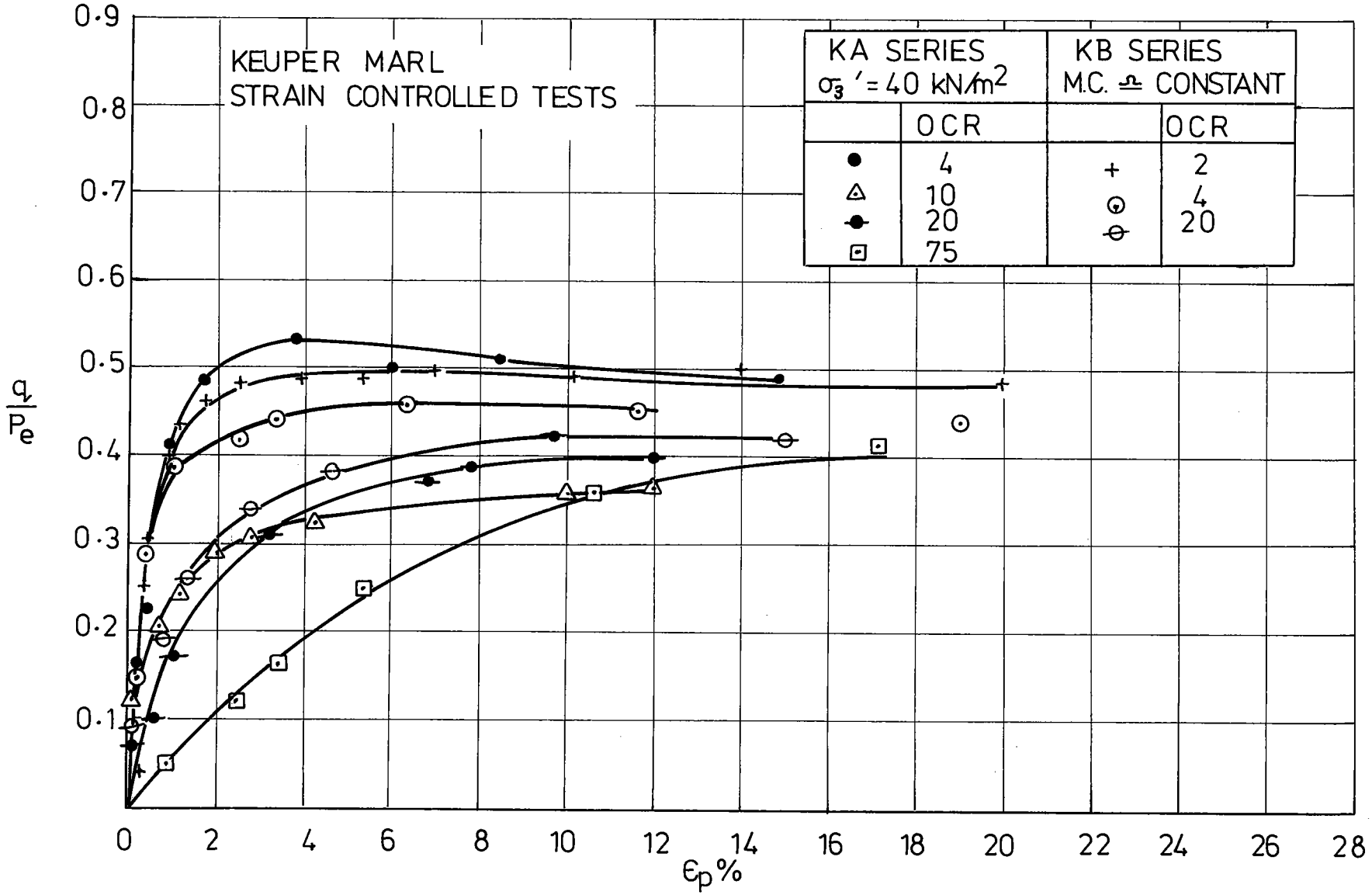

Fig. 6.7 Variation of normalised deviator stress with axial strain for strain controlled tests.

The value of q_f/p_e of 0.45 can be used to calculate the single loading strength of the material tested for any value of p_e. The actual values obtained from such tests are compared with the calculated values in Fig. 6.8 and a reasonable correlation is noted.

6.5 PLASTIC DEFORMATION UNDER CREEP AND REPEATED LOADING

The behaviour of samples under creep and repeated load has been found to be essentially very similar. The two types of behaviour will, therefore, be studied together.

The accumulation of plastic deformation under repeated loading will be shown to be directly related to flow under creep conditions. In addition, a general model will be outlined relating both creep and repeated load plastic deformations to the stress history and sample strength.

6.5.1 Undrained Stress Paths and Development of Pore water pressure

Stress paths for repeated load and single loading tests are compared in Fig. 6.9. The points represent the repeated load tests and are at values of q/p_e in which $q = q_{max}$. The tests would, in fact, move through an area of stress space represented by a parallogram enclosed by the lines representing q_{max} and $q = 0$, and with sides of slope equal to a third, since $p = q/3 + \sigma_3'$.

Comparison of the repeated load stress paths with those for strain controlled tests indicates that the equilibrium value of pore water pressure under repeated

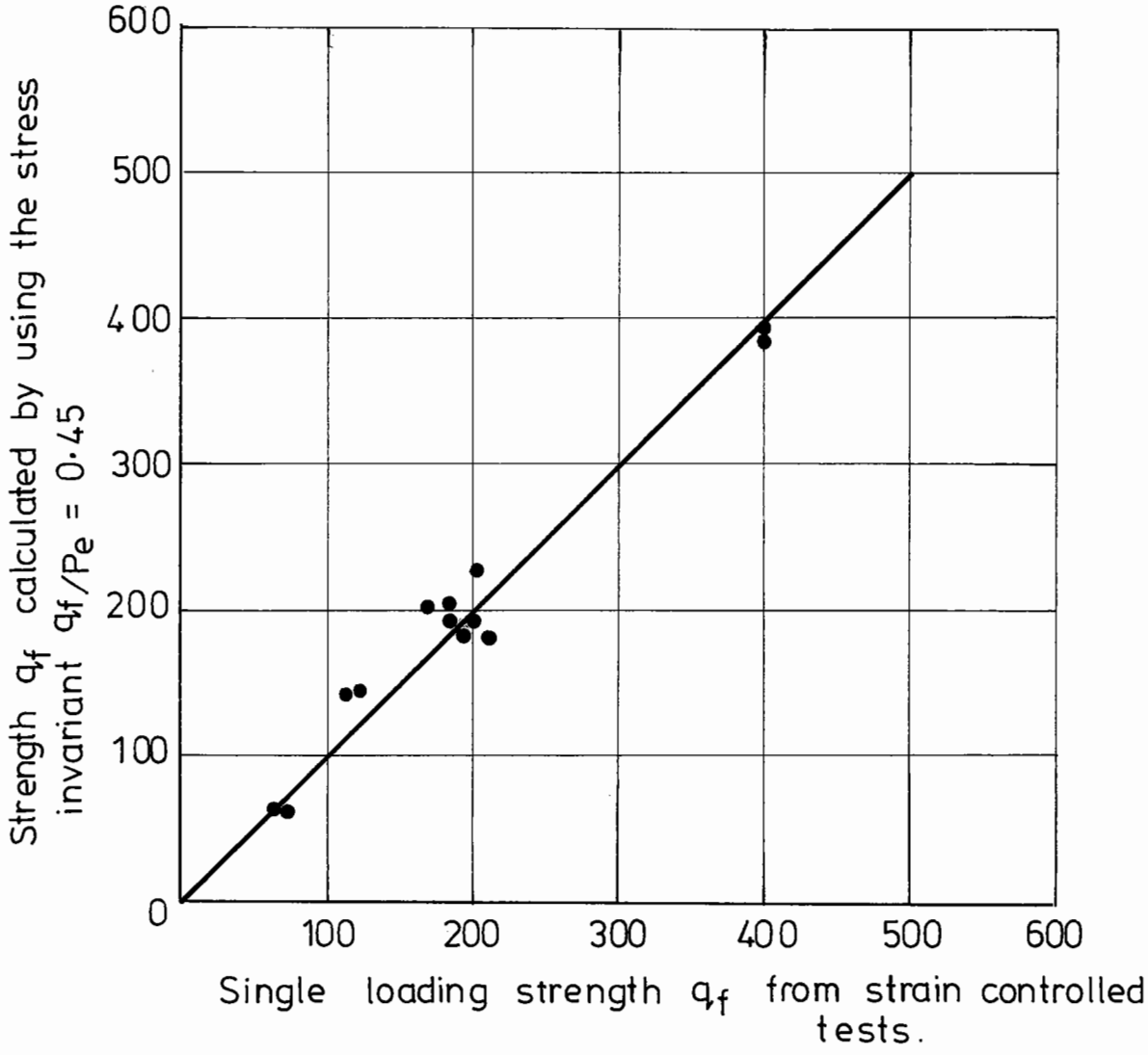

Fig. 6.8 Comparison of strength obtained from single loading tests with that calculated using the stress invariant.

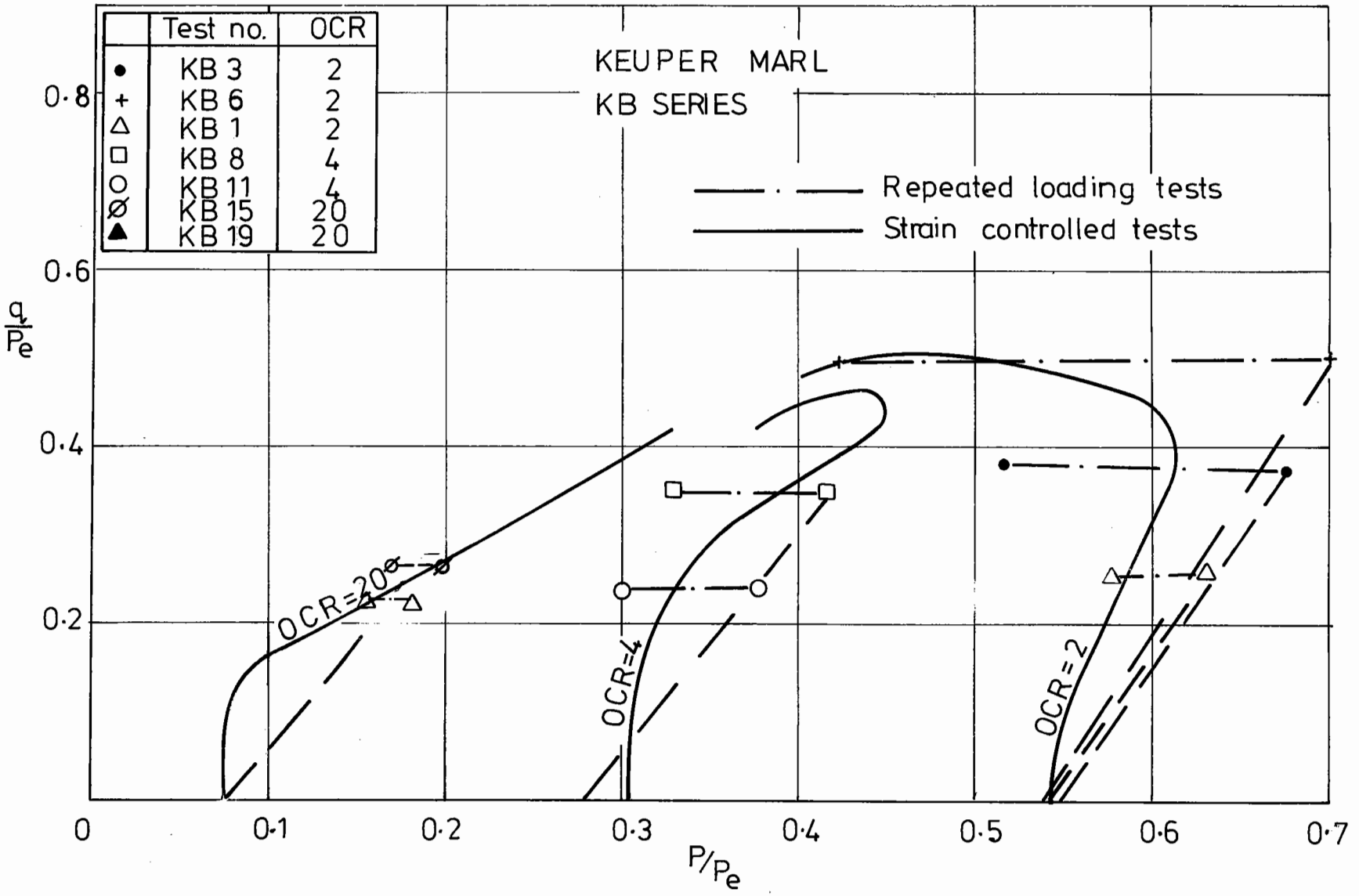

Fig.6.9 Undrained stress paths under repeated loading.

loading is greater for a given value of q than that attained in strain controlled tests. A similar conclusion was reached by Roscoe et al (1963) when comparing creep and strain controlled tests. They suggest that the time effects in any creep of soil are associated with a diffusion process. Lacerda and Houston (1973), carrying out stress relaxation tests, found the variation of pore pressure during the relaxation period is very small, lending support to the hypothesis that the magnitude of pore pressures depend exclusively on the amount of strain.

The variation of pore pressure parameter "A" with the number of cycles of applied load is shown in Figs. 6.10 and 6.11, where $A = \Delta u/(\sigma_1-\sigma_3)_{max}$. It can be seen that an equilibrium value of pore water pressure is not reached until between 10^5 and 10^6 cycles. For a very lightly over-consolidated clay, the maximum value of "A" increases with increasing deviator stress.

Undrained stress paths for creep and repeated loading are shown in Fig. 6.12. Comparison of the paths for an OCR of 10 shows that higher peak values of pore pressure are reached under creep conditions. However, in general, the stress paths are very similar.

Typical variations of pore pressure parameter "A" under creep and repeated load conditions are shown for an OCR of 10 in Figs. 6.13 to 6.15. It can be seen that for each value of applied deviator stress, the behaviour of the pore water pressure under repeated load and creep is very similar.

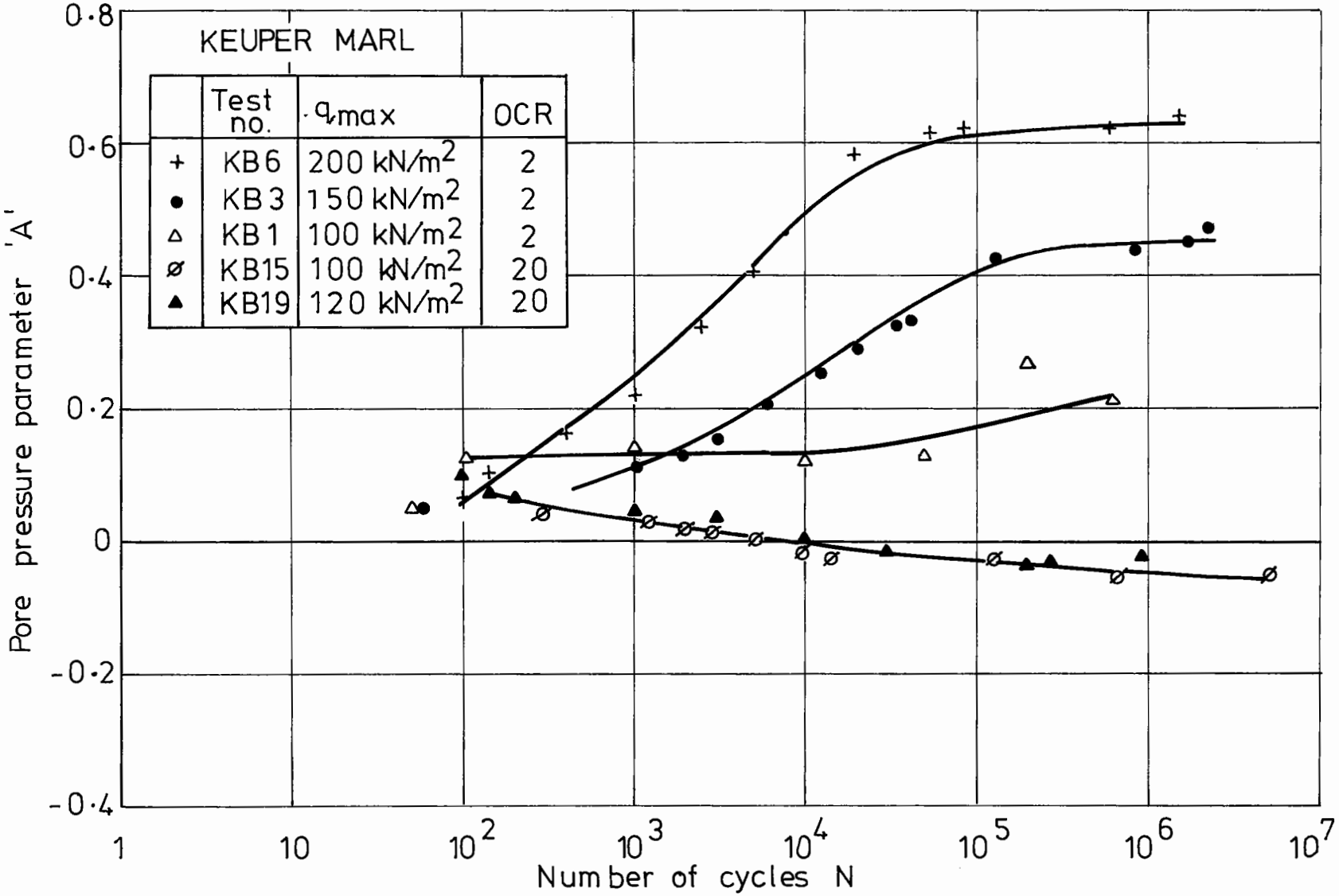

Fig. 6.10 Variation of pore water pressure parameter 'A' with number of cycles for overconsolidated keuper marl repeated load tests.

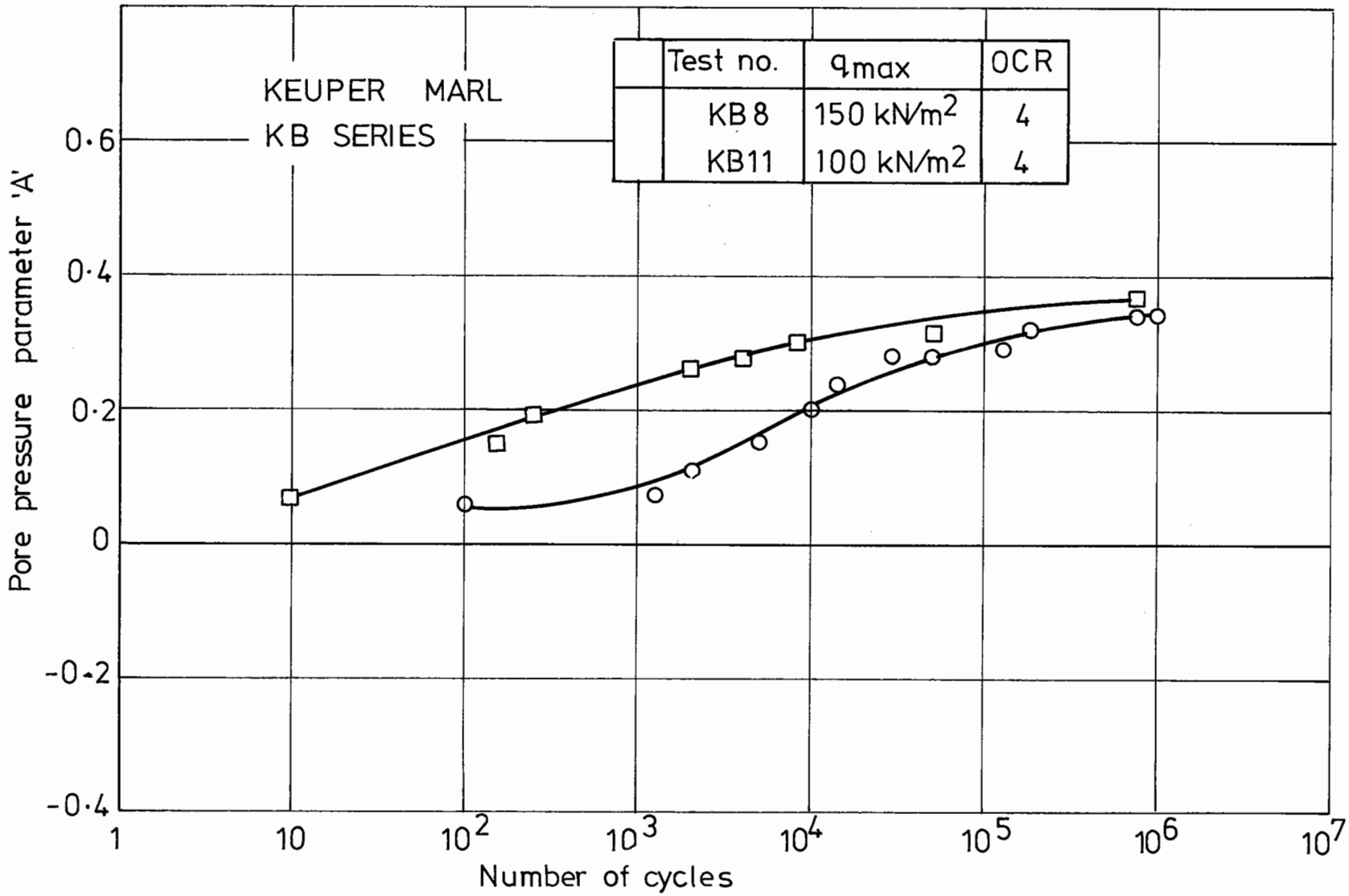

Fig. 6.11 Variation of pore water pressure parameter 'A' with number of cycles for overconsolidated keuper marl repeated load tests.

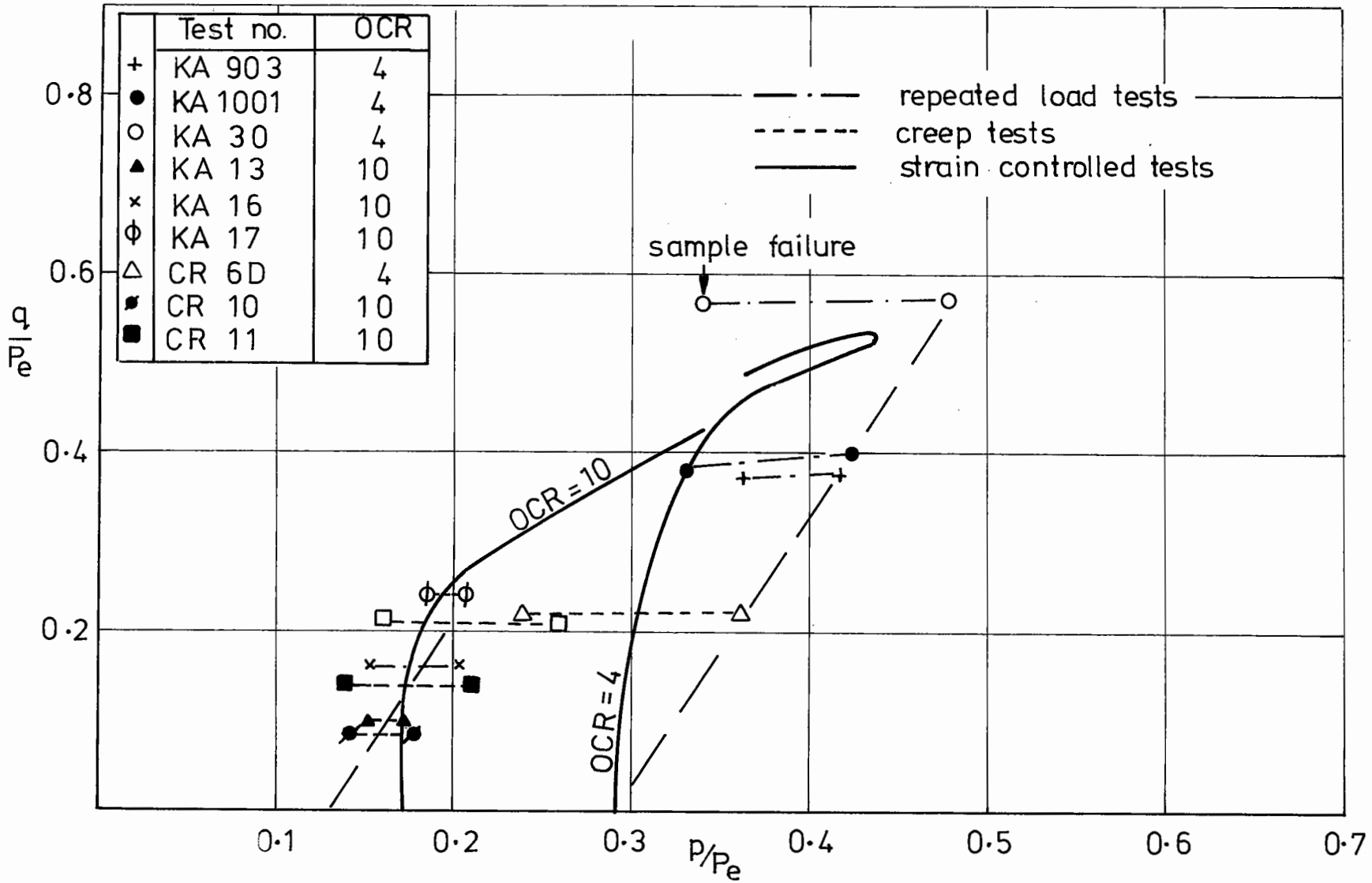

Fig. 6.12 Undrained stress paths under creep and repeated loading.

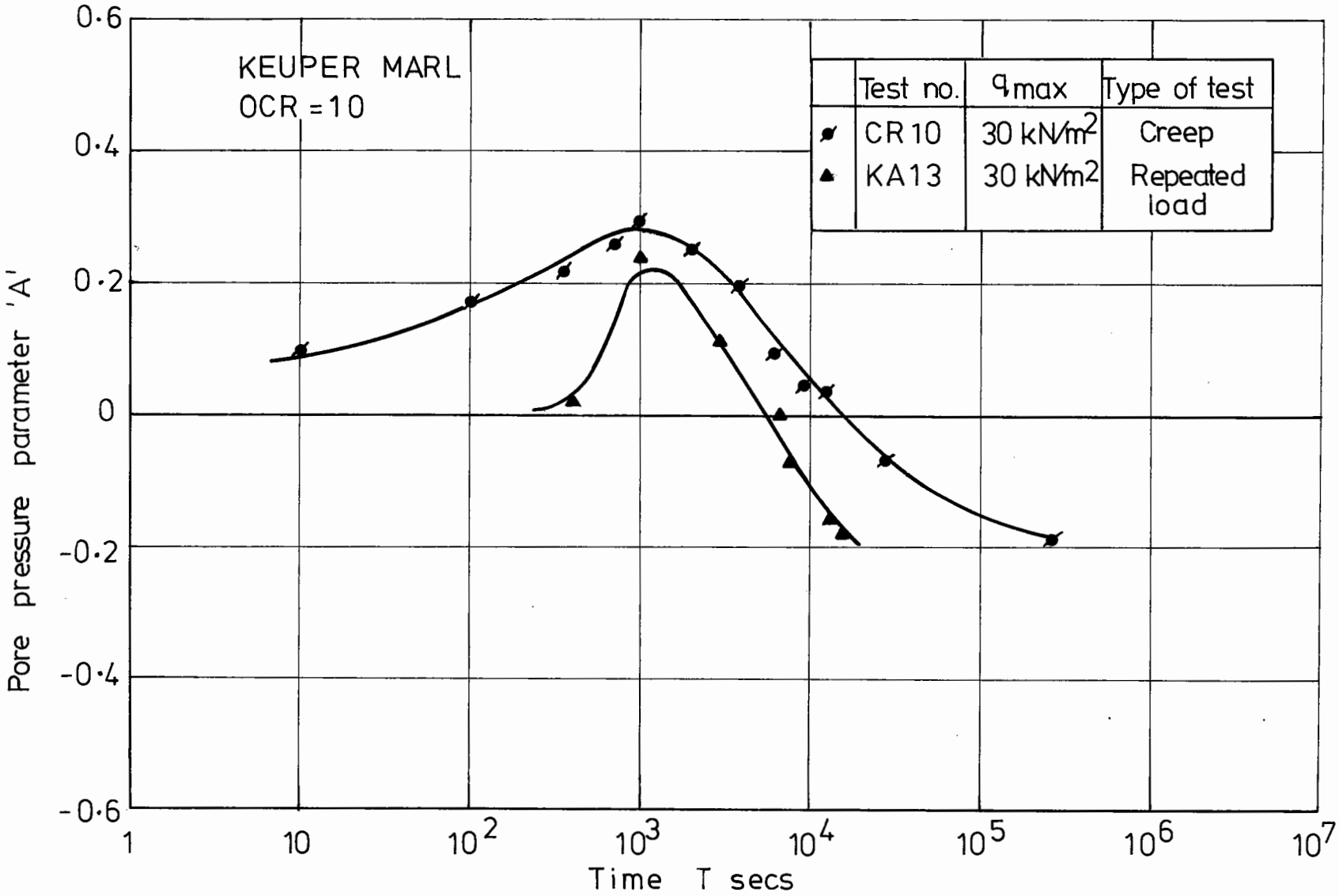

Fig. 6.13 Variation of pore water pressure parameter 'A' under creep and repeated load conditions.

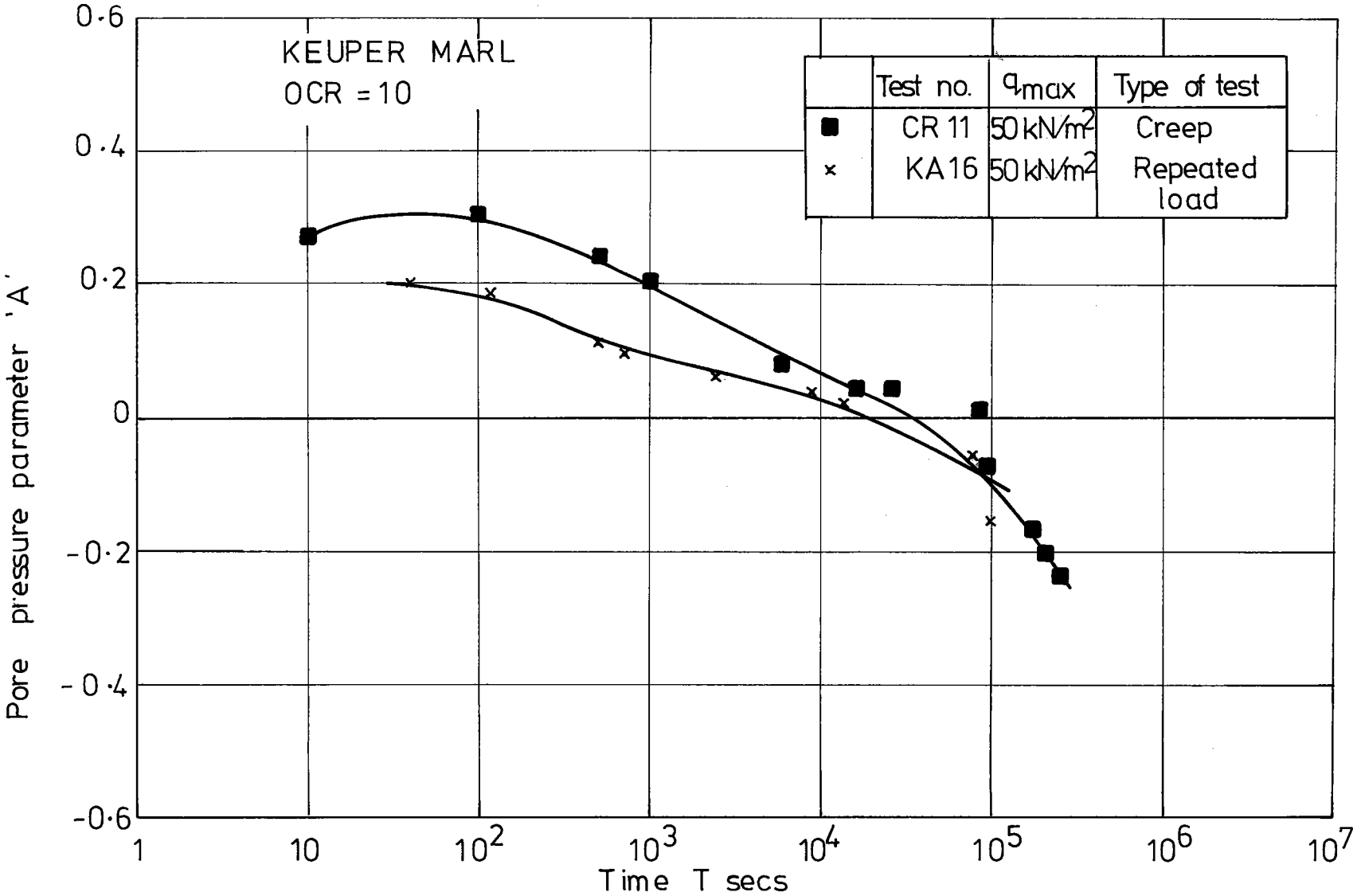

Fig. 6.14 Variation of pore water pressure parameter 'A' under creep and repeated load conditions.

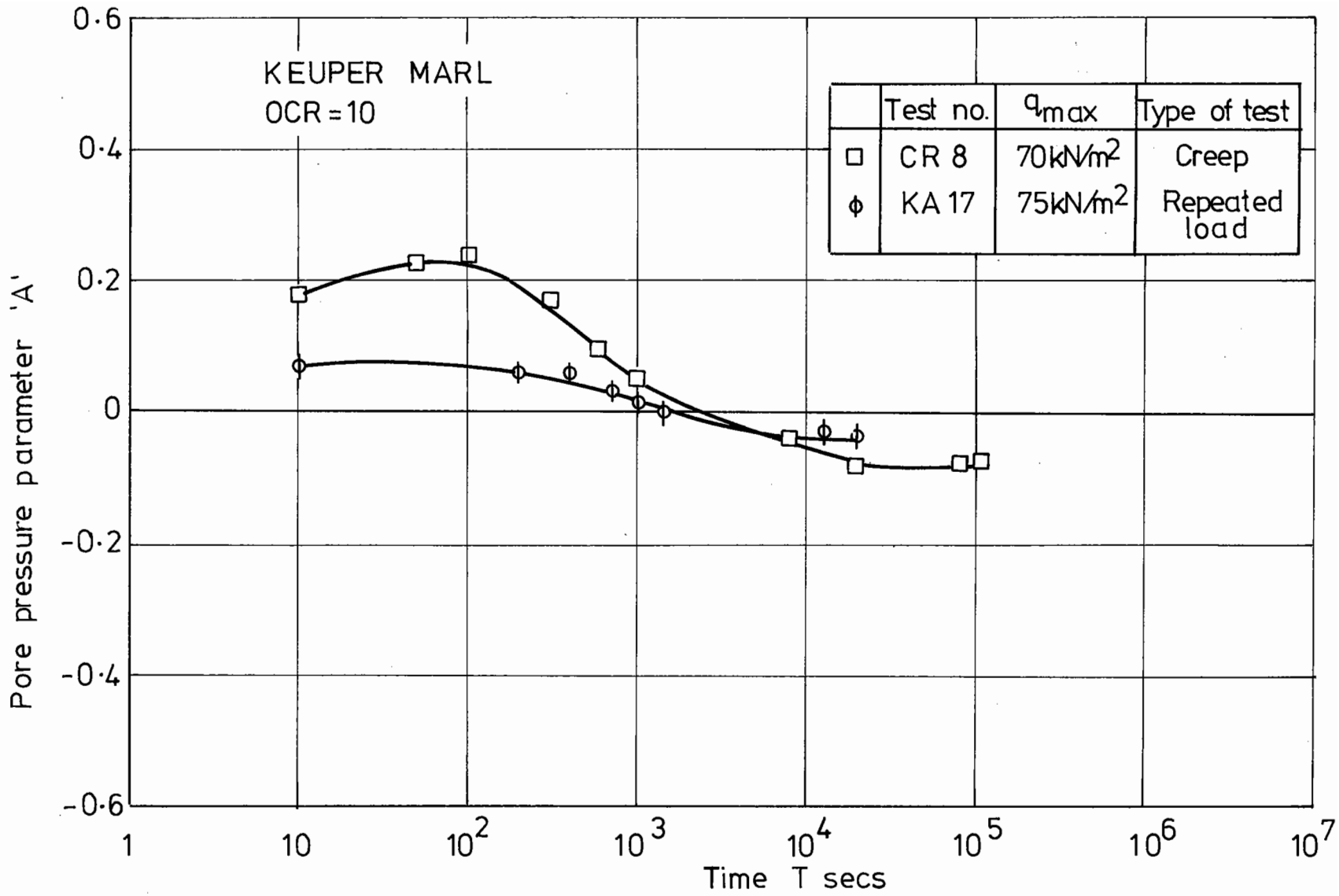

Fig. 6.15 Variation of pore water pressure parameter 'A' under creep and repeated load conditions.

6.5.2 Accumulation of Plastic Strain

Figs. 6.16 to 6.22 show the variation of plastic strain with the number of cycles for different stress levels and stress histories. A series of creep tests was carried out on samples with the same stress histories as the KA and KH repeated load tests (i.e. initial effective $\sigma_3' = 40$ kN/m^2). The variation of the plastic strain with time for these tests is shown in Figs. 6.23 to 6.26. The accumulated strain under creep stresses is, as would be expected, similar to that under repeated stresses.

A simple empirical relationship between the strain accumulated under creep and that accumulated under repeated loading was examined. Figs. 6.27 to 6.29 show the plastic strain after 5000 seconds at non-failure stresses for creep and repeated load tests. After this length of time the strain accumulated under repeated load is approximately half the value accumulated under a creep load. If the permanent strain after 5000 seconds is plotted against the bounded integral of the stress-time plot from 0 to 5000 seconds, then both types of test fall on the same line with some scatter, Fig. 6.30.

It is not possible, however, to extrapolate this relationship for times greatly in excess of that considered. Since, for most engineering purposes, it is necessary to be able to predict the plastic deformation accumulated over several decades of time, a more detailed analysis is clearly required.

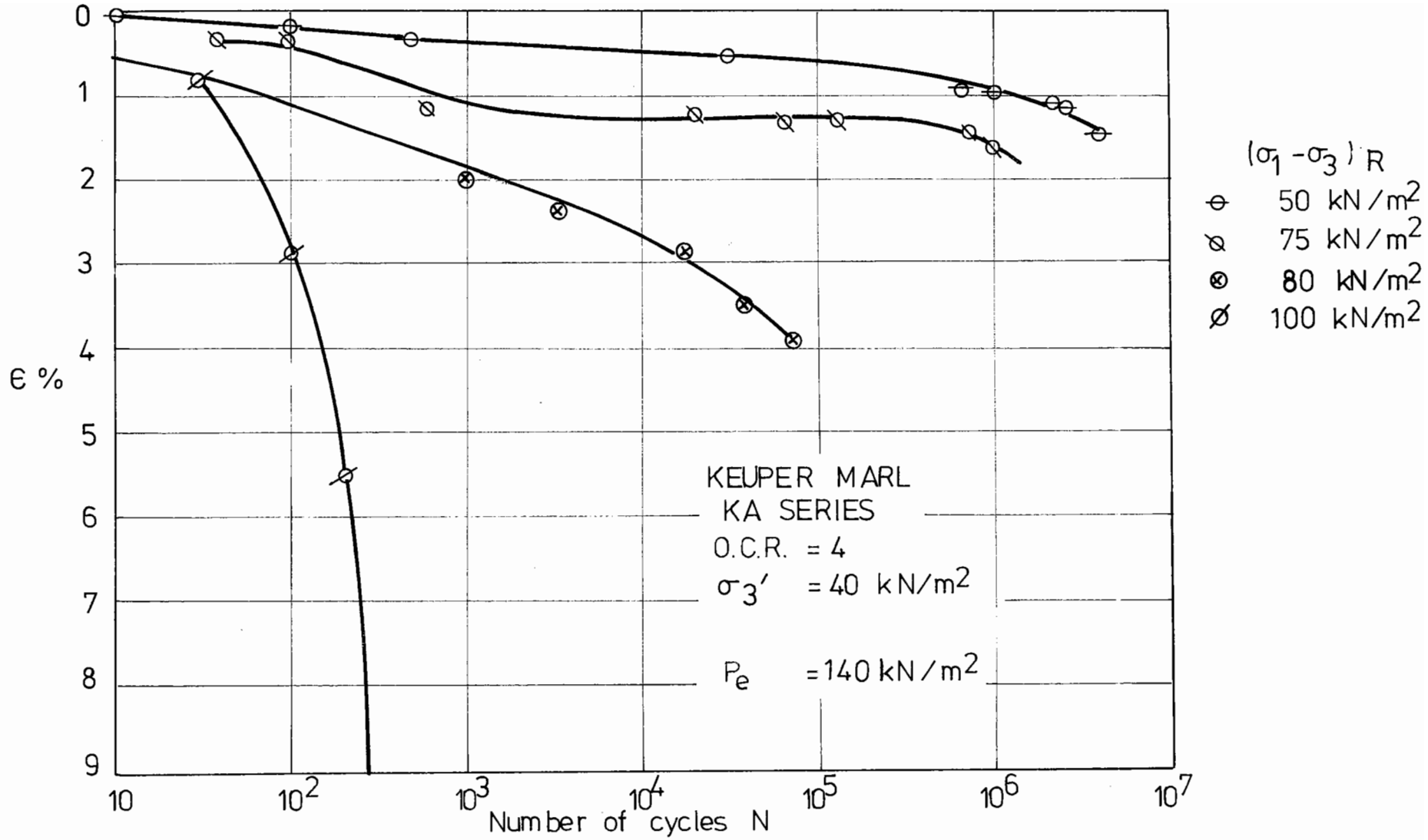

FIG.6.16 Variation of irrecoverable strain with number of cycles for different stress levels

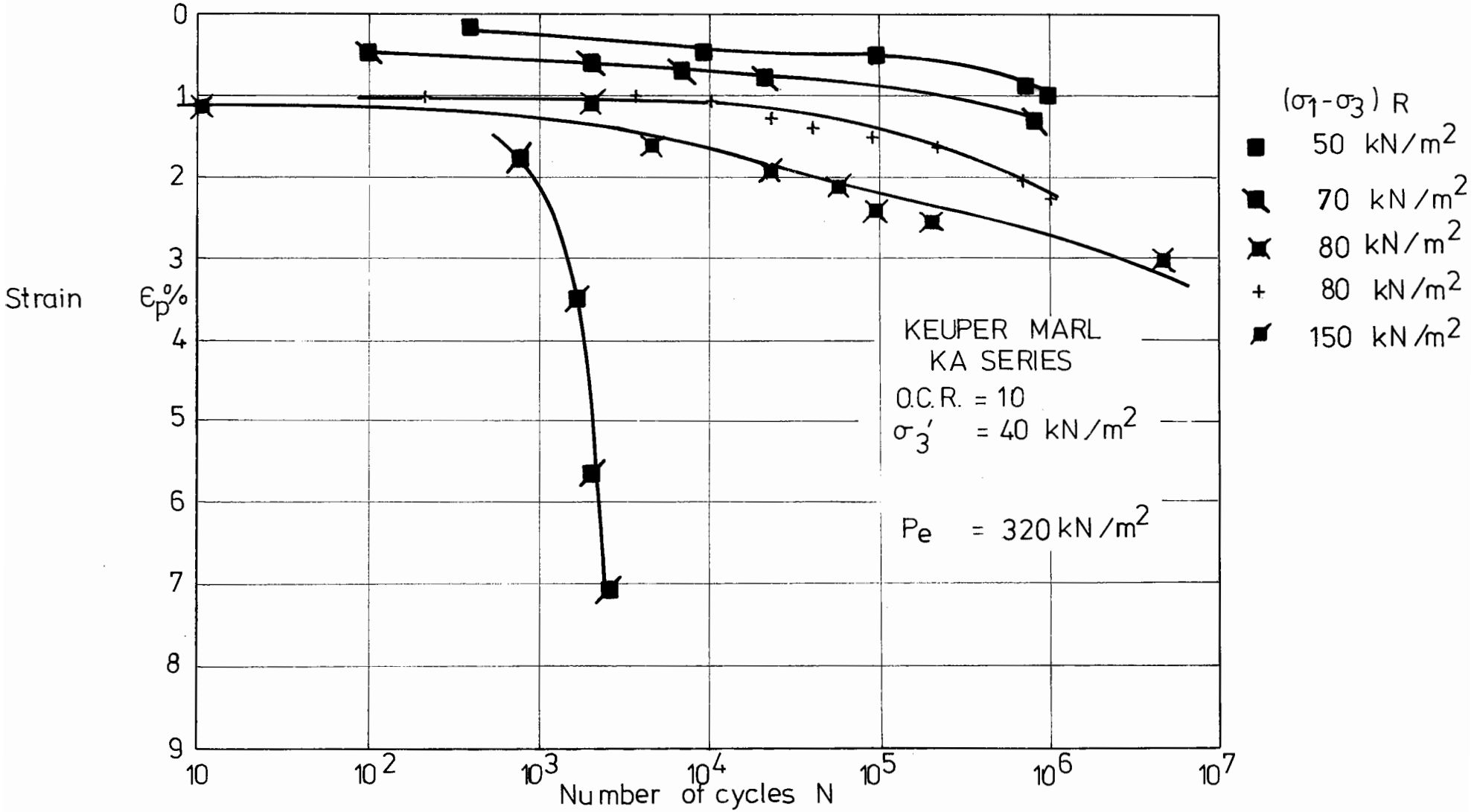

FIG. 6.17 Variation of irrecoverable strain with number of cycles for different stress levels

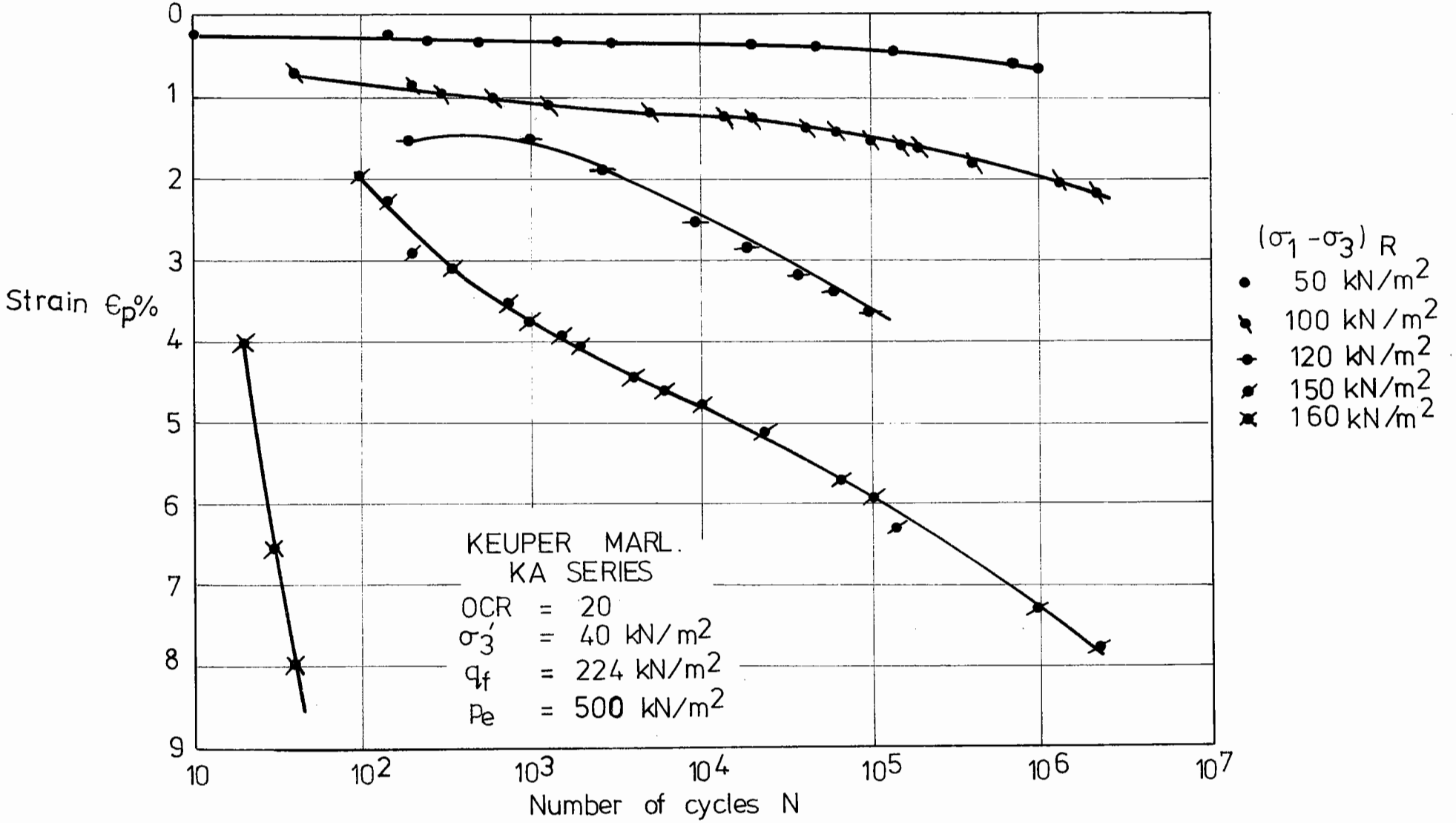

Fig. 6.18 Variation of irrecoverable strain with number of cycles for different stress levels.

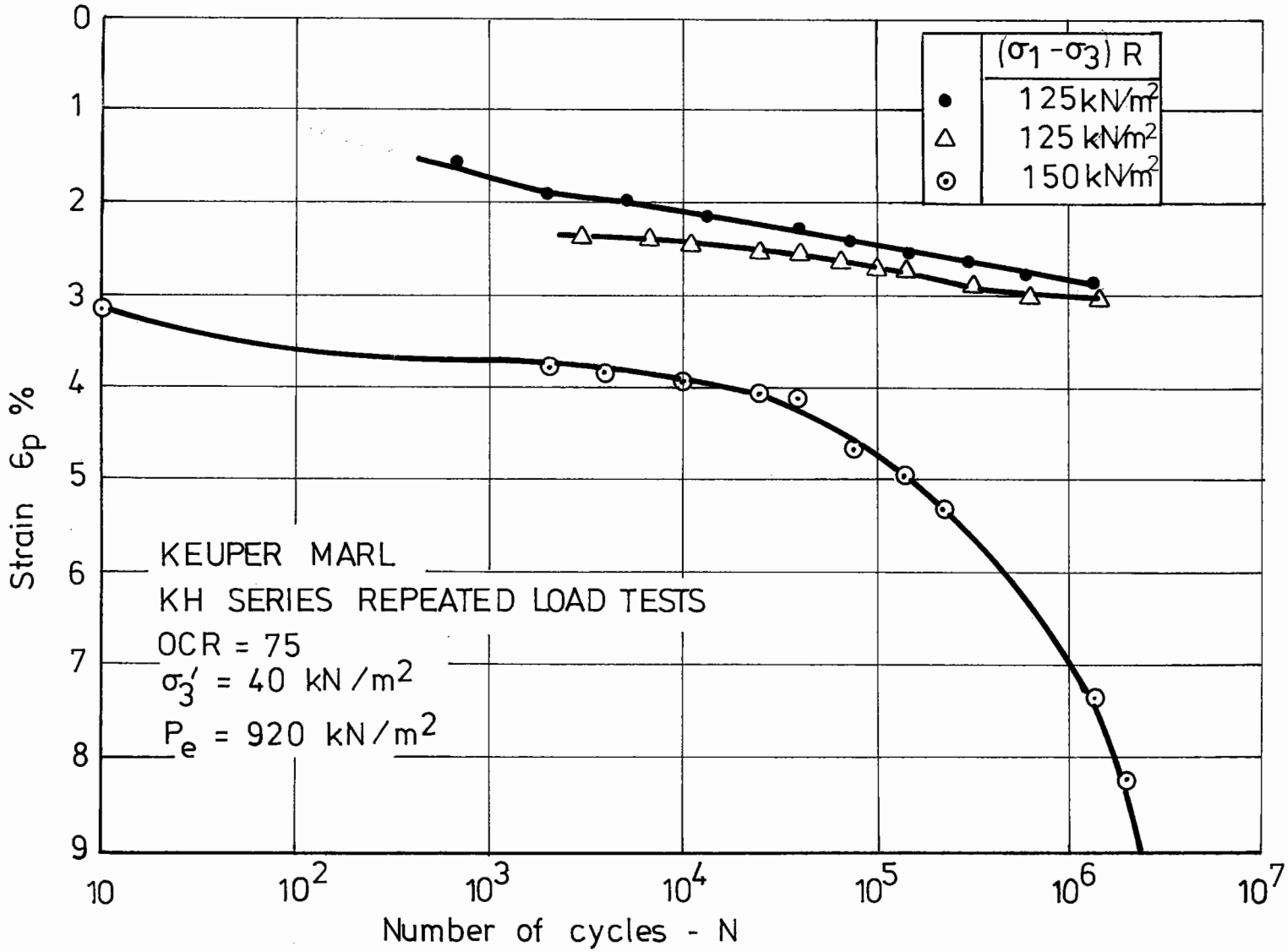

Fig. 6.19 Variation of irrecoverable strain with number of cycles for different stress levels.

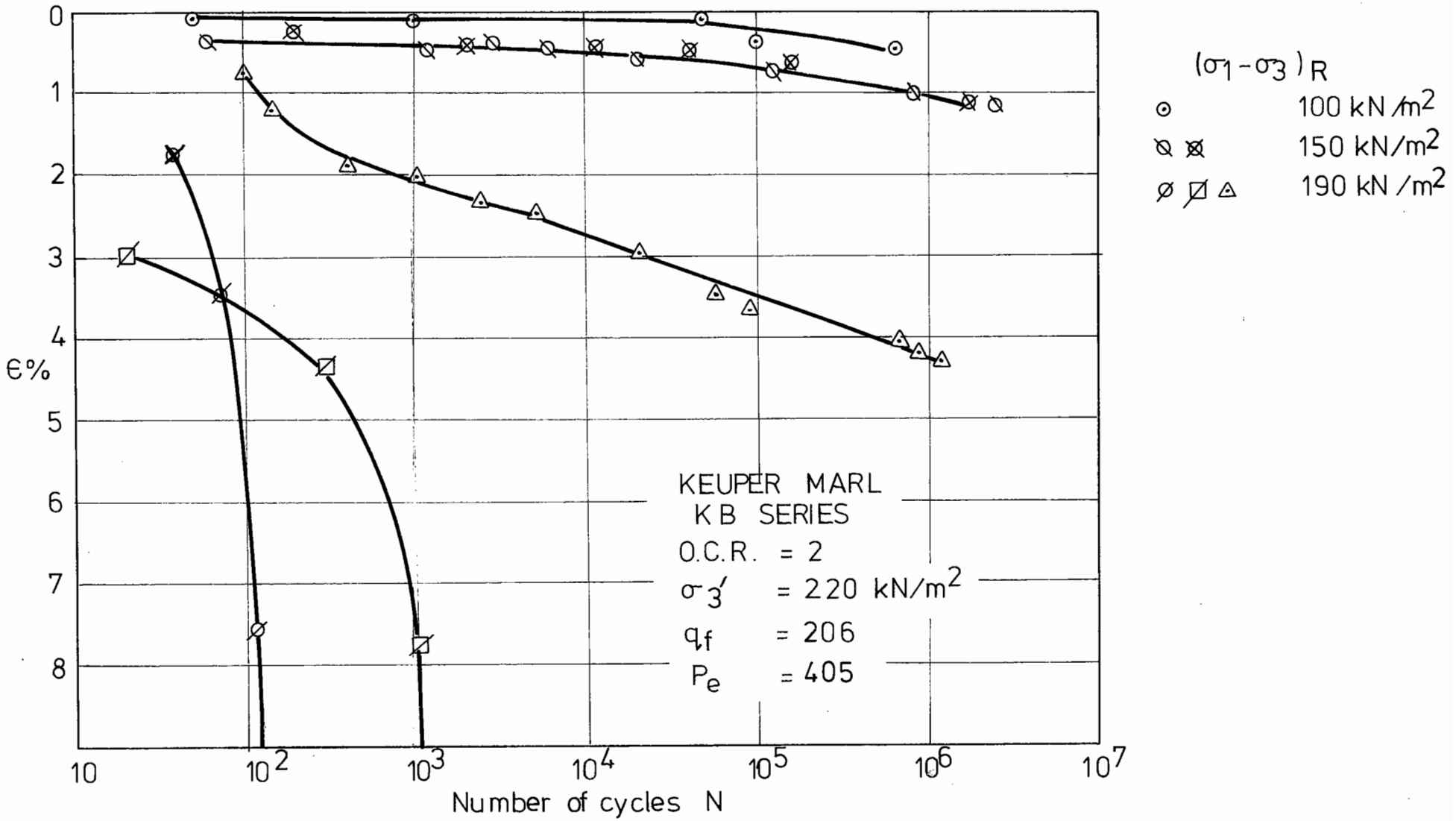

FIG 6.20 Variation of irrecoverable strain with number of cycles for different stress levels

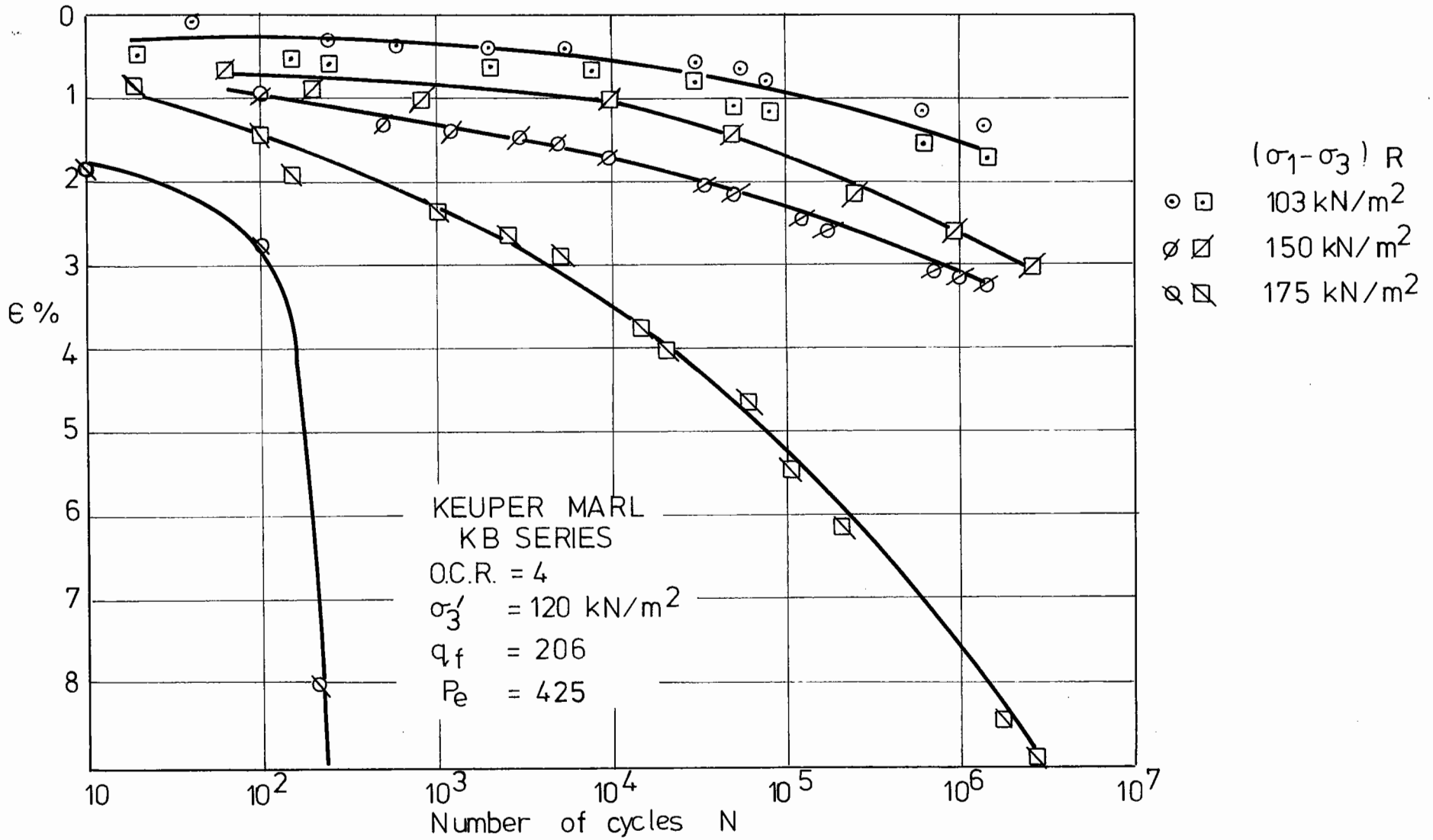

FIG. 6.21 Variation of irrecoverable strain with number of cycles for different stress levels

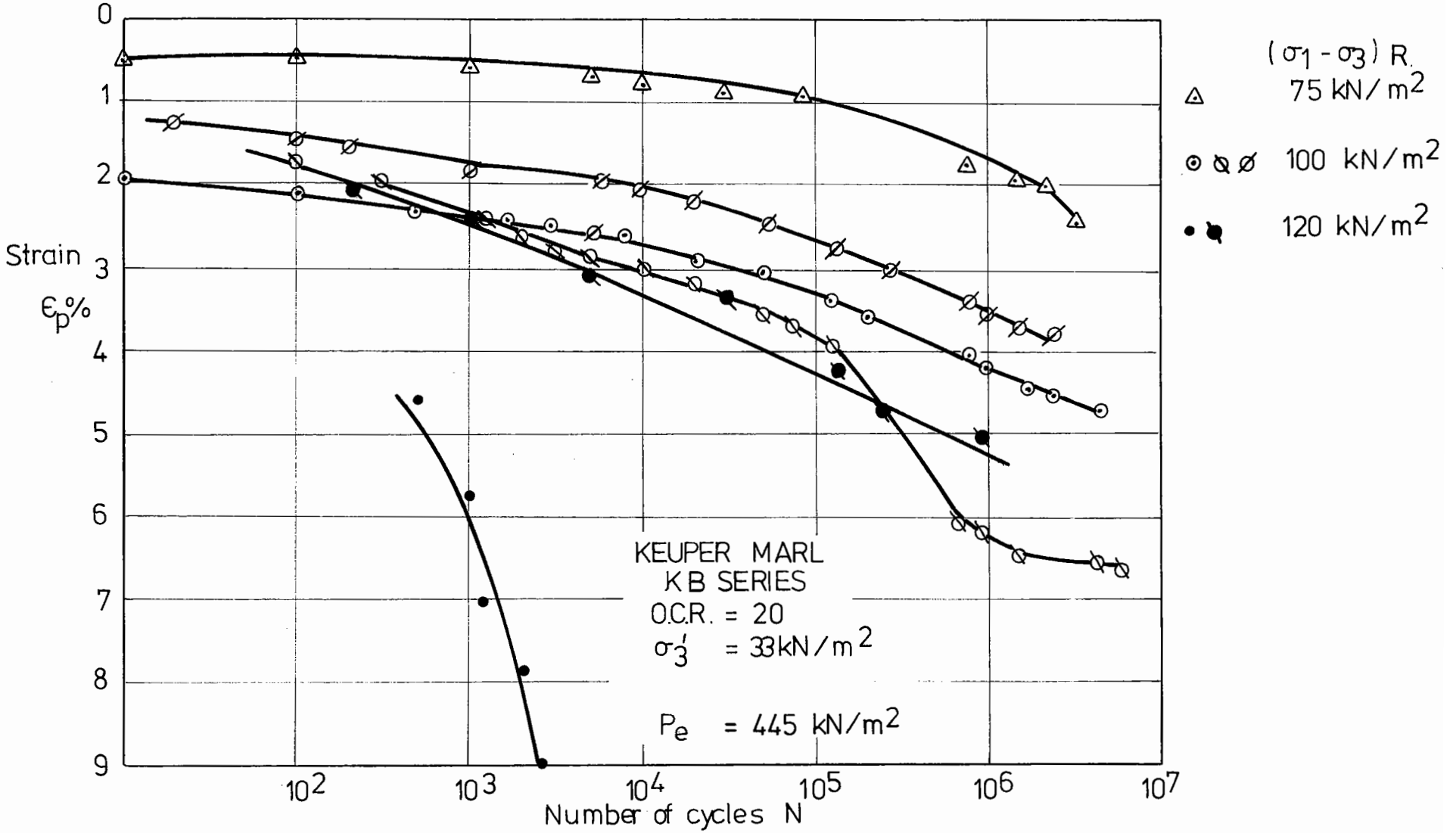

FIG. 6.22 Variation of irrecoverable strain with number of cycles for different stress levels

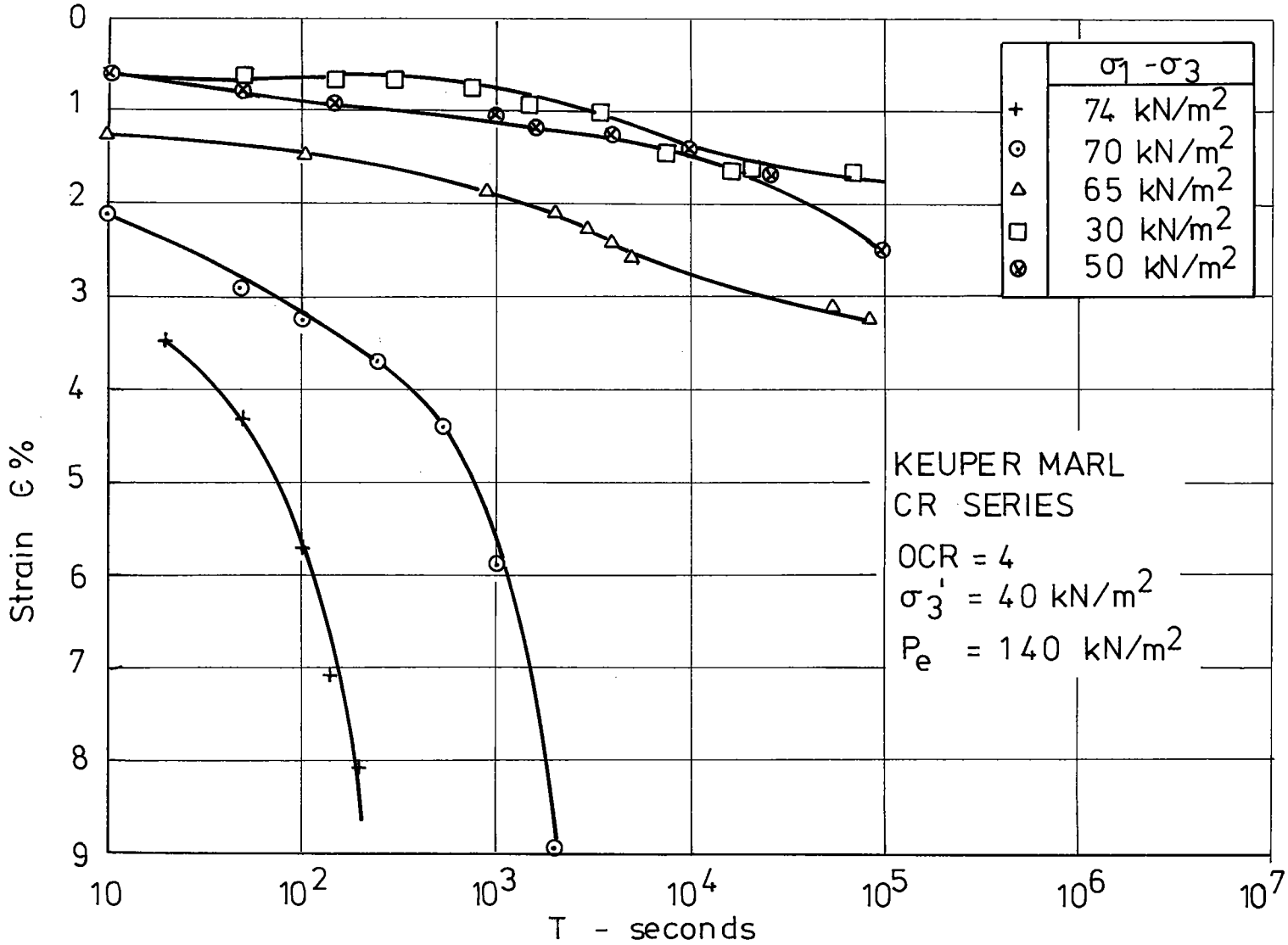

Fig. 6.23 Variation of irrecoverable strain with time under creep stress conditions

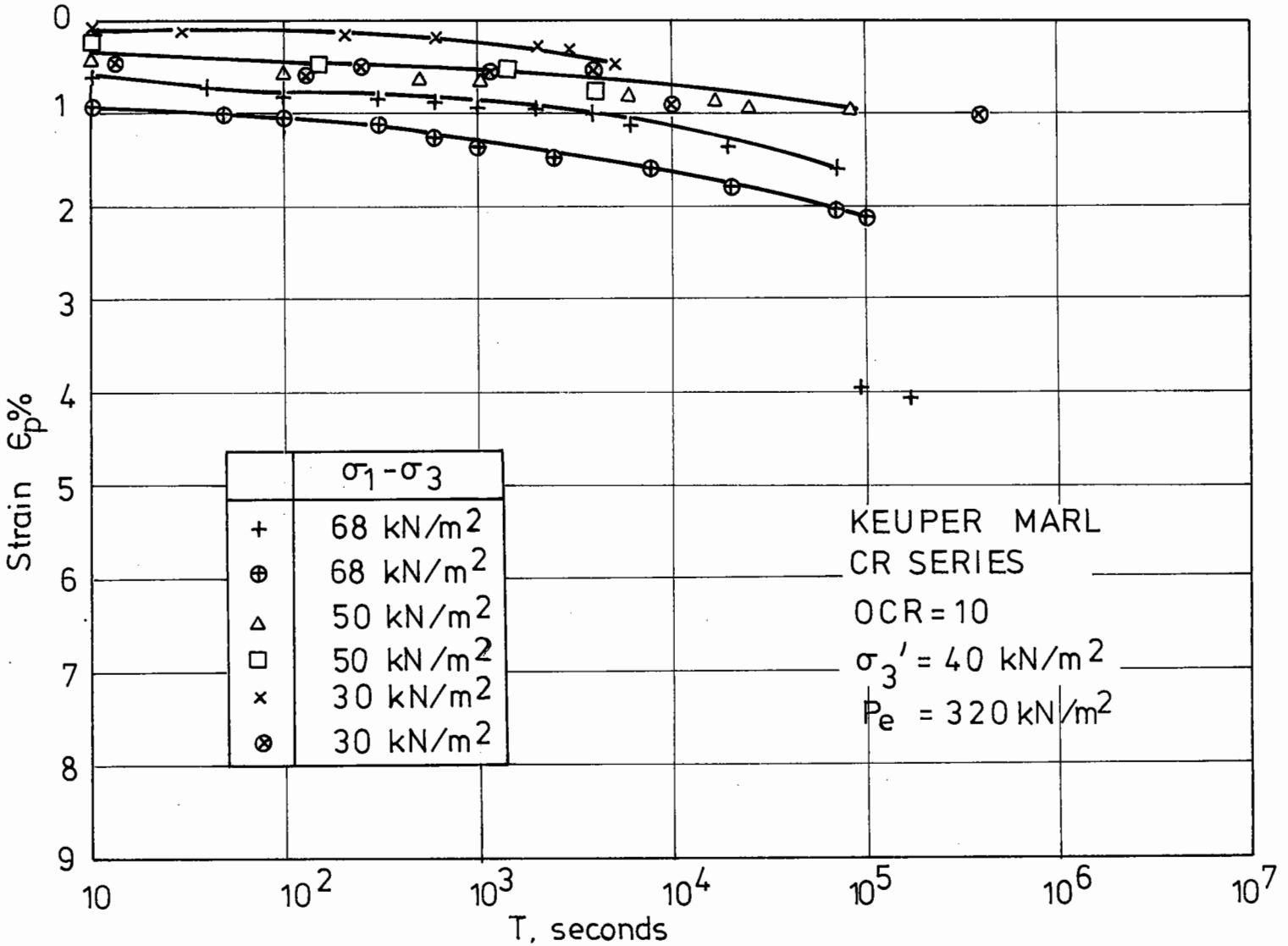

Fig. 6.24 Variation of irrecoverable strain with time under creep stress conditions.

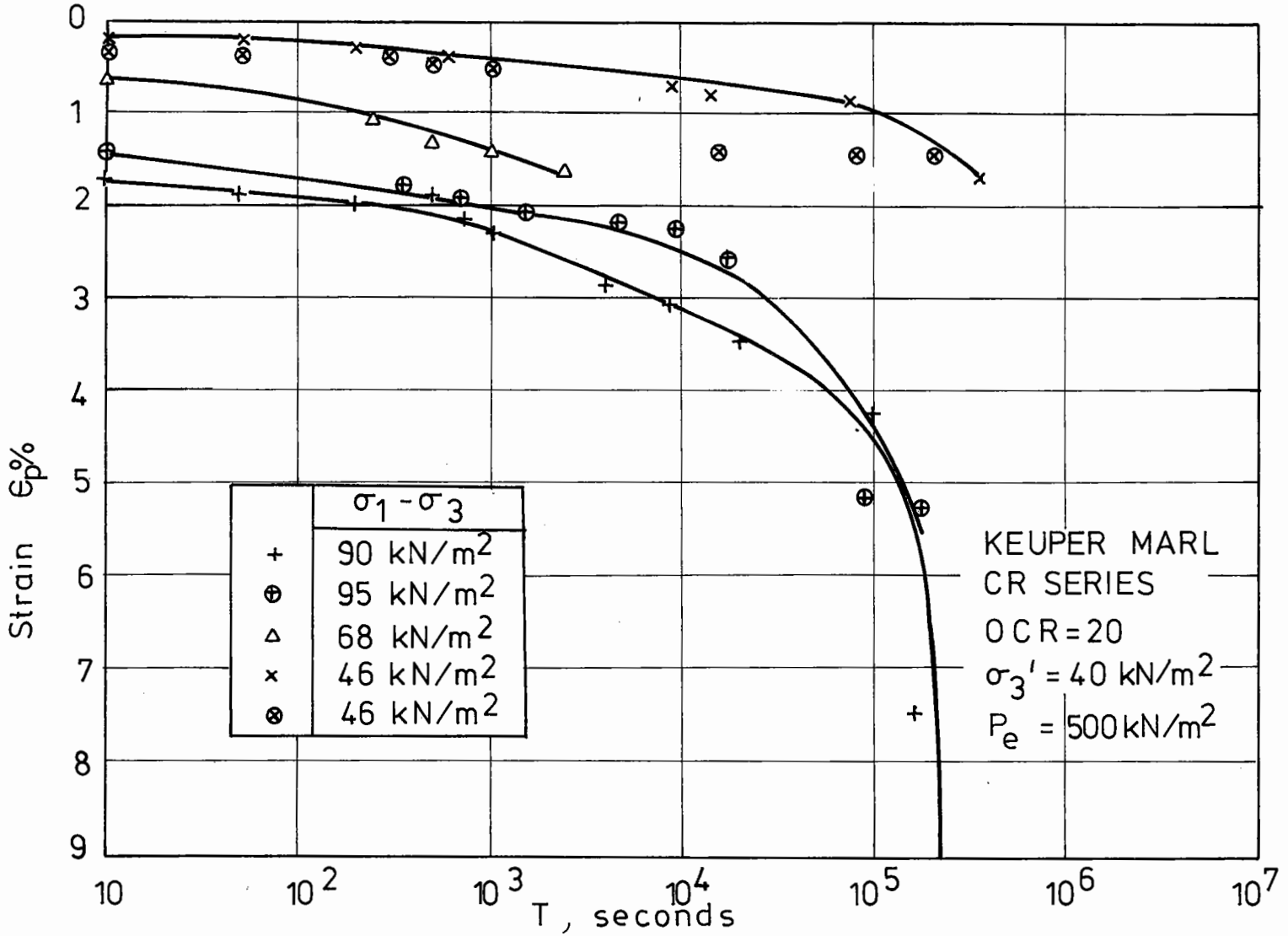

Fig. 6.25 Variation of irrecoverable strain with time under creep stress conditions.

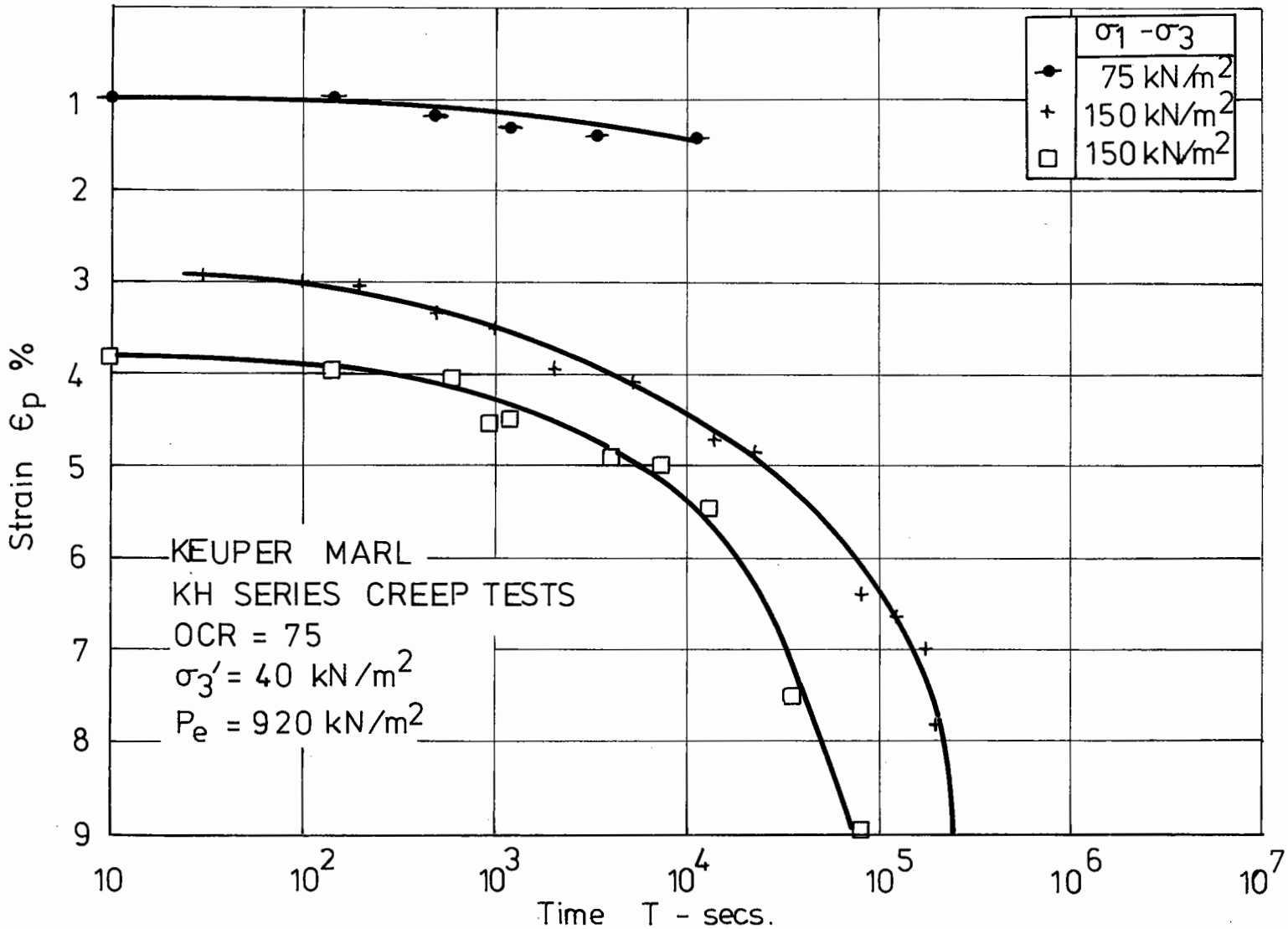

Fig. 6.26 Variation of irrecoverable strain with time under creep stress conditions.

KEUPER MARL
CR SERIES

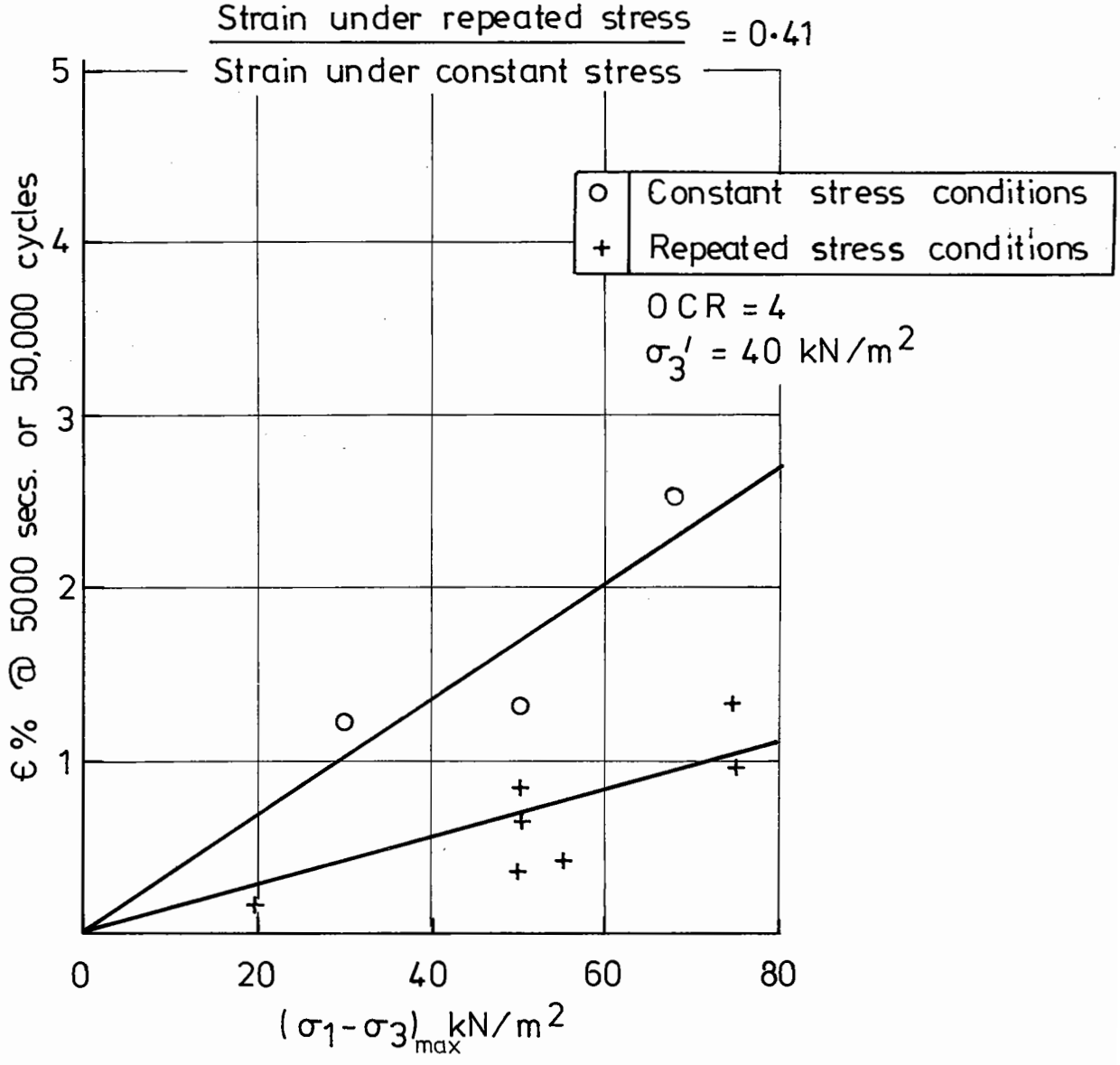

Fig. 6.27 Comparison of irrecoverable strain under repeated stress and creep stress conditions.

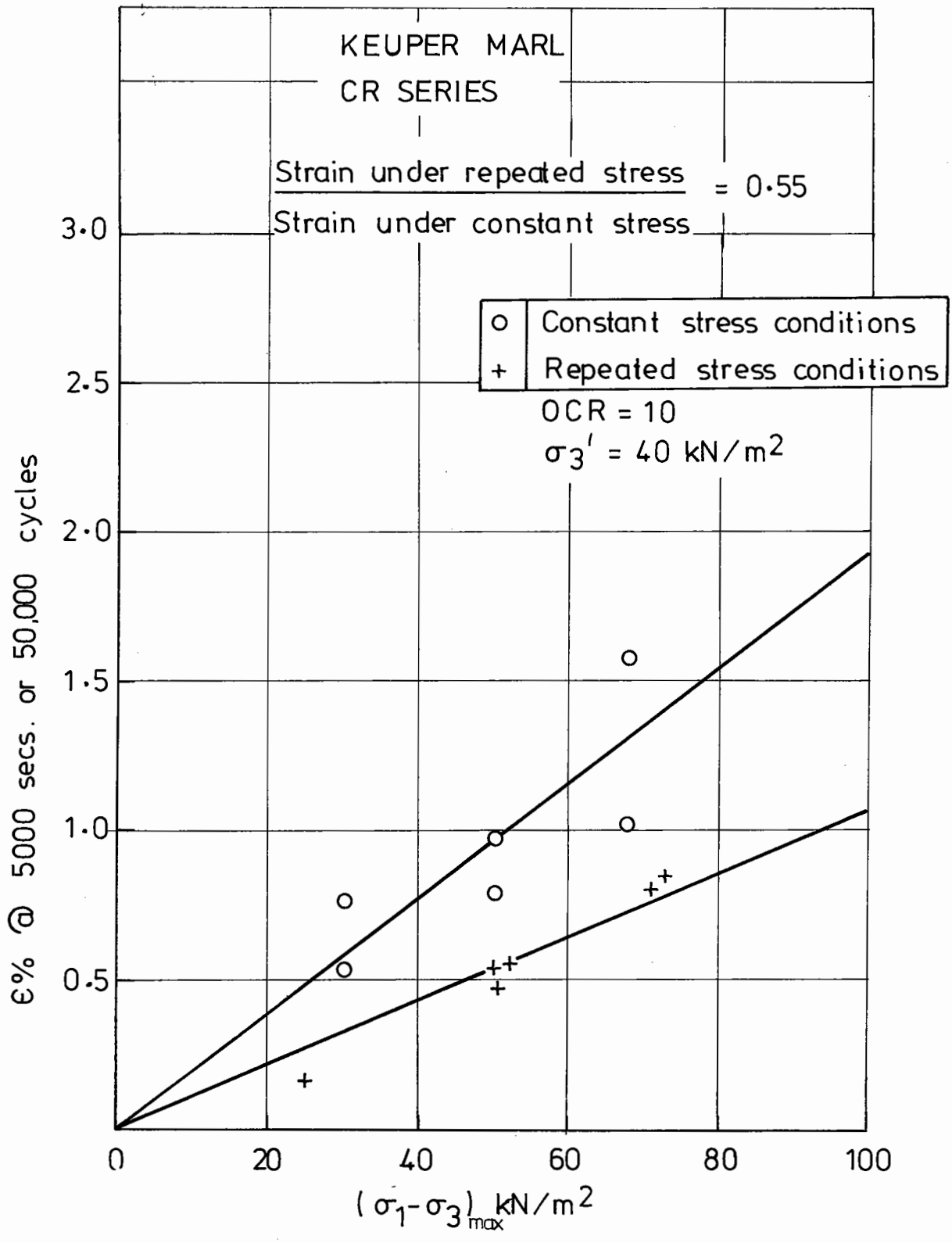

Fig. 6.28 Comparison of irrecoverable strain under repeated stress and creep stress conditions.

KEUPER MARL
CR SERIES

$$\frac{\text{Strain under repeated stress}}{\text{Strain under constant stress}} = 0{\cdot}52$$

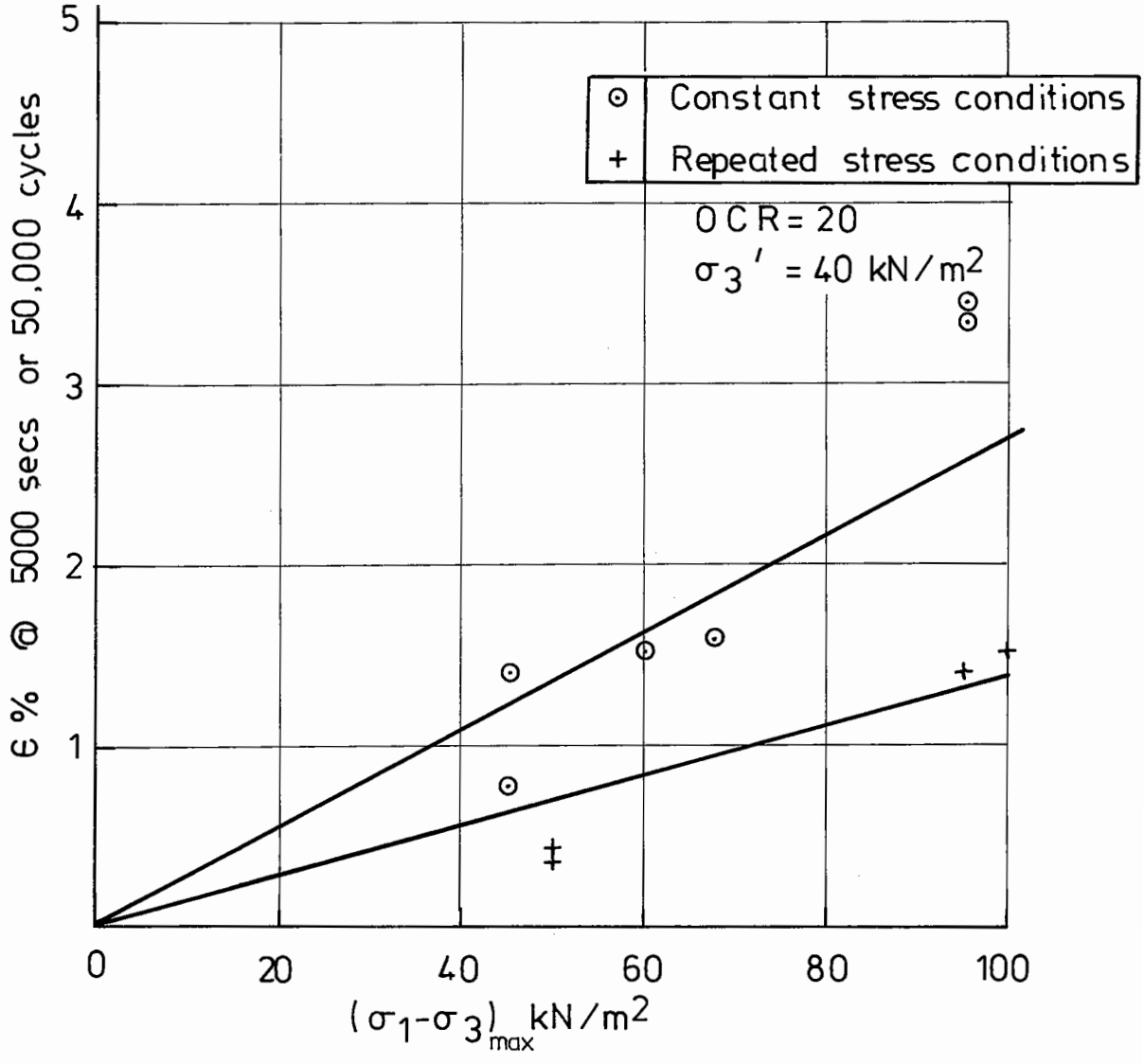

Fig. 6.29 Comparison of irrecoverable strain under repeated stress and creep stress conditions.

KEUPER MARL
CR SERIES

	OCR	Type of loading
o	4	Constant stress (creep)
+	4	Repeated stress
⊘	10	Constant stress (creep)
×	10	Repeated stress
⌀	20	Constant stress (creep)
•	20	Repeated stress

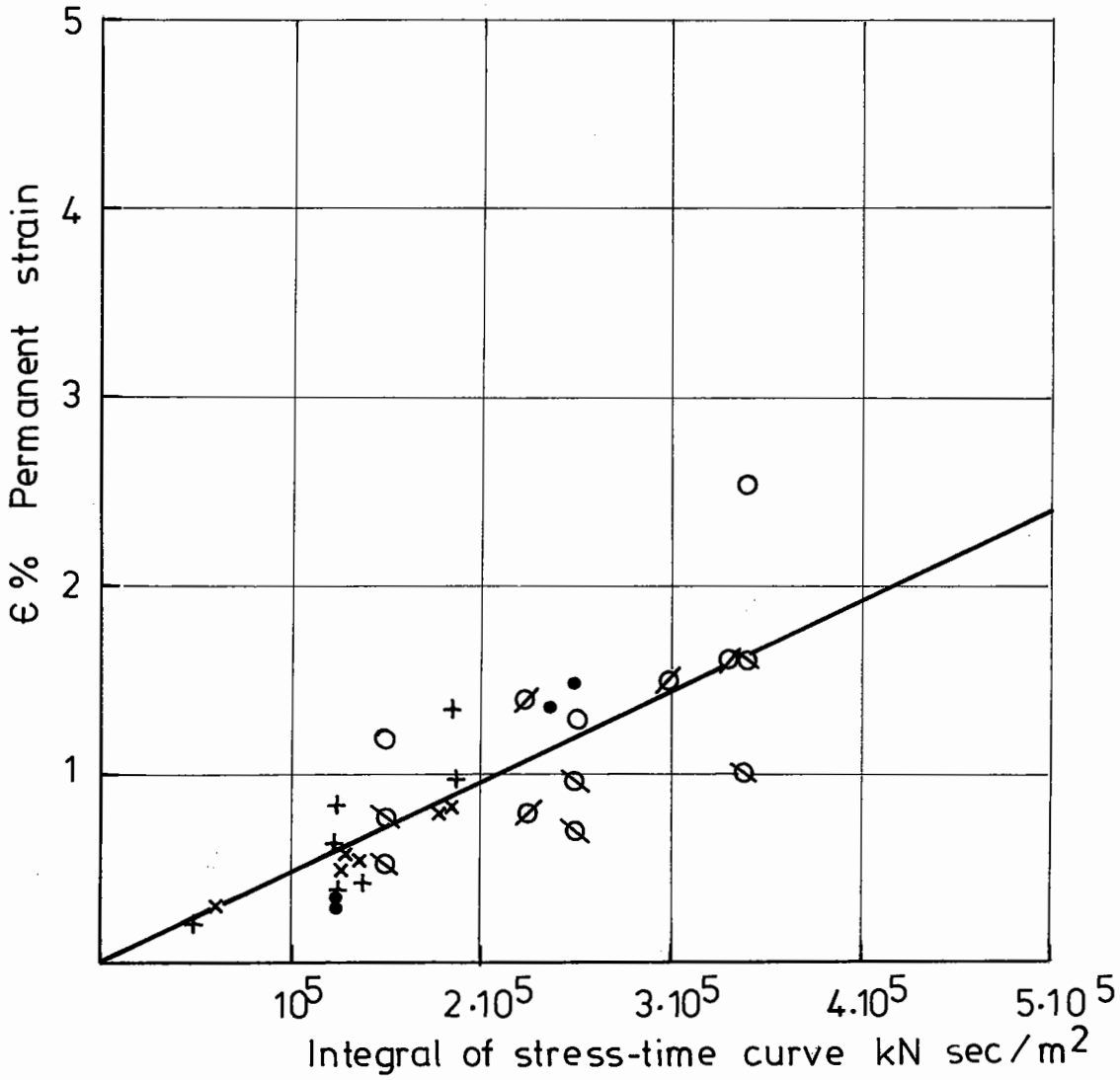

Fig.6.30 Variation of irrecoverable strain with area under stress / time curve.

lines is plotted in Fig. 6.46 for both creep and repeated loading. Only points in the area of engineering interest have been shown. This area is where sub-failure stresses can cause the accumulation of considerable plastic strain over a period of time. If the applied stresses are greater than those in this zone, then creep rupture occurs, if they are less, then the strain rates rapidly decrease to negligible proportions. Extension of the relationship at each end of the range considered would, therefore, result in an "S" shaped curve (Section 2.4.3, Fig. 2.8). Feda et al (1973) found that this curve could be approximated by a Gauss-Laplace error function. The analysis in later sections, however, will only consider those points lying on the straight line portion of this curve. Examination of Fig. 6.46 shows that the points plotted for repeated load tests lie below those plotted for creep tests.

Tests carried out on lightly over-consolidated samples (wet side) can be analysed in a similar manner; however, it is found that the slope of the log strain rate versus log time plot has a mean value of -0.87 (as opposed to -1 for the dry side). These lines are plotted in Figs. 6.47 to 6.50.

6.5.4 Relationship between Creep and Repeated Loading

If it is postulated that sine wave loading can be represented by an infinite number of creep stress increments, then, by using an approximate numerical summation, it should be possible to relate the strain rate under creep to that under repeated loading.

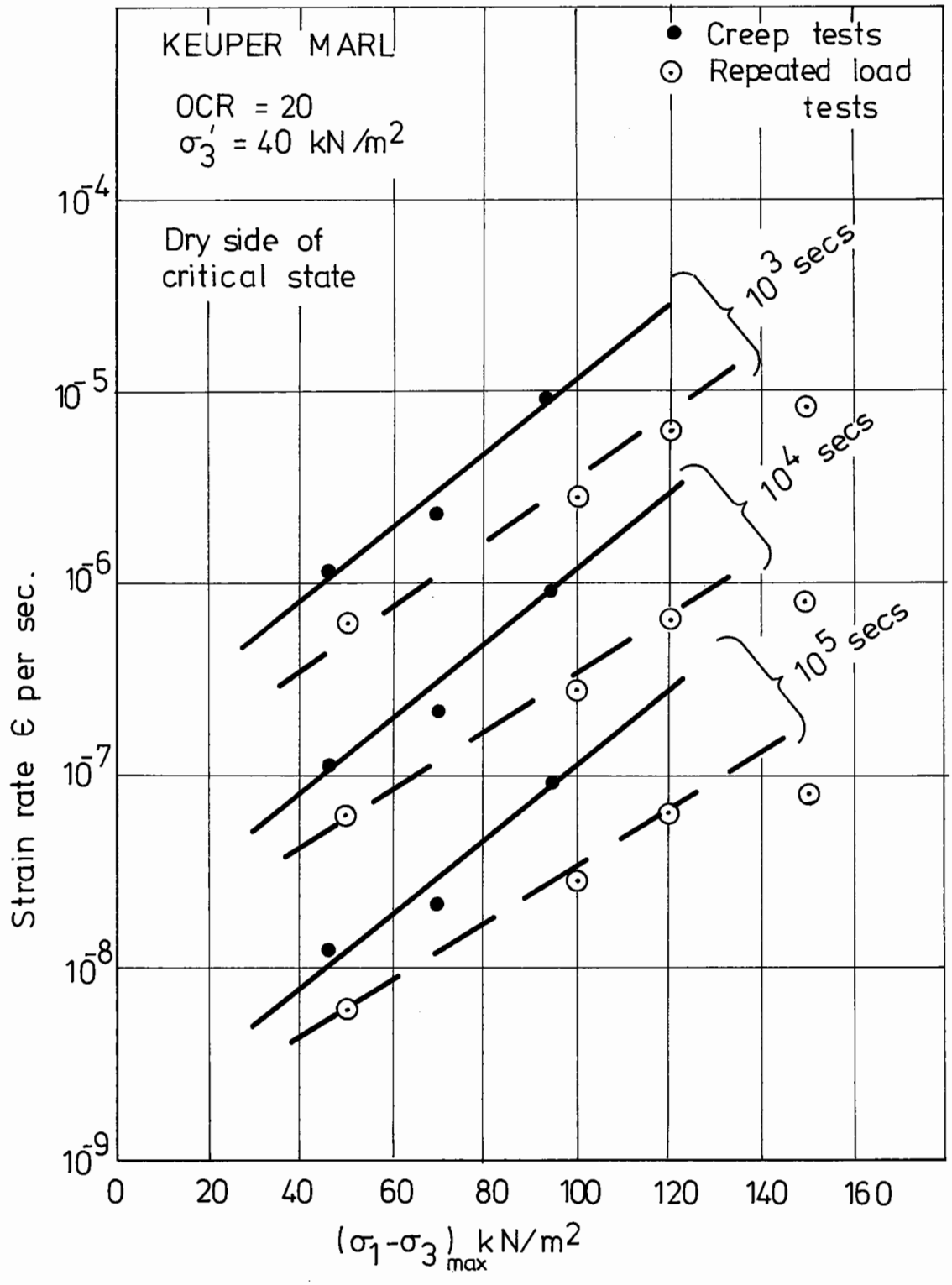

Fig. 6.46 Variation of strain rate with applied stress and time.

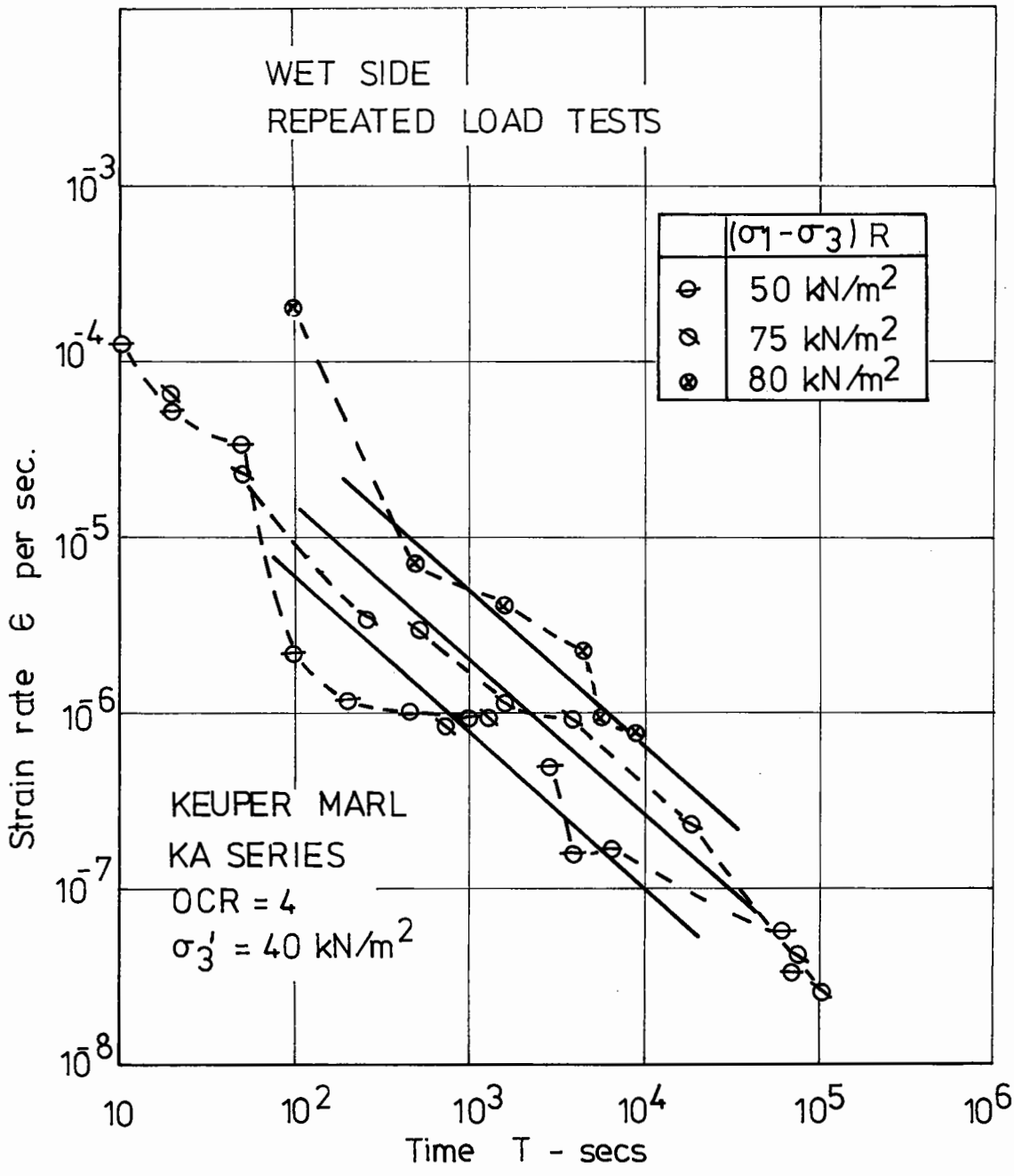

Fig. 6.47 Variation of strain rate with time.

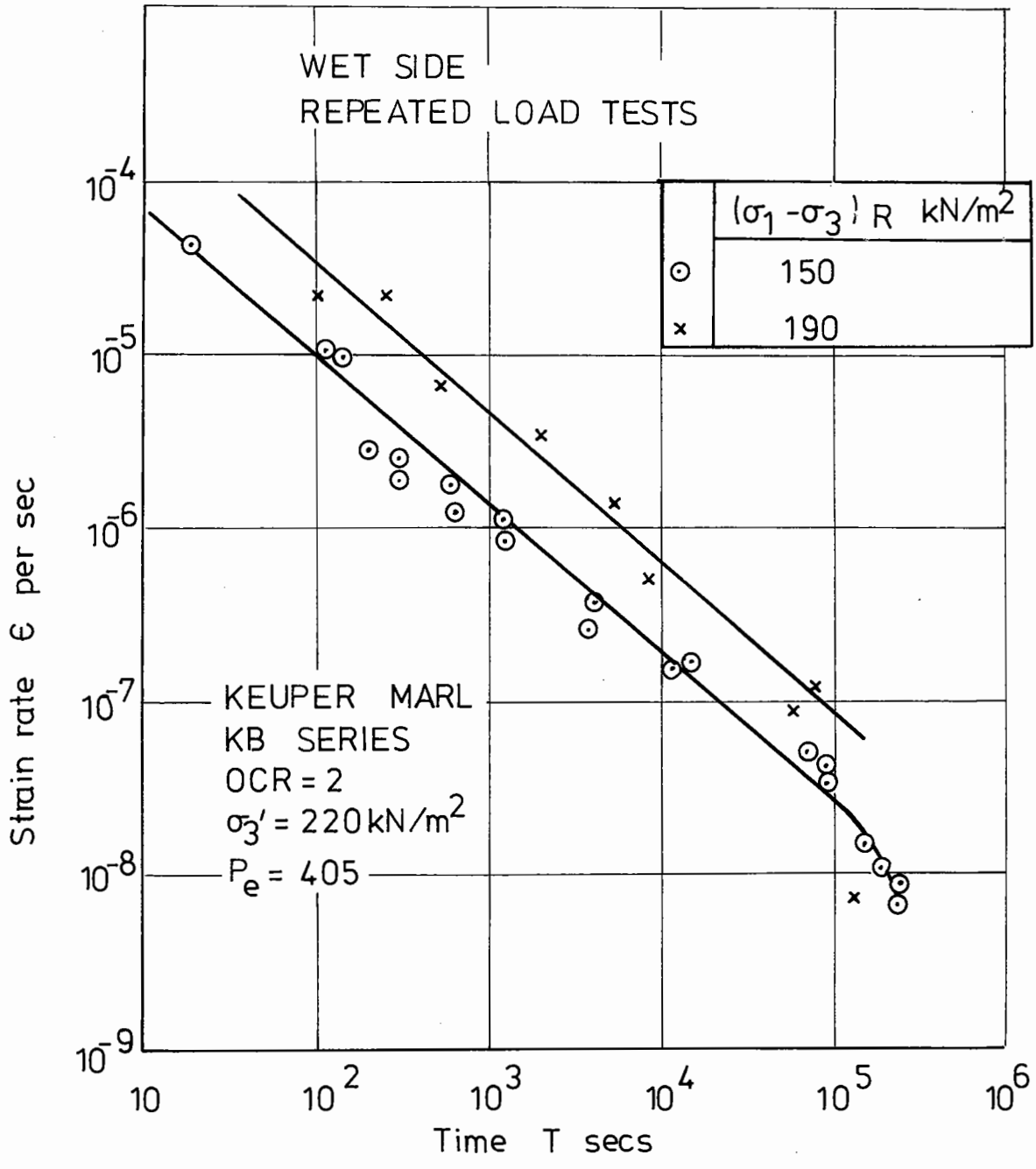

Fig. 6.48 Variation of strain rate with time

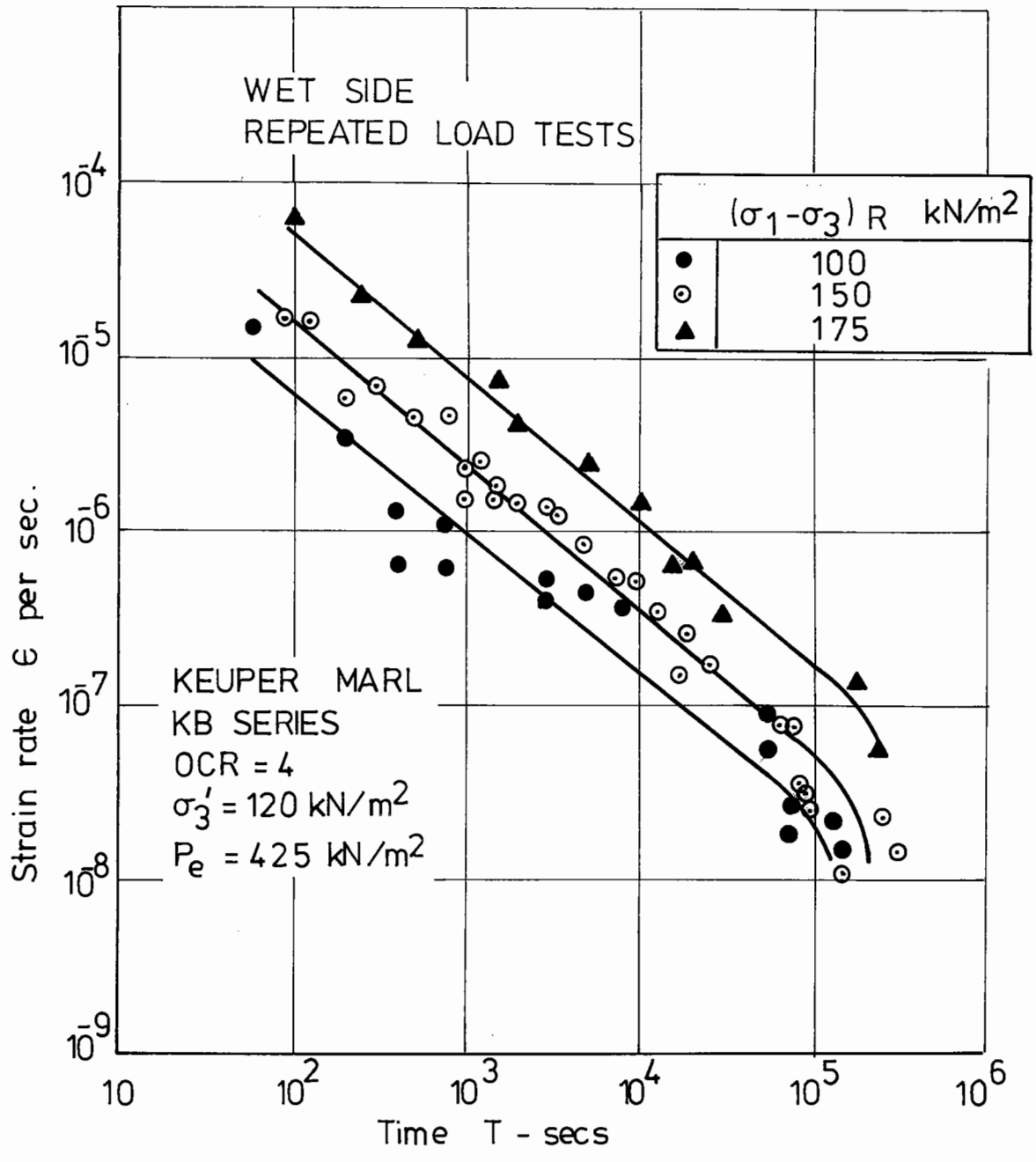

Fig. 6.49 Variation of strain rate with time.

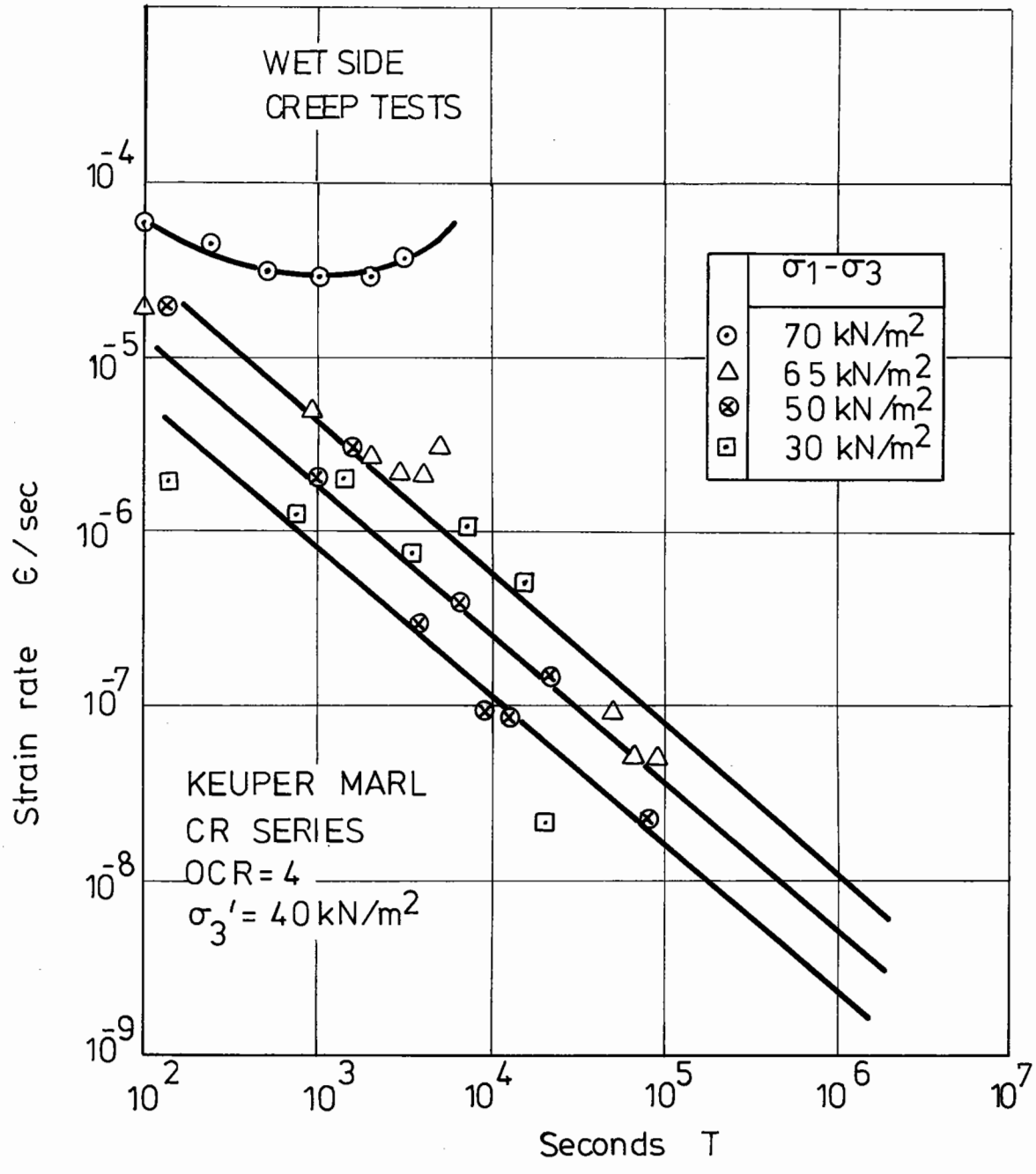

Fig. 6.50 Variation of strain rate with time.

Fig. 6.51 shows an approximate sine function represented by ten straight line sections. The mean proportion of the total stress mobilised for each section is indicated in the figure.

Figs. 6.52 to 6.54 show the relationship between the creep strain rate after 10^3 secs and the applied deviator stress for different OCR's. It is assumed that after, for example, 10^3 seconds, the strain rate during a cycle of repeated loading will vary continuously from zero to that value of creep strain rate appropriate to the maximum applied deviator stress. By averaging the creep strain rates for the ten stress increments shown in Fig. 6.51, for different maximum deviator stresses the lines shown in Figs. 6.52 to 6.54 for repeated loading were drawn (see Table 6.1). The experimental points plotted for repeated load tests show some measure of agreement with the derived lines. It is evident from this that behaviour under repeated loading can be considered as an extension of the static creep phenomenon.

6.5.5 Prediction of Accumulated Strain under Repeated Loading from Creep Data

The relationship between strain rate and time shown in Figs. 6.38 to 6.44 and 6.47 to 6.50, can be expressed in the following form:

$$\log \dot{\epsilon} = \alpha - \lambda \log T \qquad (6.1)$$

where $\dot{\epsilon}$ = strain rate, ϵ per second

T = time - seconds

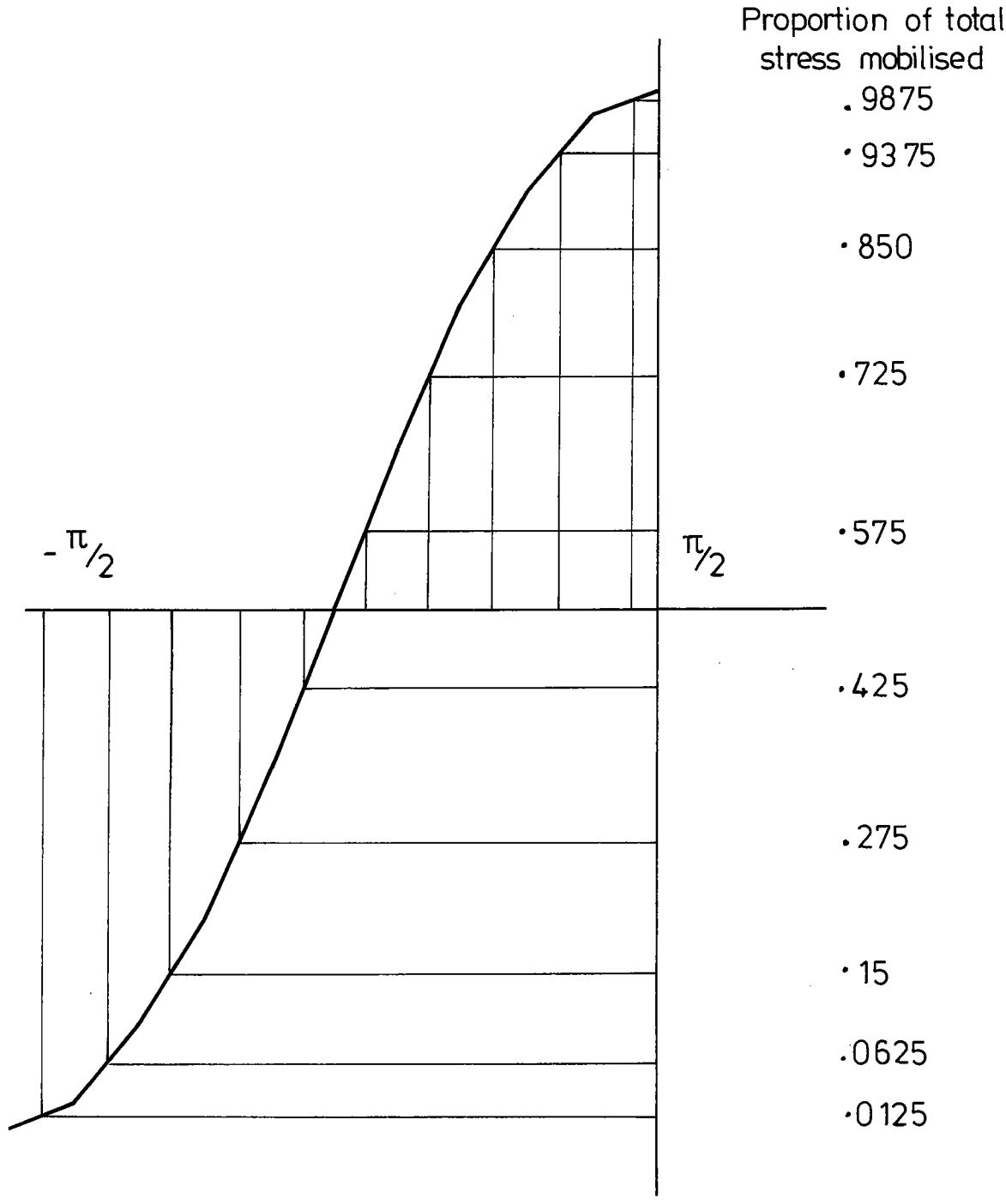

Fig. 6.51 Approximate variation of stress with time under sinusoidal load application.

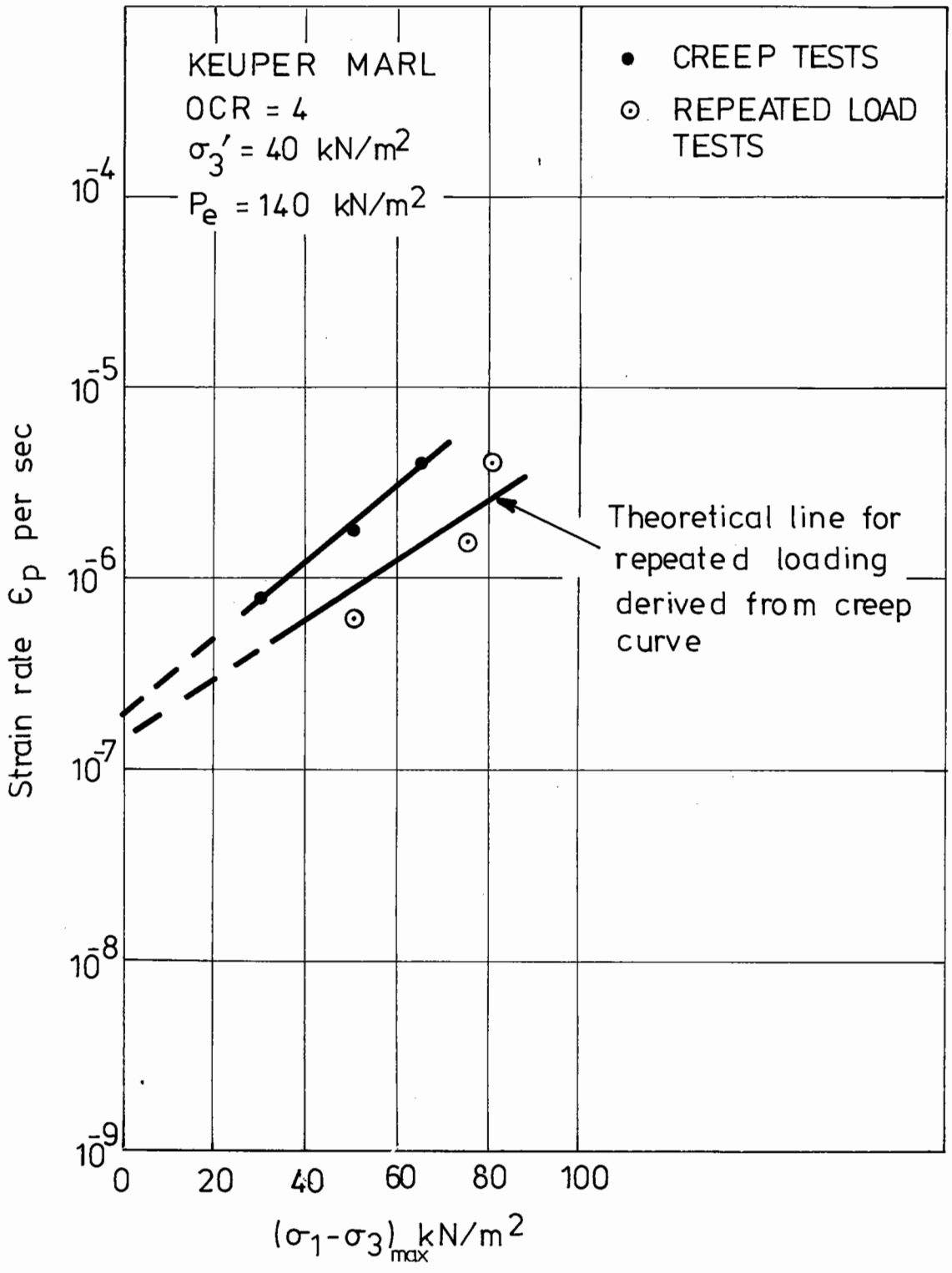

Fig. 6.52 Variation of strain rate with deviator stress after 10^3 seconds

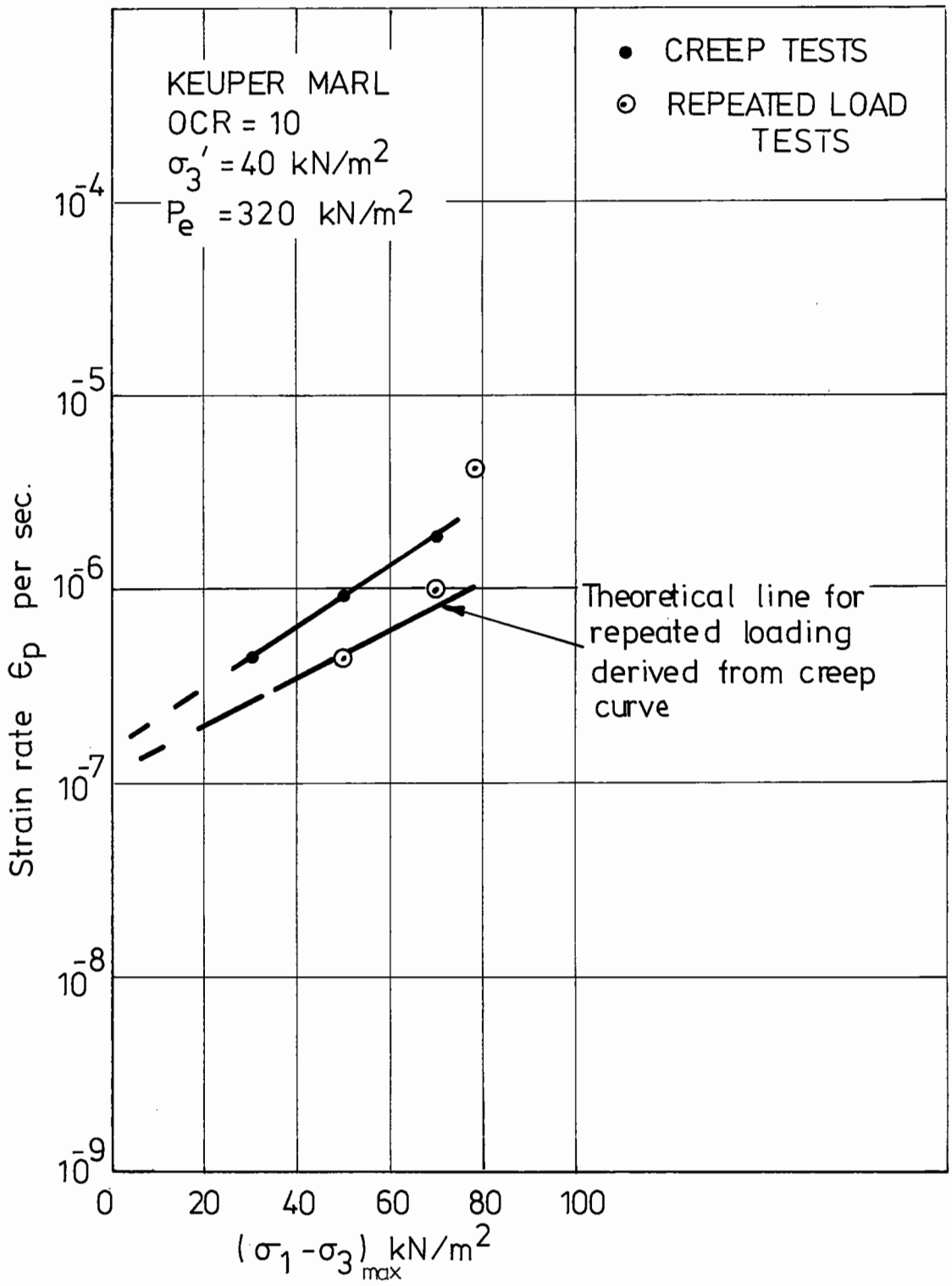

Fig. 6.53 Variation of strain rate with deviator stress after 10^3 seconds.

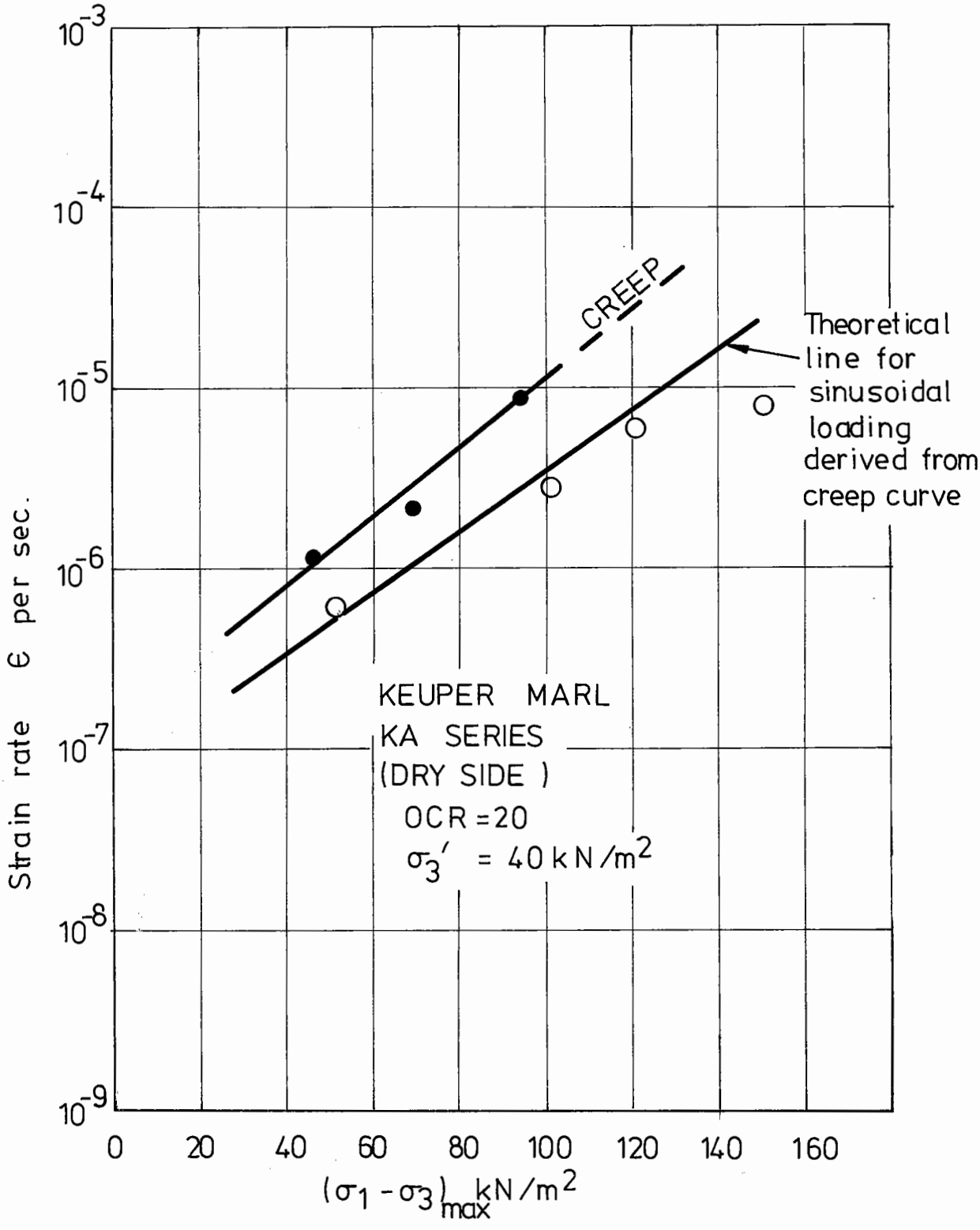

Fig. 6.54 Variation of strain rate with deviator stress after 10^3 seconds.

	Proportional stress kN/m^2	$\dot{\epsilon}$ for OCR 10 after 10^3 secs	$\dot{\epsilon}$ for OCR 4 after 10^3 secs	Proportional stress kN/m^2	$\dot{\epsilon}$ for OCR 10 after 10^3 secs	$\dot{\epsilon}$ for OCR 4 after 10^3 secs
Maximum Applied Stress	80			40		
	79	2.8×10^{-6}	7.0×10^{-6}	39	6.5×10^{-6}	1.2×10^{-6}
	75	2.3×10^{-6}	6.0×10^{-6}	37	6.0×10^{-6}	1.1×10^{-6}
	68	1.8×10^{-6}	4.8×10^{-6}	34	5.0×10^{-6}	9.5×10^{-6}
	58	1.3×10^{-6}	3.0×10^{-6}	29	4.5×10^{-6}	7.5×10^{-7}
	46	8.0×10^{-7}	1.6×10^{-6}	23	3.5×10^{-6}	6.0×10^{-7}
	34	5.0×10^{-7}	9.5×10^{-7}	17	3.0×10^{-6}	4.8×10^{-7}
	22	3.1×10^{-7}	4.0×10^{-7}	11	2.1×10^{-6}	3.1×10^{-7}
	12	2.1×10^{-7}	2.2×10^{-7}	6	-	-
	5	-	-	3	-	-
	1	-	-	0	-	-
Mean Strain Rate		1.0×10^{-6}	2.4×10^{-6}		3.0×10^{-6}	5.4×10^{-7}

Table 6.1 Examples of the Derivation of Repeated Load Strain Rate from Creep Test Data

α = strain rate at unit time

λ = gradient of the log $\dot{\epsilon}$ versus log T plot and is constant for both creep and repeated load tests on samples having the same stress history. It is defined as the decay constant.

The constant "λ" can be obtained from a creep test, but the parameter "α" is not a constant since it depends on applied stress, the stress history, and the type of loading. To obtain a value for "α" it is necessary to carry out creep tests over a range of deviator stresses. By projecting the strain rate versus time plots back to unit time a function for "α" may be obtained of the following form (see Fig. 6.45):

$$\alpha = B + C(\sigma_1 - \sigma_3) \qquad (6.2)$$

where α = log (strain rate at unit time)

= log $\dot{\epsilon}_1$

B = a constant dependent on the material and the stress history

C = gradient of the line

$(\sigma_1-\sigma_3)$ = applied deviator stress

Having obtained the above relationship for creep tests it is then possible to derive the function for "α" under repeated load conditions using the technique outlined in Section 6.5.4. This was done for OCR's of 4, 10 and 20. The functions obtained for "α" or log $\dot{\epsilon}_1$ are given below.

<u>OCR = 4</u>

Creep: $\alpha = \log_e \dot{\epsilon}_1 = 0.045(\sigma_1-\sigma_3) - 9.2 \qquad (6.3)$

Repeated load: $\alpha = \log_e \dot{\epsilon}_1 = 0.036(\sigma_1-\sigma_3) - 9.5 \qquad (6.4)$

OCR = 10

Creep: $\alpha = \log_e \dot{\varepsilon}_1 = 0.0345(\sigma_1-\sigma_3) - 8.5$ (6.5)

Repeated load: $\alpha = \log_e \dot{\varepsilon}_1 = 0.029(\sigma_1-\sigma_3) - 9.2$ (6.6)

OCR = 20

Creep: $\alpha = \log \dot{\varepsilon}_1 = 0.045(\sigma_1-\sigma_3) - 9$ (6.7)

Repeated load: $\alpha = \log \dot{\varepsilon}_1 = 0.0385(\sigma_1-\sigma_3) - 9.5$ (6.8)

Equation 6.1 can be rewritten as:

$$\dot{\varepsilon} = e^{\alpha}.T^{-\lambda} \tag{6.9}$$

where $\alpha = f(\sigma)$

Integrating equation (6.9) gives:

$$\int_{T_1}^{T_2} \dot{\varepsilon}\,dT = \int_{T_1}^{T_2} e^{\alpha}.T^{-\lambda}\,dT \tag{6.10}$$

$$\varepsilon_{T_2} = \varepsilon_{T_1} + \frac{e^{\alpha}}{1-\lambda}\left(T_2^{\,1-\lambda} - T_1^{\,1-\lambda}\right) \tag{6.11}$$

This equation allows the prediction of the strain accumulated after T_2 secs providing ε_{T_1}, λ and the function for α are known.

For the tests which were carried out, reliable data for plastic strain could not be obtained until several seconds had elapsed. Hence, the simple empirical relationship outlined in Section 6.5.2 was used to compute the plastic strain during the first 100 seconds. This relationship was that the repeated load strain is approximately half the creep strain in the early stages of

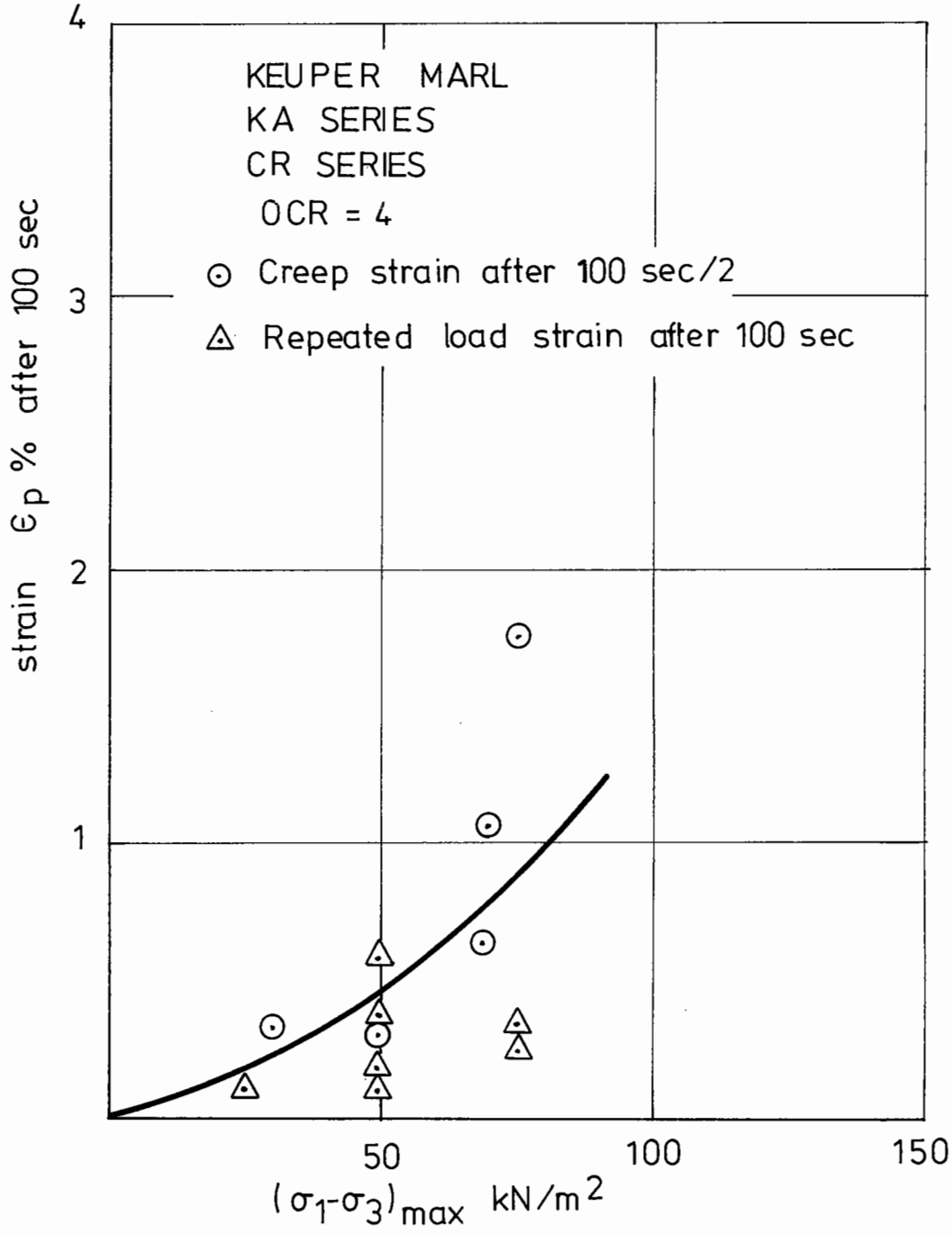

Fig. 6.55 Variation of initial strain with applied stress under creep and repeated load conditions.

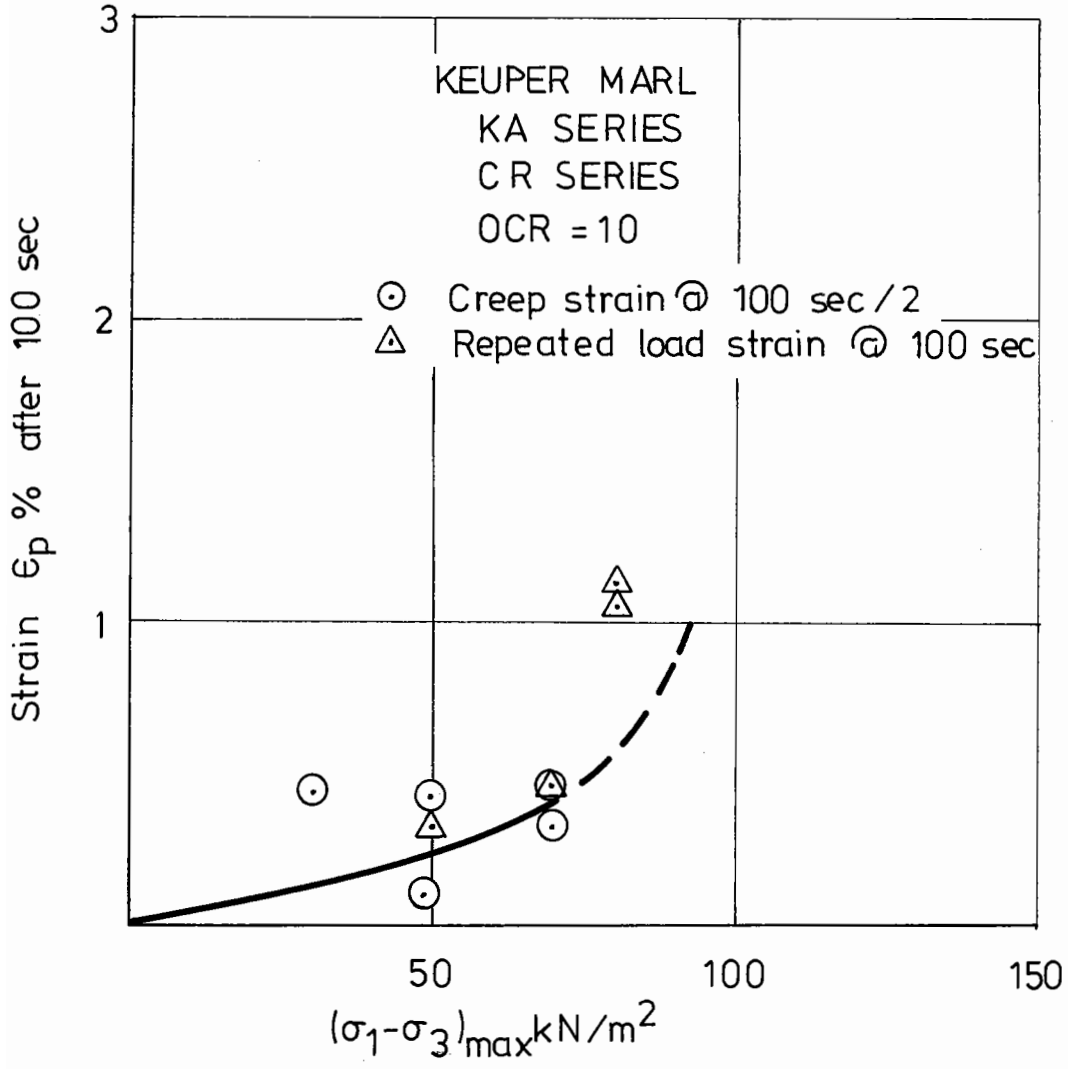

Fig. 6.56 Variation of initial strain with applied stress under creep and repeated load conditions.

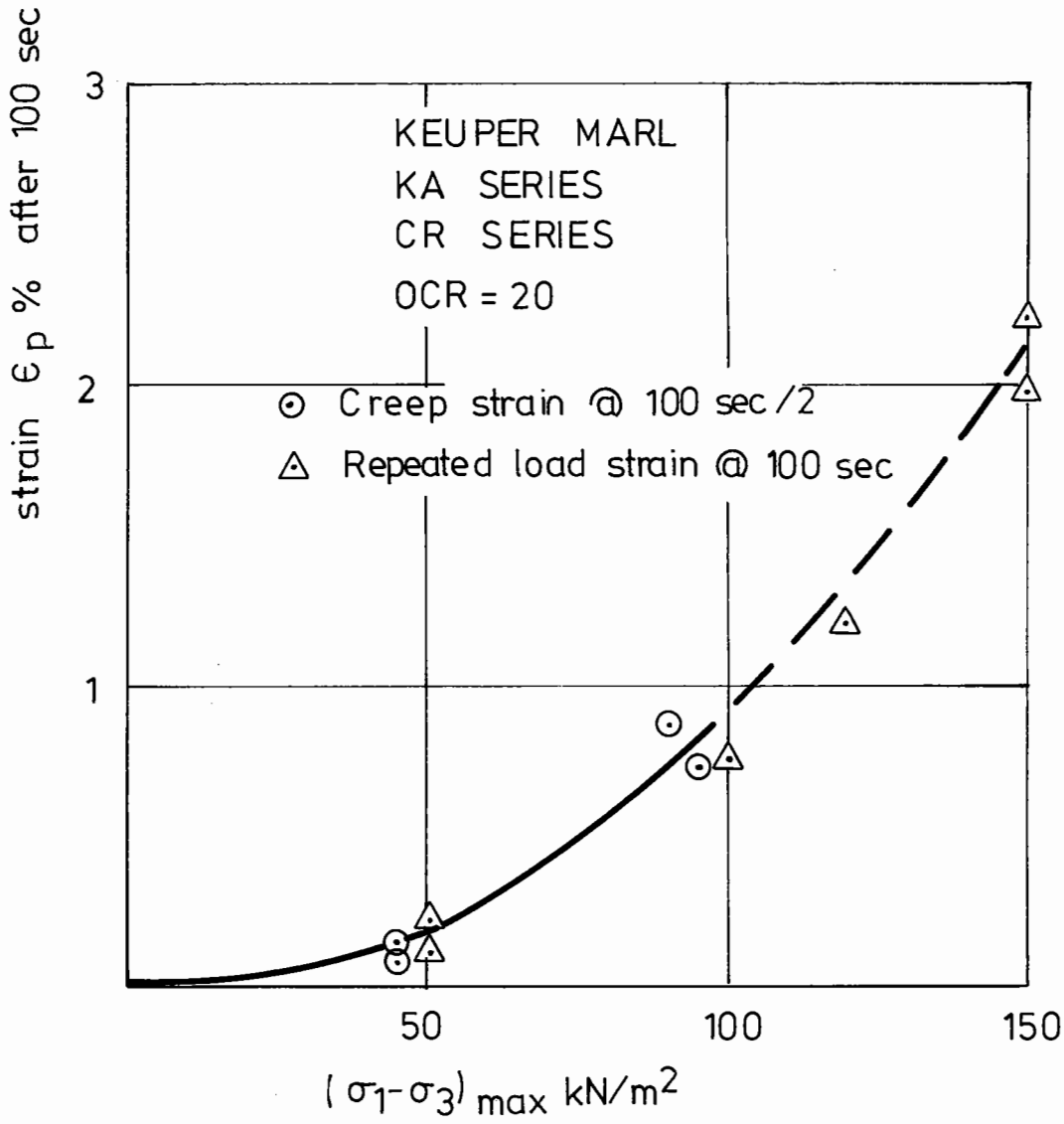

Fig. 6.57 Variation of initial strain with applied stress under creep and repeated load conditions.

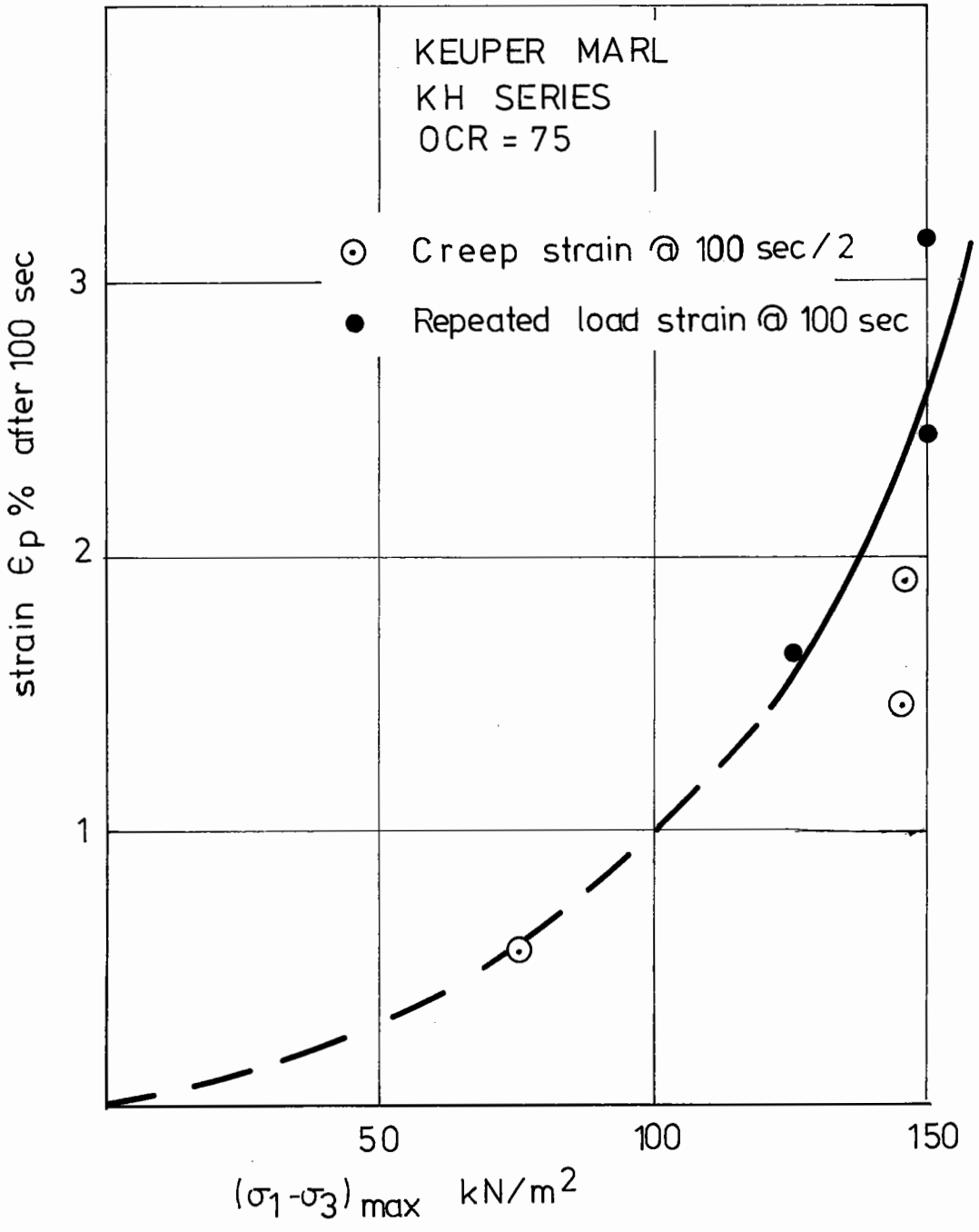

Fig. 6.58 Variation of initial strain with applied stress under creep and repeated load conditions.

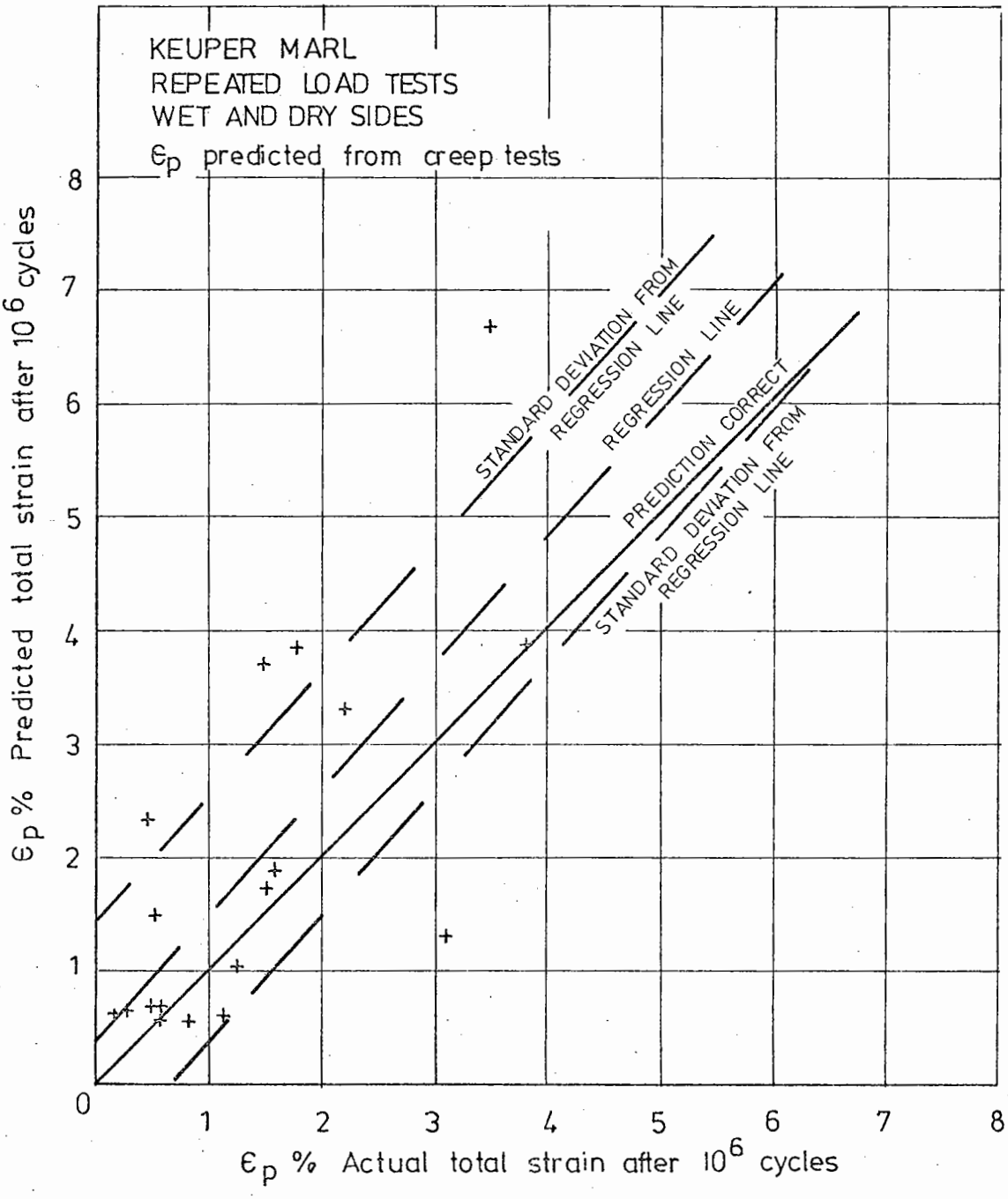

Fig. 6.59 Comparison of predicted and actual values of total strain (Prediction from creep test data)

the test. Figs. 6.55 to 6.58 indicate the accuracy of this assumption.

Using equation (6.11) and data from creep tests, predictions were made of plastic strain in repeated load tests after 10^6 cycles (Table 6.2).

6.5.5(a) Comparison between predicted and actual values of plastic strain

A comparison between predicted and actual values of total strain after 10^5 seconds or 10^6 cycles of repeated load is given in Fig. 6.59. It can be seen that there is some considerable deviation of the points from the line drawn for a correct prediction. Some measure of this deviation can be made by assuming that it is systematic. By carrying out a linear regression of the dependent variable (the predicted strain) onto the axis for the independent variable (the actual strain) a regression line was drawn of the form:

$$y = a_o + a_1 x \qquad (6.12)$$

The values of the coefficients were as follows:

$$a_o = 0.4$$

$$a_1 = 1.11$$

Coefficient of correlation = 0.73

The deviations of the predicted values from the line of regression were computed. A second assumption was made that the deviation of these values was normally distributed about the regression line, and hence the mean, the standard

Test No.	OCR	$(\sigma_1-\sigma_3)$ kN/m²	ε_p% Accumulated	Predicted ε_p% Accumulated	Predicted ε_p% Initial	Predicted Total ε_p%	Total ε_p%
KA703	4	27	0.04	0.42	0.18	0.60	0.19
KA704	4	27	0.30	0.42	0.18	0.60	0.29
KA803	4	27	1.13	0.42	0.18	0.60	1.16
KA9	4	57	1.48	1.25	0.5	1.75	1.53
KA901*	4	60	0.43	1.39	0.5	1.89	0.52
KA903*	4	57	0.21	1.25	0.5	1.75	0.21
KA10	4	load drift		-	-	-	-
KA1001	4	60	1.25	1.39	0.5	1.89	1.59
KA1003	4	52	0.34	1.04	0.45	1.49	0.52
KA1103	4	79	1.23	2.76	0.95	3.71	1.47
KA1203*	4	75	1.43	2.39	0.85	3.24	1.71
KA13*	4	26	0.13	0.411	0.1	0.51	0.13
KA14	4	26	0.05	0.411	0.1	0.51	0.05
KA15	10	50	0.31	0.31	0.25	0.56	0.59
KA16	10	50	0.53	0.31	0.25	0.56	0.85
KA17	10	load drift		-	-	-	-
KA18	10	79	0.80	0.73	0.4	1.03	1.24
KA1801	10	100	0.46	1.35	1.0	2.35	0.46
KA1802	10	157	sample failed	-	-	-	-
KA19	20	52	0.41	0.37	0.3	0.67	0.59
KA20	20	52	0.39	0.37	0.3	0.67	0.53
KA21	20	100	1.45	2.41	0.9	3.31	2.2
KA22	20	106	0.80	3.04	0.8	3.84	1.78
KA23	20	170	sample failed	25.0	2.0	-	-
KA24	20	150	5.79	16.6	2.1	18.7	7.77
KA25	20	150	4.78	16.6	2.1	18.7	6.59
KA30	4	80	1.74	2.86	1.0	3.86	3.8
KA33R	20	120	2.09	5.2	1.4	6.6	3.49
KA31R	10	82	1.05	0.802	0.5	1.302	3.04

* High friction in the seals

Table 6.2 Prediction of Total Strain after 10^6 cycles from Creep Strains

deviation and the variance were calculated. These were:

Mean = 0.0068

Standard deviation = 1.15

Variance = 1.33

For values of strain up to 6%, the "prediction correct" line lies within a standard deviation of the regression line. The regression line also suggests that the predicted values of plastic strain are systematically 11 per cent plus a small constant larger than the actual values.

6.5.6 A General Model of the Accumulation of Plastic Strain

Strain controlled tests have been examined in terms of the stress invariants p and q and the equivalent pressure p_e (Section 6.4.2). It was also shown that a sample strength could be defined in terms of the equivalent pressure p_e by the use of the invariant q_f/p_e.

Analysis of creep and repeated load tests has shown that it is possible to express the strain rate at a given time in terms of a function involving the parameters q and p_e or q_f.

By normalising the deviator stress with respect to $p_e^{\frac{1}{2}}$ two unique lines were obtained for the variation of the strain rate at a given time (Fig. 6.60). These two lines are for samples consolidated either to the wet or dry sides of the critical state (see Section 6.4.1). Separate consideration will be given below to tests falling into these two categories.

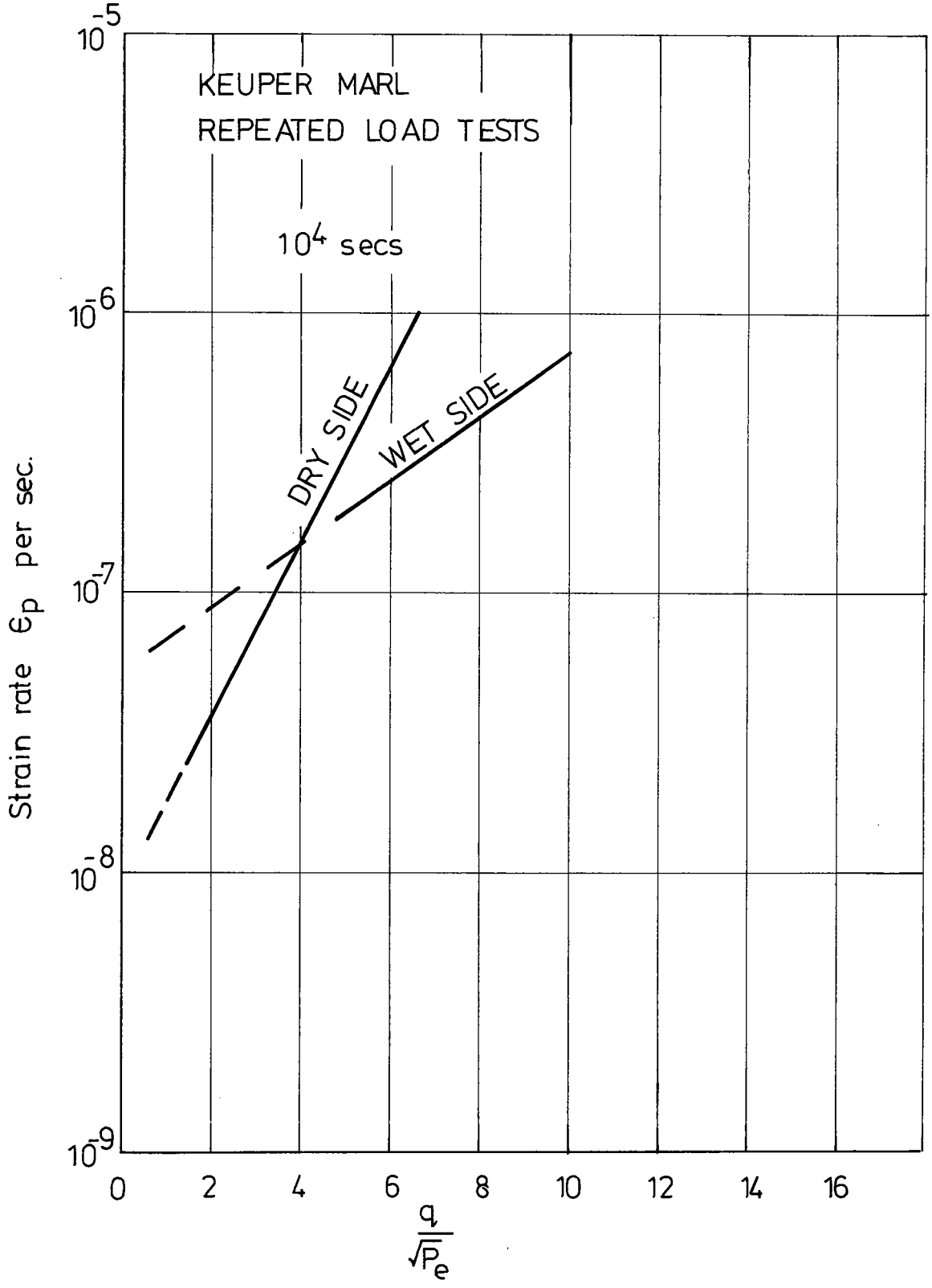

Fig. 6.60 Comparison of strain rates of samples on dry and wet sides of critical state.

In order to determine the stress history of site samples, it is necessary to estimate the preconsolidation pressure; methods for doing this have been developed by Casagrande (1936), Burmister (1942) and Schmertmann (1955) and are outlined in Appendix E.

6.5.6(a) Model for repeated load tests on the "dry" side

The variation of the strain rate after 10^4 seconds is plotted against the normalised maximum deviator stress q_{max} for repeated load tests in Fig. 6.61. Using the data tabulated in Table 6.3 a line of regression was fitted to these tests.

The equation for this line was:

$$\log_e \dot{\epsilon}_{10^4} = 0.706 . q_{max} . p_e^{-\frac{1}{2}} - 18.4 \qquad (6.13)$$

(coefficient of correlation = 0.93)

A similar equation was obtained for creep tests (Table 6.4, Fig. 6.62):

$$\log_e \dot{\epsilon}_{10^4} = 0.774 . q . p_e^{-\frac{1}{2}} - 18.2 \qquad (6.14)$$

(coefficient of correlation = 0.92)

Using the summation technique outlined in Section 6.5.4 a theoretical repeated loading line was derived from equation (6.14) and is shown in Fig. 6.63. It can be seen that for the general case, this line does not coincide with the regression line plotted through the repeated load tests.

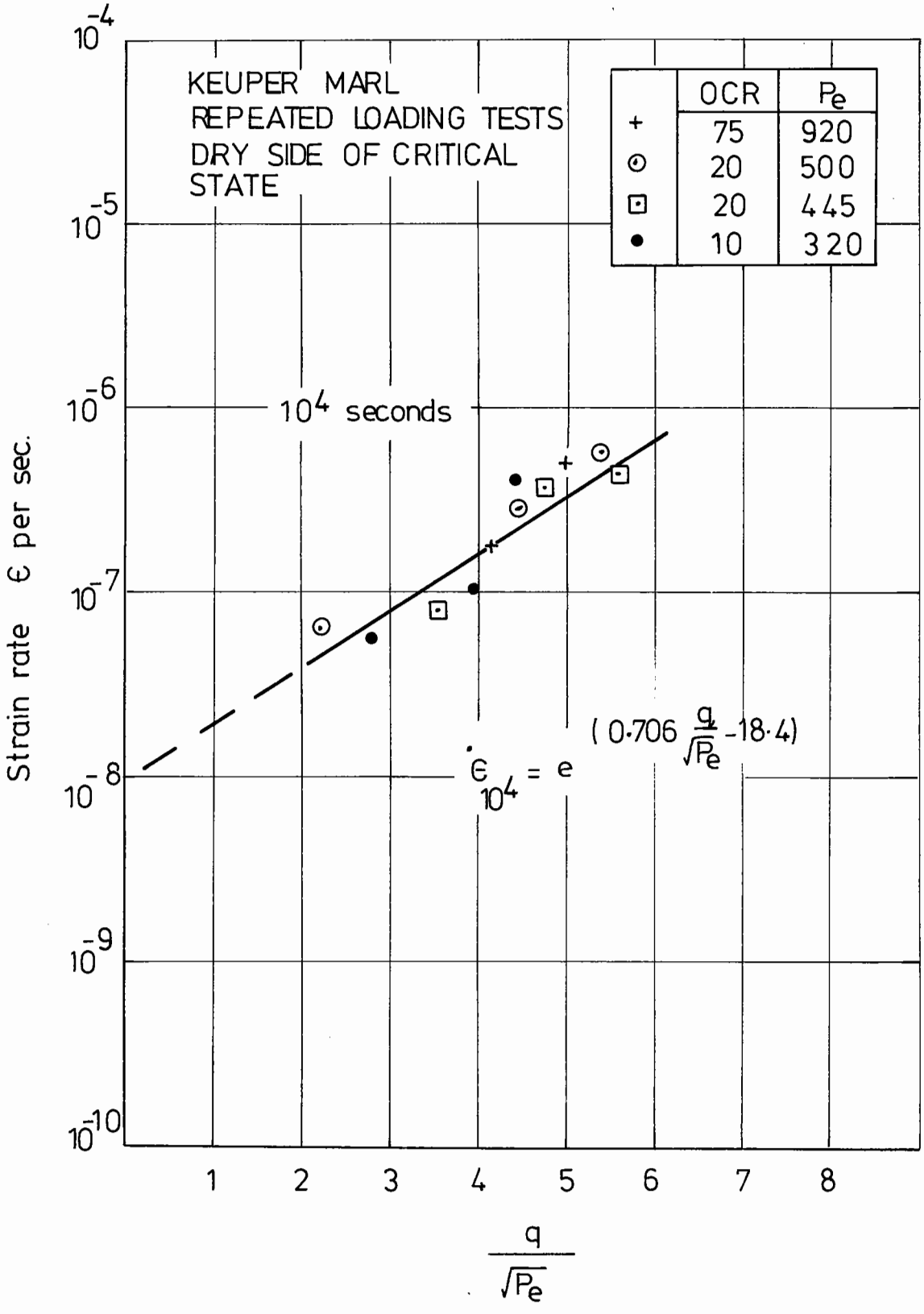

Fig. 6.61 Variation of strain rate with normalised deviator stress at 10^4 seconds (repeated load tests)

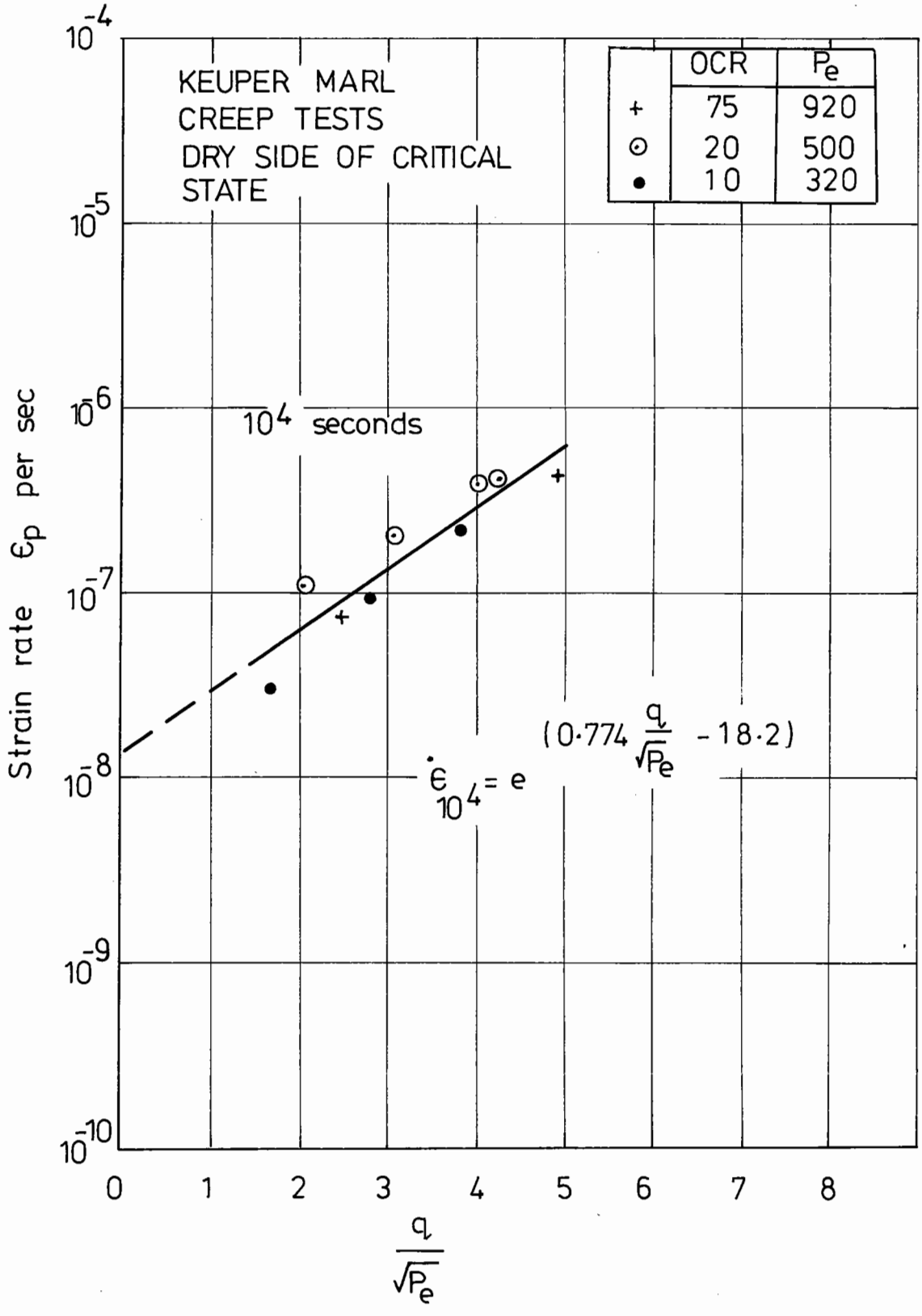

Fig. 6.62 Variation of strain rate with normalised deviator stress at 10^4 seconds for dry side (creep tests)

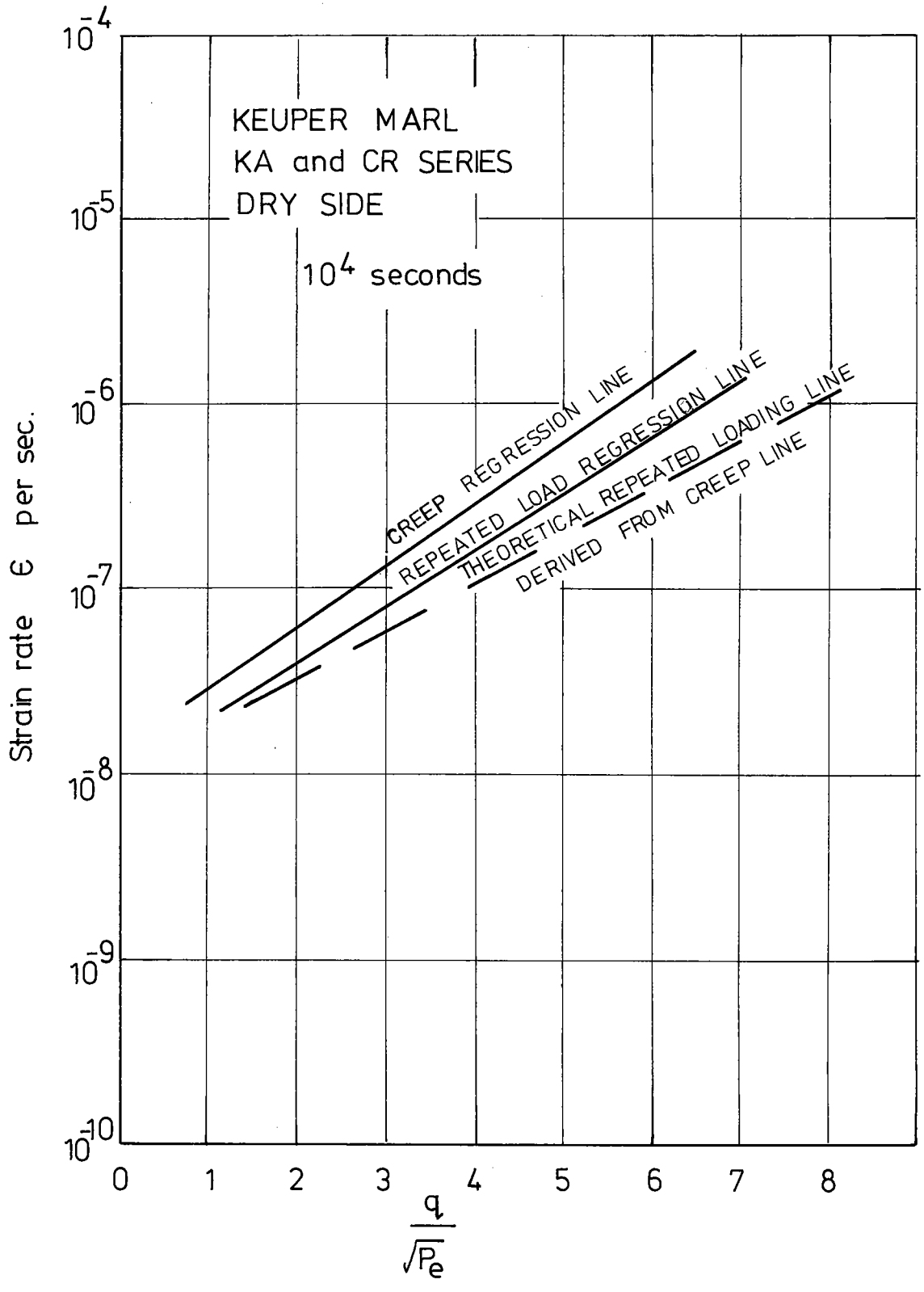

Fig. 6,63 Comparison of creep, repeated loading and theoretical lines for the variation of strain rate with normalised deviator stress.

OCR	p_e	q	$q/\sqrt{p_e}$	$\dot{\epsilon}$ @ 10^4 secs
20	500	50	2.236	6.1×10^{-8}
20	500	100	4.472	2.8×10^{-7}
20	500	120	5.367	5.2×10^{-7}
20	500	150	6.708	8.0×10^{-7}
10	320	80	4.47	4.0×10^{-7}
10	320	70	3.9	1.0×10^{-7}
10	320	50	2.79	5.1×10^{-8}
20	445	75	3.54	7.5×10^{-8}
20	445	100	4.73	3.5×10^{-7}
20	445	120	5.67	4.2×10^{-7}
75	920	125	4.09	1.8×10^{-7}
75	920	150	4.94	4.8×10^{-7}

Table 6.3 Strain rates for repeated load tests "dry" side

Equation (6.9) can be rewritten for the general case, as:

$$\dot{\epsilon} = e^{\alpha'} . T^{-\lambda} \qquad (6.15)$$

where $\alpha' = f(q, p_e)$

and $\lambda = 1$ (for the dry side)

Integrating with respect to T:

$$\int_{T_1}^{T_2} \dot{\epsilon} dT = e^{\alpha'} \int_{T_1}^{T_2} T^{-\lambda} \, dT \qquad (6.16)$$

OCR	p_e	q	$q/\sqrt{p_e}$	$\dot{\varepsilon}$ @ 10^4 secs
75	920	150	4.94	4.2×10^{-7}
75	920	75	2.45	7.0×10^{-8}
20	500	46	2.05	1.1×10^{-7}
20	500	68	3.04	2.0×10^{-7}
20	500	90	4.02	4.0×10^{-7}
20	500	95	4.25	4.0×10^{-7}
10	320	30	1.68	3.0×10^{-8}
10	320	50	2.79	9.5×10^{-8}
10	320	68	3.81	2.3×10^{-7}

Table 6.4 Strain rates for creep tests "dry" side

For the special case of $\lambda = 1$:

$$\varepsilon_{T_2} = \varepsilon_{T_1} + e^{\alpha'}.(\log_e T_2 - \log_e T_1) \qquad (6.17)$$

$\exp(\alpha') = \dot{\varepsilon}_1$ = strain rate after 1 second

Equations (6.13) and (6.14) can be rewritten for the T = 1 sec situation to give the following expressions for α':

$$\text{Repeated load:} \quad \alpha' = 0.706.q.p_e^{-\frac{1}{2}} - 9.2 \qquad (6.18)$$

$$\text{Creep:} \quad \alpha' = 0.774.q.p_e^{-\frac{1}{2}} - 9.0 \qquad (6.19)$$

Using equations (6.17) and (6.18) computations were made of the predicted accumulated strain from 10^2 to 10^5

seconds (10^3 to 10^6 cycles) (Table 6.5). Some data from Lashine et al (1971) is included. Using the statistical techniques explained in Section 6.5.5(a), a comparison was made between the predicted and actual values of strain. Assuming a systematic error using this method of prediction, the line for a correct prediction lies within a standard deviation of the error for values of strain up to 8% (Fig. 6.64).

The coefficients for the regression line were:

$$a_o = 0.295$$

$$a_1 = 1.1$$

Coefficient of correlation = 0.87

The mean error from the regression line = 0.001%

Standard deviation = 1.104

Variance = 1.21

An attempt has been made to predict the total plastic strains for repeated load data, where creep tests have been carried out under the same conditions. This was done by using the value of strain for the first 100 seconds given by Figs. 6.55 to 6.58 and the accumulated strain from the general model (Table 6.6). A measure of the prediction is given in Fig. 6.65.

The coefficients for the regression line were:

$$a_o = -0.036$$

$$a_1 = 1.16$$

Coefficient of correlation = 0.935

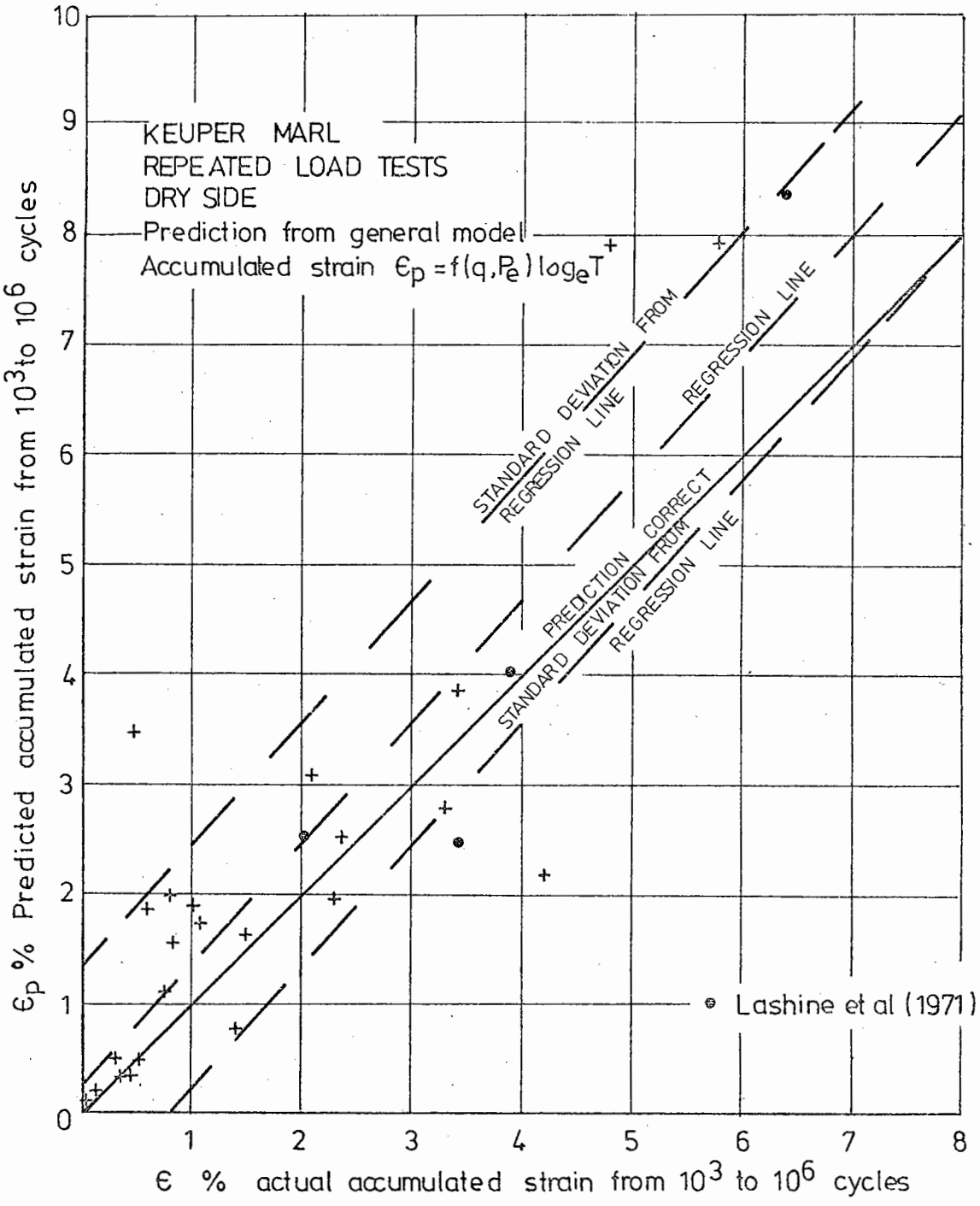

Fig. 6.64 Comparison of predicted and actual values of accumulated plastic strain (Dry side)

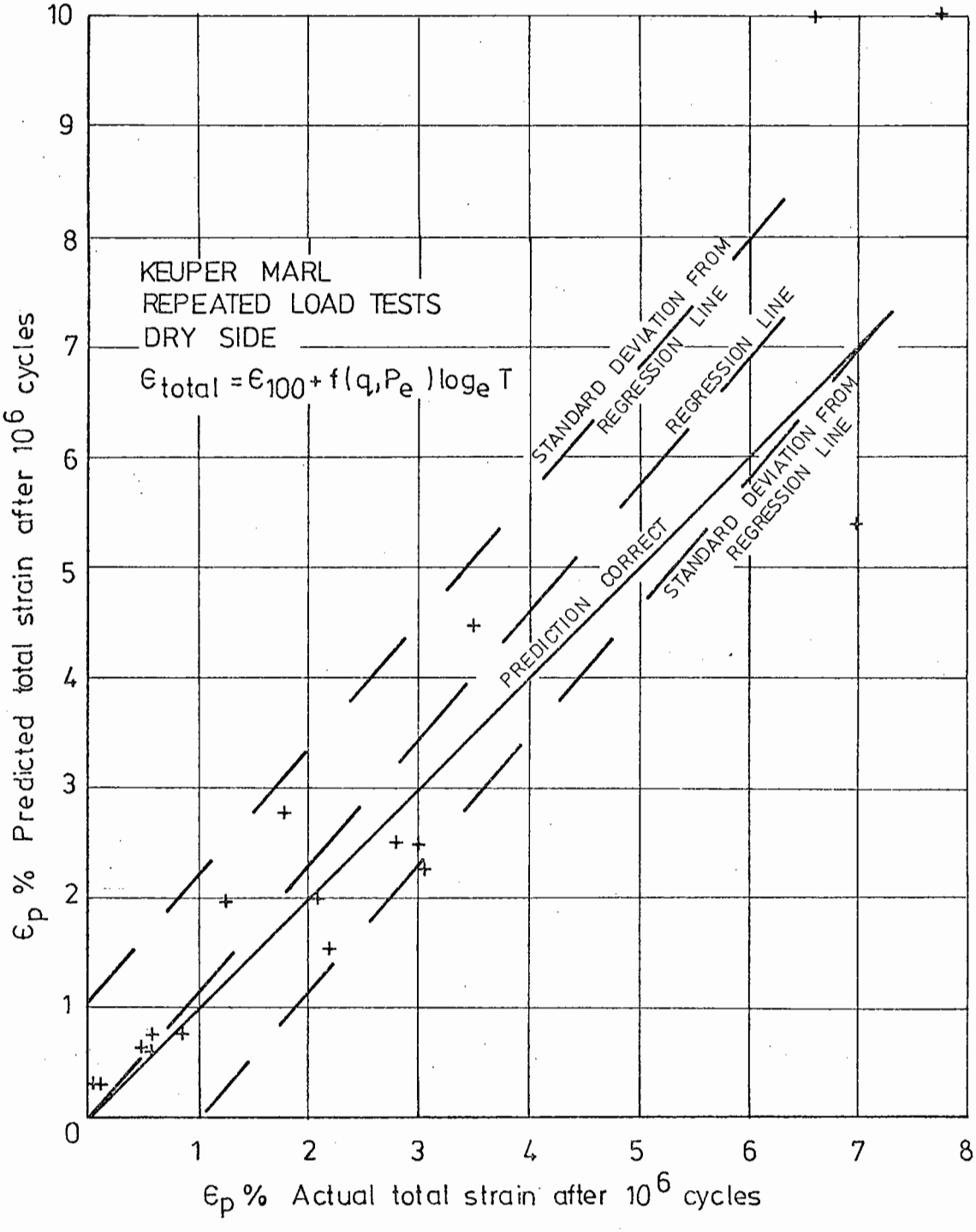

Fig. 6.65 Comparison of predicted and actual values of total plastic strain (Dry side)

Test No.	OCR	p_e kN/m²	q kN/m²	ϵ_p% accumulated 10^2 to 10^5 secs	ϵ_p% accumulated 10^2 to 10^5 secs predicted from general model	Comments
KA15	10	320	50	0.31	0.49	
KA16	10	320	50	0.53	0.49	
KA17	10	320	-	-	-	Load drift
KA18	10	320	79	0.80	1.56	
KA1801	10	320	100	0.46	3.5	
KA1802	10	320	157	-	34	Failed
KA19	20	500	52	0.41	0.35	
KA20	20	500	52	0.39	0.35	
KA21	20	500	100	1.45	1.63	
KA22	20	500	106	0.80	1.97	
KA23	20	500	170	-	14.9	Failed
KA24	20	500	150	5.79	7.9	
KA25	20	500	150	4.78	7.9	
KA33R	20	500	120	2.09	3.06	
KA31R	10	320	82	1.05	1.76	
KA13	10	210	26	0.13	0.19	
KA14	10	320	23	0.05	0.17	
KB14	20	445	100	2.27	1.97	
KB15	20	445	103	4.21	2.17	
KB16	20	445	116	-	-	Failed
KB17	20	445	73	1.41	0.79	
KB18	20	445	107	2.35	2.49	
KB19	20	445	120	3.43	3.85	
KB32	20	445	83	0.75	1.11	
KH4	75	920	159	3.3	2.80	
KH5	75	920	142	1.0	1.89	
KH6	75	920	142	0.59	1.89	
Lashine et al (1971)	10	468	110	2.0	2.51	
"	20	413	103	3.4	2.48	
"	20	413	117	3.9	4.04	
"	20	413	138	6.4	8.39	
"	20	413	159	-	17.4	

Table 6.5 Predicted and Actual Accumulated Strains for the "Dry" Side

6.5.3 Rate of Accumulation of Plastic Strain

For purposes of studying the variation of strain-rate with time the samples are divided into two categories. These are: (1) samples falling on the wet side of the critical state, and (2) those falling on the dry side.

Figs. 6.31 to 6.37 show the variation of the logarithm of the strain-rate with the logarithm of time, for samples on the dry side, for both creep and repeated load tests.

Lashine (1973) suggested that for repeated load tests, if the slope of the strain rate vs time plot (on log-log axes) was greater than a certain value, rupture would occur in a finite period of time. Finn and Shead (1973) give a similar finding for creep tests. They plotted the locus of the turning points of the strain rate-time plots for samples subjected to stresses causing rupture in a finite time. They found this locus to be parallel to the lines for sub-failure stresses. If any test tended towards this locus, then rupture occurred after a finite period of time. It is not the author's intention to study samples which fell in this zone, but rather to characterise the behaviour of the samples subjected to sub-failure stresses.

There are a number of possible reasons for the scatter of results exhibited in Figs. 6.31 to 6.37. As outlined in the description of the equipment, it was not always possible to maintain a constant stress for either repeated load or creep tests due to drift of the null position of the servo valve. In addition, as shown by Mitchell (1964), Campanella et al (1968) and Parr (1972), temperature has a

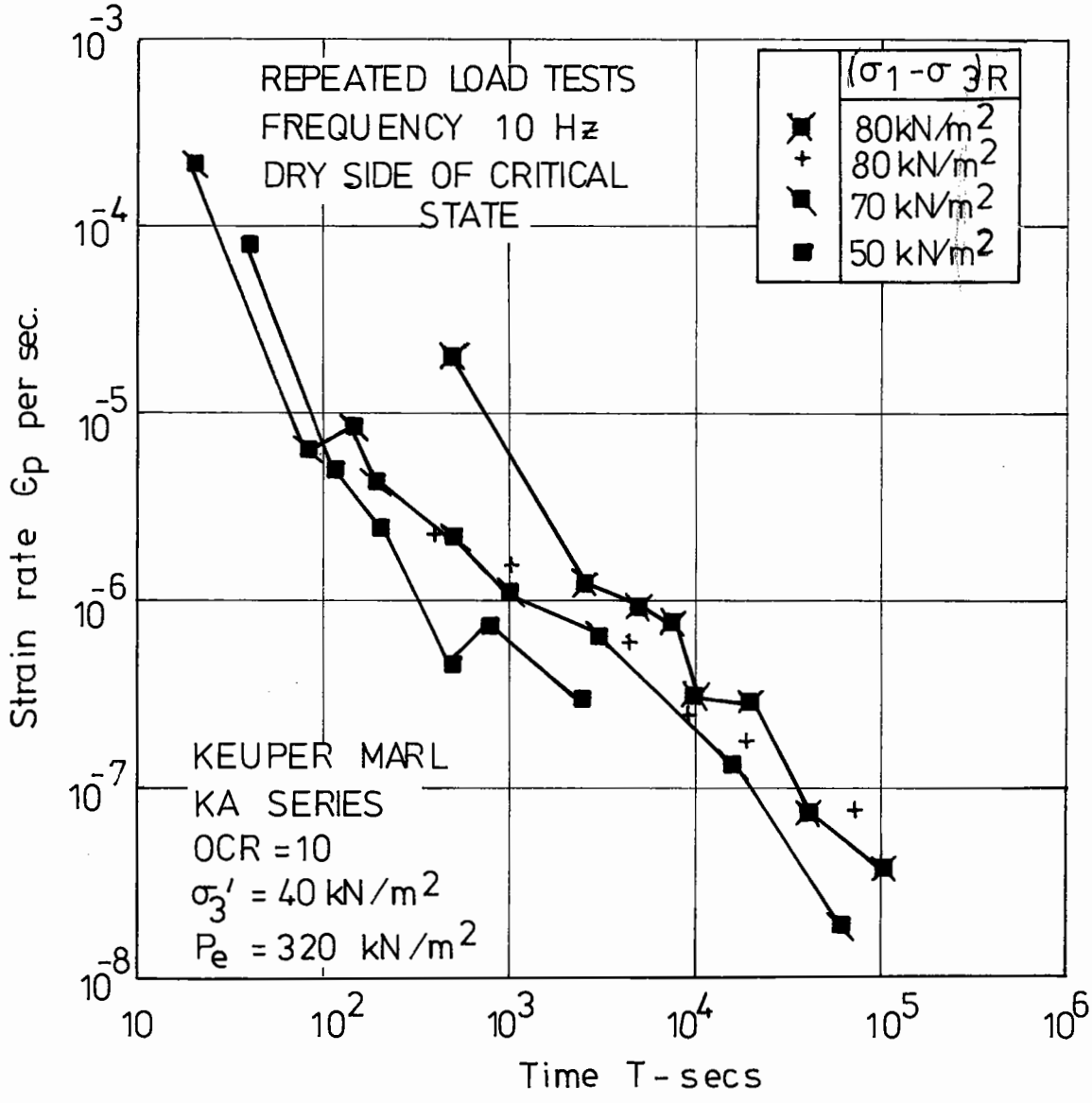

Fig. 6.31 Variation of strain rate with time.

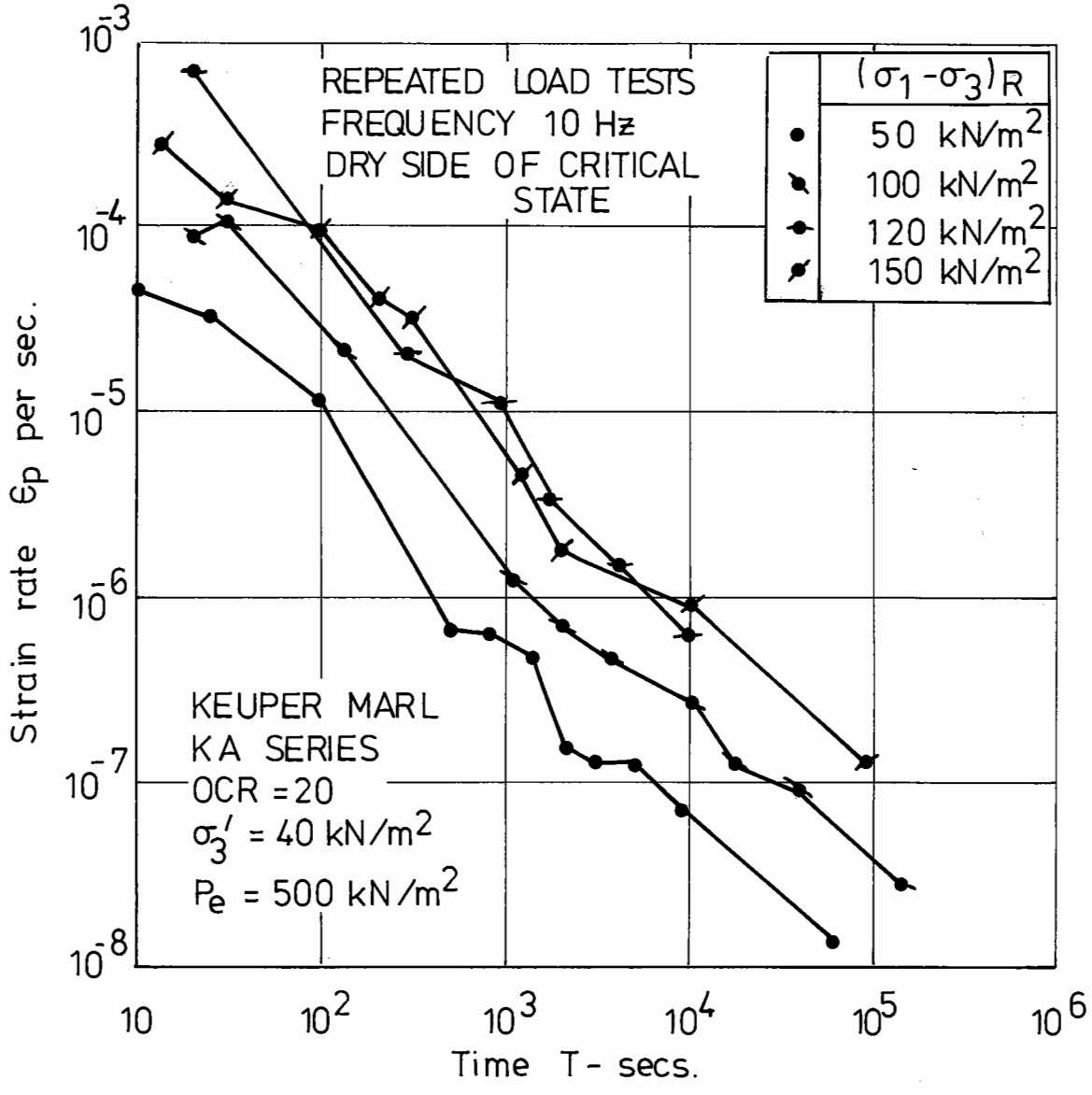

Fig. 6.32 Variation of strain rate with time.

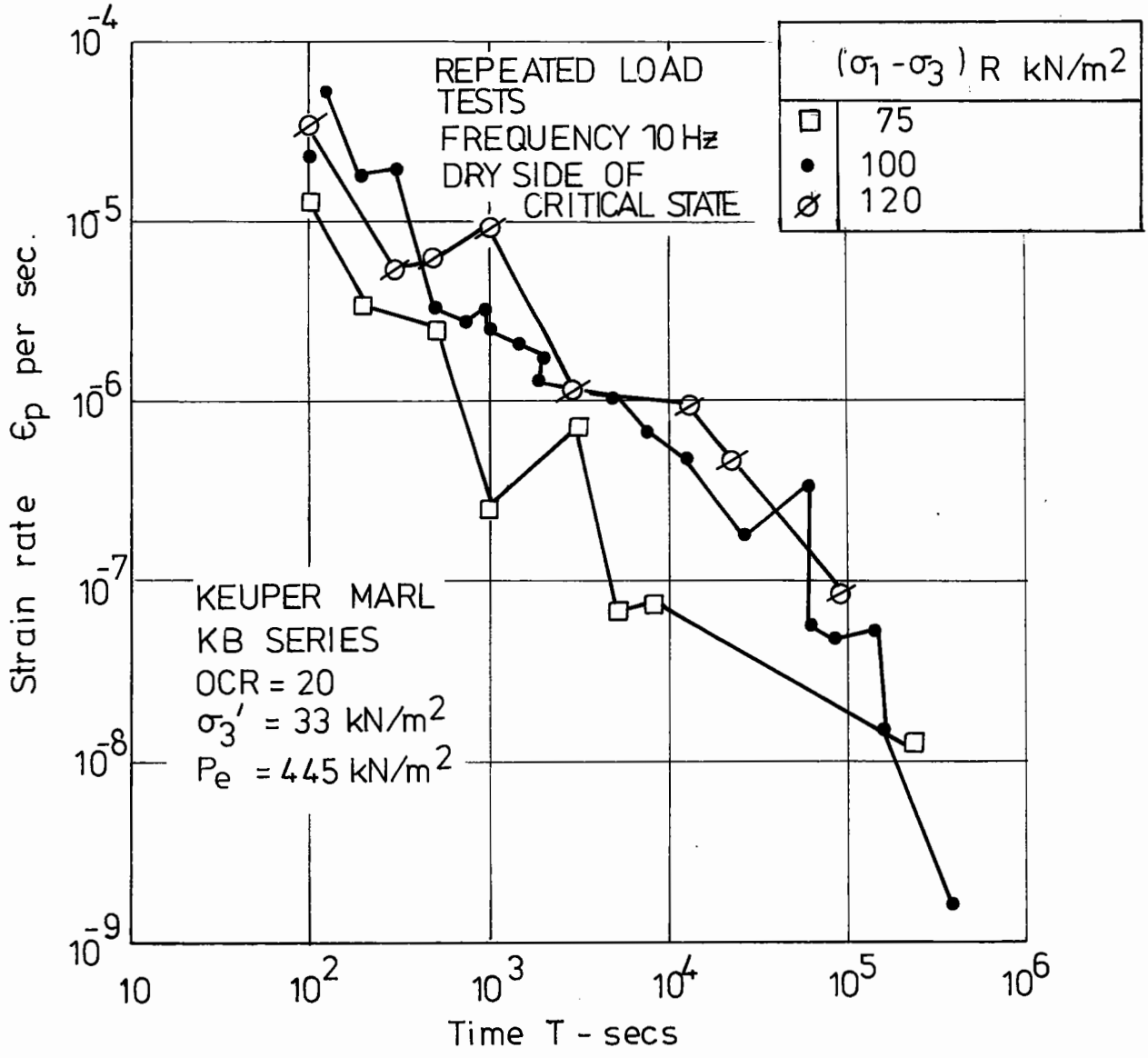

Fig. 6.33 Variation of strain rate with time.

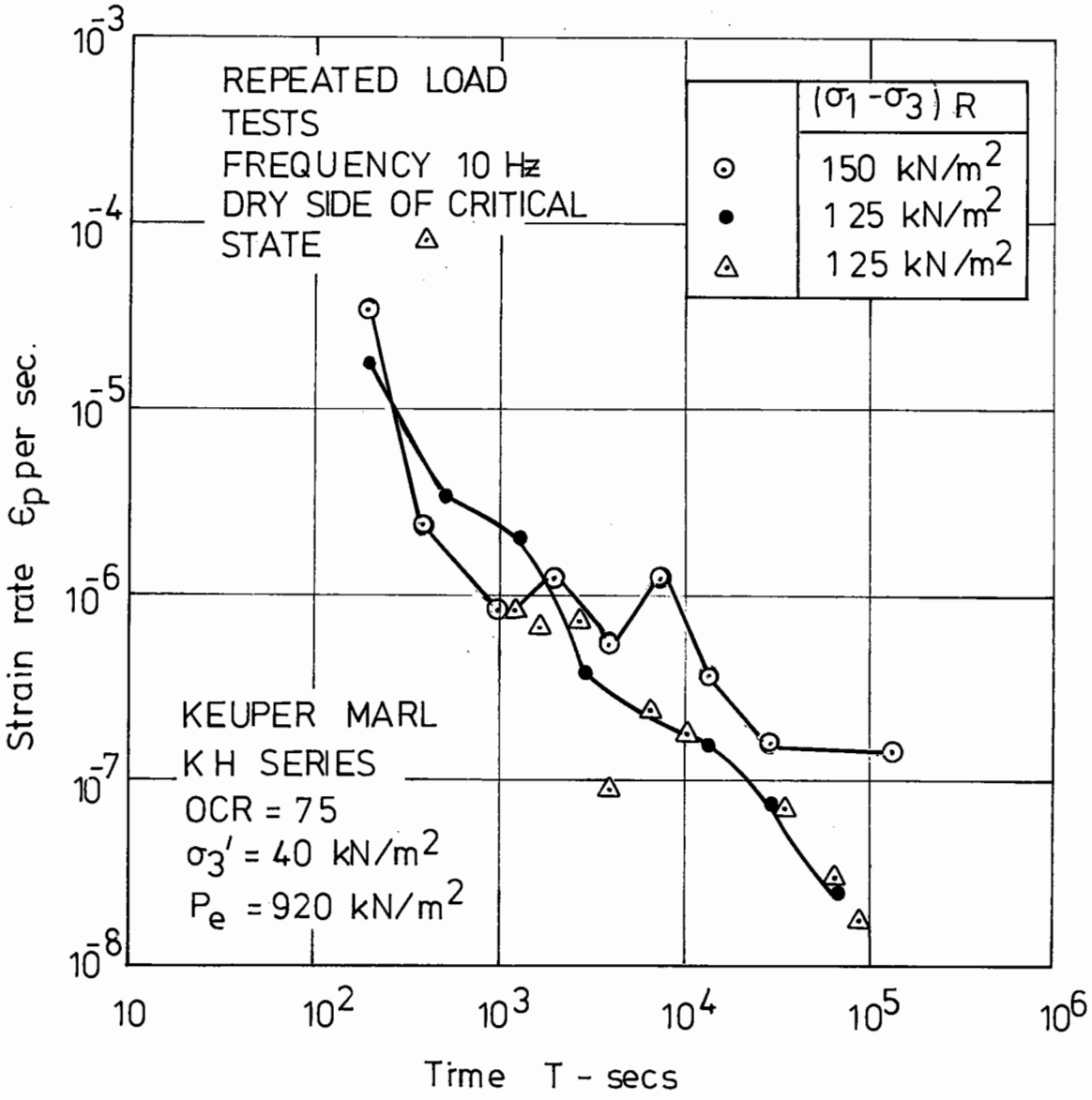

Fig. 6.34 Variation of strain rate with time.

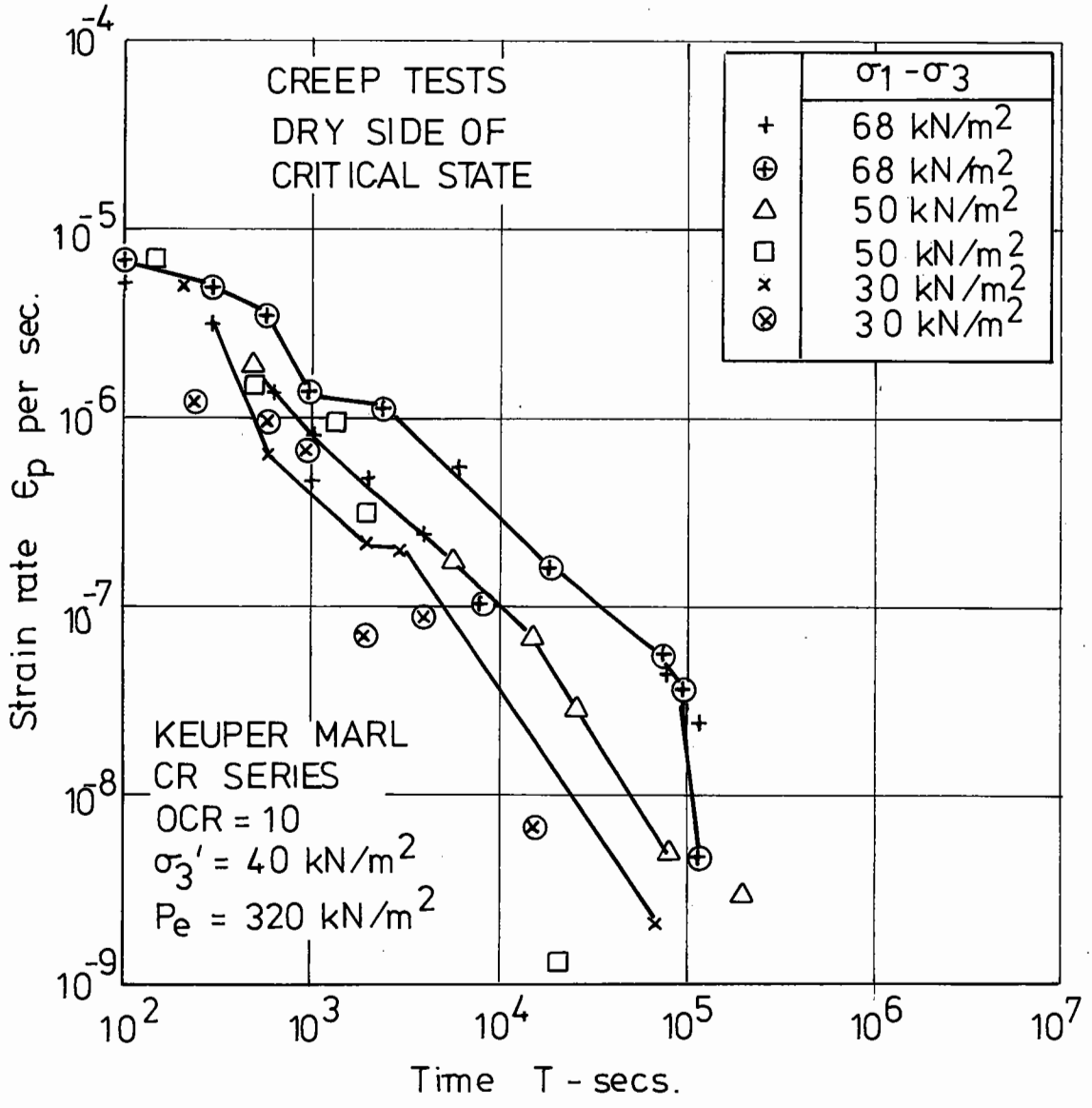

Fig. 6.35 Variation of strain rate with time.

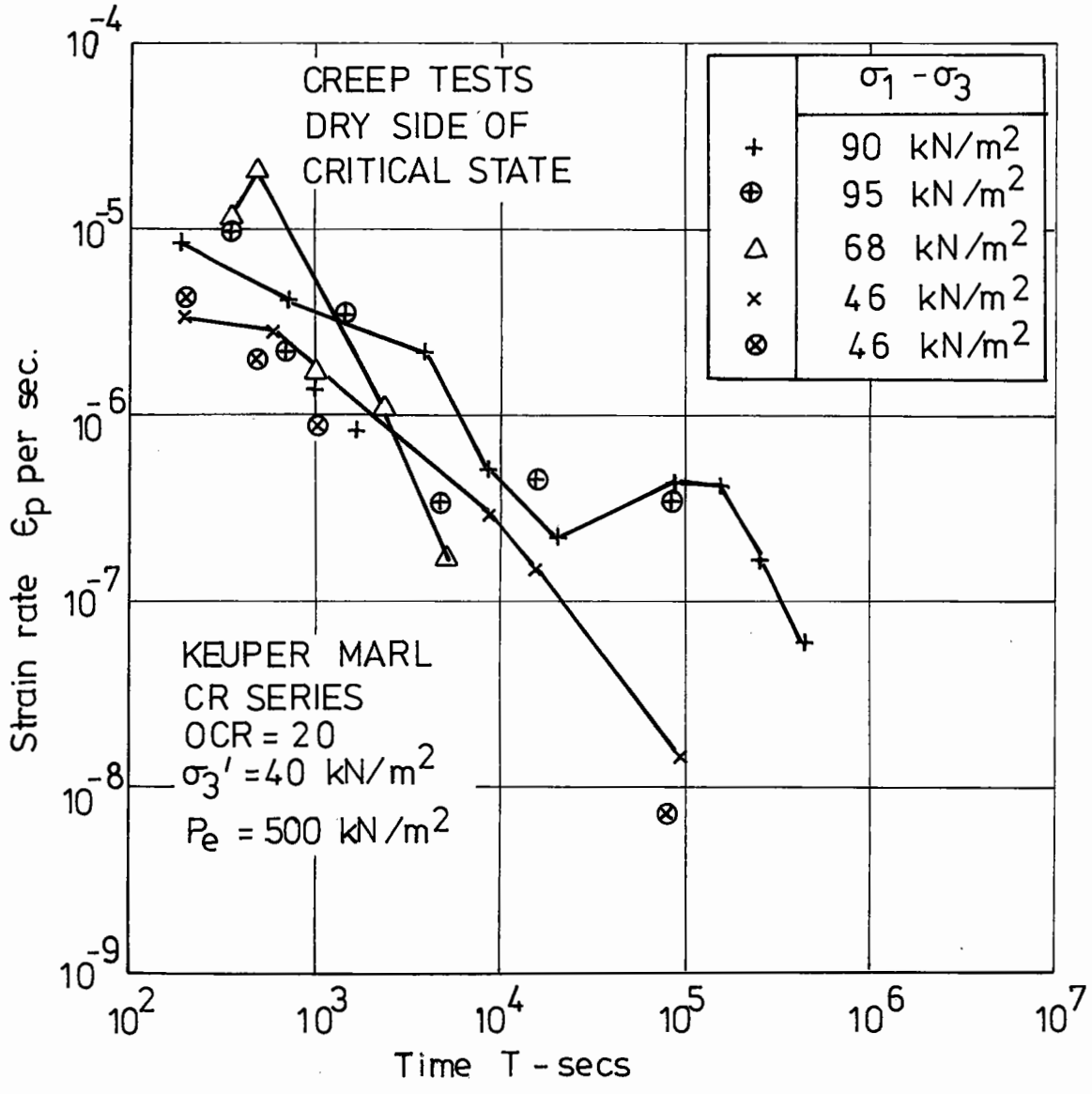

Fig.636 Variation of strain rate with time.

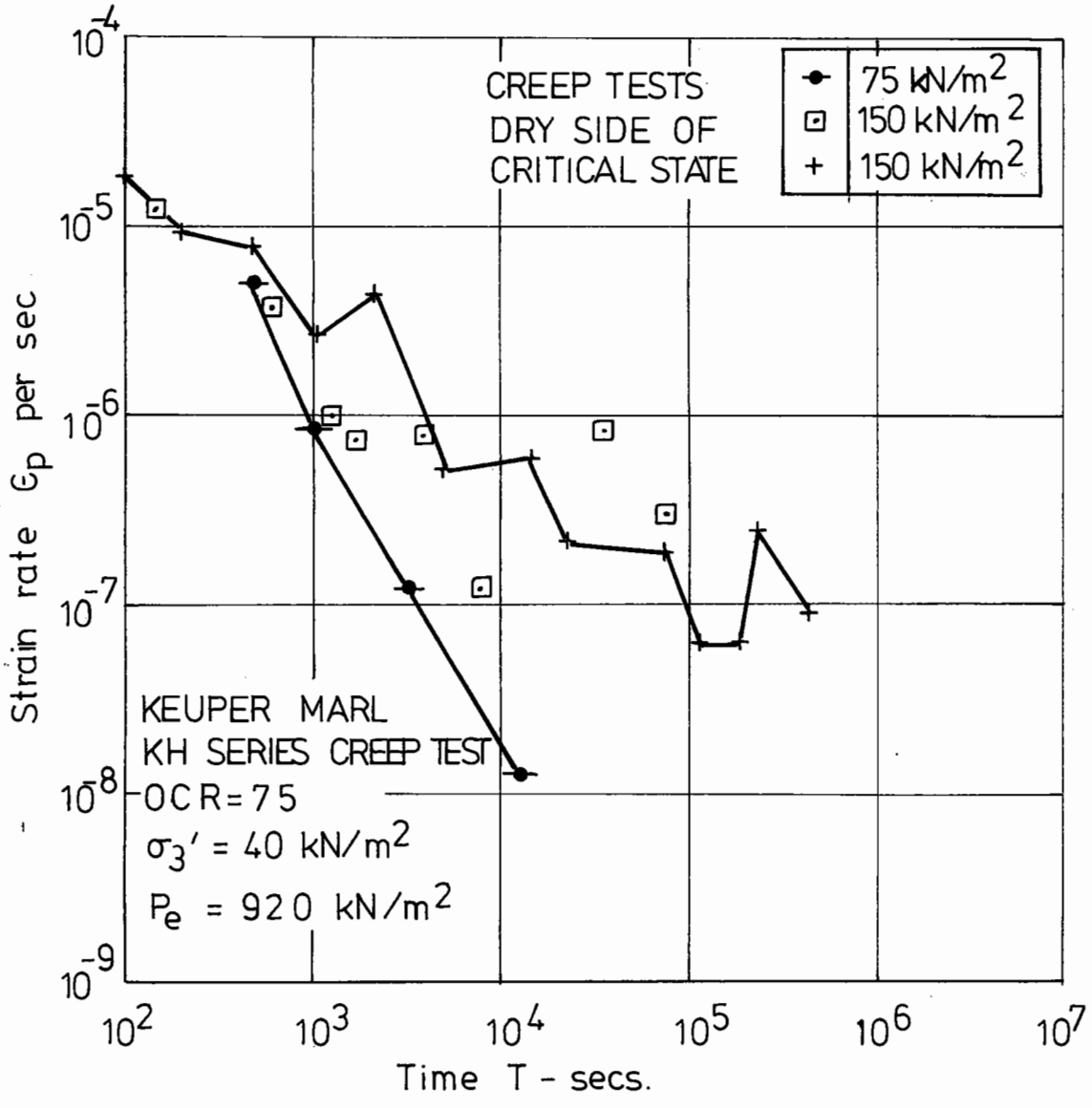

Fig. 6.37 Variation of strain rate with time.

considerable effect on creep behaviour. Although tests were carried out in a room where the temperature was controlled, variations up to $\pm 3^{o}C$ could occur.

It has, in addition, been shown by Ter-Stepanian (1973) that during creep of remoulded clay samples, plastic deformation can occur in a "jump-like" fashion due to the replacement of less durable random structures by oriented ones. Parr (1972), testing undisturbed fissured samples of London clay under very closely controlled conditions, found considerable instabilities during the accumulation of plastic strain. Bishop and Lovenbury (1969), testing drained samples of London clay, considered limited instabilities to be a significant characteristic of undisturbed clays under repeated loading.

The mean slopes of the variation of the logarithm of strain rate with the logarithm of time were found to be the same for both the creep and the repeated load tests. Lines of the same slope were fitted by eye to all the experimental points. The slope which seemed to give the best fit in the majority of cases was equal to -1. These lines are shown in Figs. 6.38 to 6.44. It can be seen from these lines that at a given time the strain-rate is a function of the applied stress.

By plotting the variation of strain rate against the maximum deviator stress a series of parallel lines is obtained at different times (Fig. 6.45). This is similar to that plotted by Singh and Mitchell (1968) and Holzer et al (1972), Fig. 2.5. A typical set of these

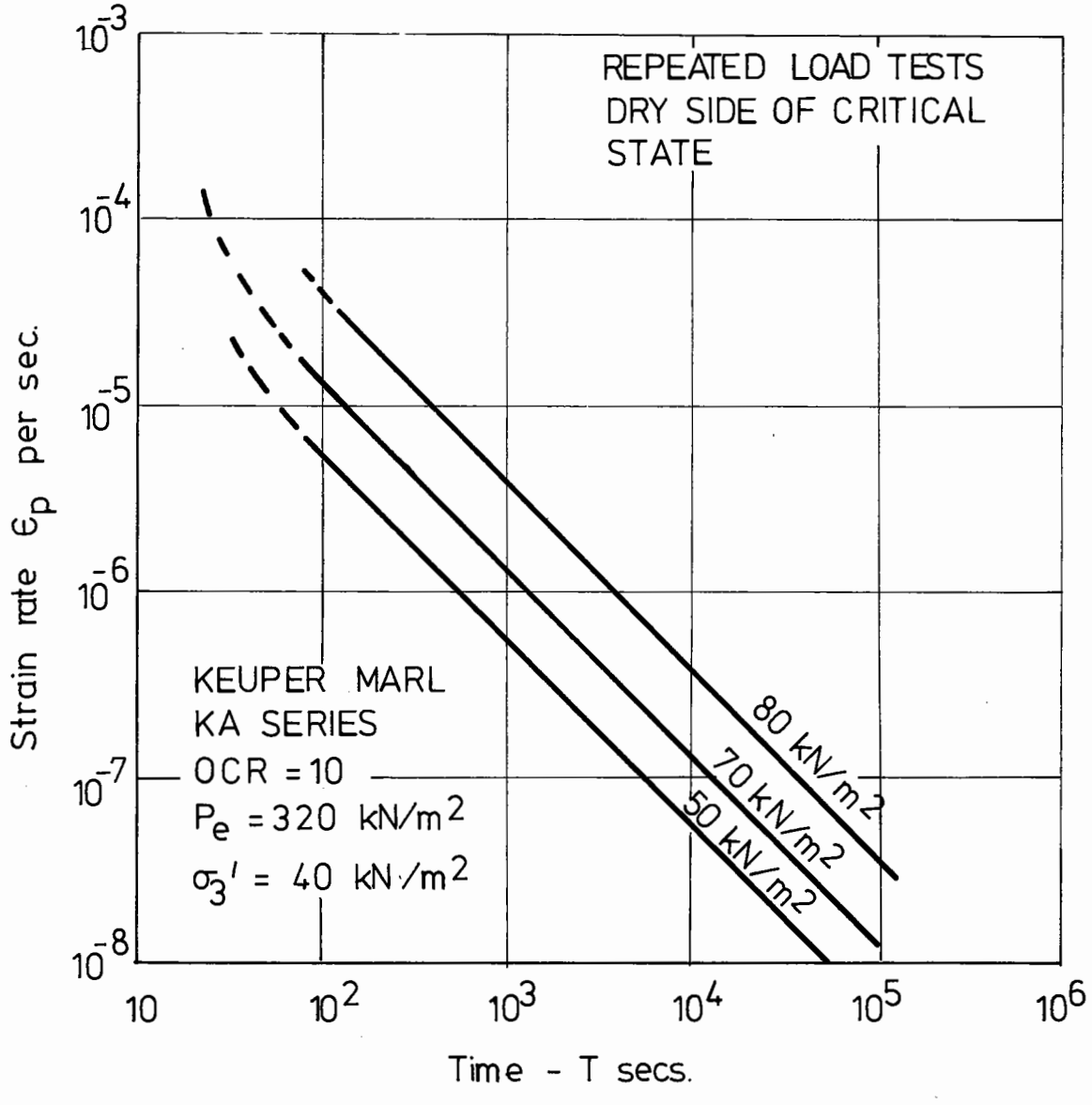

Fig. 6.38 Mean variation of strain rate with time.

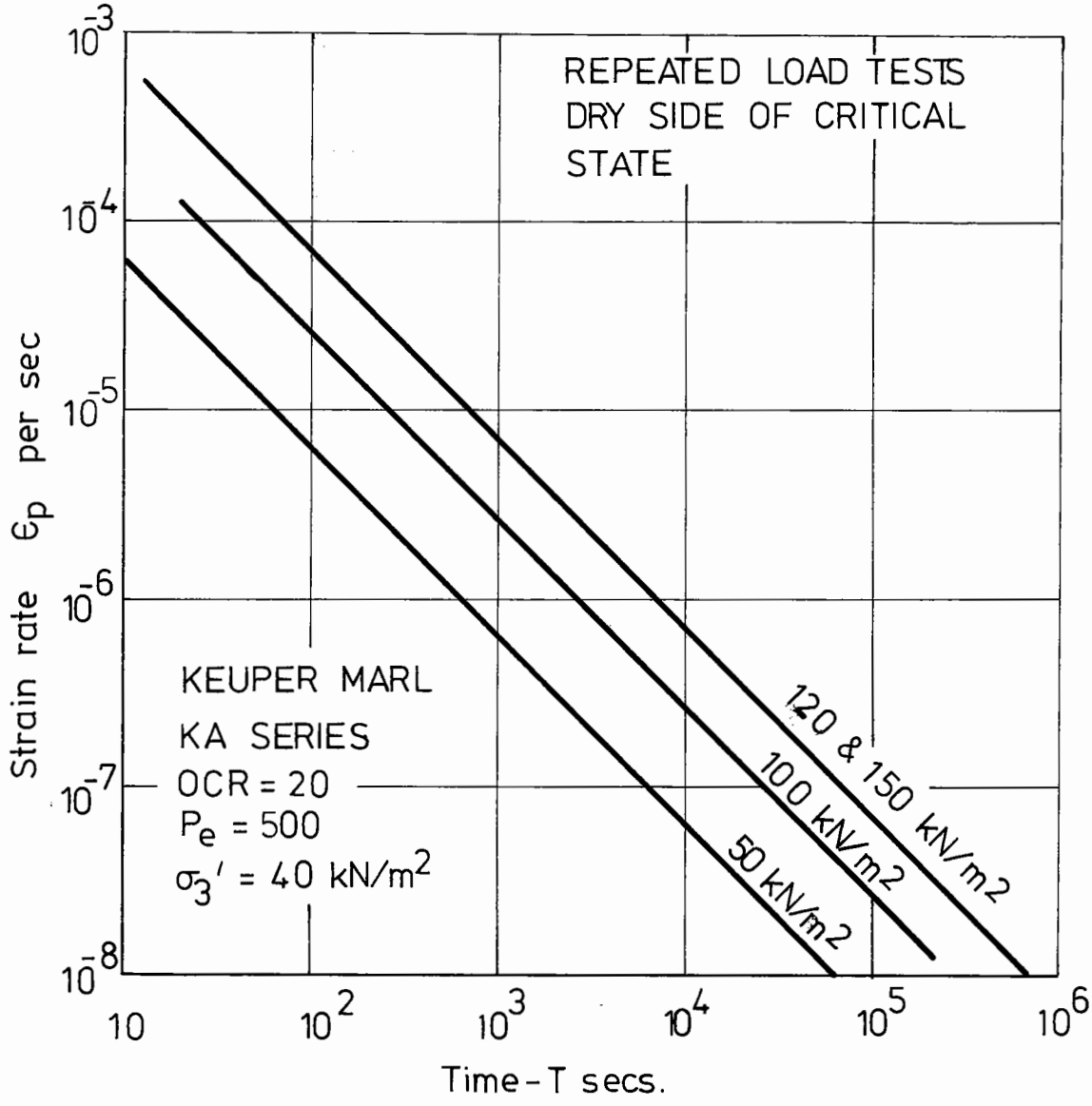

Fig. 6.39 Mean variation of strain rate with time.

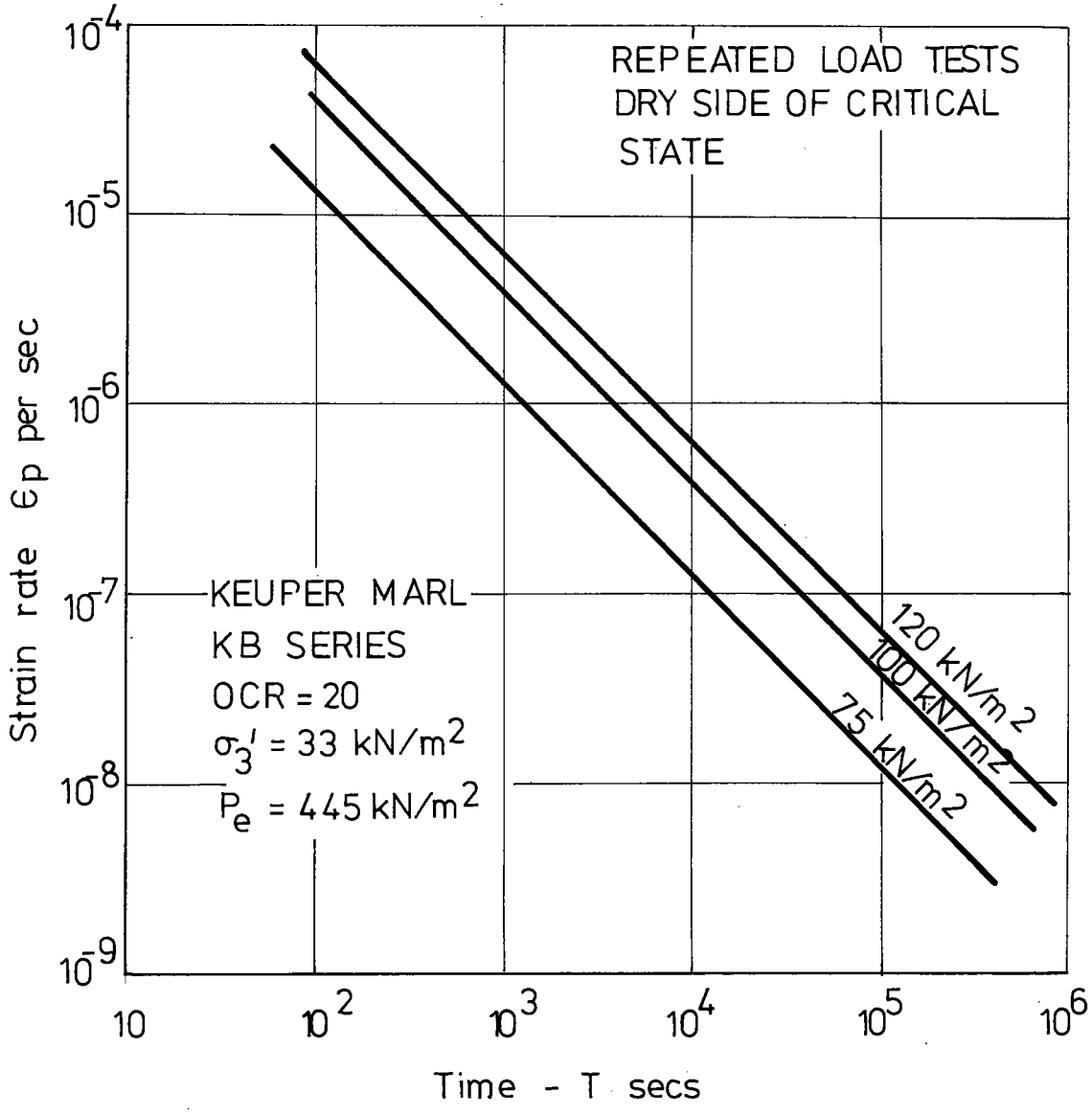

Fig. 6.40 Mean variation of strain rate with time.

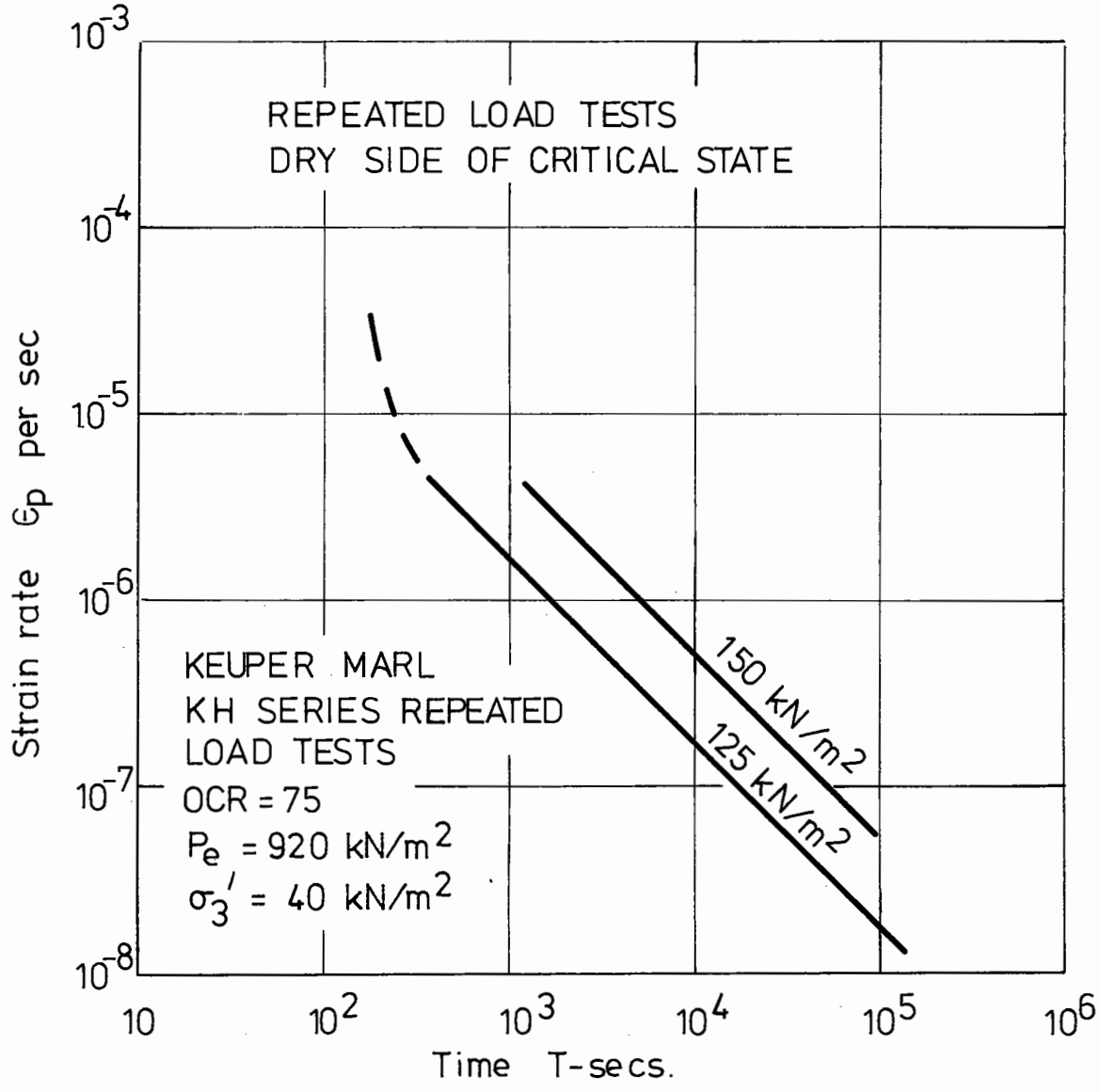

Fig. 6.41 Mean variation of strain rate with time.

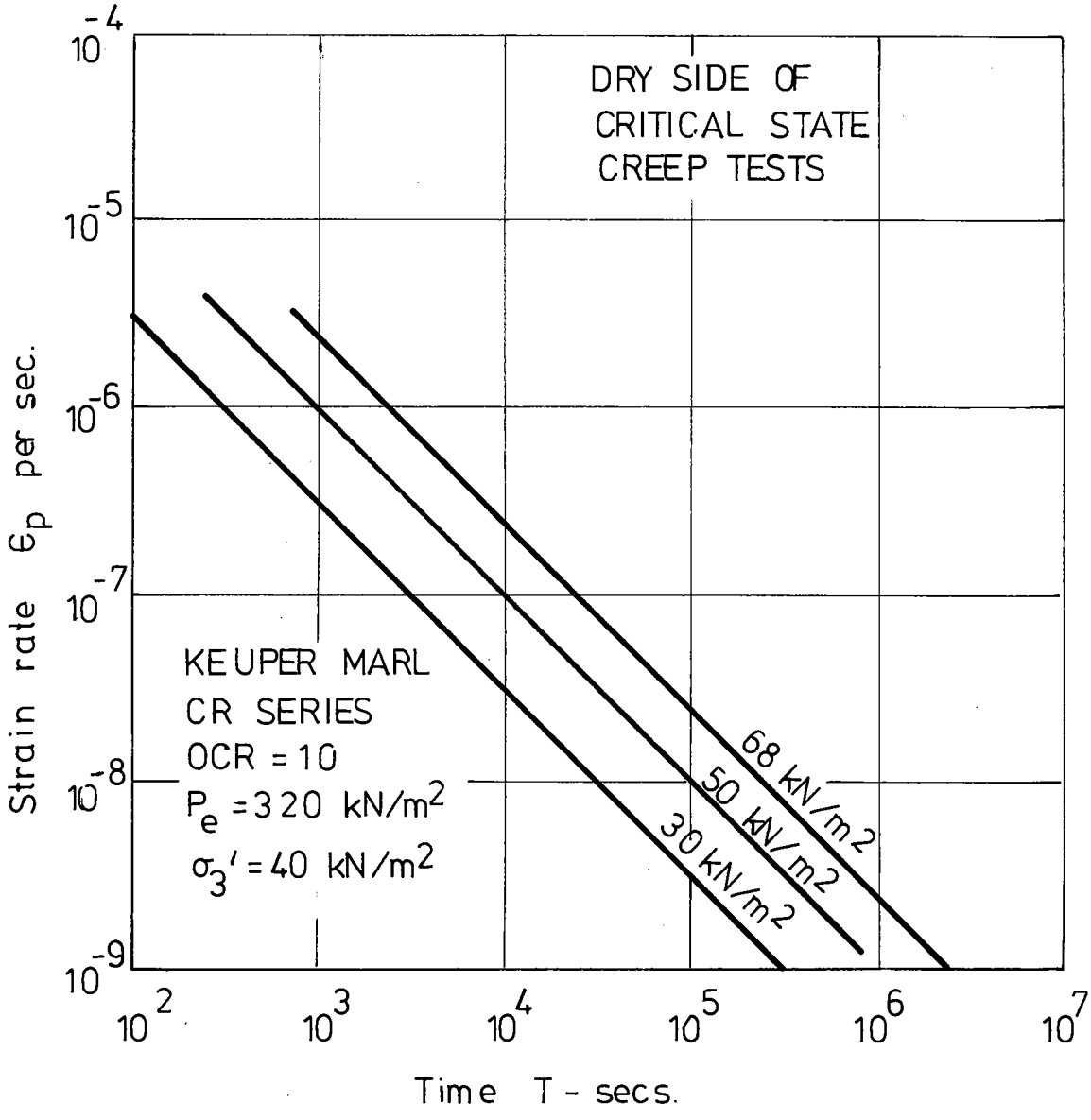

Fig. 6.42 Mean variation of strain rate with time.

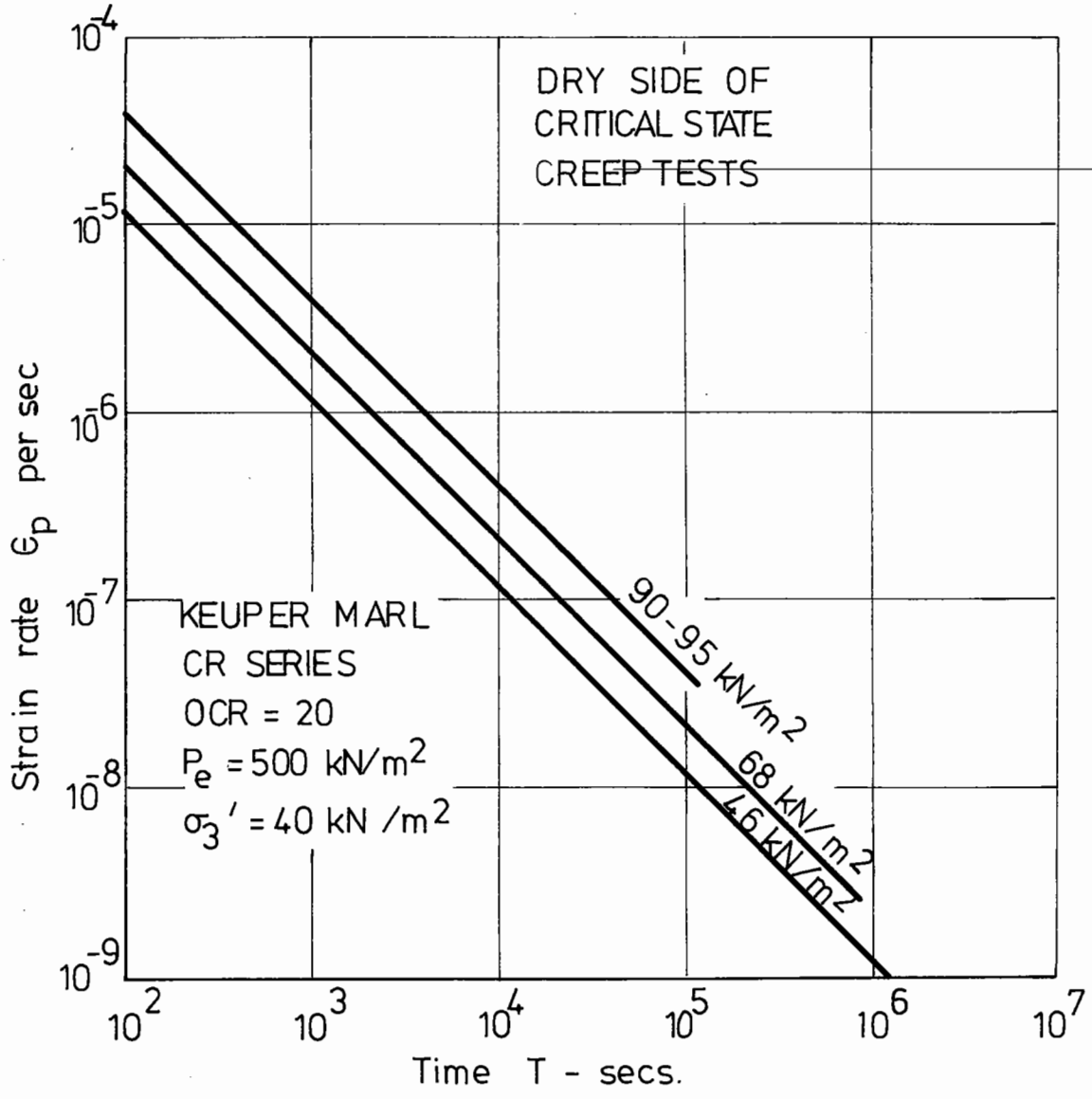

Fig. 6.43 Mean variation of strain rate with time.

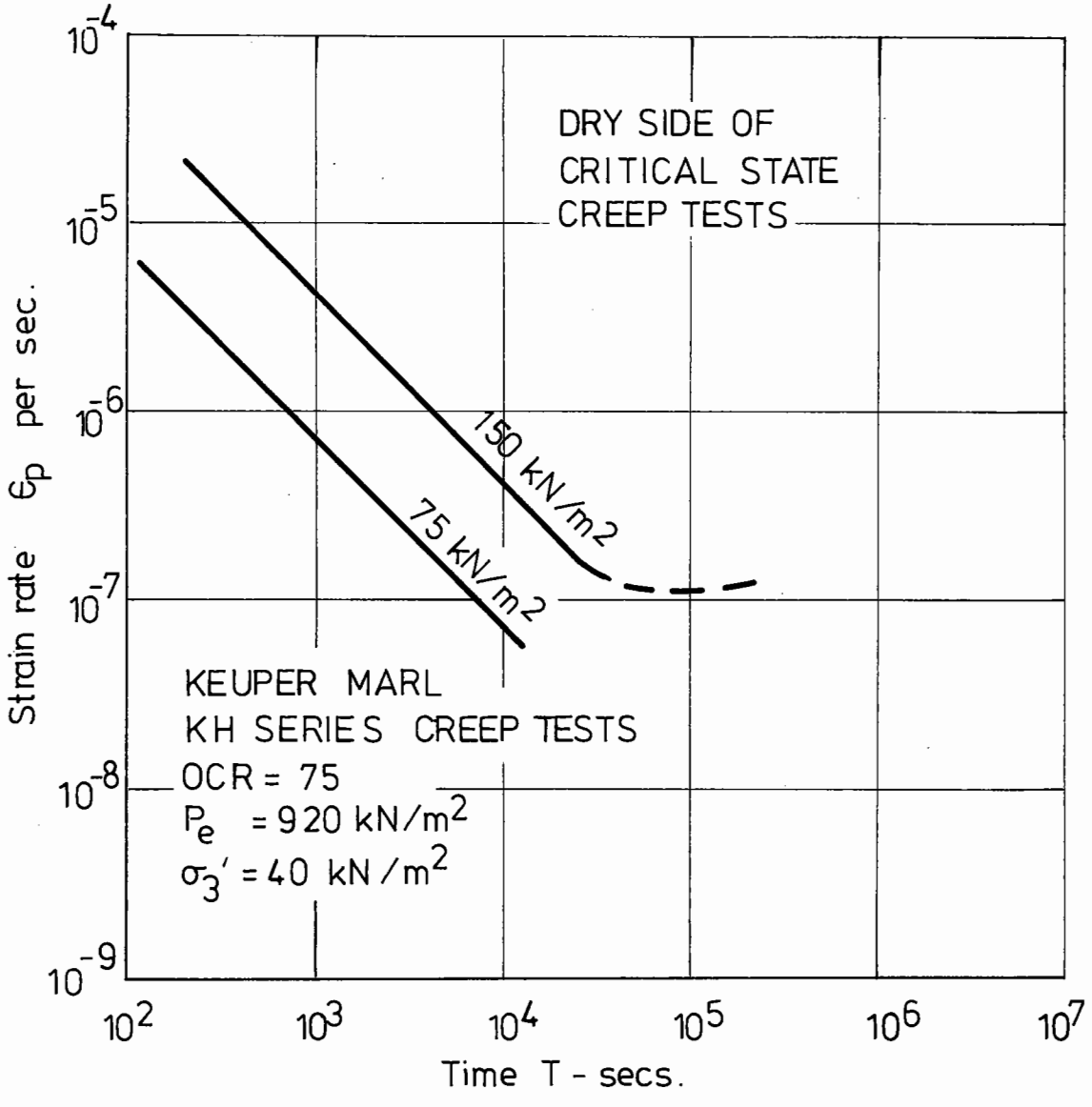

Fig. 6.44 Mean variation of strain rate with time.

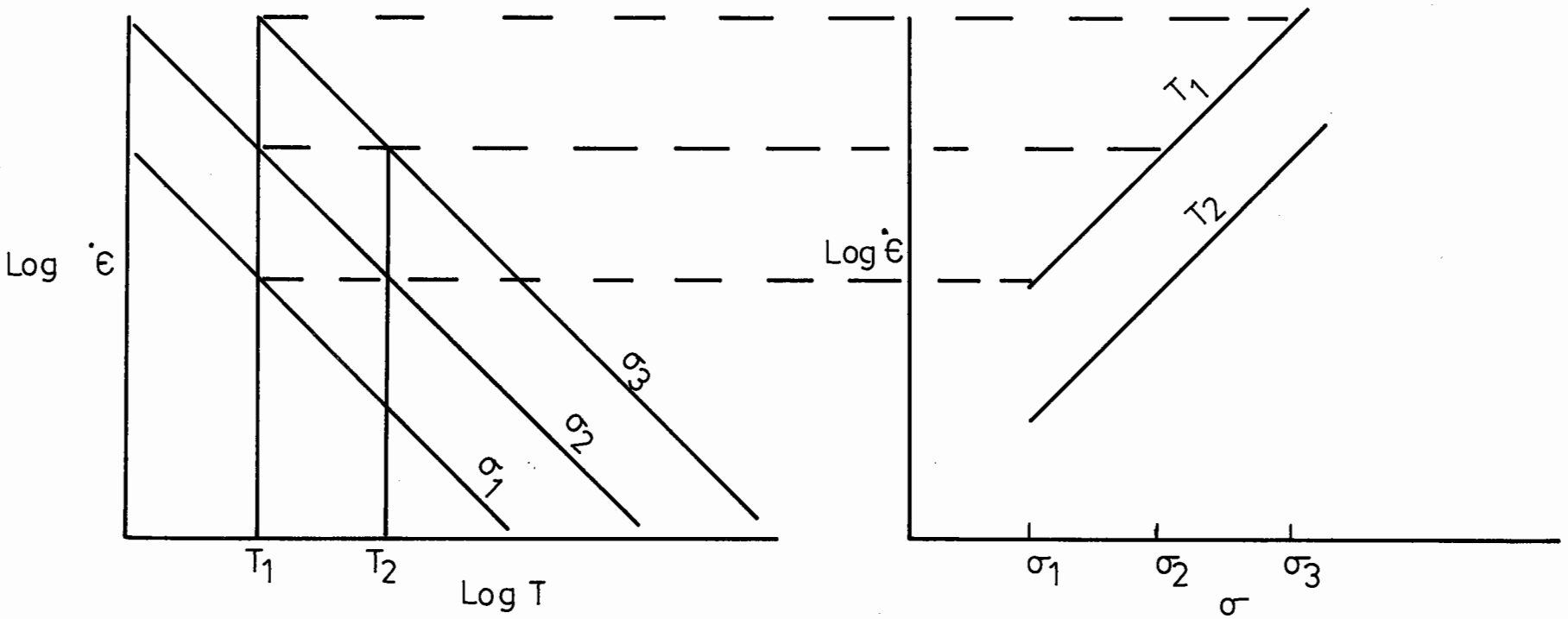

Fig. 6.45 Derivation of function for variation of strain-rate with respect to stress.

Test No.	OCR	Actual ϵ_p	ϵ_p initial predicted	ϵ_p accumulated predicted $q/\sqrt{p_e}$ model	ϵ_p total predicted
KA13	10	0.13	0.1	0.19	0.29
KA14	10	0.05	0.1	0.17	0.27
KA15	10	0.59	0.25	0.49	0.74
KA16	10	0.85	0.25	0.49	0.74
KA17	10	3.47	1.0	-	-
KA18	10	1.24	0.4	1.56	1.96
KA1802	10	Failed	-	34	Failed
KA20	20	0.59	0.3	0.35	0.65
KA19	20	0.53	0.3	0.35	0.65
KA21	20	2.20	0.9	1.63	2.53
KA22	20	1.78	0.8	1.97	2.77
KA23	20	Failed	2.0	14.9	Failed
KA24	20	7.77	2.1	7.9	10.0
KA25	20	6.59	2.1	7.9	10.0
KA31R	10	3.04	0.5	1.76	2.26
KA31	10	2.1	1.0	1.0	2.0
KA33R	20	3.49	1.4	3.06	4.46

Table 6.6 Predicted and Actual Total Strains for the "Dry" Side

The mean error from the regression line = 0.005

Standard deviation = 1.09

Variance = 1.20

Considering first the prediction of accumulated strain, Fig. 6.64, it can be seen that the systematic deviation from a true prediction is of the order of 10% plus a small constant value. When a further step is added and the total strain is predicted, this systematic deviation increases to 16%. Providing the assumption of normal distribution is a correct one, then 64% of the predicted values of total strain for the dry side will be within 16% of the actual value $\pm$ 1.09% and for the accumulated strain 64% of the predicted values will lie within 10% of the actual value $\pm$ 1.1%.

It was not found possible to quantify the degree to which the variability was due to experimental error or to inherent variability of the material behaviour.

6.5.6(b) Model for repeated load tests on the "wet" side

A similar model to that already explained for the "dry" side was developed for samples on the wet side of the critical state. The variation of the strain rate with the stress parameter $q.p_e^{-\frac{1}{2}}$ is shown in Fig. 6.66 for both creep and repeated load tests (see Tables 6.7 and 6.8). The functions governing α' (see equation (6.15)) are given below:

$$\text{Repeated load:} \quad \alpha' = 0.254\ q.p_e^{-\frac{1}{2}} - 8.78 \qquad (6.20)$$

$$\text{Creep:} \quad \alpha' = 0.485\ q.p_e^{-\frac{1}{2}} - 8.78 \qquad (6.21)$$

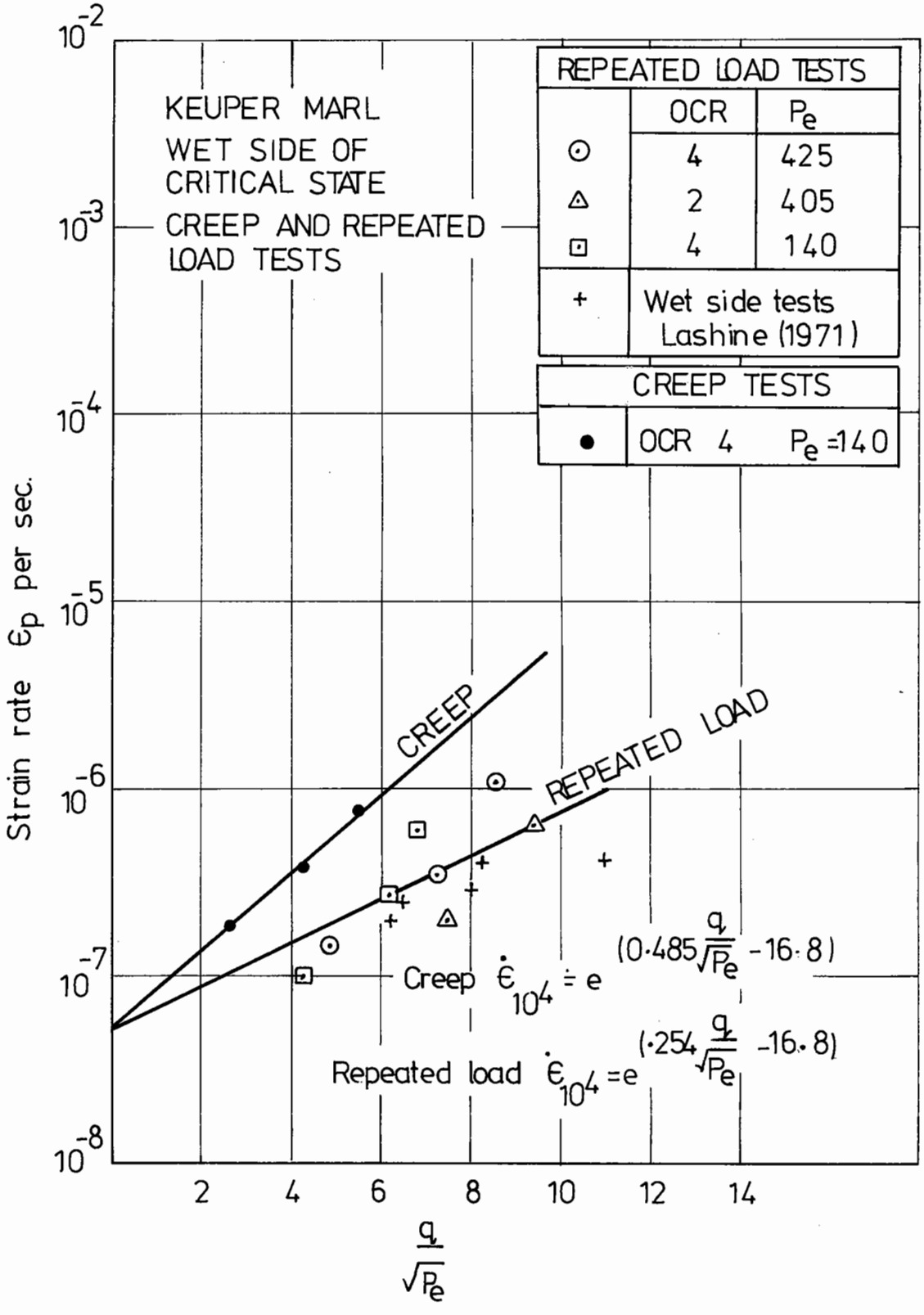

Fig. 6.66 Variation of strain rate with normalised deviator stress at 10^4 secs for wet side (creep and repeated load tests).

OCR	p_e	q	$q/\sqrt{p_e}$	$\dot{\varepsilon}$ @ 10^4 secs
4	425	100	4.85	1.6×10^{-7}
4	425	150	7.27	3.6×10^{-7}
4	425	175	8.48	1.1×10^{-6}
2	405	150	7.45	2.0×10^{-7}
2	405	190	9.44	6.6×10^{-7}
4	140	50	4.23	1.0×10^{-7}
4	140	75	6.34	2.7×10^{-7}
4	140	80	6.76	6.2×10^{-7}
2	555	152	6.45	2.5×10^{-7} *
2	555	193	8.19	4.0×10^{-7} *
4	628	155	6.18	2.0×10^{-7} *
4	628	200	7.98	2.9×10^{-7} *
4	628	272	10.85	4.1×10^{-7} *

* Lashine et al (1971)

Table 6.7 Strain rates for repeated load tests "wet" side

OCR	p_e	q	$q/\sqrt{p_e}$	$\dot{\varepsilon}$ @ 10^4 secs
4	140	30	2.54	1.8×10^{-7}
4	140	50	4.23	3.7×10^{-7}
4	140	65	5.49	7.9×10^{-7}

Table 6.8 Strain rates for creep tests "wet" side

Fig. 6.67 compares the derived theoretical repeated load line with the actual creep and repeated load lines. It can be seen that in this case as opposed to the case for the "dry" side, the theoretical line lies above the actual line.

The value of λ used for the wet side was 0.87. By substituting α' for α in equation (6.11) the accumulated plastic strain between 10^3 and 10^6 cycles was predicted for repeated loading (Table 6.9, Fig. 6.68). As for the dry side, data from Lashine et al (1971) is included and shows good agreement with the author's tests. The regression line through the points shown in Fig. 6.68, for the range considered, lies very close to the line for a correct prediction. The author does not consider that there is any significant systematic deviation from the model proposed.

6.5.7 Plastic Strain Related to Sample Strength

It has already been shown in Section 6.4.2 that the equivalent pressure p_e is directly related to the sample strength q_f obtained from a strain controlled test. The functions for α' used in the prediction models for both "dry" and "wet" sides can, therefore, be considered as functions of q and q_f.

If the normalised stress paths and strain contours for strain controlled tests plotted in Fig. 6.6 are examined, it can be seen that for a given mobilised proportion of q_f the strain is less on the "wet" than on

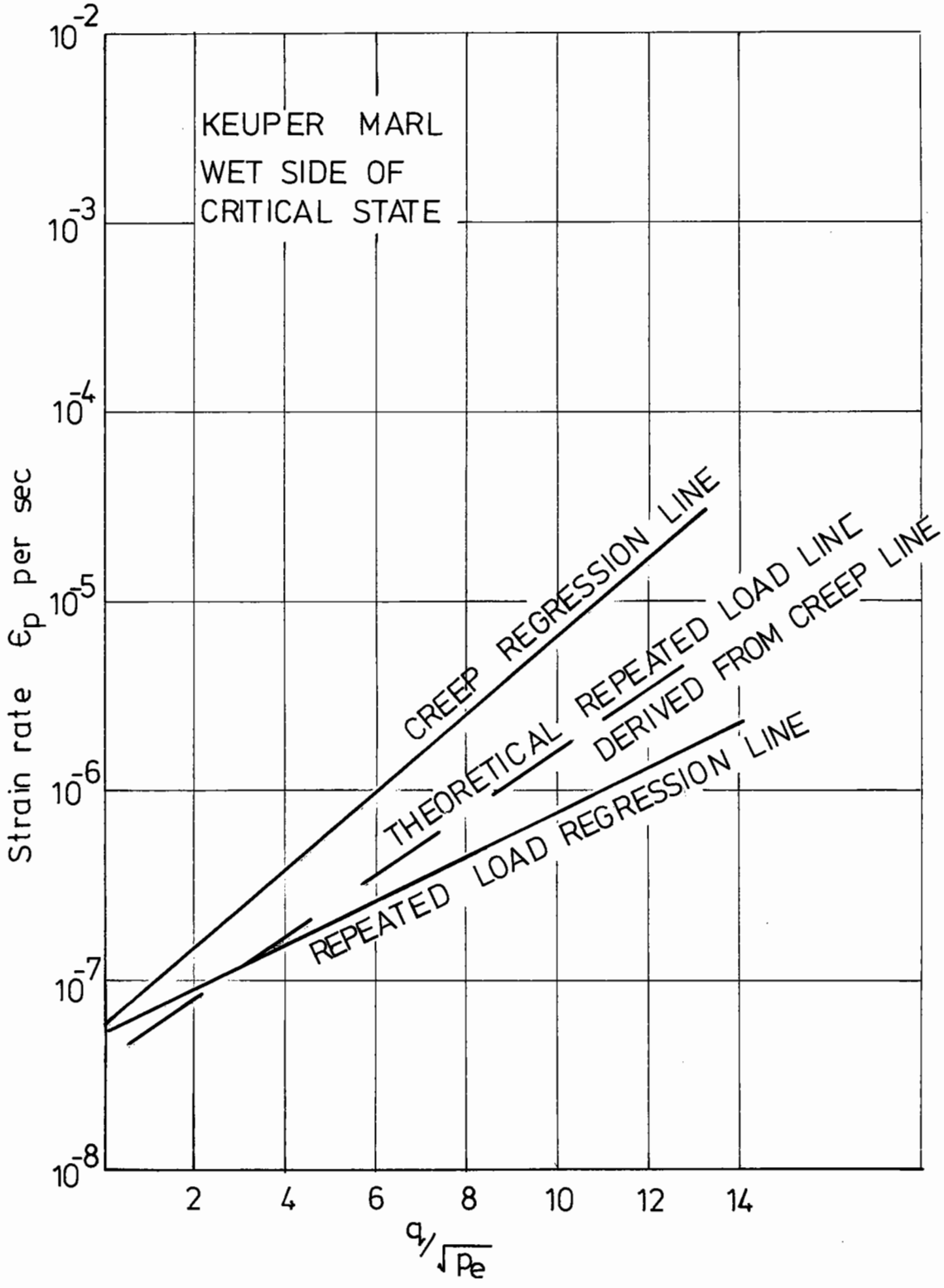

Fig. 6.67 Comparison of creep, repeated load and theoretical repeated load lines for the variation of strain rate with normalized deviator stress.

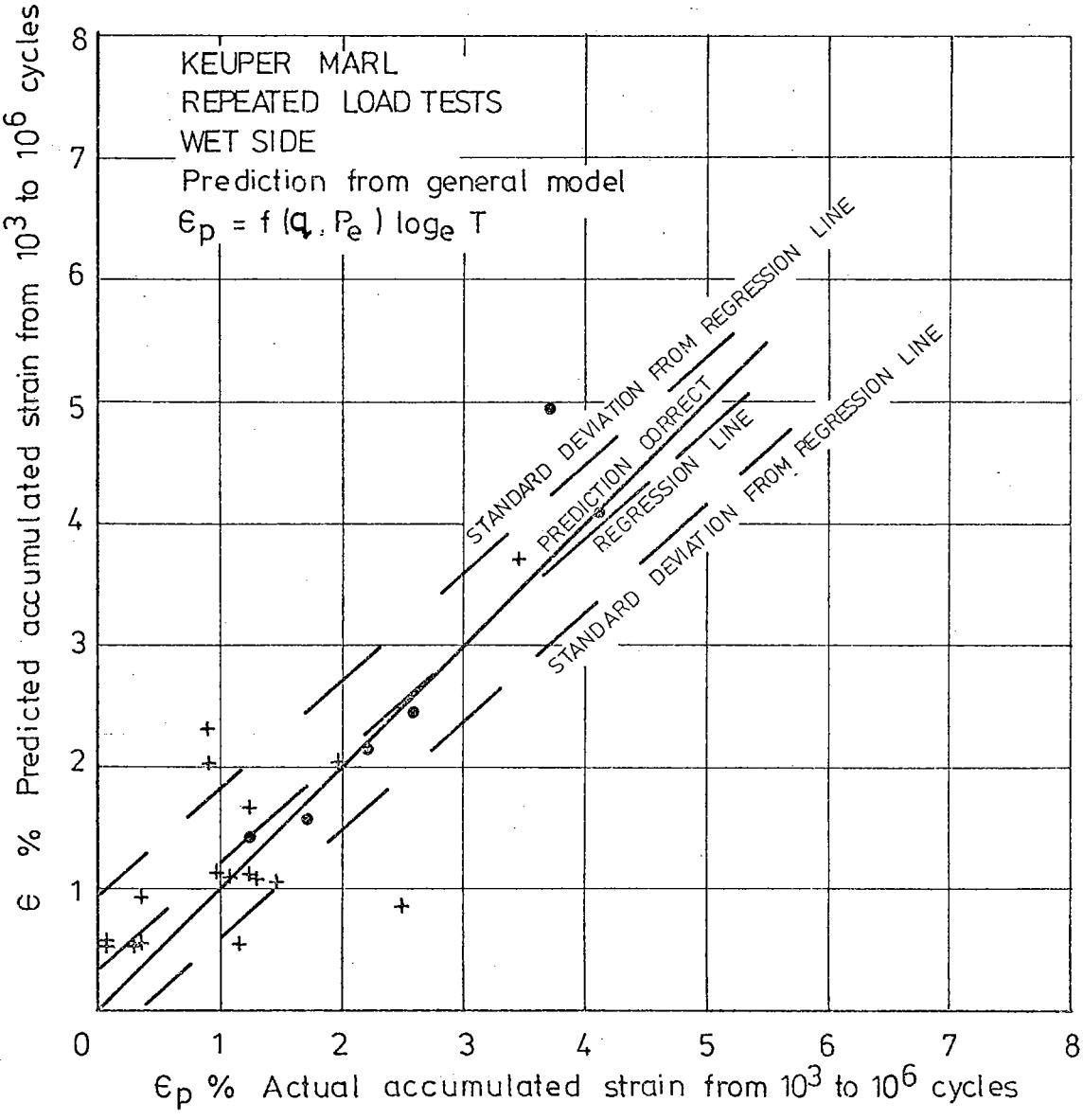

Fig.6.68 Comparison of predicted and actual accumulated strain for repeated load tests (Wet side)

Test No.	OCR	p_e kN/m²	q kN/m²	ε_p% 10^6 cycles	ε_p% 10^6 cycles predicted	Comments
KA703	4	140	27	0.04	0.55	
KA704	4	140	27	0.30	0.55	
KA803	4	140	27	1.13	0.55	
KA9	4	140	57	1.48	1.04	
KA901	4	140	60	0.43	1.11	High friction in seals
KA903	4	140	57	0.21	1.04	High friction in seals
KA10	4	140	-	-	-	Rig failure
KA1001	4	140	60	1.25	1.11	
KA1003	4	140	52	0.34	0.937	
KA1103	4	140	79	1.23	1.67	
KA1203	4	140	75	1.43	1.53	High friction in seals
KA13	4	140	26	0.13	0.53	High friction in seals
KA14	4	140	26	0.05	0.53	
KA30	4	140	80	2.5	0.85	Values for 10^5 cycles
KB1	2	405	104	0.36	0.57	Values for 10^5 cycles
KB2	2	405	195	-	3.58	Failed
KB3	2	405	152	0.81	2.08	
KB4	2	405	160	0.87	2.3	
KB5	2	405	195	-	3.58	Failed
KB6	2	405	198	3.45	3.72	
KB7	2	405	103	0.98	1.12	
KB9	4	425	153	1.97	2.01	
KB10	4	425	103	1.11	1.09	
KB11	4	425	101	1.28	1.06	
KB12	4	425	190	-	3.18	Failed
Lashine et al (1971)	2	628	152	1.2	1.43	
"	2	628	193	2.2	2.16	
"	2	628	275	3.7	4.96	
"	4	555	152	1.7	1.57	
"	4	555	193	2.6	2.45	
"	4	555	241	4.1	4.11	

Table 6.9 Predicted and Actual Accumulated Strains for the "Wet" Side

the "dry" side. It would, therefore, be expected that under repeated load conditions the accumulated strain and, therefore, the strain rate at any given time, would also be less for the wet side. Fig. 6.60 shows that for the tests carried out that this was in fact the case.

The sample strength is not, however, an independent variable since it depends on the voids ratio of the clay. p_e can be considered as a measure of the voids ratio and is, therefore, a more fundamental parameter than the sample strength.

6.5.8 The Effect of Rest Periods on the Accumulation of Plastic Strain

Many engineering situations involving repeated loading of soil have rest periods interspersed between trains of load pulses. A series of tests was, therefore, carried out on the Keuper marl to determine the effects of the length of the rest periods and the number of load pulses between rest periods.

It is necessary to re-examine the concept of resilient modulus since rest period loading indicated a considerable delayed elastic response existed for the saturated marl.

The variation of plastic strain with number of cycles for lightly over-consolidated marl takes the same form under rest period loading as it does under continuous loading (see Figs. 6.69 to 6.71). The length of rest period or the number of cycles between rest periods do not cause any consistent trend as far as the accumulation of plastic strain is concerned.

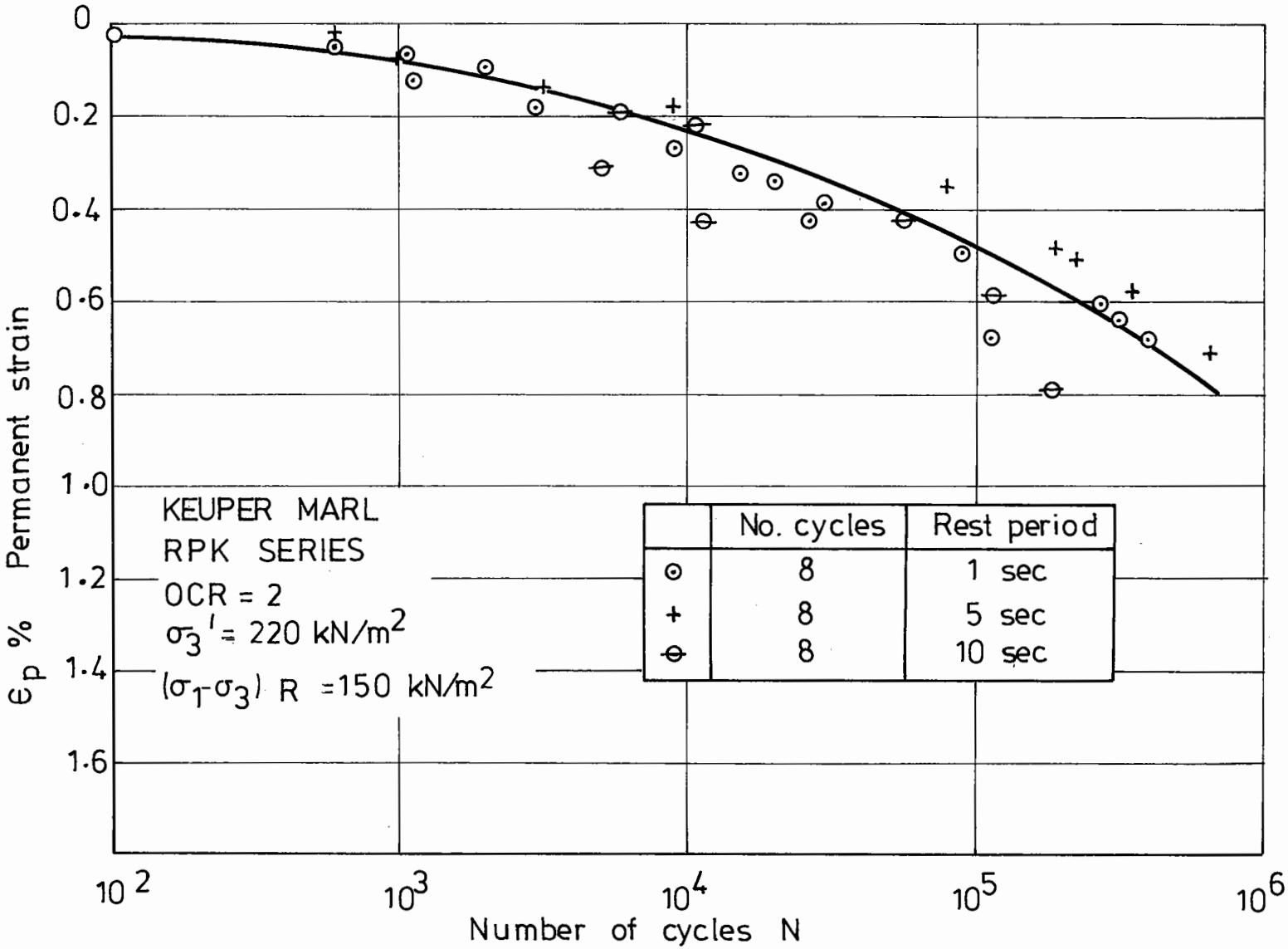

Fig. 6.69 Effect of rest periods on the variation of plastic strain with number of load applications.

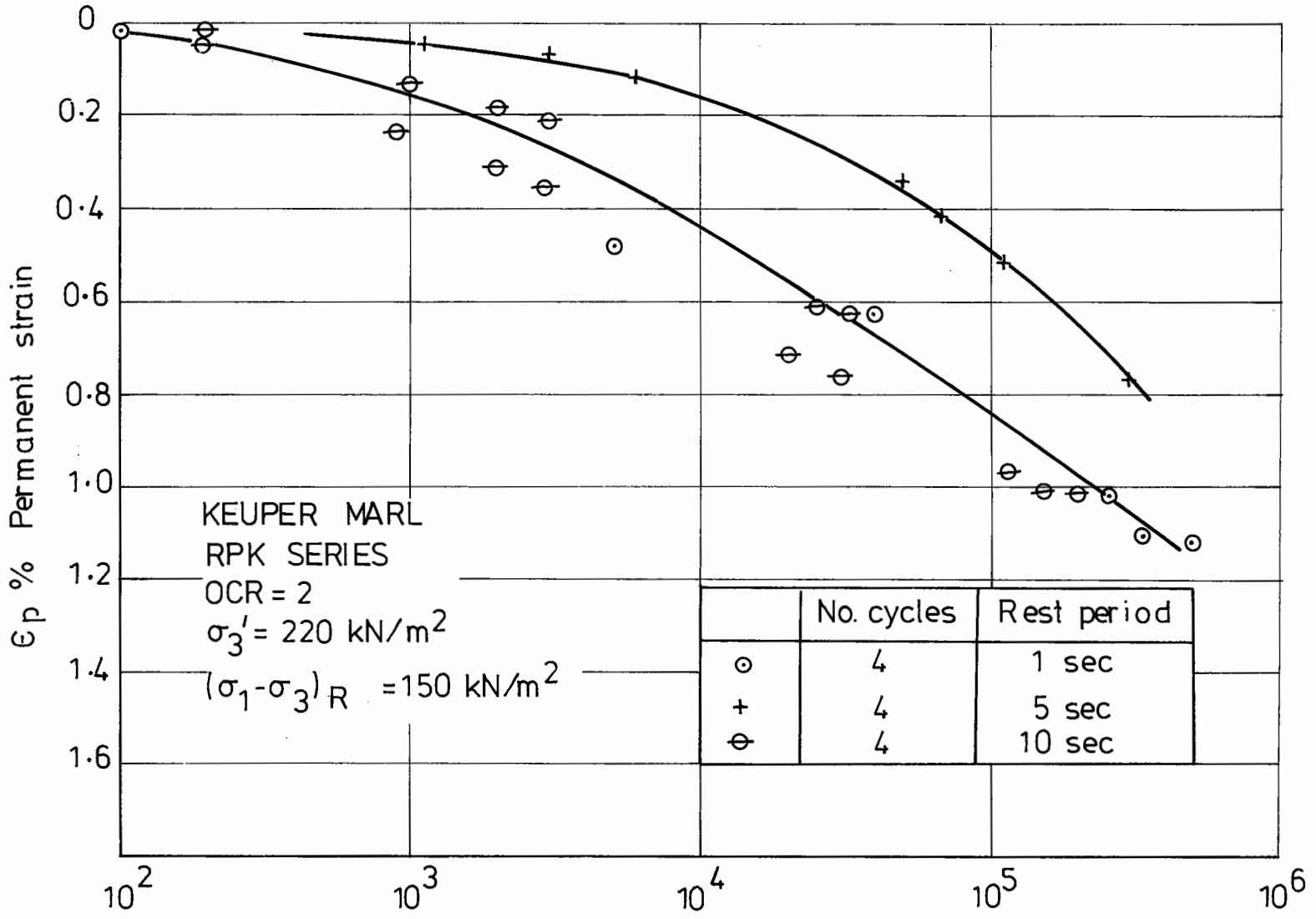

Fig. 6.70 Effect of rest periods on the variation of plastic strain with number of load applications.

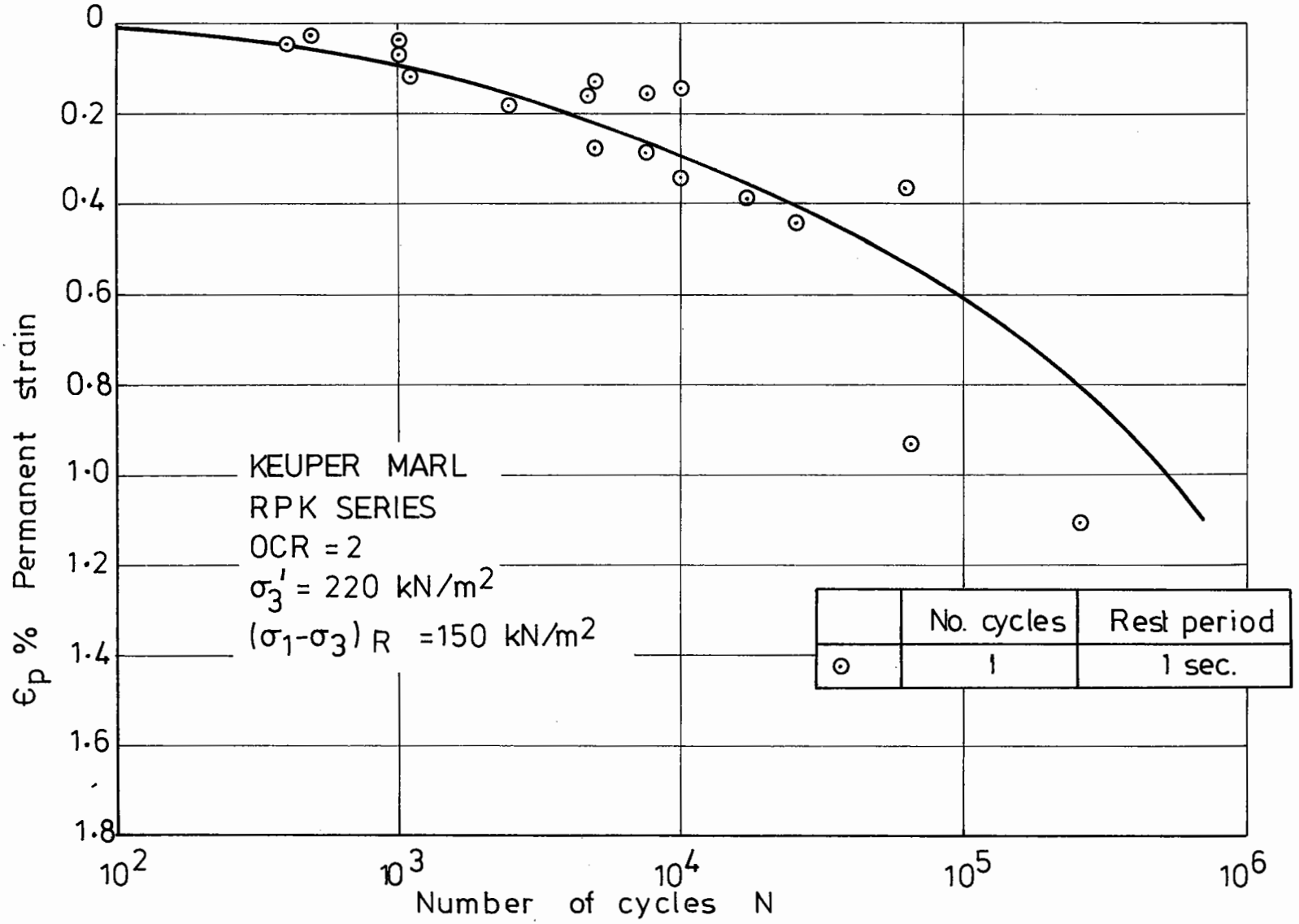

Fig 6.71 Effect of rest periods on the variation of plastic strain with number of load applications.

For the purposes of comparison of rest period loading with continuous loading the strain rate was plotted against the loading time on a log-log basis (Figs. 6.72 to 6.74). Comparison of the strain rates for samples on the "wet" side suggests that there is a slight tendency for rest period loading to cause an increase in the strain rate (and hence the strain) as most of the points lie above the line for continuous loading; the difference is not, however, considered to be significant.

In addition to carrying out tests on a lightly over-consolidated marl on the wet side a limited number of tests were carried out on samples consolidated to the dry side. Strains accumulated on these samples are tabulated in Table 6.10. The loading for these tests consisted of eight maximum deviator stress pulses of 75 kN/m^2 followed by differing lengths of rest period. Strain rates for rest period loading generally lie between the lines drawn for continuous loading at maximum deviator stresses of 70 kN/m^2 and 80 kN/m^2 (Figs. 6.75 to 6.77). There was no significant change in the strain rates for rest periods of different lengths. Similar findings are reported by Newland (1971) who, when investigating a normally consolidated clay, showed that the imposition of a rest period in a "creep" test gave no real effect in terms of the plastic strain developed with time.

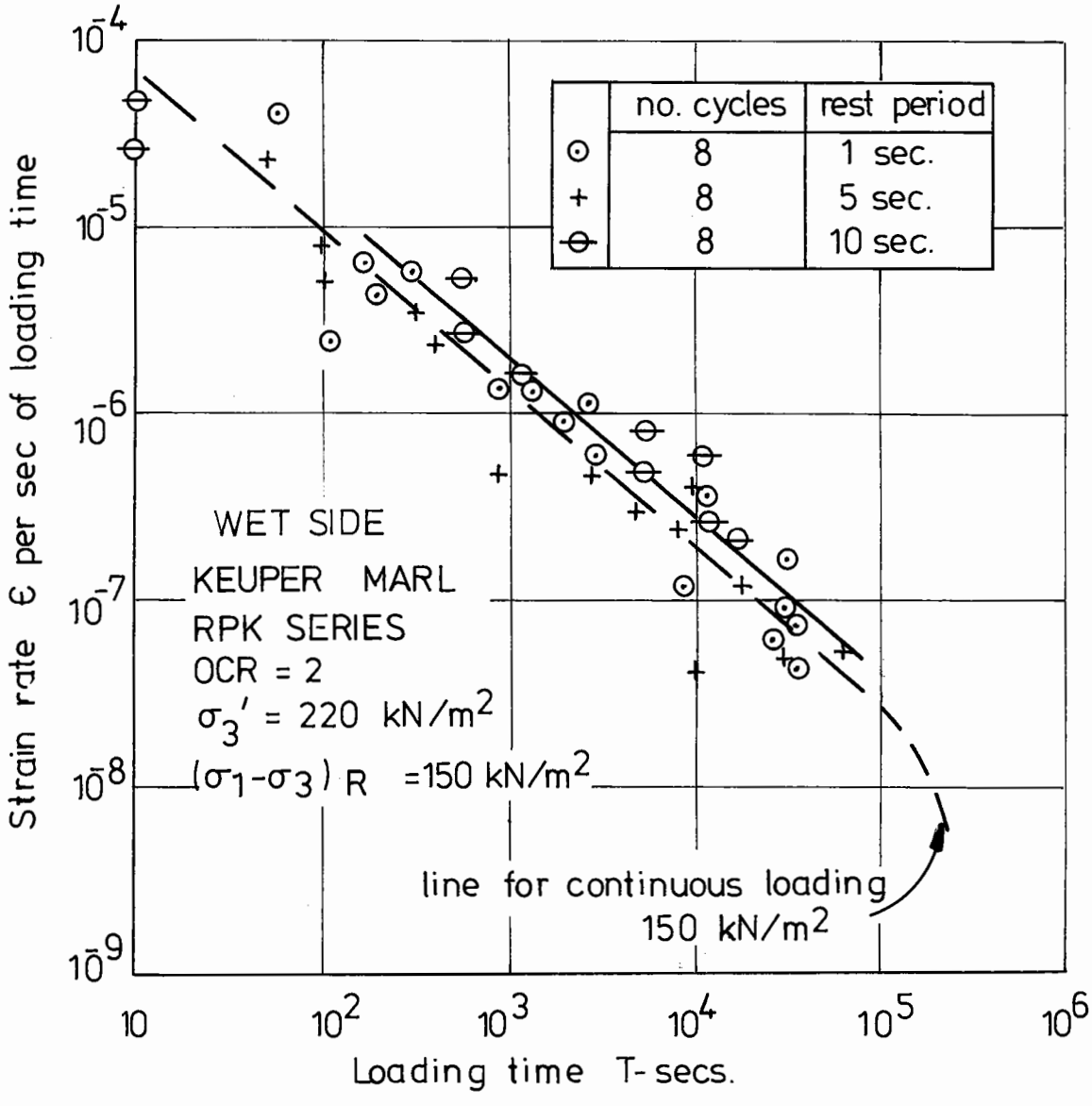

Fig. 6.72 Strain rate variation under rest period loading.

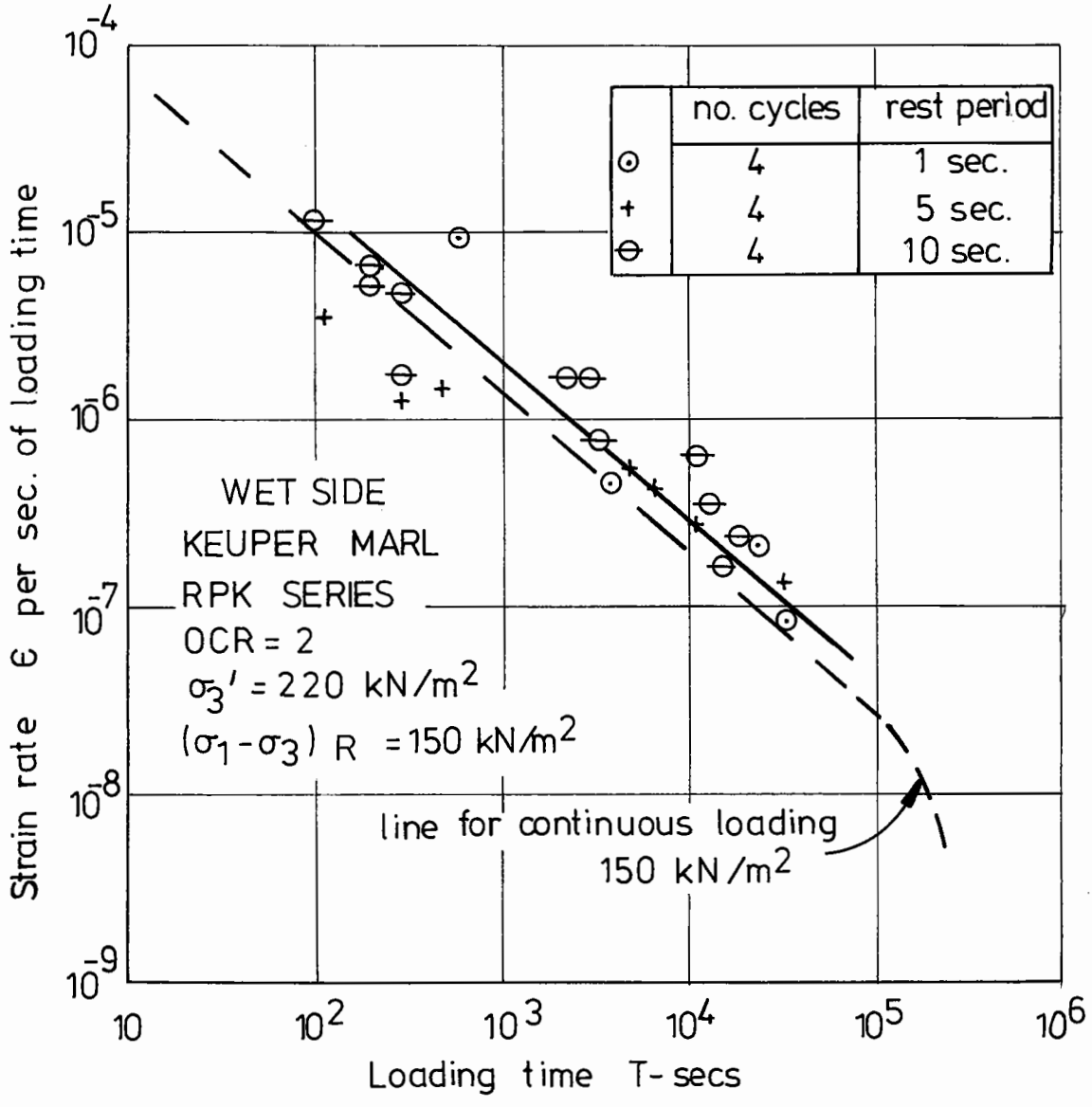

Fig. 6.73 Strain rate variation under rest period loading

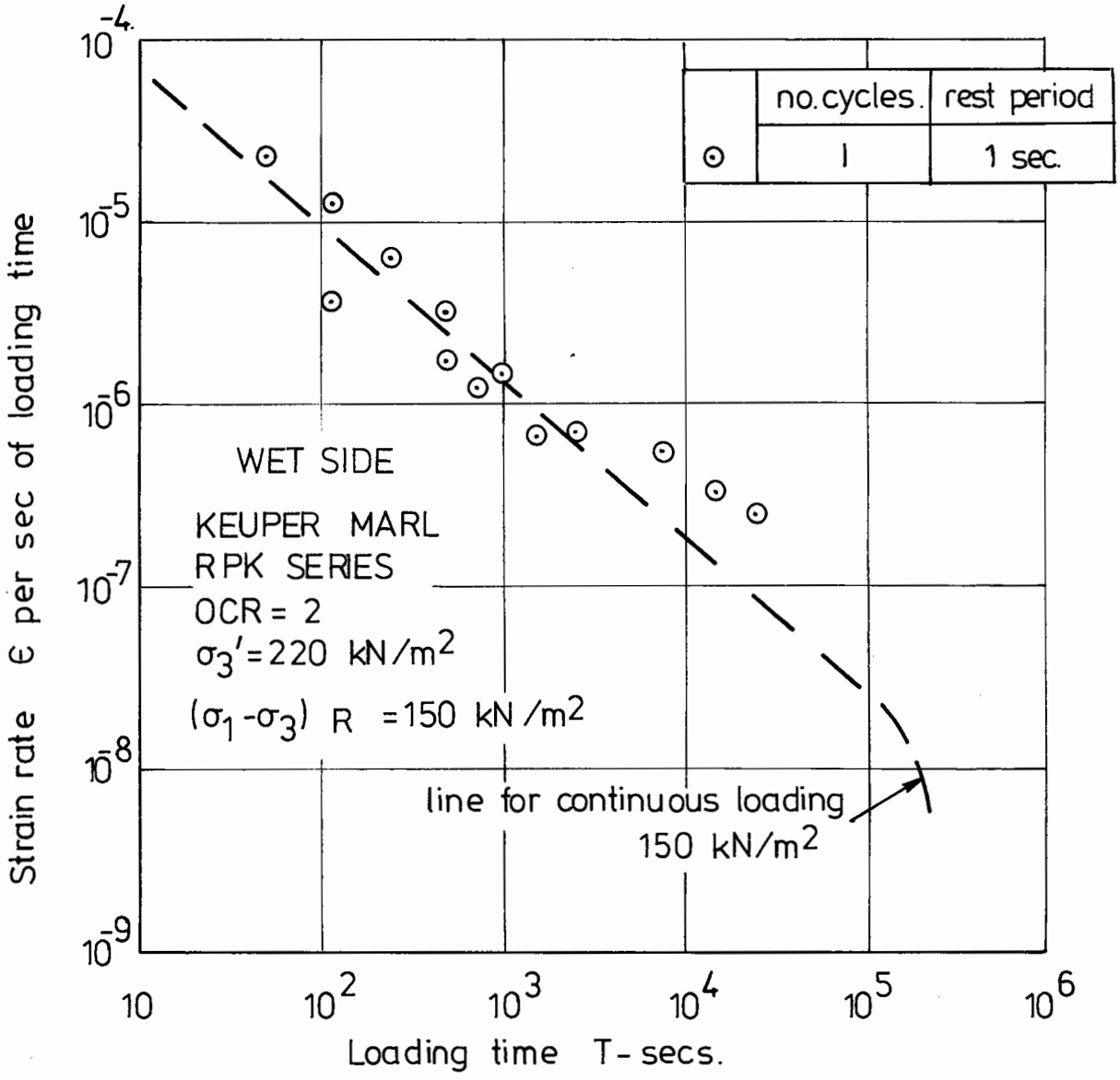

Fig. 6.74 Strain rate variation under rest period loading.

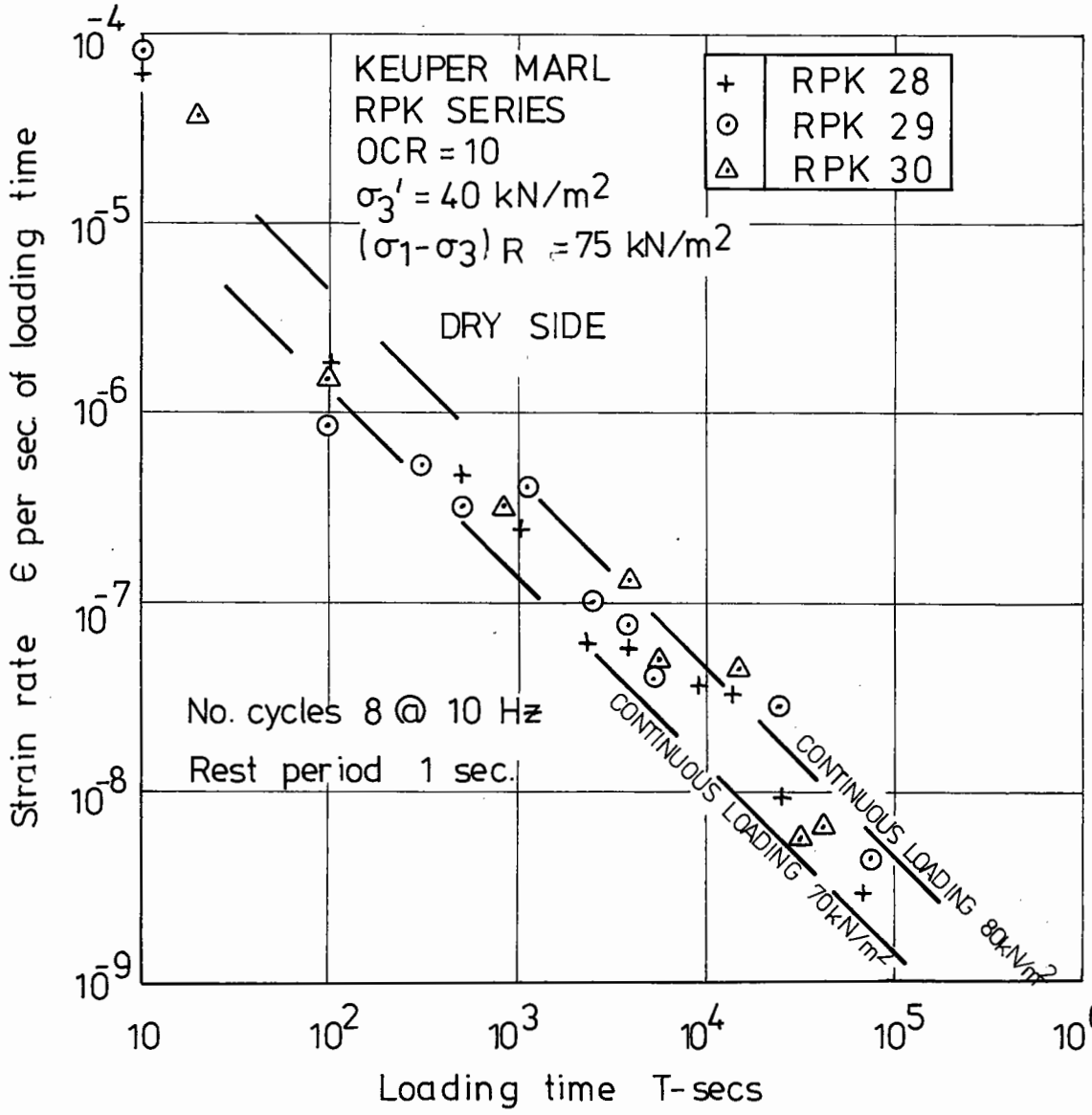

Fig.6·75 Strain rate variation under rest period loading.

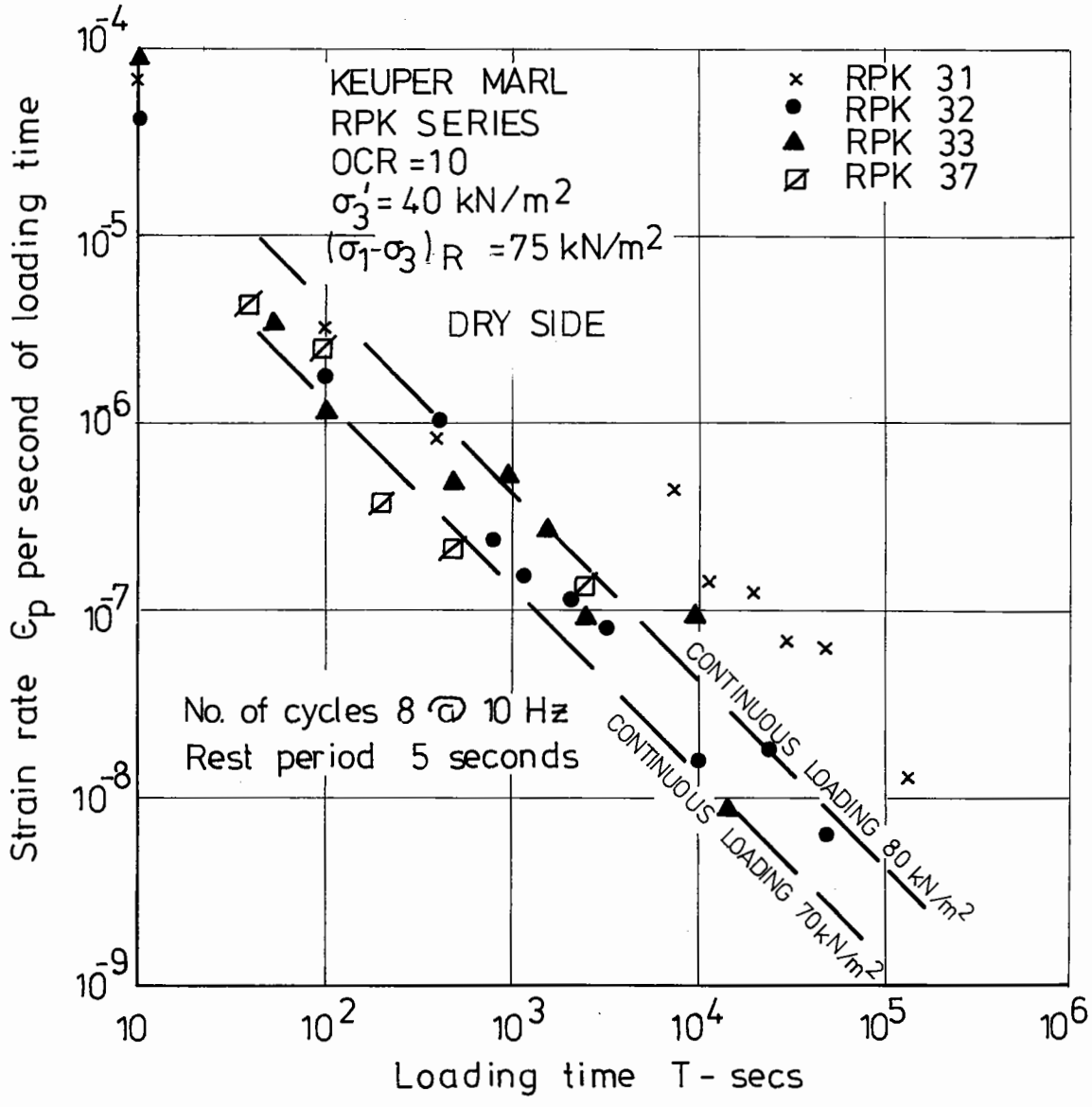

Fig. 6.76 Strain rate variation under rest period loading.

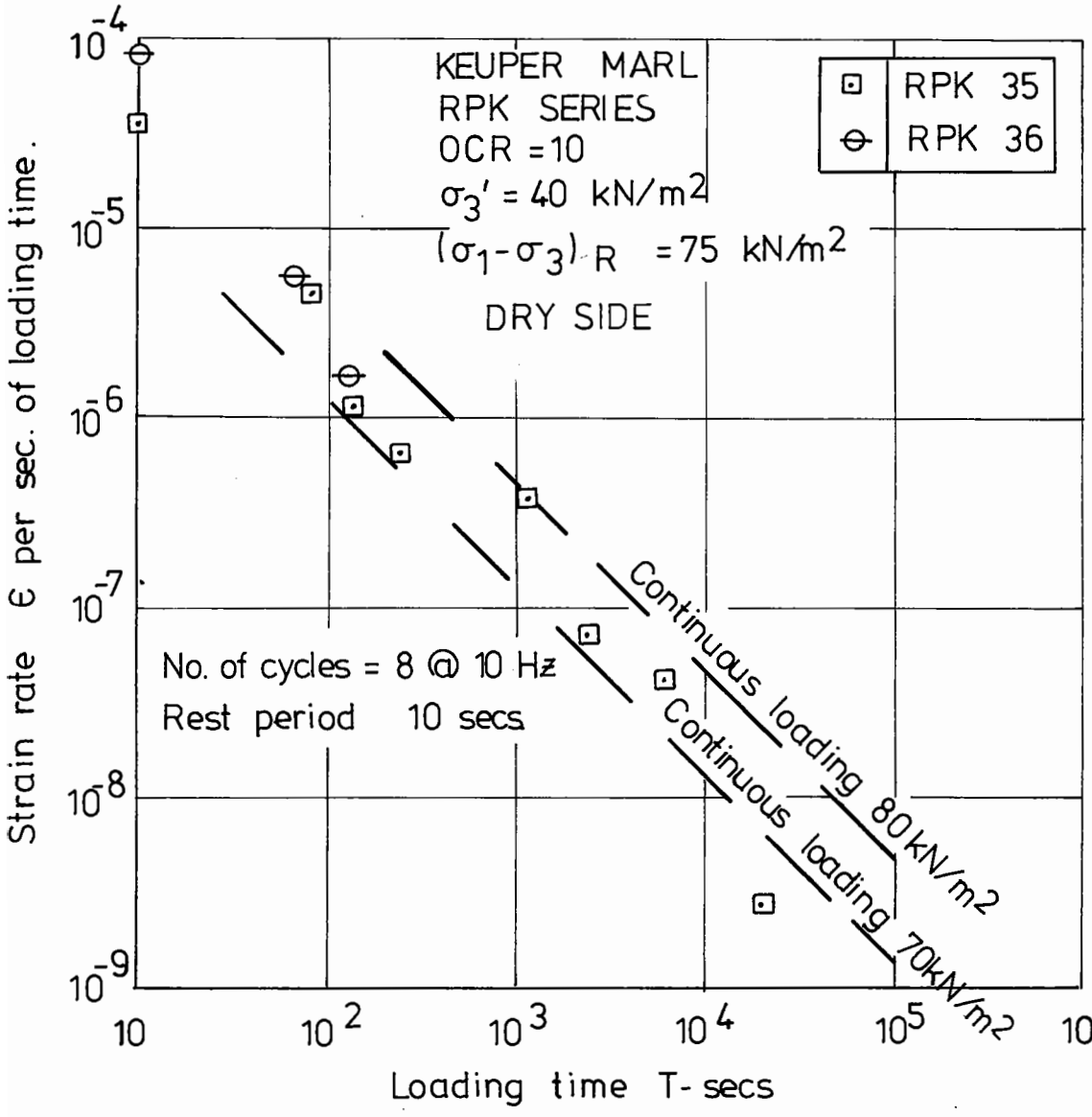

Fig. 6·77 Strain rate variation under rest period loading.

Test No.	OCR	Repeat Period		q_{max} kN/m^2	ε_p% accumulated from 1 to 10^4 cycles	ε_p% accumulated from 1 to 10^5 cycles	ε_p% total @ 10^5 cycles
		No. of Cycles	Rest Period				
RPK 28	10	8	1 sec	75	0.5	1.23	1.8
RPK 29	10	8	1 sec	75	0.48	1.0	1.8
RPK 30	10	8	1 sec	75	0.4	0.85	1.4
RPK 31	10	8	5 sec	75	0.7	3.1	3.76
RPK 32	10	8	5 sec	75	0.7	1.07	1.49
RPK 33	10	8	5 sec	75	0.68	1.75	2.67
RPK 35	10	8	10 sec	75	0.78	1.47	1.79
RPK 36	10	8	10 sec	load drift			
RPK 37	10	8	5 sec	75	0.34	-	-

Table 6.10 Accumulated plastic strain under rest period loading for samples on the "dry" side

6.6 RECOVERABLE DEFORMATION UNDER REPEATED LOADING

When using layered elastic or finite element computer analyses of flexible pavement structures, it is essential to be able to characterise the resilient properties of the subgrade. The current state of knowledge only allows an estimate of the resilient modulus of the unbound materials to be made from a CBR test which is a static test to failure.

It will be shown that for a saturated Keuper marl the resilient deformation is essentially independent of the voids ratio or stress history but is a function of the applied stresses.

Tests using rest period loading have shown a large delayed elastic component which should be allowed for when resilient moduli are being estimated for pavement design purposes.

6.6.1 Resilient Modulus

The resilient modulus is a term that has been commonly adopted to define the stiffness of materials under repeated loading. It is defined as the ratio of the amplitude of the deviator stress to the amplitude of the vertical strain on the sample.

The resilient modulus varies with both stress and time. Values of resilient modulus have been plotted against the number of cycles for some typical tests in Figs. 6.78 to 6.80. The variation of the modulus with time depends on the OCR. For an OCR of 2 there is a considerable decrease in

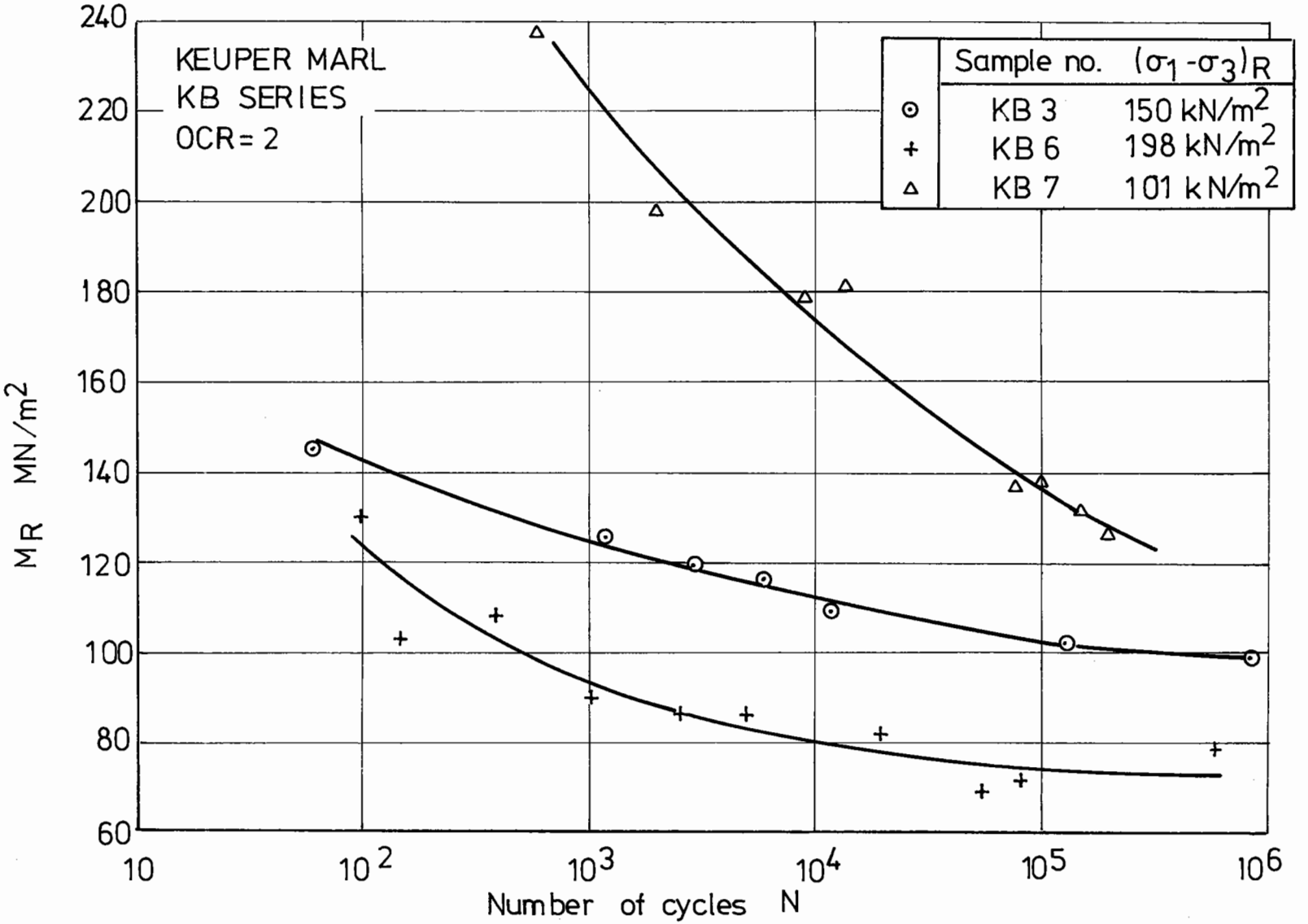

Fig. 6.78 Variation of resilient modulus with number of cycles for lightly overconsolidated keuper marl

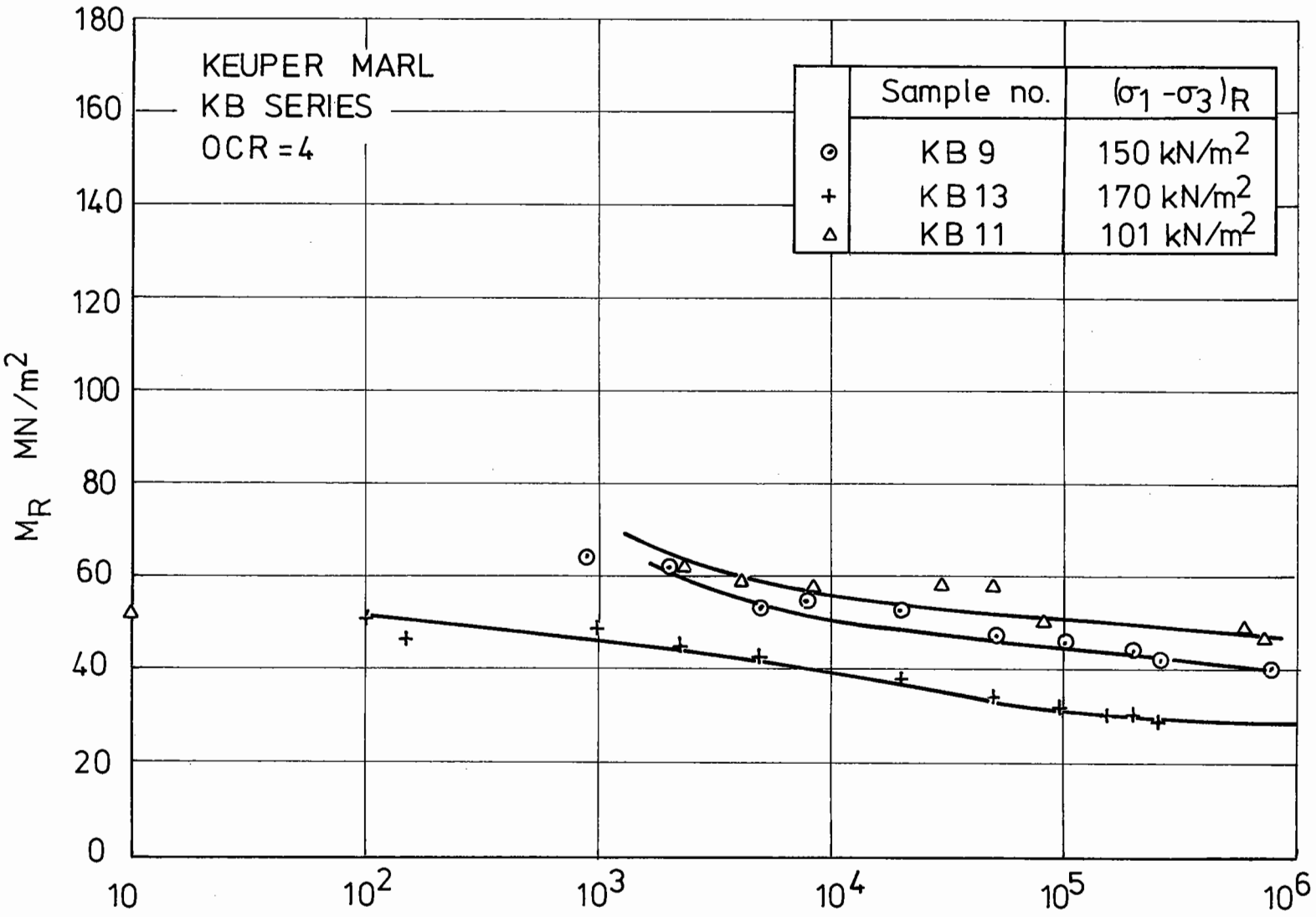

Fig. 6.79 Variation of resilient modulus with number of cycles for overconsolidated keuper marl.

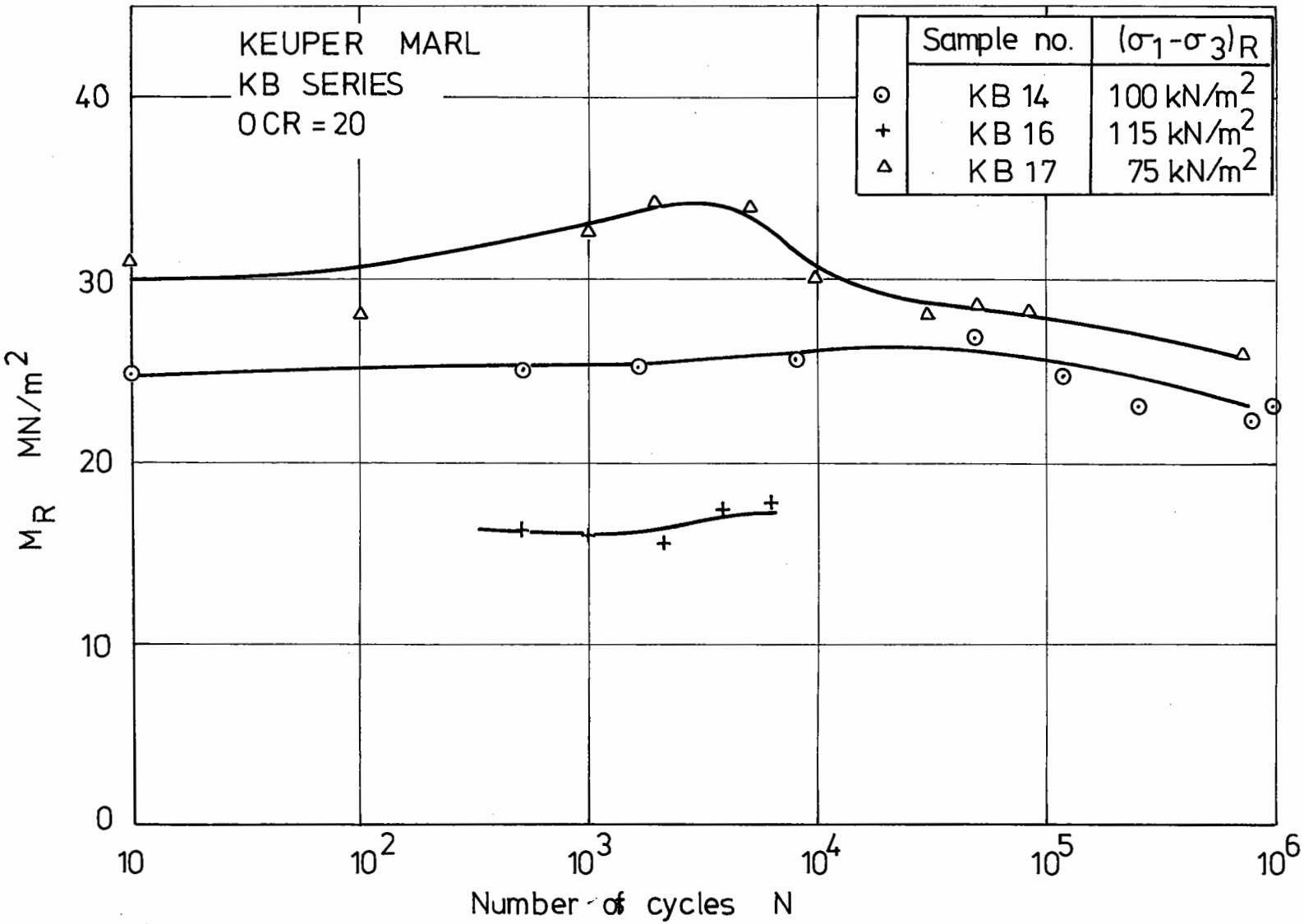

Fig. 6,80 Variation of resilient modulus with number of cycles for heavily overconsolidated keuper marl.

resilient modulus with time. As the OCR increases, the decrease becomes less marked until for a highly over-consolidated clay (Fig. 6.80) there is no marked change at all. It is suggested the decrease in the modulus is due to a decrease in the effective confining stress. This would be far greater for the lightly over-consolidated samples where high pore water pressures are developed compared with the highly over-consolidated samples where virtually no change in pore pressure occurs under repeated load conditions (see Fig. 6.10). In contrast to the stiffening effect of the confining stress, it can be seen that an increase in the deviator stress has a softening effect. Lashine et al (1971) carried out a series of tests which seemed to indicate that the resilient modulus decreased as the OCR increased (Fig. 6.81). However, when the KA series of tests (carried out at a constant initial effective confining stress of 40 kN/m^2) are plotted on the same axes, it can be seen that all three OCR's lie on the same curve. Fig. 6.82 shows the variation of the resilient modulus with the deviator stress for a constant initial confining stress. By replotting the results of Lashine et al (1971) it can be shown that for a given deviator stress the resilient modulus varies directly with the confining stress (Fig. 6.83). By normalising the deviator stress with respect to the initial effective confining stress, it can be seen that both these results and those from the present tests lie approximately on the

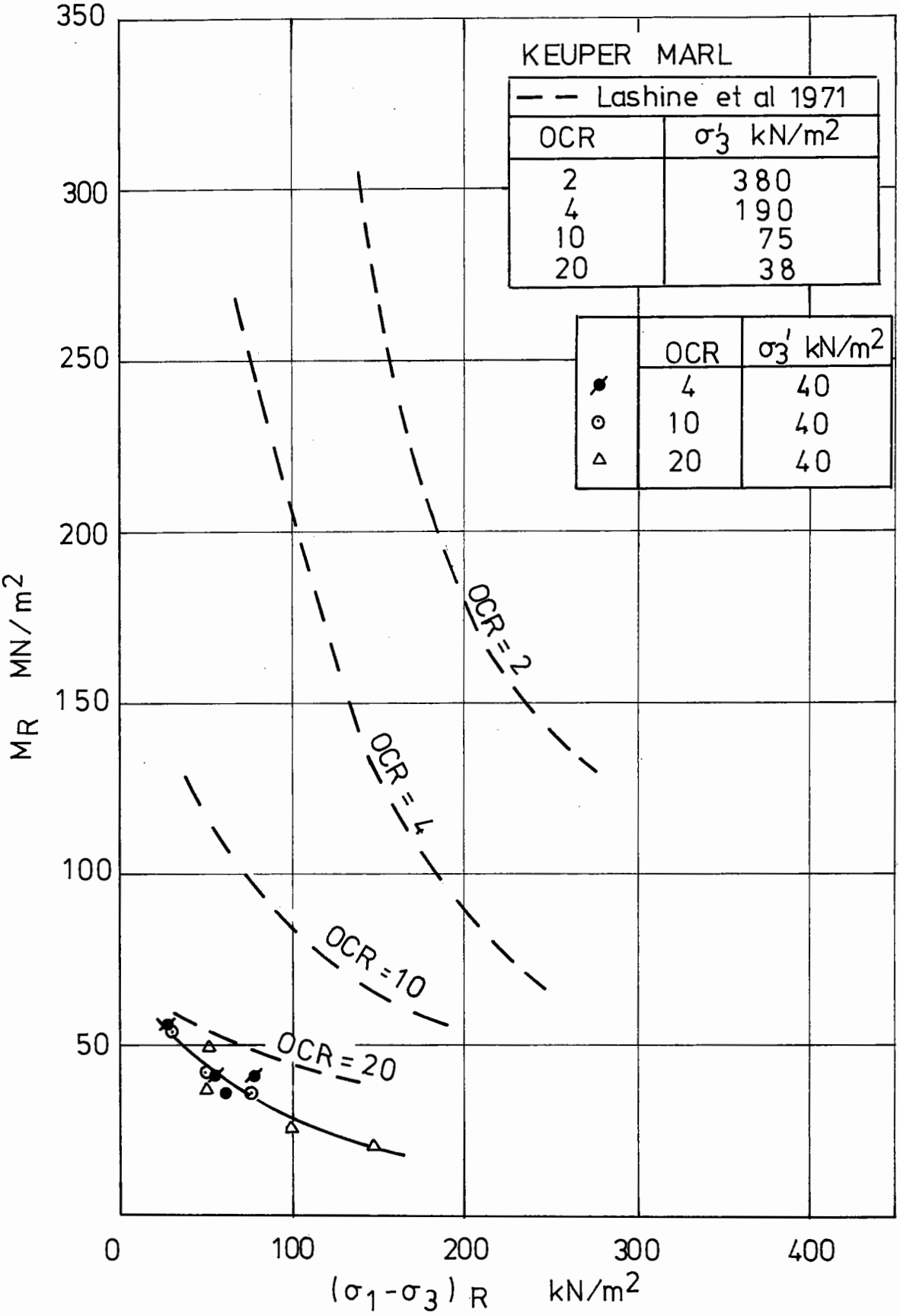

Fig. 6.81 Variation of resilient modulus with deviator stress overconsolidation ratio and effective confining pressure (after 10^5 cycles)

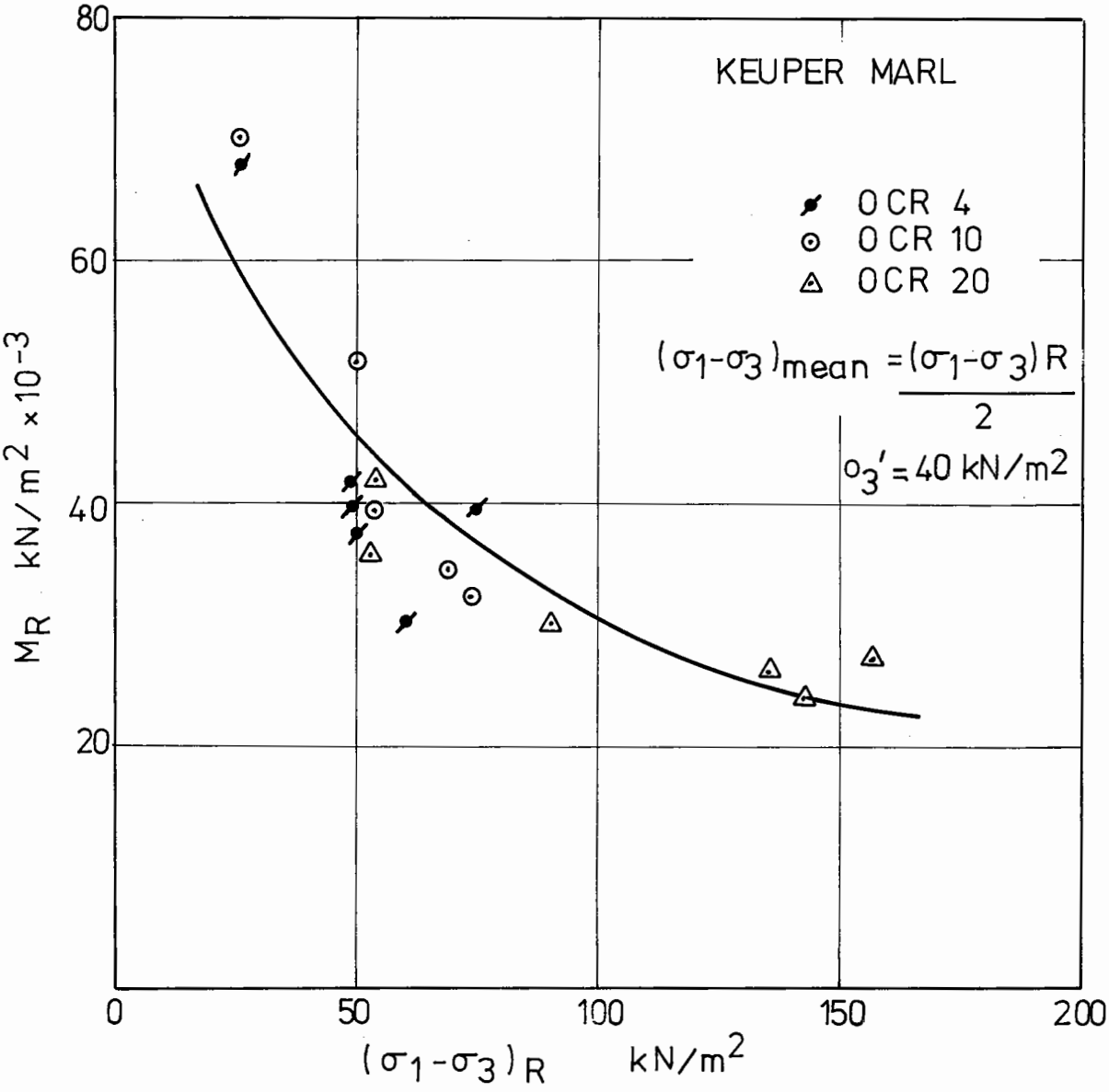

FIG. 6.82 Variation of resilient modulus with cyclic deviator stress for different overconsolidation ratios and constant effective confining pressure (After 10^5 cycles)

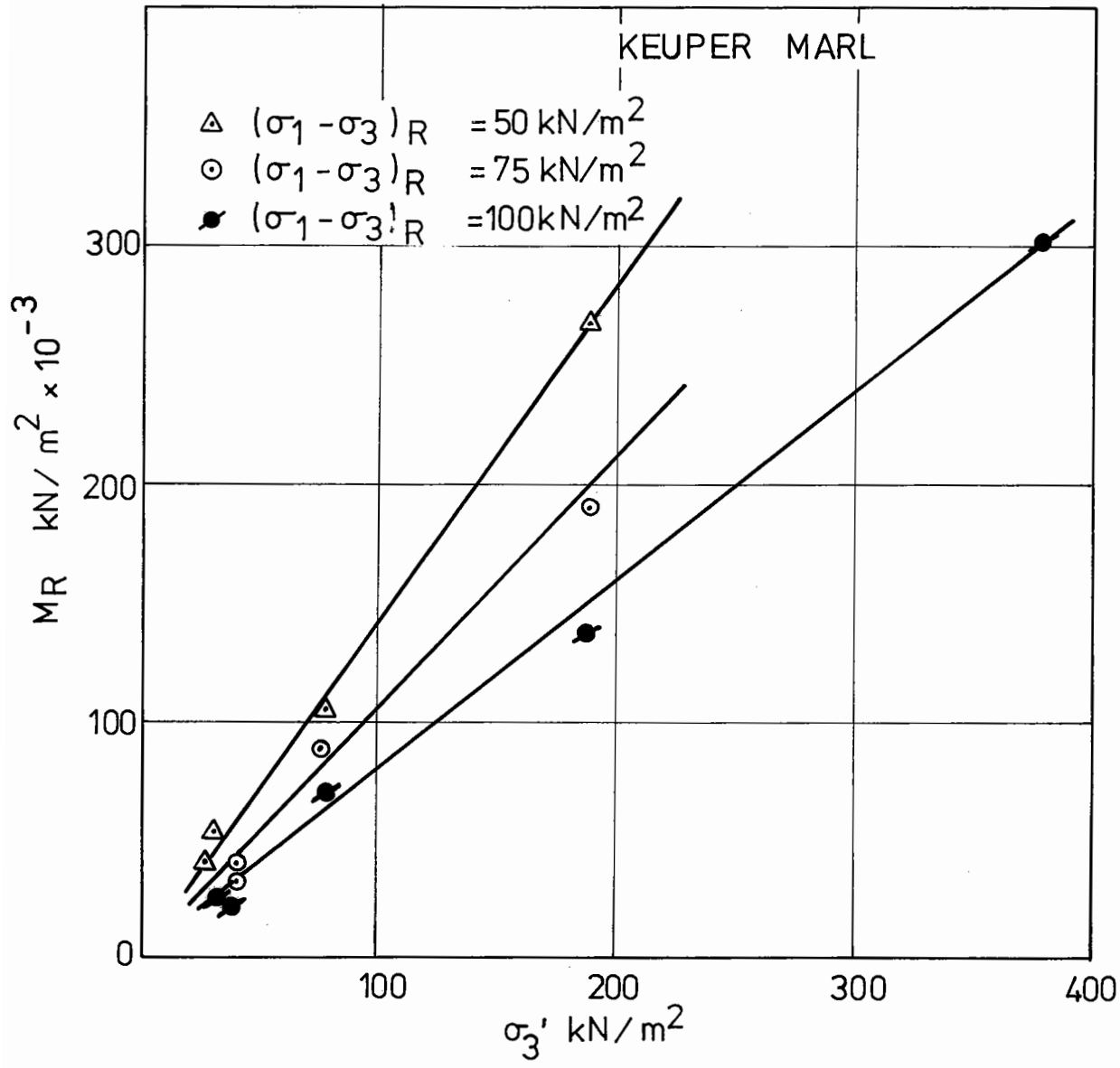

FIG. 6.83 Variation of resilient modulus with effective confining pressure and cyclic deviator stress for overconsolidated keuper marl.

same curve (Fig. 6.84). It is noted, however, that Lashine's experimental points lie above the present ones and this is considered to be due to modifications carried out on the triaxial cell to reduce friction in the loading ram and hence obtaining a truer measure of sample stiffness.

It is, therefore, maintained that the resilient modulus is thus shown to be independent of the OCR and is a function of the applied stresses. This is supported by Parry and Amerasinghe (1973) who showed that the recoverable portion of the shear strain for isotropically consolidated specimens is independent of the stress history. Similarly, Humphries and Wahls (1968) found the OCR to be insignificant in the determination of the dynamic shear modulus of kaolinite. It was found that the effective pressure was the dominant factor.

Defining σ_{3i}' as the initial effective confining stress and excluding Lashine's experimental data, then the resilient modulus can be expressed as follows:

$$M_R = 50.5 \frac{(\sigma_1-\sigma_3)_R^{-0.69}}{\sigma_{3i}'} \qquad (6.22)$$

Fig. 6.85

A coefficient of correlation of 0.844 was obtained for this relationship.

The tests at an OCR of 75 were carried out to determine any effects that there might be due to changes in moisture content by increasing the range of moisture contents studied. These tests, however, lie on the same line as the others. It can, therefore, be concluded that the moisture content is

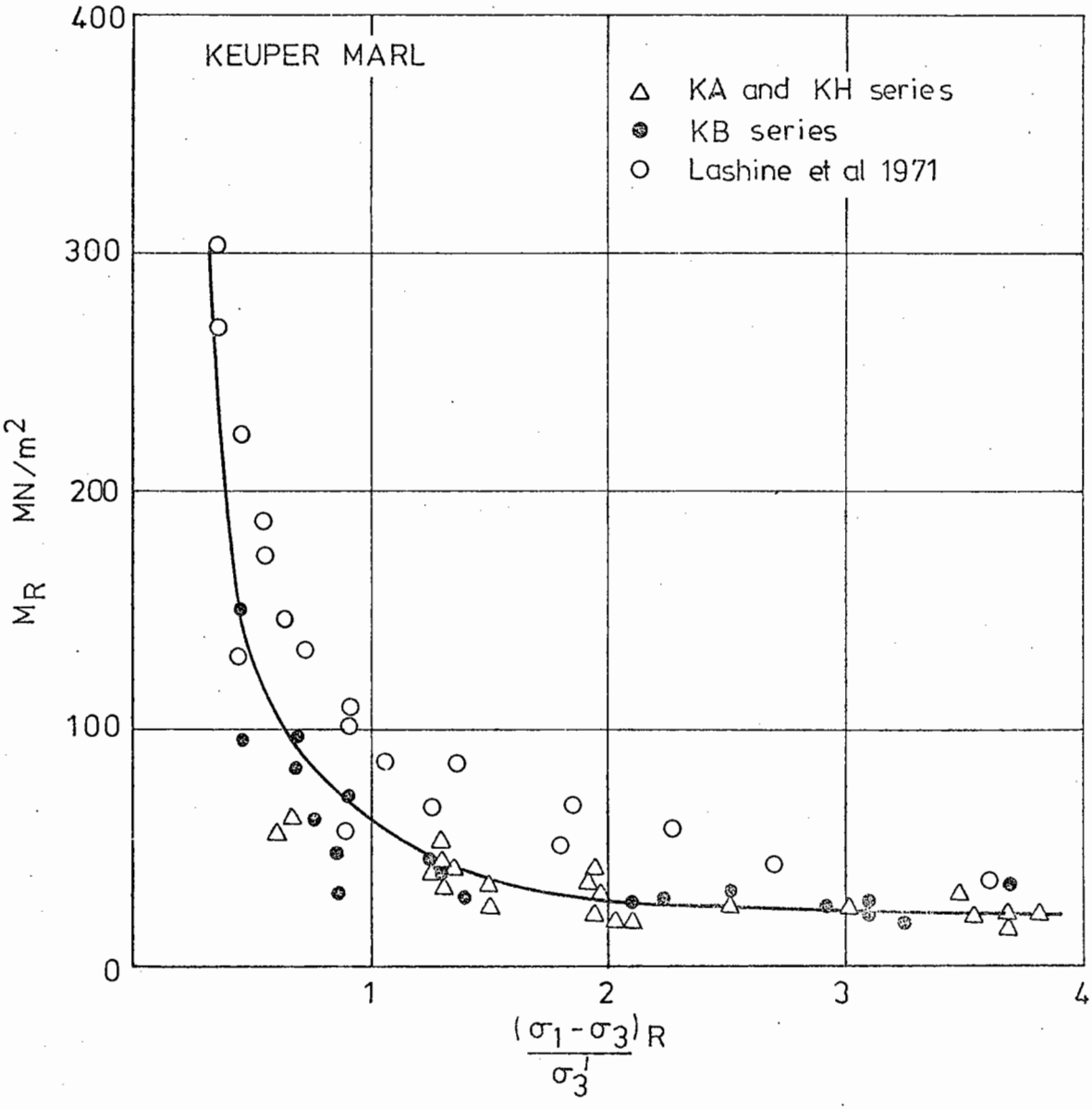

Fig. 6.84 Variation of resilient modulus with the normalized deviator stress.

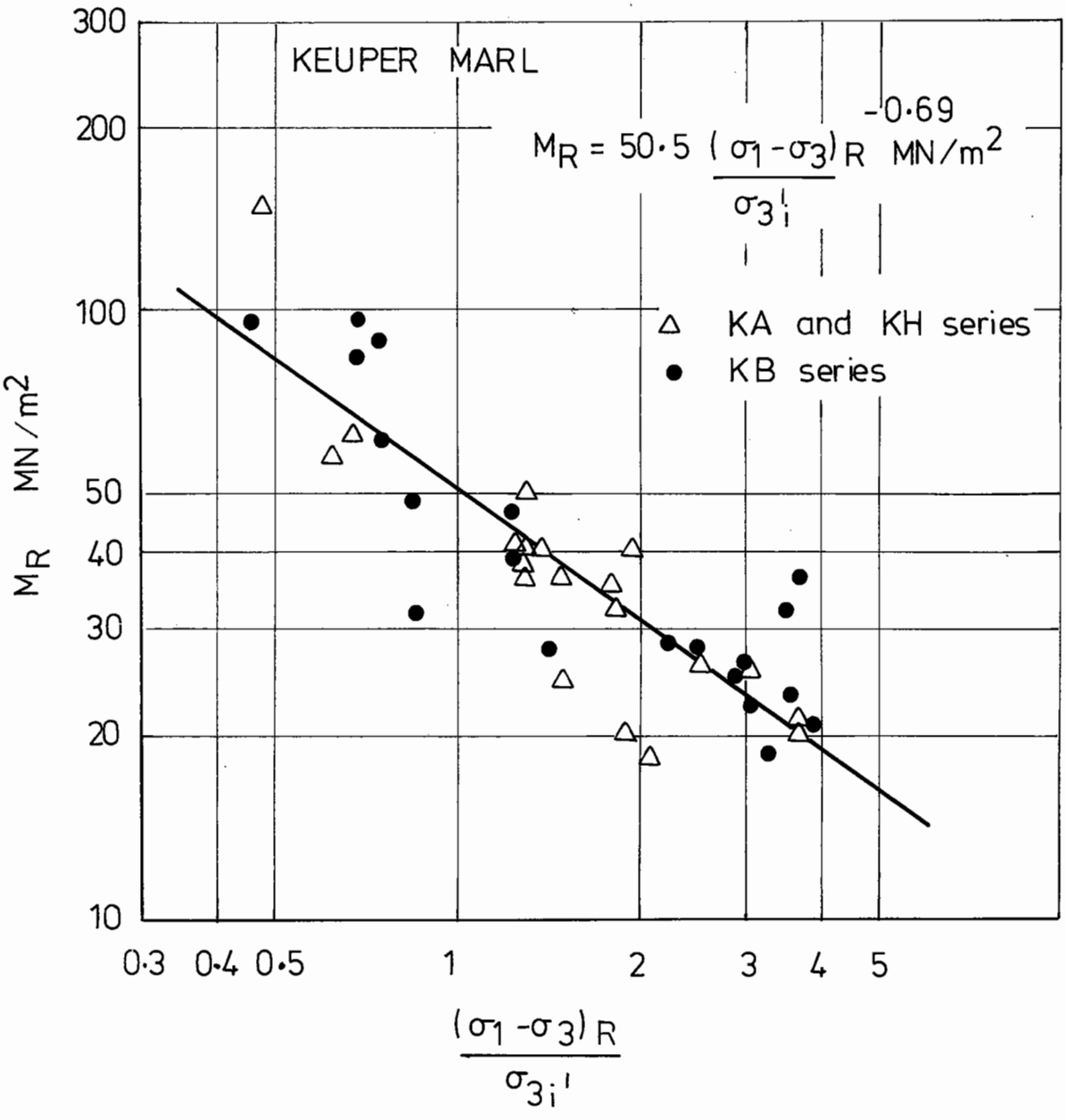

Fig.6.85 Variation of the resilient modulus with the stress ratio $\frac{(\sigma_1-\sigma_3)_R}{\sigma_3'_i}$

not a significant parameter in the determination of the repeated elastic modulus.

Much of soils testing relative to the pavement design problem has been carried out using repeated load tests on partially saturated clays. For these materials it has been found that the resilient modulus is a function of the deviator stress and the soil suction. The suctions of partially saturated clays tend to have very high values and can be considered as a measure of the initial effective confining stress. Results from Dehlen (1969) plotted on the same axes as Fig. 6.85 give a line of similar slope (Brown, 1974) (2). Richards (1970) has also shown the soil suction to be an important determinant of the resilient modulus.

6.6.2 The Effect of Rest Periods on the Recoverable Deformation

Two kinds of recoverable deformation are discernable during rest period loading. One component is purely elastic and the other is delayed elastic.

The delayed elastic component exists for both lightly over-consolidated and more heavily over-consolidated clays. Some idea of the relative magnitude of the delayed component of deformation can be obtained from Fig. 6.86, which shows typical traces from the load cell, LVDT and pore water pressure transducer.

Figs. 6.87 and 6.88 show the variation of the total modulus (determined from the total recoverable strain) and the purely elastic modulus for OCR's of 2 and 10. The two different moduli were computed from data recorded using an

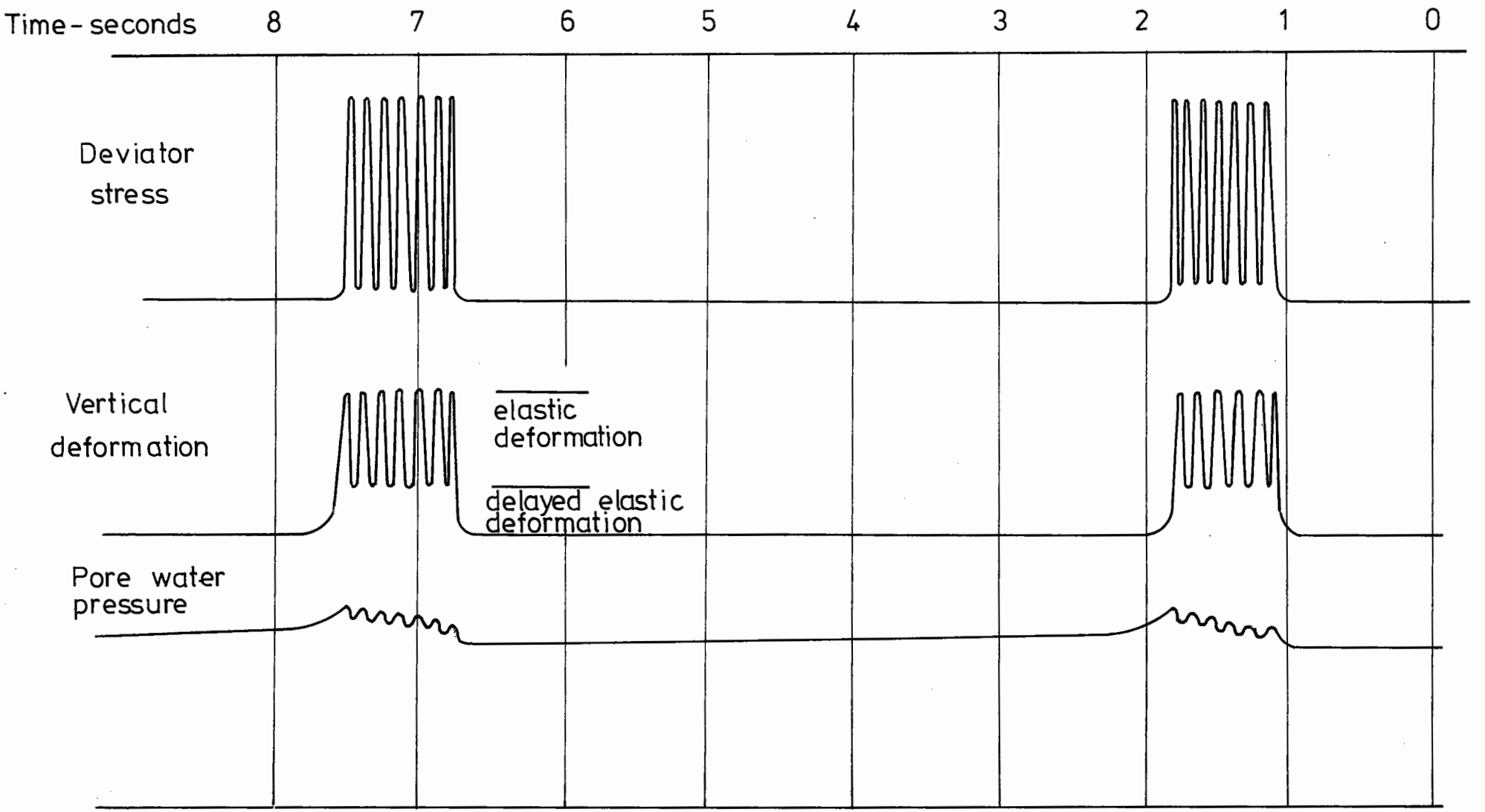

Fig. 6.86 Typical traces recorded during rest period loading.

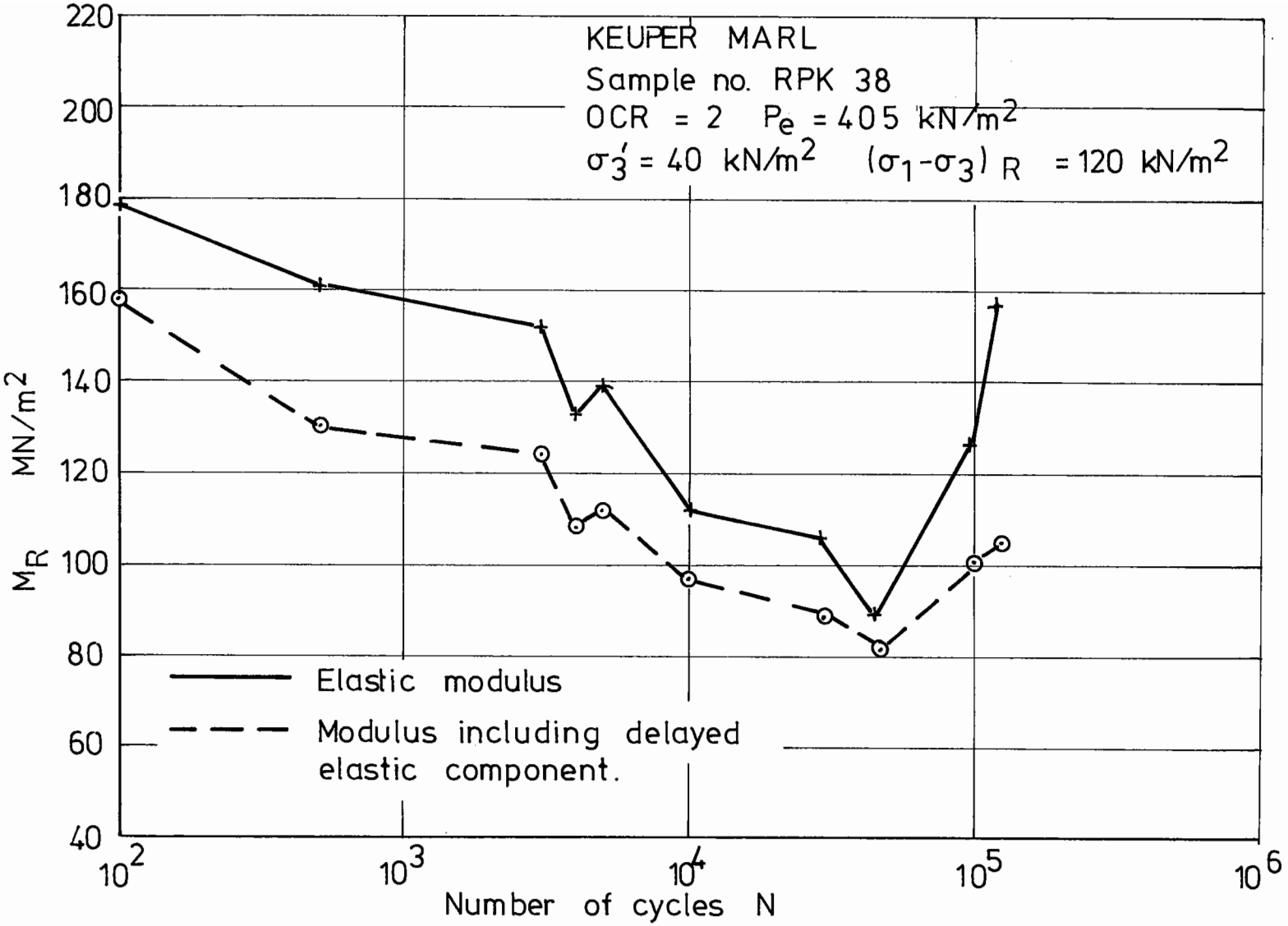

Fig. 6.87 Comparison of elastic and delayed elastic resilient modulus.

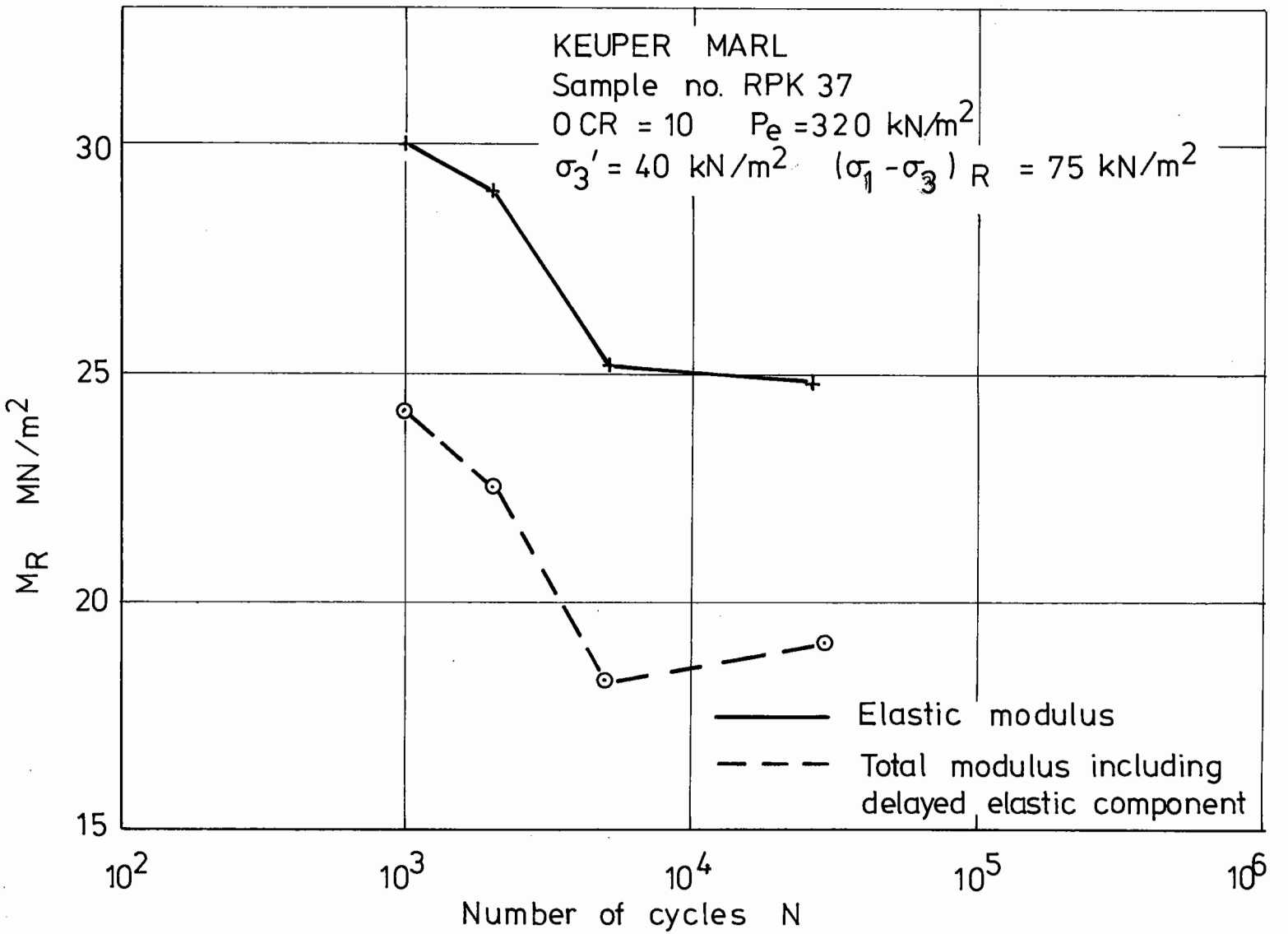

Fig. 6.88 Comparison of elastic and delayed elastic resilient modulus.

ultra-violet recorder. For the lightly over-consolidated samples the total modulus is between 80% and 85% of the purely elastic modulus for most of the test. In the case of the more heavily over-consolidated sample, the total modulus is between 75% and 80% of the elastic modulus.

Fig. 6.89 shows the variation of the total modulus with number of cycles, for varying lengths of rest period and 8 load cycles between each rest. These results do not show any significant difference for different lengths of rest period. Examination of u.v. traces showed that over 95% of the delayed elastic recovery occurred in less than one second. The shortest rest period used was one second, which would explain why no measurable difference was noted between the different lengths of rest period used. Krizek et al (1971), carrying out strain controlled relaxation tests on clay samples, showed 99% of the relaxation occurred in 1 second. Fig. 6.90 shows a similar behaviour for lightly over-consolidated samples. Again, the results do not seem to show any discernible difference for different lengths of rest period.

A comparison of the effect of the application of different numbers of cycles between rest periods showed a marked softening in terms of the total modulus as the number of cycles decreased (Fig. 6.91). It is, therefore, suggested that the delayed elastic component of deformation is dependent on the number of continuous cycles, decreasing as the number of continuous cycles increases.

The total modulus can be as small as 50% of the purely

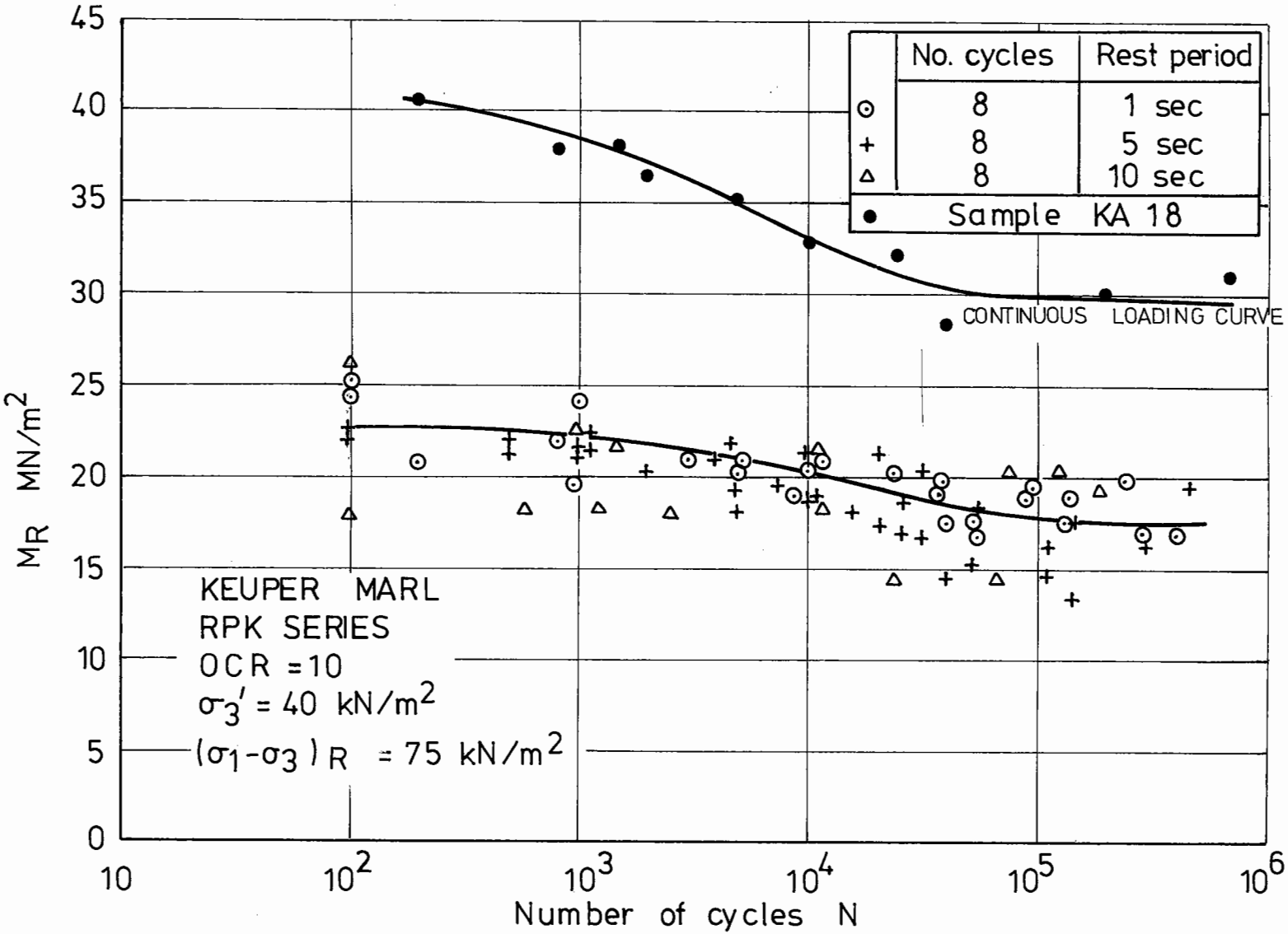

Fig.6.89 Variation of total resilient modulus with number of cycles of rest period loading.

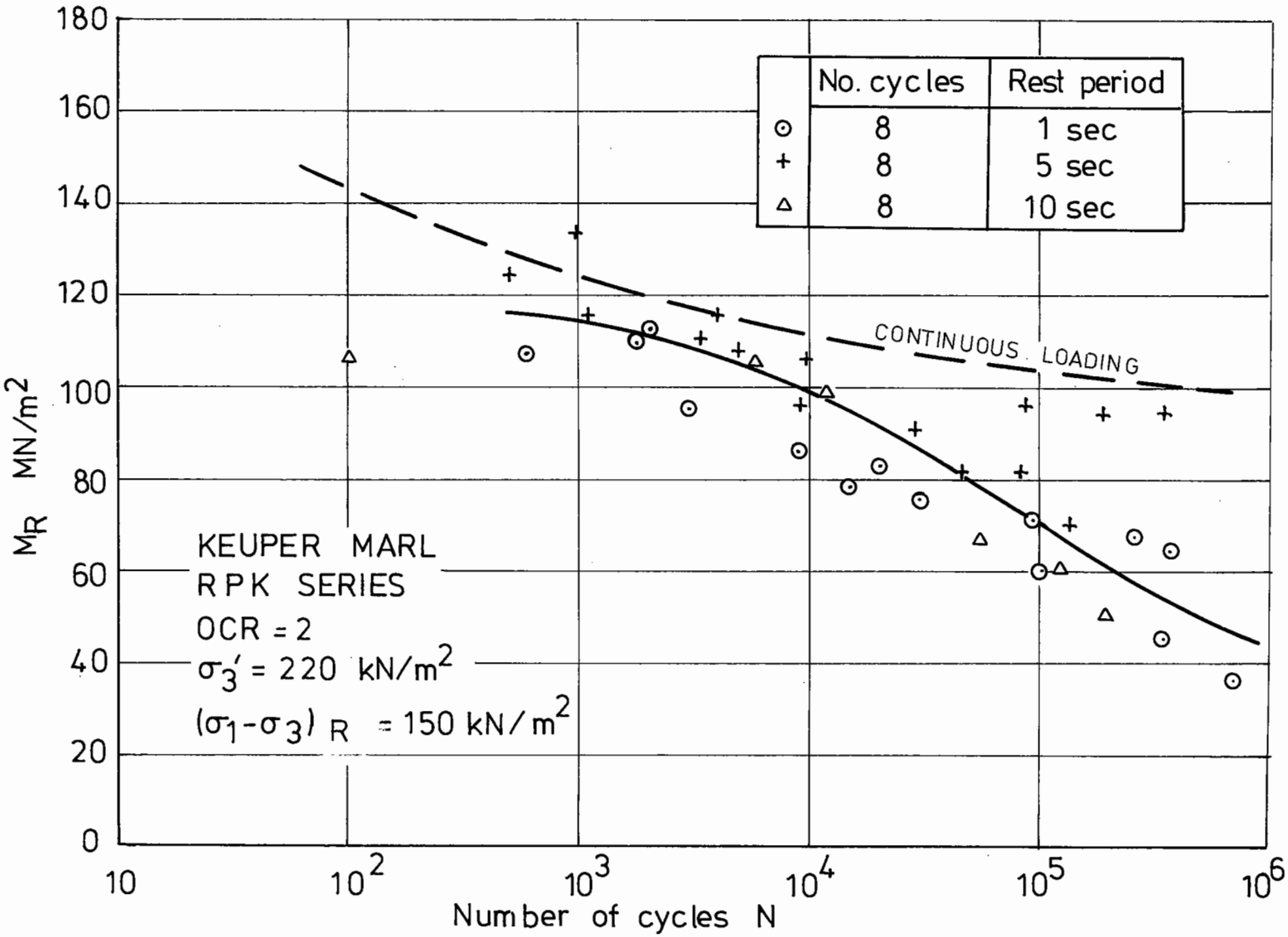

Fig. 6.90 Variation of total resilient modulus with number of cycles of rest period loading

Fig. 9.13 Variation of total resilient modulus with number of cycles to repeated load triaxial test

elastic modulus. Pneumatic repeated load testing equipment as used by Seed and others (Seed and Fead, 1959) does not apply a continuous cyclic load and would, therefore, give values of total modulus and not purely elastic modulus.

CHAPTER SEVEN

TESTS ON BREEDON GRAVEL

7.1 INTRODUCTION

The tests on the granular material consisted of two phases. The first being a preliminary investigation of the effect of the sequence of loading on the resilient and permanent deformations. The second phase was an investigation into the effects of cyclic cell pressure. In order to compare the resilient deformations under cyclic cell pressures with those measured under constant cell pressures, it was necessary to develop a method of measuring lateral strains. This was done using strain coils and their method of use is described in Appendix B.

7.2 THE MATERIAL

A crushed stone aggregate passing a $\frac{3}{8}$" sieve, supplied by the Breedon and Cloud Hill Gravel Company was used for all the tests. The grading curve for the material (Fig. 7.1) shows that it lies within the grading limits of material used extensively by British Rail in their track foundations (Meldon Dust).

The moisture content/dry density relationship was determined using both modified and standard AASHO compaction, (Fig. 7.2). With the latter the optimum moisture content was found to be 6% and the maximum dry density 2280 kg/m^3. Using the standard AASHO compaction, the optimum moisture

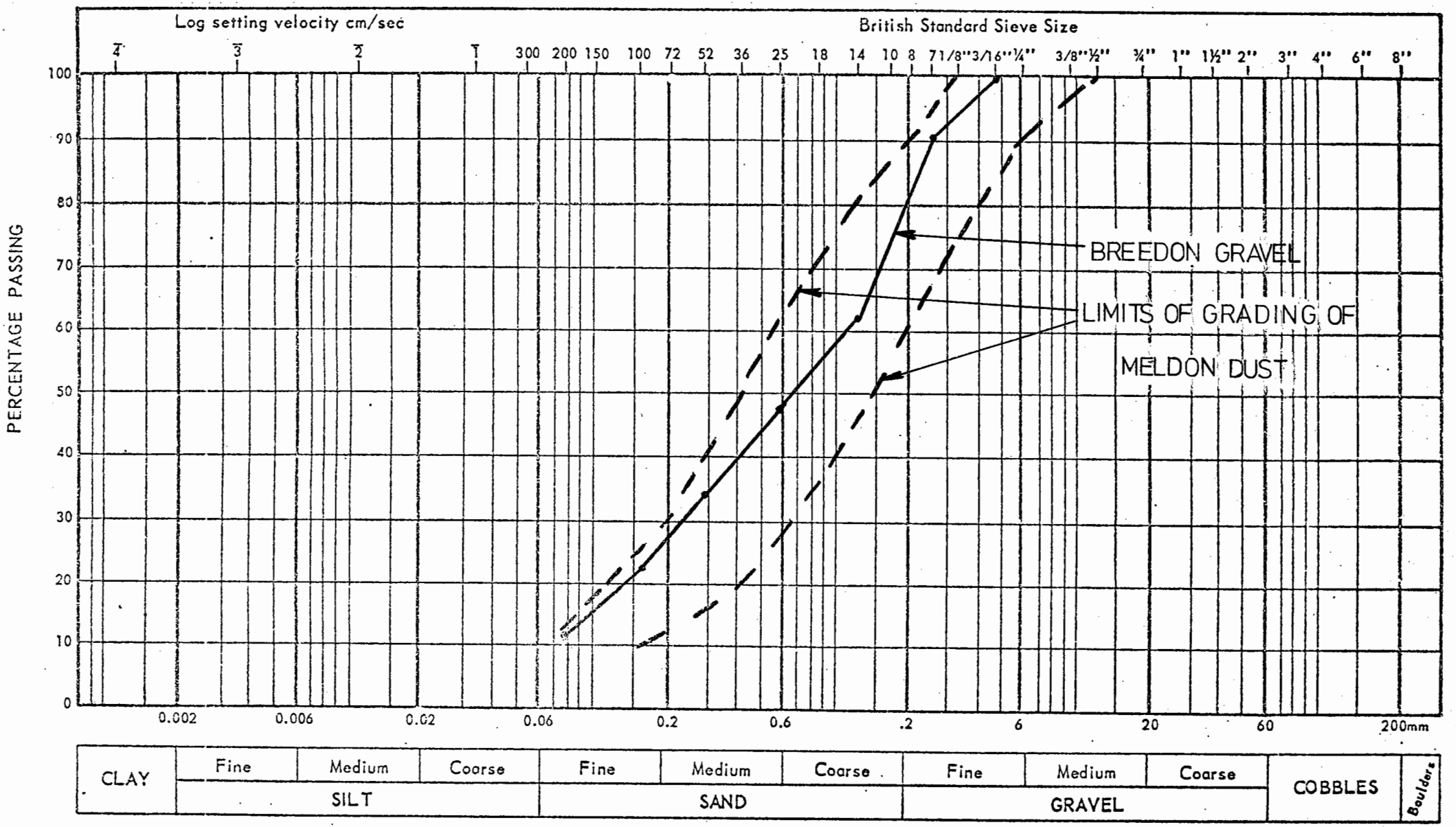

Fig. 7.1 Breedon gravel particle size distribution

content was found to be 6.5% at a dry density of 2227 kg/m^3.

It was decided to use the standard AASHO compaction at a moisture content of 7-7.5% as this gave samples which were stiff enough to handle. This coincides with the shaded zone on Fig. 7.2 in the region just wet of optimum.

The specific gravity of the particles was measured and found to be 2.72. Control moisture contents taken during compaction and after testing showed the moisture content to be in the region of 7.5% $\pm$ 0.5%. The dry densities of the samples after compaction were found to be 2219 kg/m^3 $\pm$ 16 kg/m^3.

7.3 DEFINITION OF RESILIENT MODULUS

The greater part of repeated load soil testing carried out to date has been done under triaxial test conditions, but with only the vertical stress being cycled. A definition of resilient modulus M_R has evolved from this as:

$$M_R = \frac{(\sigma_1 - \sigma_3)_R}{\varepsilon_R} \qquad (7.1)$$

where $(\sigma_1 - \sigma_3)_R$ = the repeated component of the deviator stress

and ε_R = the resilient vertical strain.

As is illustrated in Fig. 7.3, under constant cell pressure conditions, the amplitude of the vertical stress component (σ_1) is the same as the amplitude of the deviator stress $(\sigma_1 - \sigma_3)$. The resilient modulus is, therefore, analogous to Young's modulus.

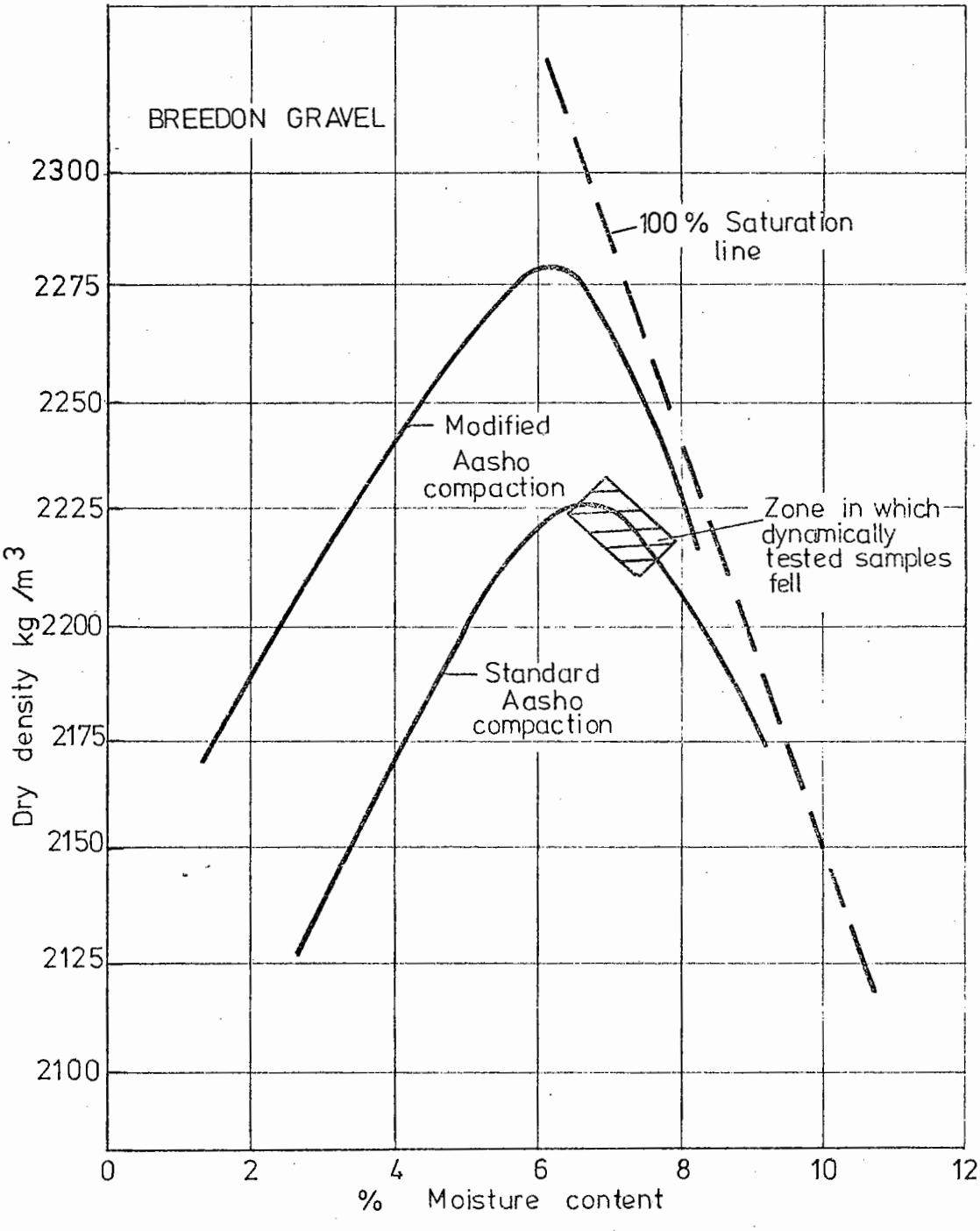

FIG. 7.2 Variation of moisture content with dry density

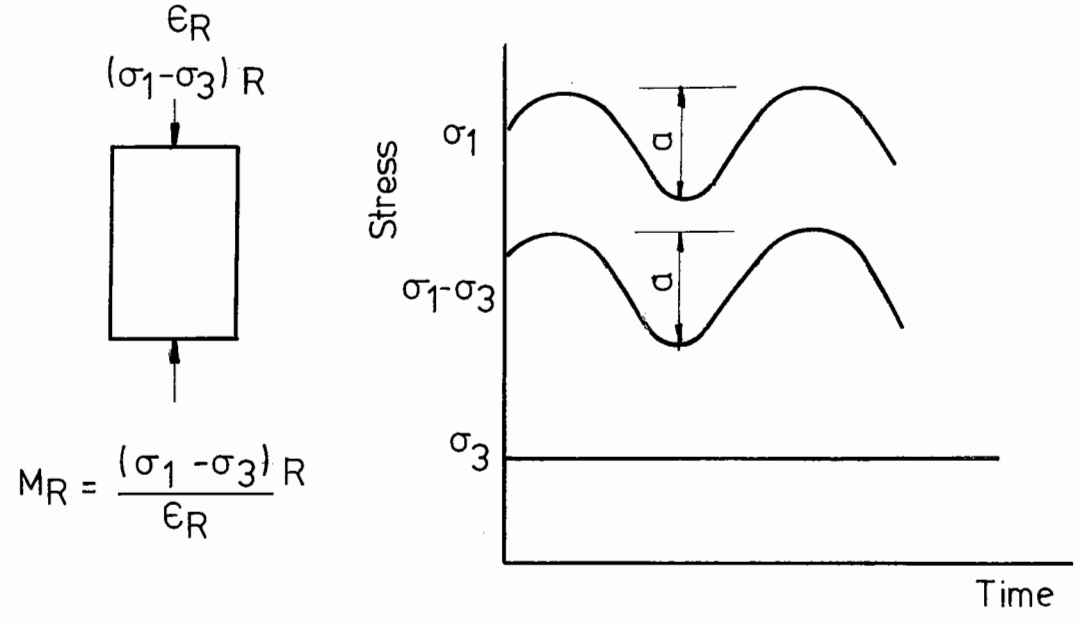

FIG. 7.3 SAMPLE SUBJECTED TO CYCLIC DEVIATOR STRESS

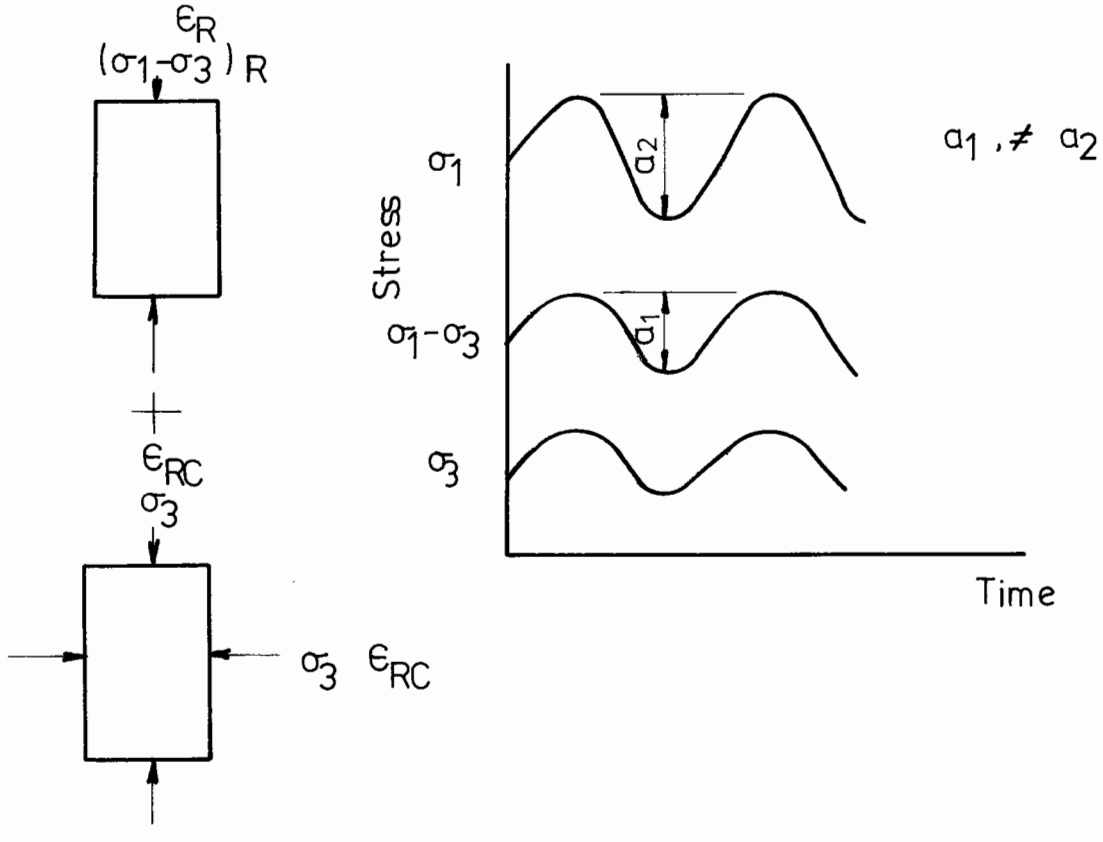

FIG. 7.4 SAMPLE SUBJECTED TO CYCLIC CONFINING STRESS AND CYCLIC DEVIATOR STRESS.

In the case of cyclic cell pressure, however, the amplitude of the vertical stress is not the same as the amplitude of the deviator stress and care must be taken in properly defining the modulus, Fig. 7.4.

Assuming that the material behaves isotropically, and considering only the cyclic components of stress and strain, then M_R can be calculated from the following equations in which it has been regarded as analogous to Young's modulus.

For the vertical direction:

$$M_R = \frac{\sigma_1}{\epsilon_1} - 2\nu_R \frac{\sigma_3}{\epsilon_1} \tag{7.2}$$

and for the horizontal direction:

$$M_R = \frac{\sigma_3}{\epsilon_3} - \nu_R\left(\frac{\sigma_1}{\epsilon_3} + \frac{\sigma_3}{\epsilon_3}\right) \tag{7.3}$$

Equating (7.2) and (7.3) gives the resilient Poisson's ratio as:

$$\nu_R = \frac{\sigma_1\epsilon_3 - \sigma_3\epsilon_1}{2\sigma_3\epsilon_3 - \epsilon_1(\sigma_1 + \sigma_3)} \tag{7.4}$$

and the resilient modulus as:

$$M_R = \frac{(\sigma_1 - \sigma_3)(\sigma_1 + 2\sigma_3)}{\epsilon_1(\sigma_1 + \sigma_3) - 2\epsilon_3\sigma_3} \tag{7.5}$$

7.4 PRELIMINARY TEST RESULTS

A preliminary test series was carried out to determine the effect of increasing stress sequences on both the resilient and permanent deformations, under cyclic cell pressure conditions. This test series was carried out

before the lateral strain measurement equipment had been fully developed.

The test series showed that the resilient properties can be accurately measured using sequences of sub-failure stresses. Permanent deformation, however, is dependent on the load sequence. Lashine et al (1971) showed that the resilient behaviour reached an equilibrium after approximately 10^4 cycles of loading. Hence all resilient properties considered are after the equilibrium condition has been reached.

Because there were no lateral strain measurements for this test series, it was necessary to assume a value of resilient Poisson's ratio of 0.35. Using this, values of resilient modulus were compared for incremental and single stage loading. Fig. 7.5 shows that points for single stage loading lie on the incremental loading curve. This means that for the purposes of determining resilient characteristics it is only necessary to test a small number of samples with sequences of varying load.

Considering now the accumulation of permanent strain, tests were carried out at two cyclic cell pressures for different deviator stress. Figs. 7.6 and 7.7 show the accumulation of plastic strain with the number of cycles of applied stress. It can be seen that an equilibrium value of permanent strain is reached after approximately 10^4 cycles.

A comparison of the permanent strains under sequential loading with those accumulated under single stage loading

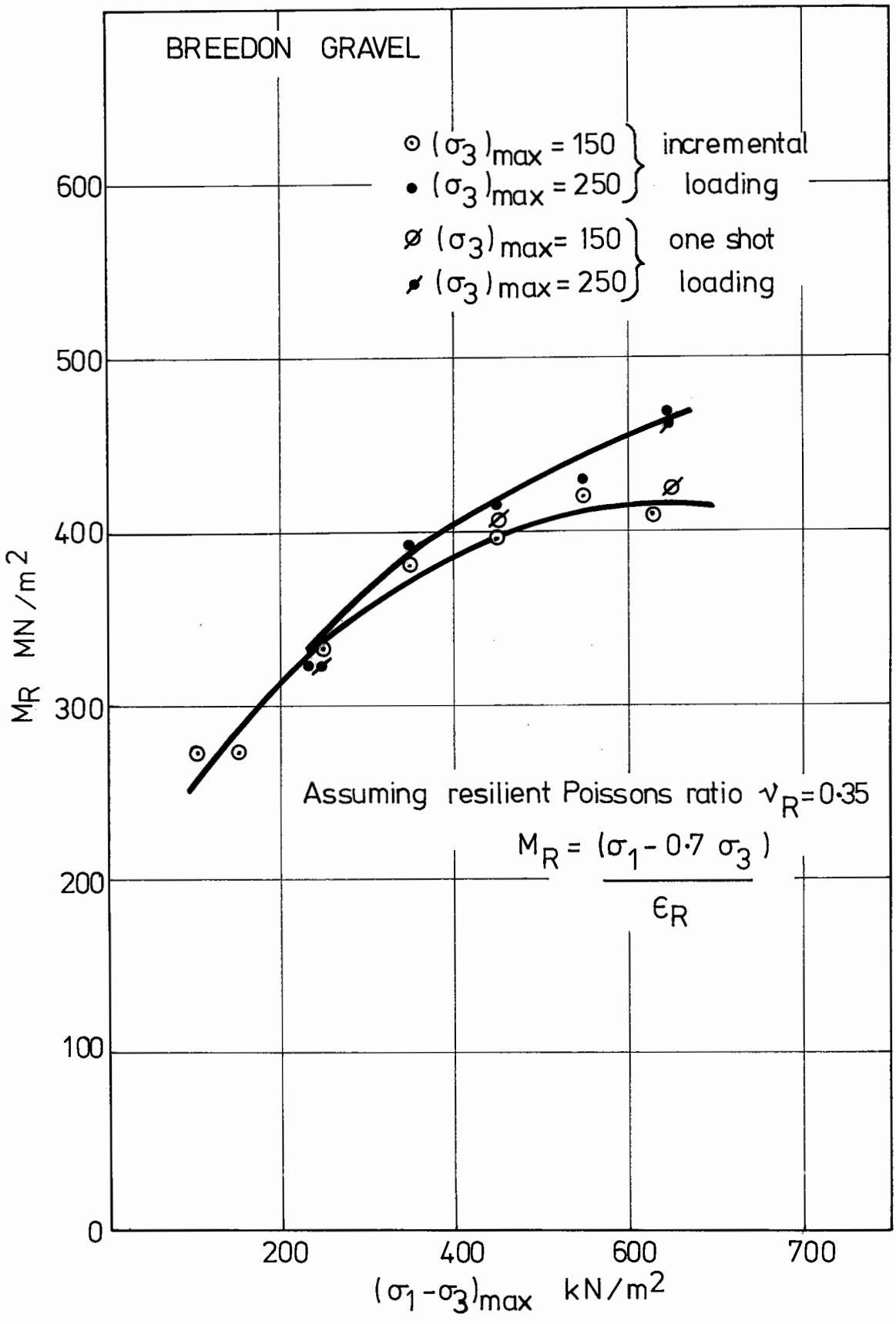

FIG. 7.5 Effect of loading sequence on the resilient modulus for varying cell pressures.

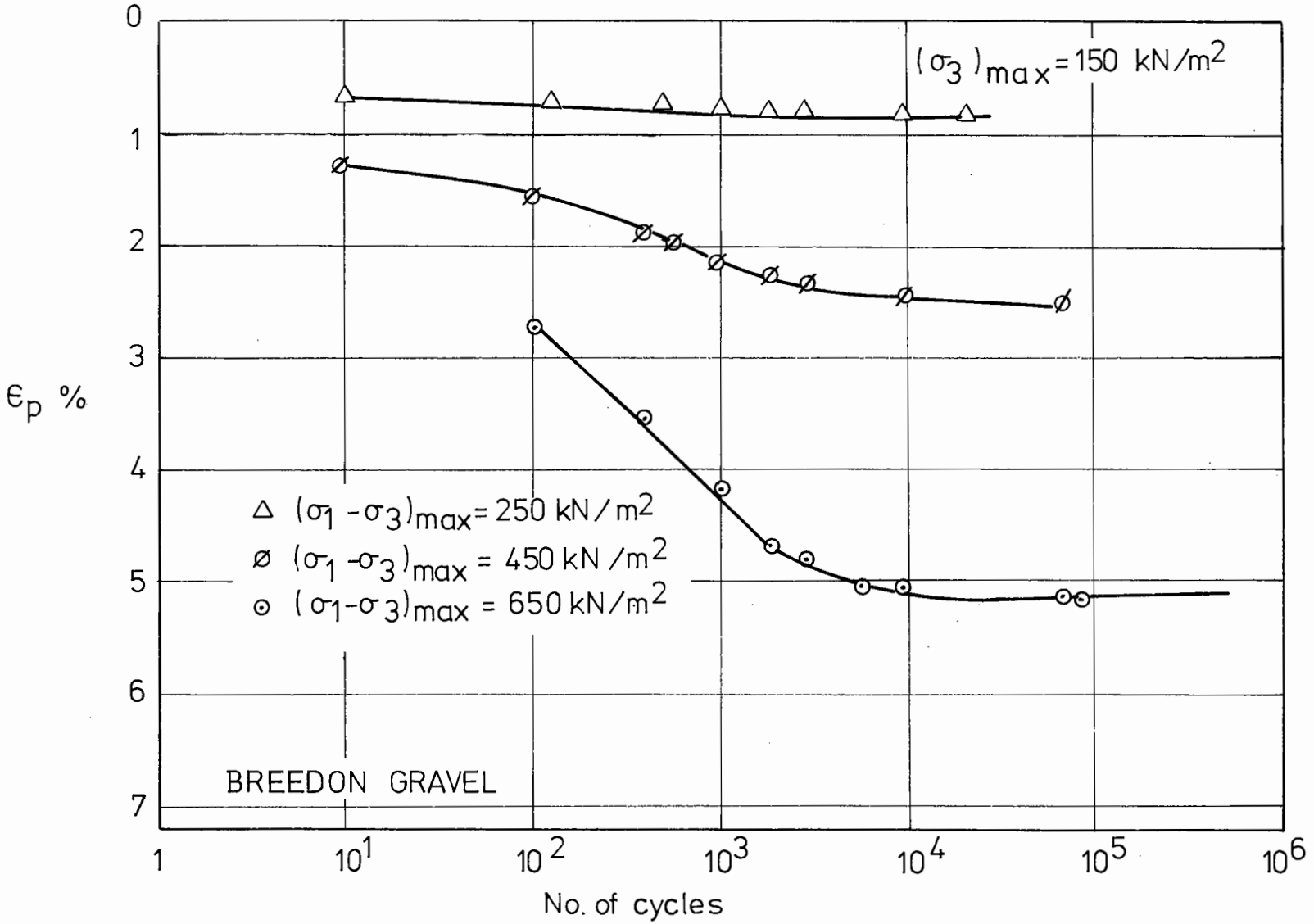

FIG. 7.6 Variation of axial strain with number of cycles and maximum deviator stress.

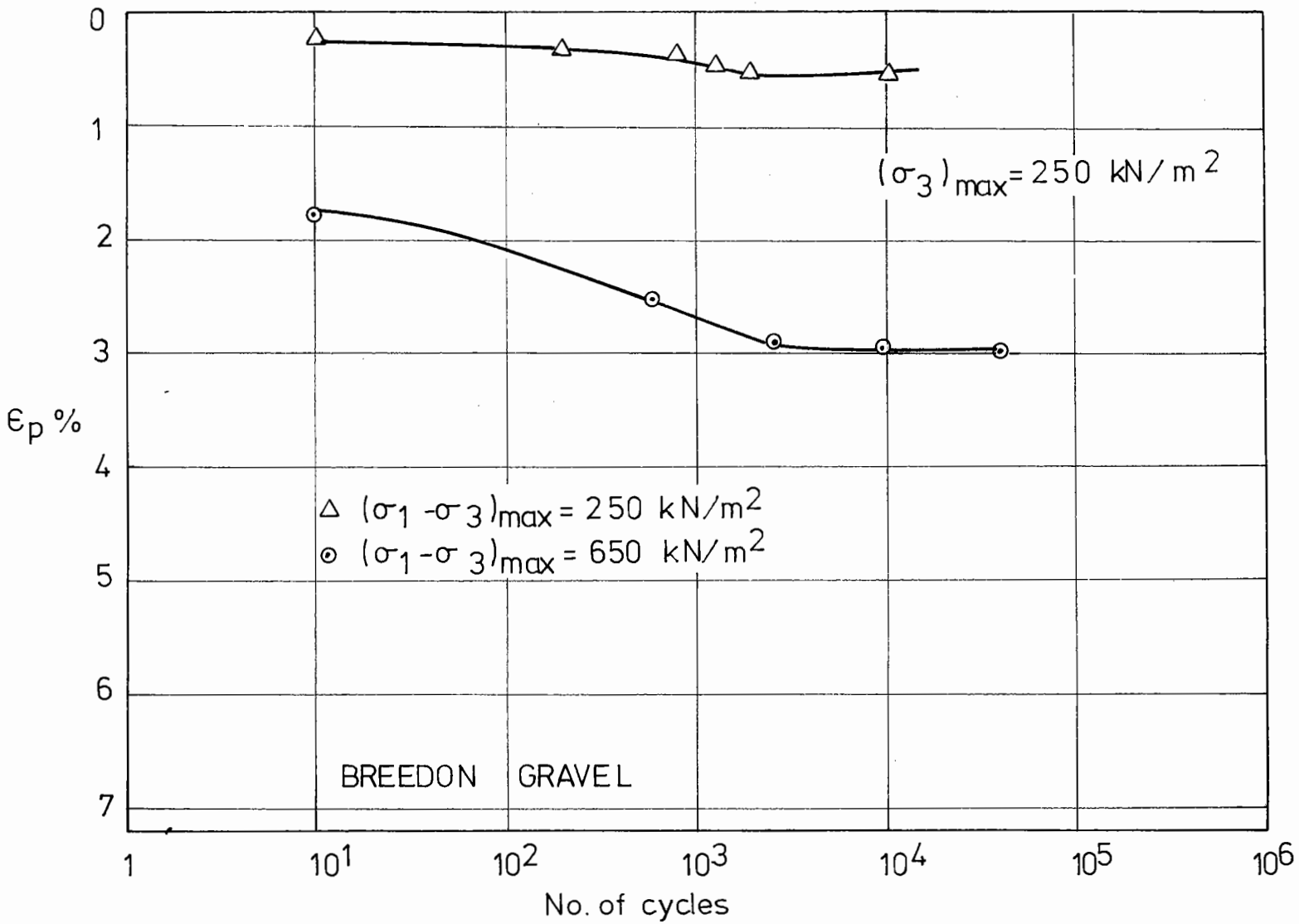

FIG. 7.7 Variation of axial strain with number of cycles and maximum deviator stress

is given in Figs. 7.8 and 7.9. Application of the maximum deviator stress without a conditioning sequence causes a great increase in the permanent strain. It is thought that under a relatively small deviator stress a reorientation of the particles occurs, to form a more stable structure which is better able to resist the higher deviator stresses. Under a larger deviator stress this reorientation still occurs but because of the initially unstable structure large permanent strains occur, before an equilibrium is reached.

For the purposes of the comparison of permanent strain data then, the loading sequences applied to a sample are important. It was decided, therefore, only to use data from single stage loading for permanent strain characterisation.

7.5 THE EFFECTS OF CYCLIC CELL PRESSURE

For the purposes of pavement design, it is necessary to characterise both the permanent and resilient strains. Tests were carried out for both to determine whether a level of constant confining stress existed which was equivalent to a given cyclic stress and could hence be used in a materials testing procedure involving equipment without the facility for cycling the cell pressure.

An equivalent constant confining stress was found to exist for permanent strain. However, when the resilient properties are considered in terms of the resilient modulus and the resilient Poisson's ratio an apparent difference in behaviour between the constant and cyclic cases was found.

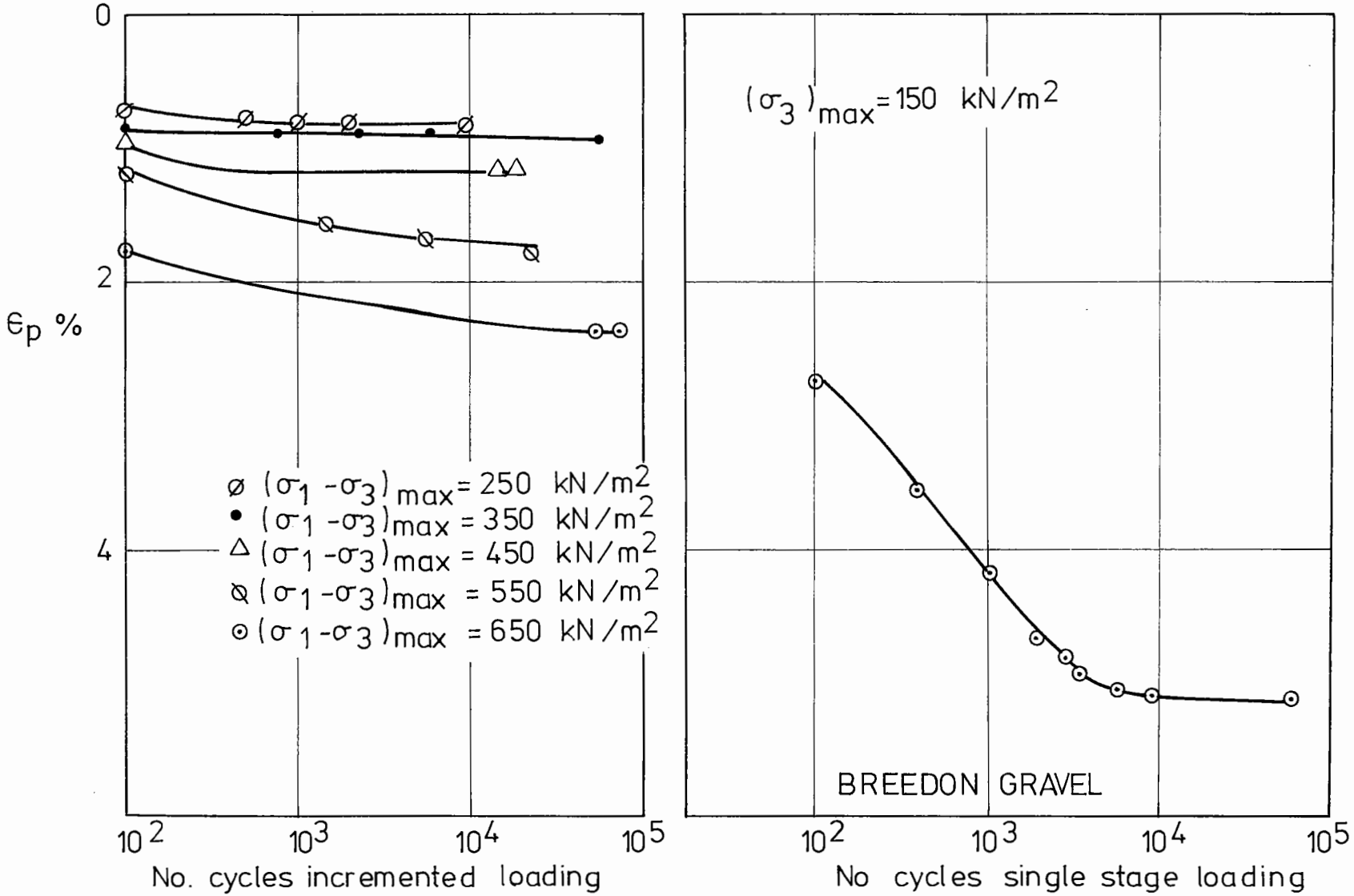

FIG. 7.8 Comparison of axial strain for incremented loading with that for single stage loading.

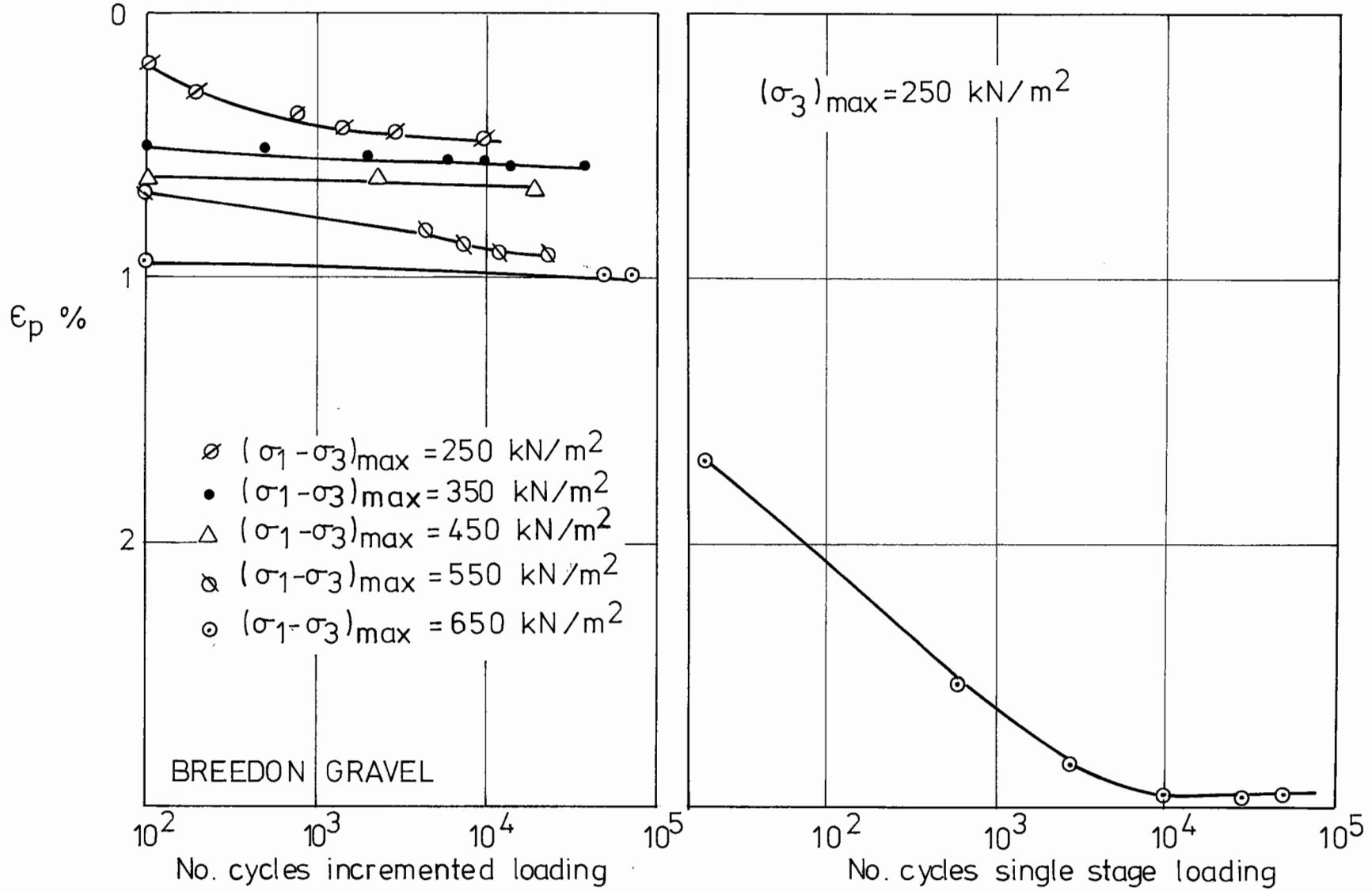

FIG. 7.9 Comparison of axial strain for incremented loading with that for single stage loading.

A more fundamental analysis, however, revealed a continuity of behaviour for the two cases.

7.5.1 Permanent Strain

For the purposes of characterising the effects of different types of confining stress one level of cyclic deviator stress was applied. In each case this stress was cycled from zero to a maximum value so that the mean was always half the maximum.

For a constant confining stress a linear relationship exists between the permanent strain and the deviator stress normalised with respect to the confining stress (Lashine et al, 1971). It was shown that this relationship still holds in the case of cyclic cell pressure if the normalising parameter is taken as the mean value of the confining stress (Fig. 7.10).

7.5.2 Resilient Modulus and Poisson's Ratio

For the purpose of linear elastic analysis of pavement structures, it is necessary to have values for both the resilient modulus M_R and the resilient Poisson's ratio, ν_R.

It has already been shown by Hicks (1970) and others that the resilient modulus is dependent on both the confining and deviator stresses. By examining the behaviour under a constant deviator stress it is possible to examine the effect of the mean level and repeated component of the cyclic cell pressure. The resilient modulus for cyclic confining stress tests was computed as shown in Section 7.3.

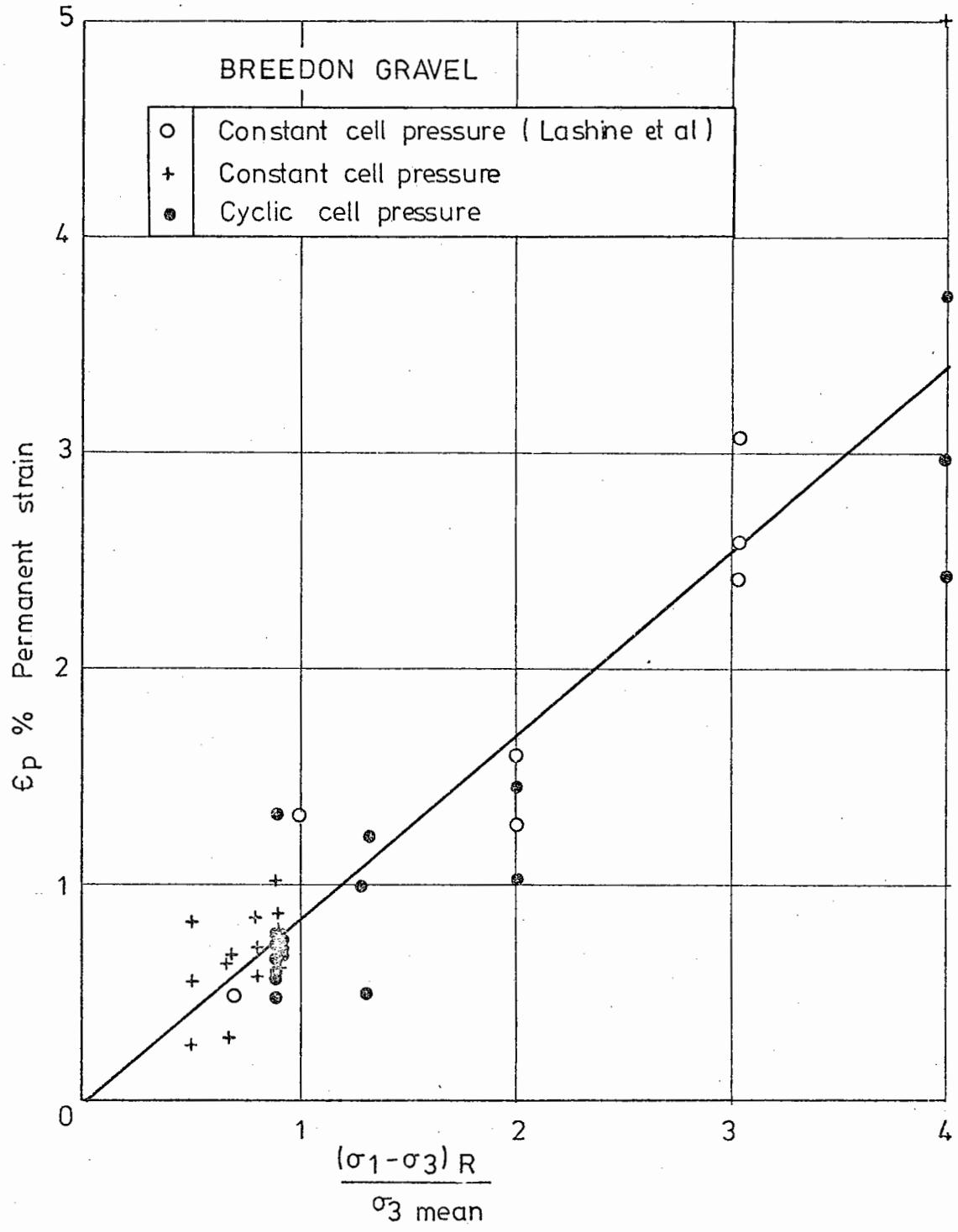

Fig.7.10 Variation of permanent strain with the ratio of the deviator stress to the mean confining pressure.

The variation of resilient modulus with confining stress for all types of test is shown in Fig. 7.11. This figure shows that it is the mean value of the confining stress which is the determinant of the resilient modulus for a given deviator stress. The amplitude of the repeated component of the cell pressure did not have any quantifiable effect on the modulus.

Pavement analyses are sensitive to the value of Poisson's ratio (Hicks, 1970) and it is, therefore, important to evaluate it under cyclic cell pressure conditions.

Under a static confining stress (Fig. 7.12) the resilient Poisson's ratio varies from less than 0.1 to values in excess of 0.5 where dilation of the samples was occurring. The resilient Poisson's ratio was shown to be a linear function of the principal stress ratio when plotted on a logarithmic basis. A similar relationship was found by Allen and Thompson (1973).

The resilient Poisson's ratio from tests with cyclic confining stress was also plotted as a function of the principal stress ratio over the same range of stress ratios as for tests with a constant confining stress. However, Fig. 7.13 shows that it is found to be virtually constant, most points lying in the region between 0.2 and 0.1.

7.5.3 Repeated Loading Stress Paths

In order to better understand the behaviour of the material it has been examined in terms of the repeated

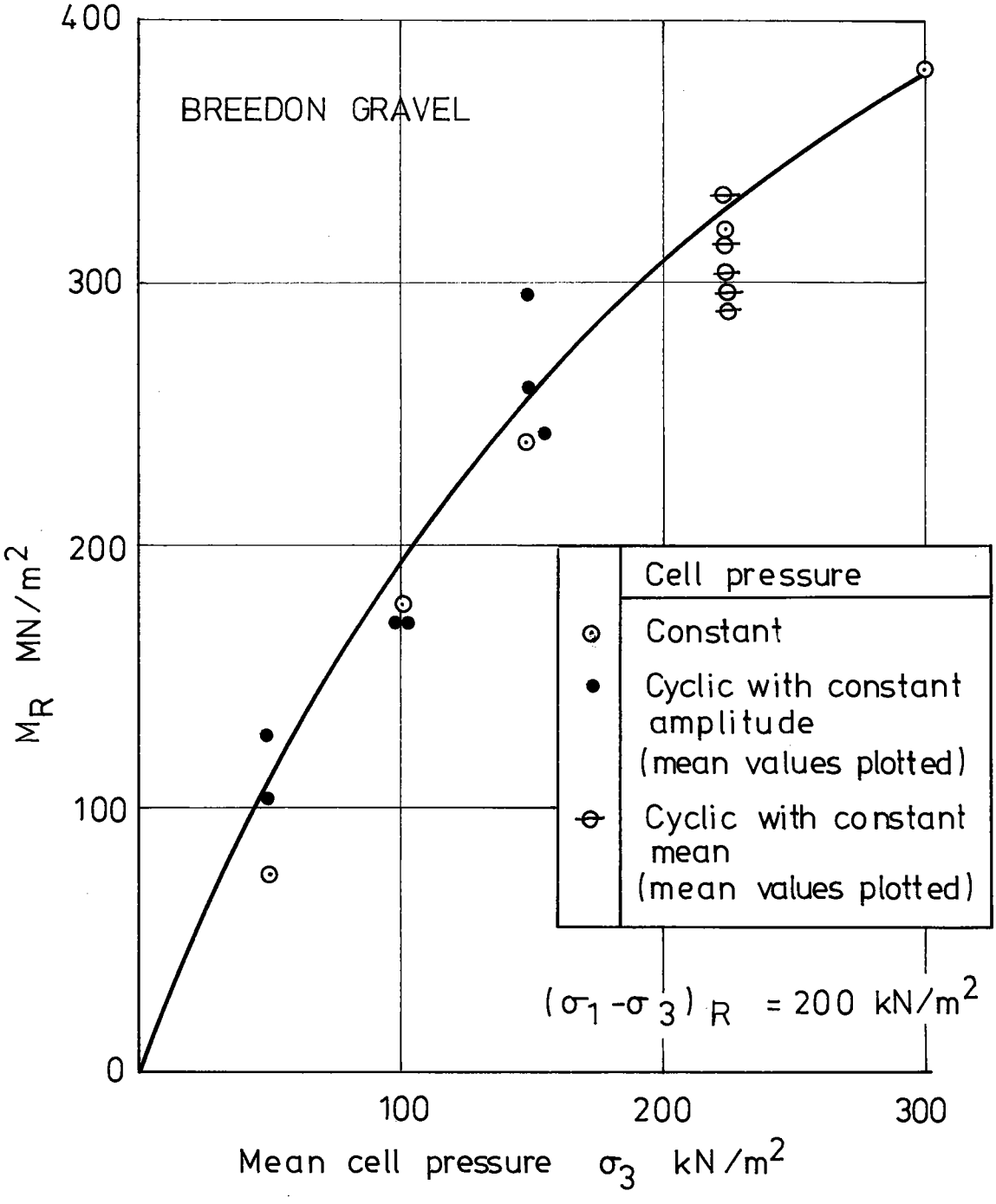

Fig. 7.11 Comparison of resilient modulus under constant and cyclic cell pressure conditions.

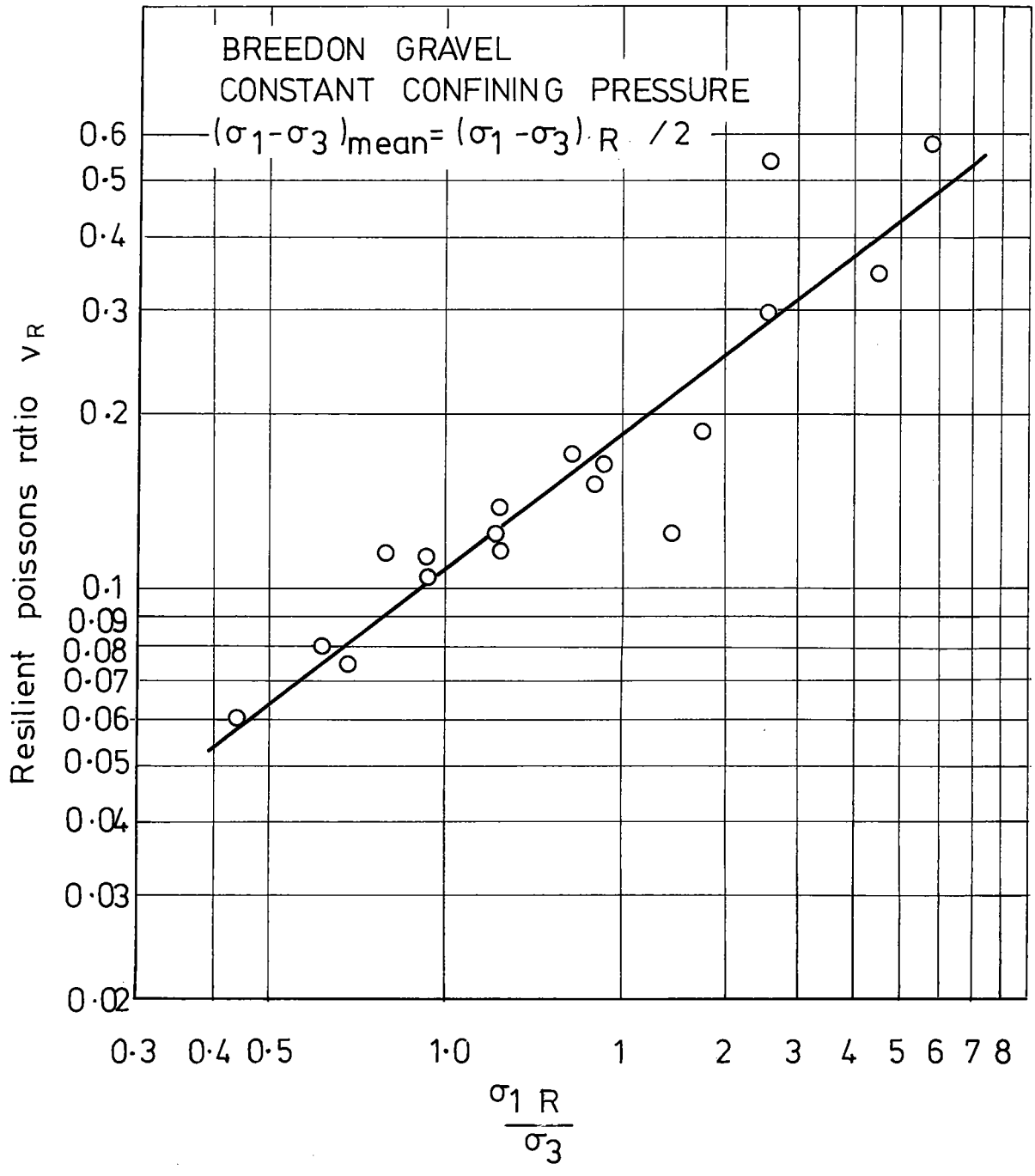

Fig. 7.12 Variation of resilient poissons ratio with principal stress ratio for a constant confining stress.

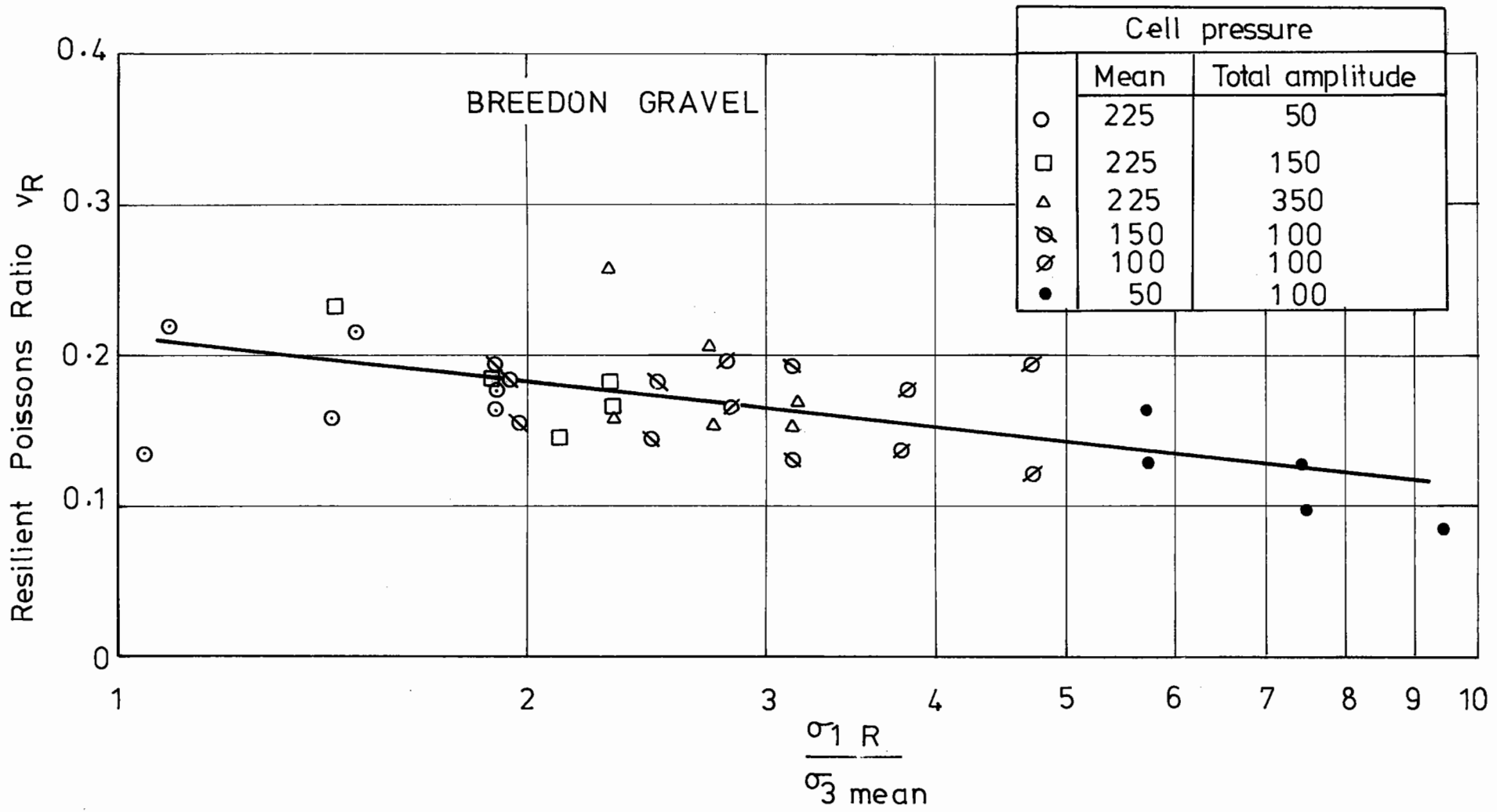

Fig. 7.13 Variation of resilient poissons ratio with stress ratio for a cyclic confining stress.

stress paths using the invariants p and q where:

the deviator stress: $q = (\sigma_1 - \sigma_3)$ (7.6)

and the mean normal stress:

$$p = \frac{(\sigma_1 + \sigma_2 + \sigma_3)}{3} \quad (7.7)$$

These two parameters are normally defined in terms of effective stresses but as the tests were drained and the strains of major interest were those after some 10^5 cycles, total stresses can be equated to effective stresses. "q" is directly proportional to the octahedral shear stress which is defined as:

$$\tau^2_{oct} = \frac{1}{9}\left[(\sigma_1 - \sigma_2)^2 + (\sigma_2 - \sigma_3)^2 + (\sigma_3 - \sigma_1)^2\right] \quad (7.8)$$

Scott (1965)

which for the triaxial test reduces to:

$$\tau_{oct} = \frac{\sqrt{2}}{3}(\sigma_1 - \sigma_3) \quad (7.9)$$

In addition, p is the same as the octahedral normal stress:

$$\sigma_{oct} = \tfrac{1}{3}(\sigma_1 + \sigma_2 + \sigma_3) \quad (7.10)$$

For the special case of the deviator stress cycling from zero, any repeated stress path can be defined using three parameters, Fig. 7.14. These are:

p_R - the repeated mean normal stress,

q_R - the repeated deviator stress,

p_m - the mean value of the mean normal stress.

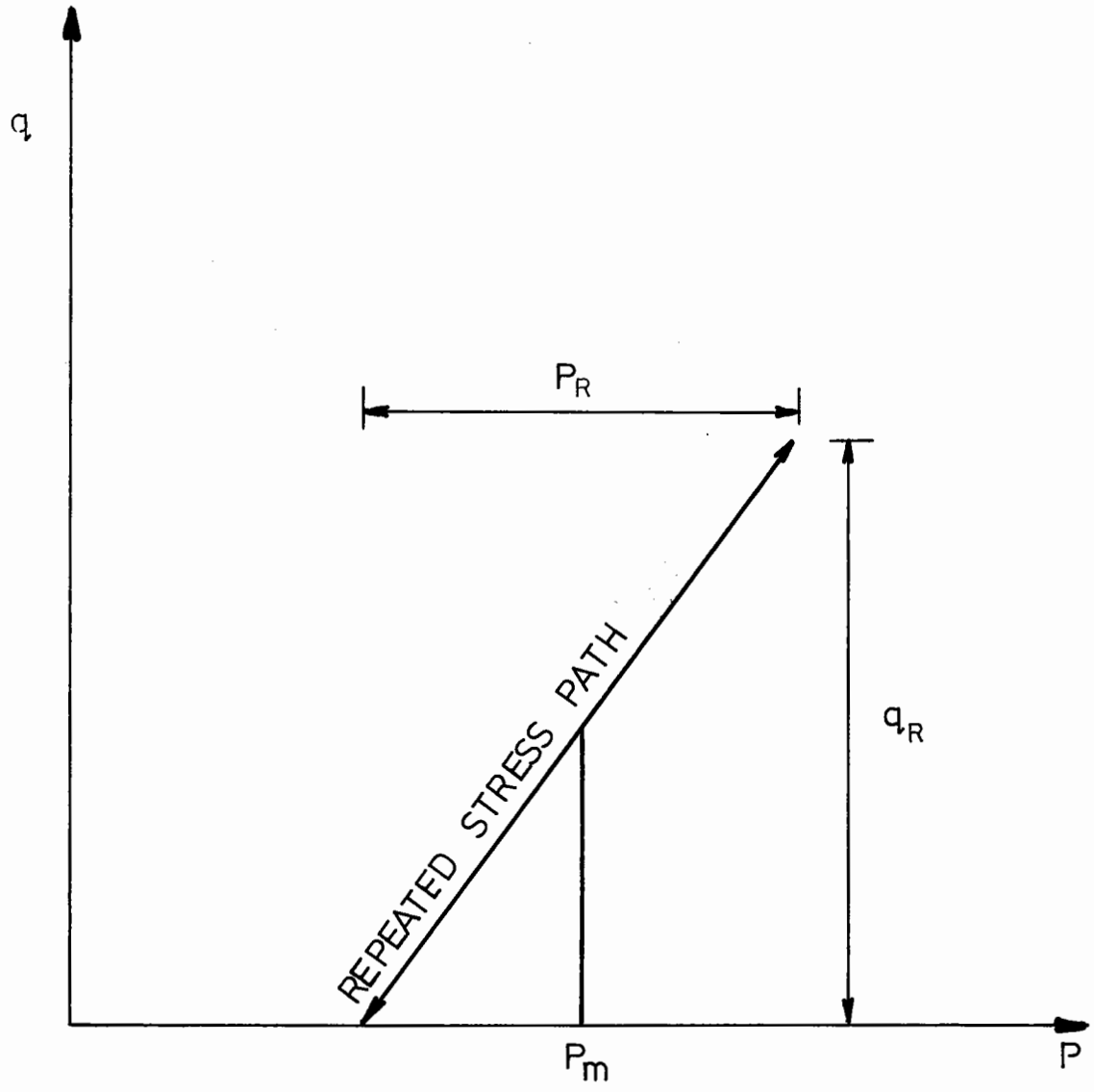

Fig. 7.14 Definition of the repeated stress path.

If the stress path did not cycle from q = 0, then a fourth parameter would be needed, say q_m, the mean deviator stress (Boyce et al, 1974).

The stress paths for the constant confining stress tests are a series of parallel lines of slope equal to 3 (Fig. 7.15).

If the confining stress is cycled in phase with the deviator stress, then the stress paths take the form of those illustrated in Fig. 7.16. The slopes of these vary according to the ratio of q_R to p_R.

7.5.4 Volumetric and Shear Strains

In order to characterise the stress-strain behaviour of the two types of test it is necessary to consider two further parameters; these are, the resilient volumetric and shear strains which are defined as follows:

Resilient volumetric strain: $$v_R = \epsilon_1 + 2\epsilon_3 \qquad (7.11)$$

Resilient shear strain: $$\epsilon_R = \frac{2\sqrt{2}}{3}(\epsilon_1 - \epsilon_3) \qquad (7.12)$$

The volumetric strain is three times the octahedral normal strain which is defined as:

$$\epsilon_{oct} = \tfrac{1}{3}(\epsilon_1 + \epsilon_2 + \epsilon_3) \qquad (7.13)$$

The resilient shear strain, ϵ_R, as defined is derived from the definition of octahedral shear strain, φ_{oct}, where:

$$\varphi_{oct}^2 = \frac{4}{9}\left[(\epsilon_1 - \epsilon_2)^2 + (\epsilon_2 - \epsilon_3)^2 + (\epsilon_3 - \epsilon_1)^2\right] \qquad (7.14)$$

Scott (1965)

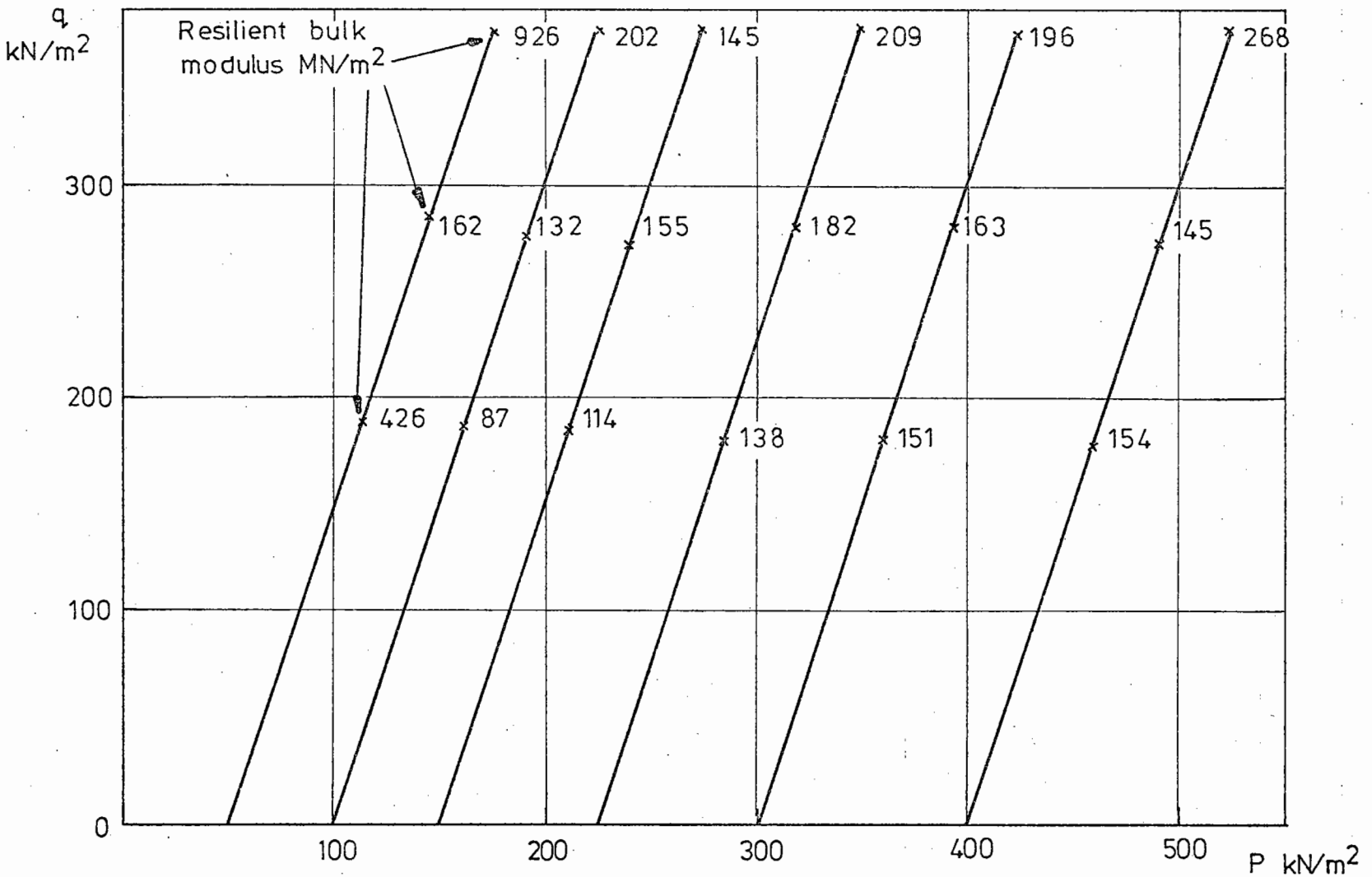

Fig. 7.15 Stress paths for constant confining stress tests.

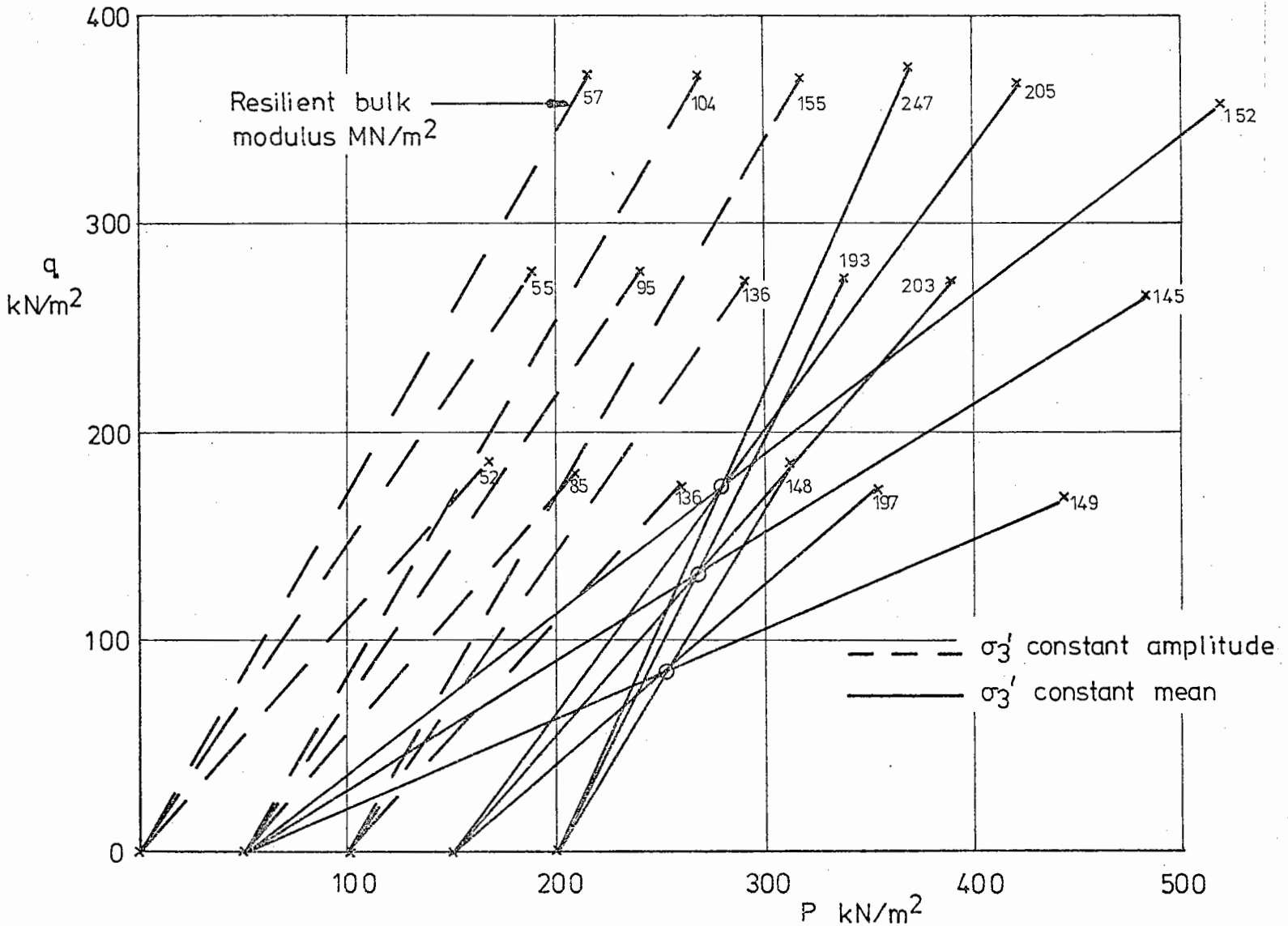

Fig. 7.16 Stress paths for cyclic confining stress tests.

which, for the special case of the triaxial test, reduces to:

$$\varphi_{oct} = \frac{2\sqrt{2}}{3} (\varepsilon_1 - \varepsilon_3) \qquad (7.15)$$

Compressive strains are defined as positive. The bulk modulus is defined as:

$$K = \frac{\sigma_{oct}}{3 \cdot \varepsilon_{oct}} \qquad (7.16)$$

and the shear modulus is defined as:

$$G = \frac{\tau_{oct}}{\varphi_{oct}} \qquad (7.17)$$

From these definitions follow the definitions of resilient bulk modulus:

$$K_R = \frac{p_R}{v_R} \qquad (7.18)$$

and resilient shear modulus:

$$G_R = \frac{\sqrt{2}}{3} \cdot \frac{q_R}{\varepsilon_R} \qquad (7.19)$$

By establishing equations (7.18) and (7.19) in terms of the volumetric octahedral strain and stress and the octahedral shearing strain and stress, the volumetric and shearing components are separated from each other.

The behaviour of the bulk modulus and shear modulus is best examined in terms of simple stress-strain relationships. Previous work by Lashine et al (1971) has shown that both the cyclic and mean components of stress affect stress-strain relationships for this material. A unique stress-

strain relationship was found to exist if v_R was plotted against p_R normalised with respect to p_m (Fig. 7.17). It can be seen from this curve that, except where dilation is occurring with the resultant negative volumetric strains, the relationship is continuous and points for both constant and cyclic confining stresses lie on the same curve. There does not seem to be any systematic effect due to the value of q_R.

The tests carried out under constant confining stress all lie on the lower portion of the curve. This fact, it will be shown, is significant when considering Poisson's ratio. The slope of this line is a measure of the volumetric compliance which is the same as the reciprocal of the bulk modulus. As p_R increases, the bulk modulus decreases and as p_m increases, the bulk modulus increases. This trend can be seen on Fig. 7.16. This result is similar to that found by Lashine et al (1971) for the resilient modulus, where a stiffening occurred as the mean level of the deviator stress was increased and a softening occurred as the amplitude was increased.

A similar relationship can be plotted of resilient shear strain against normalised deviator stress (Fig. 7.18), (Tables 7.1 and 7.2). In a similar fashion to the relationship for resilient volumetric strain, the resilient shear strain increases as the ratio q_R/p_m increases. It is not, however, affected by the level of the repeated mean normal stress (p_R). Once again, tests carried out with a cyclic confining stress lie on the same curve as those with

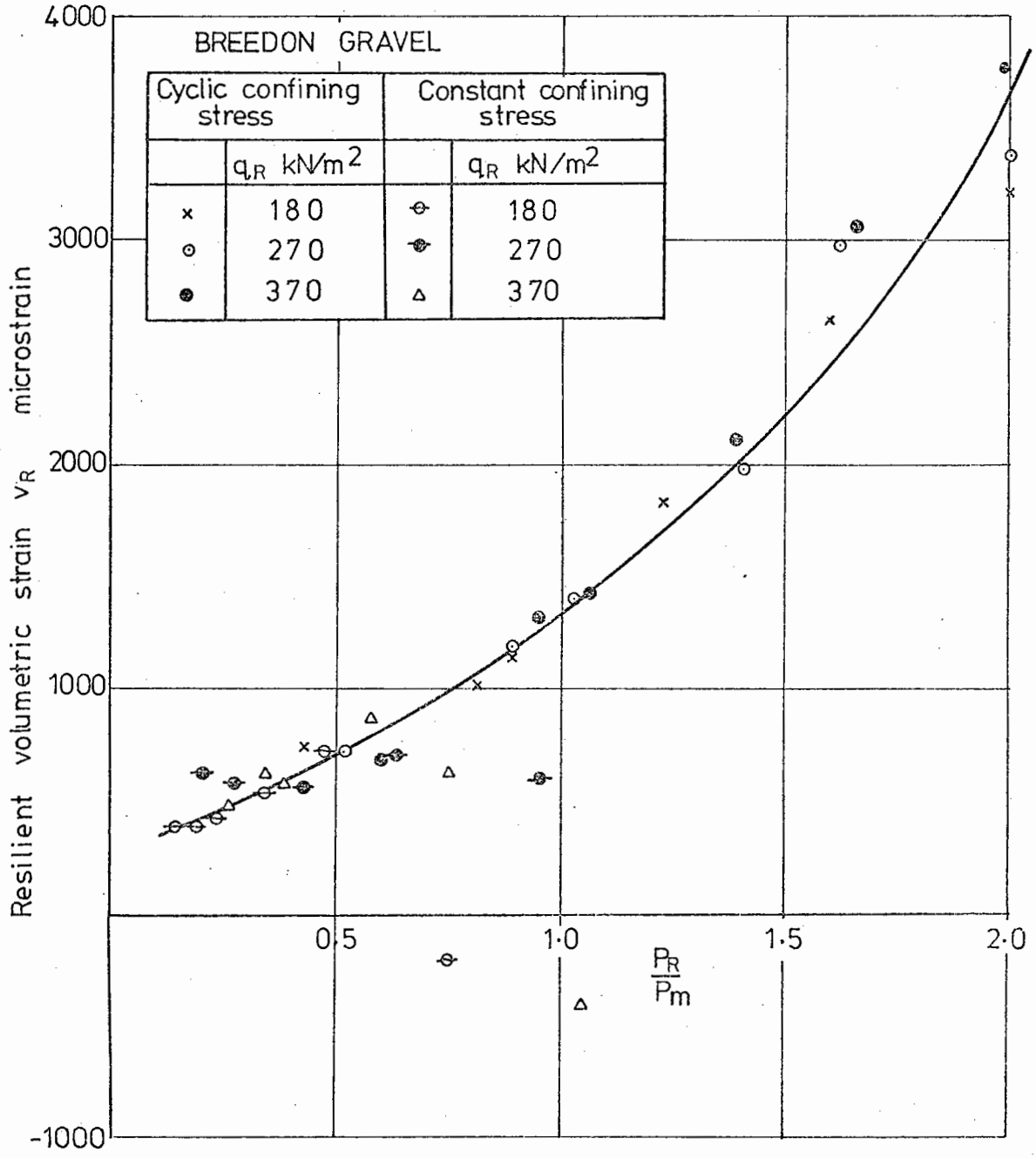

Fig. 7.17 Variation of resilient volumetric strain with the normalized mean normal stress.

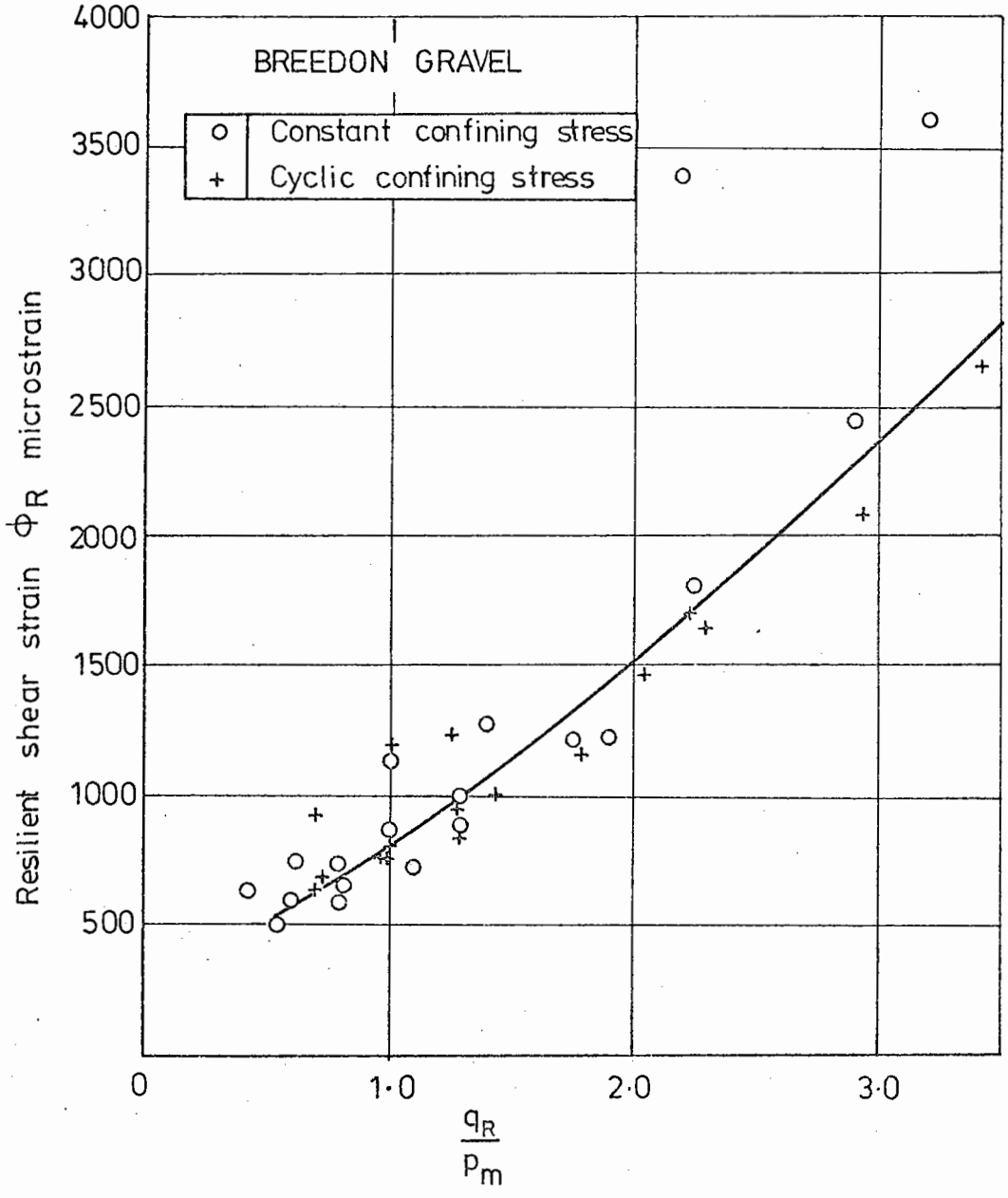

Fig. 7.18 Variation of resilient shear strain with normalised deviator stress.

a constant confining stress. The two points where excessively high shear strains occur coincide with the wayward points on Fig. 7.17 for samples which were dilating. It should, however, be noted that the range of shear strains is similar for both types of test. The gradient of this curve is a measure of the shear compliance. It can be seen that as q_R increases there is a slight decrease in the shear modulus and that as p_m increases, there is an increase.

As the shear strain increases to values greatly in excess of the volumetric strain, there is a marked increase in Poisson's ratio (Fig. 7.19). Considering the case of a constant confining stress, Poisson' ratio would be expected to increase as the shear strains increase (while, as already shown, the volumetric strains remain virtually constant). It can be seen that a marked increase in Poisson's ratio occurs only under conditions when the shear strains become high relative to the volumetric strains and that this situation did not occur when the cell pressure was cycled.

p_m	q_R kN/m²	p_R/p_m	q_R/p_m	Volumetric strain (microstrain)	Shear strain (microstrain)
84	188	0.75	2.2	-203	3371
131	186	0.47	1.4	707	1274
183	185	0.34	1.0	538	1147
254	178	0.23	0.6	428	587
320	181	0.19	0.55	399	484
420	177	0.14	0.42	381	629
445	272	0.20	0.61	622	739
460	365	0.26	0.79	471	729
361	368	0.34	1.0	623	878
270	280	0.34	1.1	512	706
284	370	0.43	1.3	589	982
198	272	0.46	1.3	584	908
146	275	0.42	1.9	692	1229
215	375	0.58	1.75	859	1222
164	371	0.75	2.26	612	1804
99	286	0.96	2.9	588	2454
116	372	1.07	3.2	-401	3609
346	278	0.27	0.8	571	633

Table 7.1 Values of Resilient Parameters for Constant Confining Pressure

p_m	q_R kN/m^2	p_R/p_m	q_R/p_m	Volumetric strain (microstrain)	Shear strain (microstrain)
255	185	0.43	0.72	743	670
269	274	0.51	1.02	714	749
285	375	0.60	1.32	687	828
252	173	0.81	0.69	1034	632
270	272	0.89	1.0	1177	791
286	368	0.95	1.29	1325	961
248	169	1.6	0.68	2654	927
267	265	1.62	1.0	2983	1160
284	357	1.65	1.25	3086	1226
179	177	0.88	1.0	1156	753
185	270	1.03	1.45	1393	994
208	371	1.05	1.78	1411	1149
129	182	1.22	1.41	1838	1147
135	276	1.4	2.04	1998	1420
160	369	1.38	2.3	2104	1627
84	188	2.0	2.24	3228	1697
93	274	2.0	2.94	3369	2076
108	370	1.91	3.42	3798	2664

Table 7.2 Values of Resilient Parameters for Cyclic Confining Pressure

CHAPTER EIGHT

UNBOUND MATERIAL BEHAVIOUR IN THE PAVEMENT SYSTEM

8.1 INTRODUCTION

An attempt has been made to incorporate the materials tested in this study into a theoretical pavement structure.

Three layer structures have been considered, with the Keuper marl as a subgrade, Breedon gravel as a sub-base and a single bituminous bound layer consisting of a dense bitumen macadam (Fig. 8.1).

Pavement systems were selected for two design lives; 10^6 and 10^7 standard axles. These systems were then analysed at three different temperatures. The stresses and strains were computed using a layered elastic computer programme known as BISTRO (Peutz et al, 1968).

Using the computed stresses, an estimate has been made of the accumulation of permanent deformation for the complete structures considering subgrades of different stress histories.

8.2 THE CONCEPT OF A STANDARD AXLE

Wheel loads of varying types and configuration can be reduced to an equivalent number of standard axles. The standard axle most generally used in 8.2 tonnes. The concept of a standard axle assumes that a given vehicle load L, can be reduced in terms of damage to a pavement

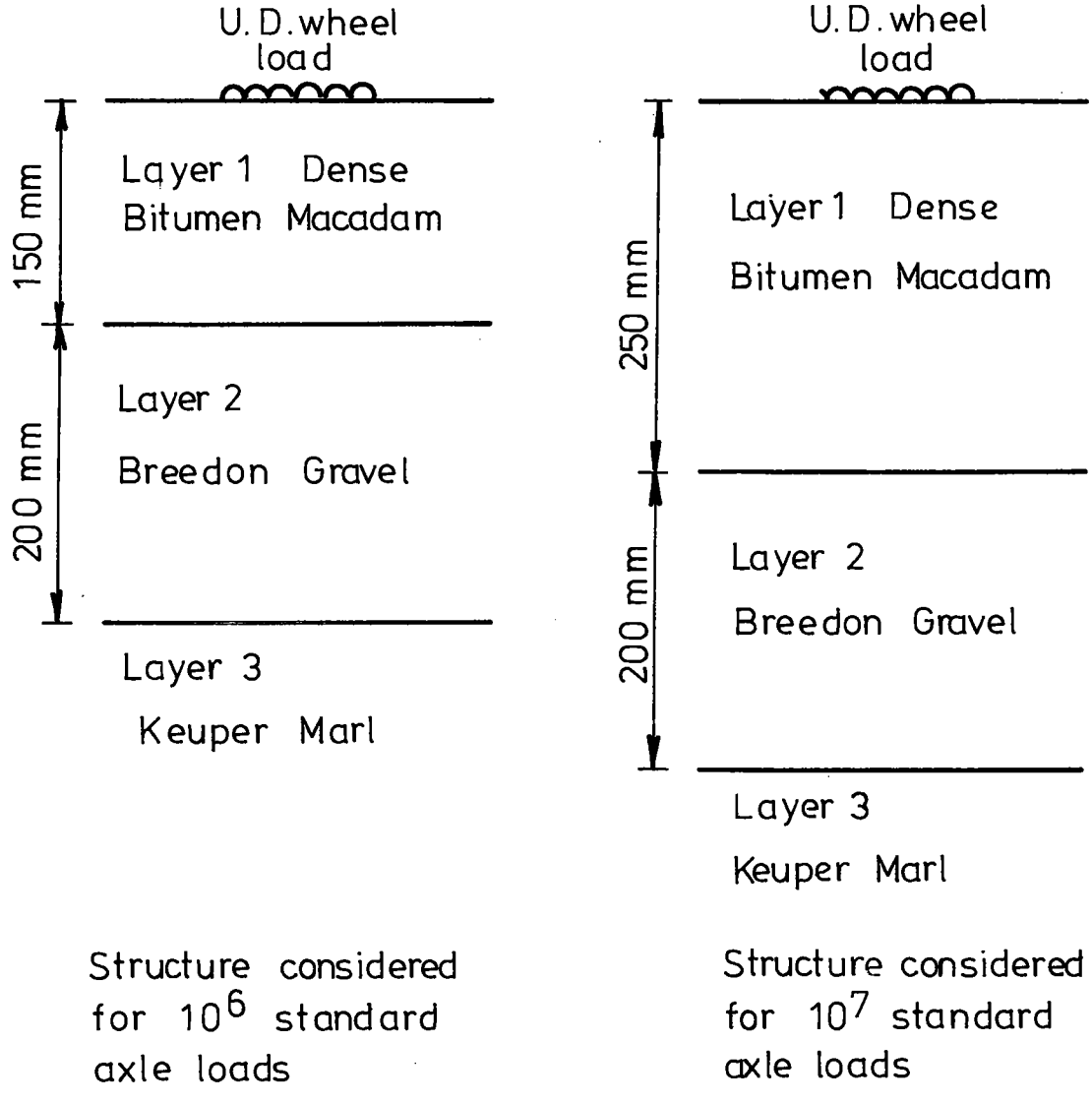

Fig. 8.1 Theoretical pavement structures.

structure to F applications of a standard wheel load S, such that:

$$F = \left(\frac{L}{S}\right)^n$$

The power of n found by most investigators is about 4 (Peattie, 1974). Table 8.1 lists typical equivalence factors for different classes of axle load. It can be seen that the damage caused by light vehicles is negligible. Fig. 8.2 shows the equivalence factor plotted against the axle load on a semi-logarithmic scale. This graph is similar and can be considered analogous to those plotted for Keuper marl of strain rate against some stress function. Therefore, as far as clays are concerned, the concept of a standard axle is a useful tool in any determination of plastic strain.

Axle load class - tonnes	Equivalence factor F
0 - 1.81	0.0002
1.81 - 3.63	0.001
3.63 - 5.44	0.09
5.44 - 7.26	0.35
7.26 - 9.07	1.00
9.07 - 10.89	2.30
10.89 - 12.70	4.40
12.70 - 14.52	7.60
14.52 - 16.33	12.1
Over 16.33	22.8

Table 8.1 Equivalence Factors

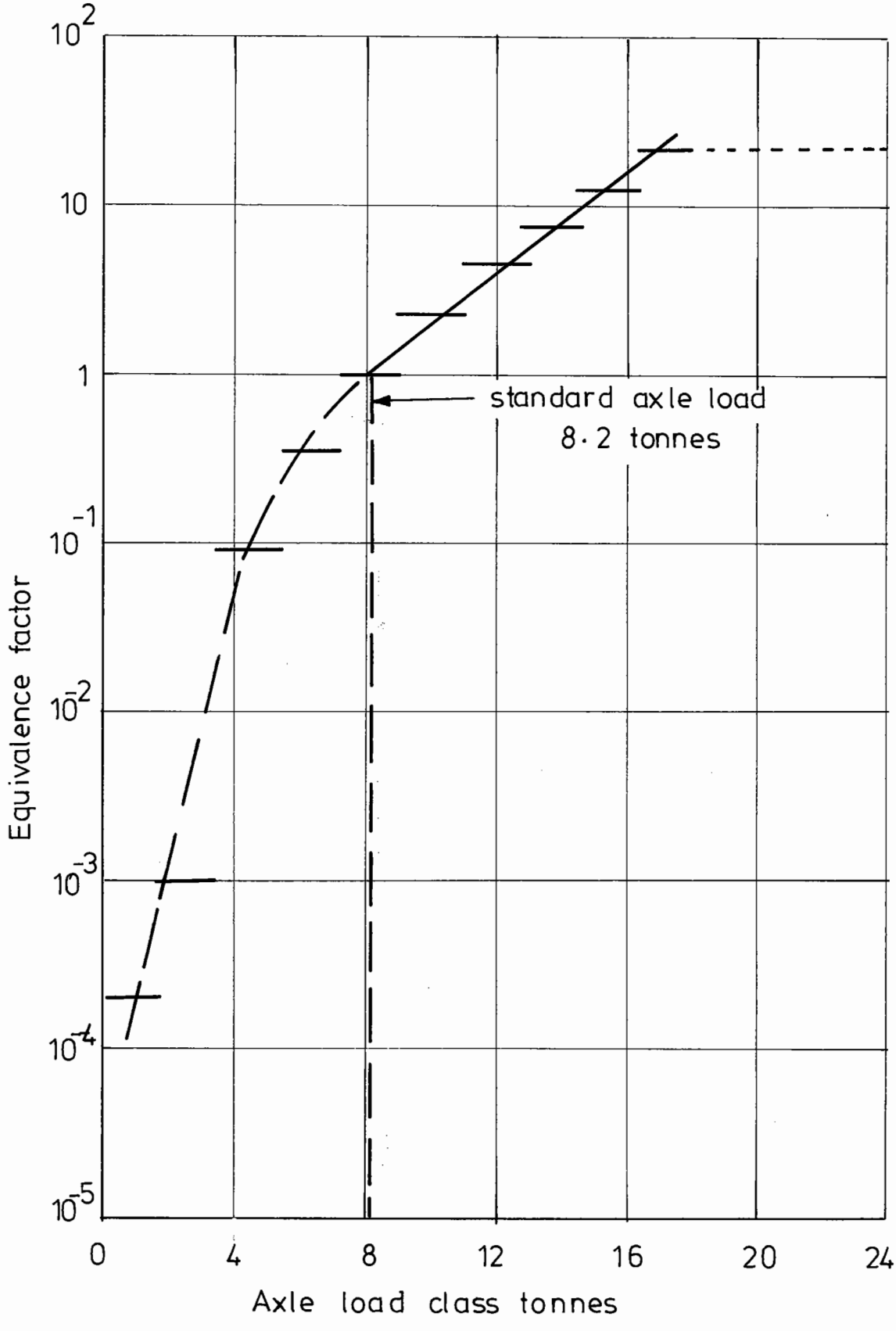

Fig. 8.2 Variation of equivalence factor with axle load

Analyses were carried out for 10^6 and 10^7 standard axles.

A single wheel configuration was used since other configurations are not likely to have much effect at depth (Peattie, 1974). The radius of the loaded area was assumed to be 0.16 m and the pressure acting on this area is hence 500 kN/m^2.

8.3 MATERIALS IN THE PAVEMENT STRUCTURE

8.3.1 Bituminous Layer

A single bituminous layer only was considered in the theoretical pavement systems. A dense bitumen macadam was chosen on which tests have been carried out to allow some prediction of permanent strain (Snaith, 1973).

The properties of this layer are affected by both temperature and vehicle speed. The stiffness of the bituminous layer was determined using the method given by Brown (1974) (1) for a vehicle speed of 30 kph and three temperatures of 20, 30 and 40°C. The stiffnesses for the different layer thicknesses and temperatures are given in Table 8.2.

A Poisson's ratio of 0.4 was chosen for this layer.

8.3.2 Breedon Gravel

Although this material would not be used in a road as a sub-base, it was chosen for the second layer because some data is available on the permanent and resilient stress-strain characteristics.

System No.	Temperature ^{o}C	Design Applications	Thickness of DBM mm	Stiffness of DBM MN/m^2	Tensile strain in DBM μ strain	Allowable tensile strain in DBM μ strain	Compressive strain in subgrade μ strain	Allowable strain in subgrade μ strain
1	20	10^6	150	8250	155	140	587	450
2	20	10^7	250	8000	74	75	251	240
3	30	10^6	150	3200	315	140	985	450
4	30	10^7	250	3100	159	75	455	240
5	40	10^6	150	1040	651	140	1650	450
6	40	10^7	250	1000	363	75	856	240

Table 8.2 Critical Strains in Pavement Systems

The modulus of this material is stress dependent and hence an initial estimate of 150 MN/m^2 was made for the value of modulus. Using this value a first analysis of the pavement structure was made using BISTRO which gave an approximate stress distribution. The modulus of granular materials is primarily dependent on the horizontal stress (Hicks, 1970, Lashine, 1971). Using data given by Lashine (1971), and the mean value of horizontal stress, taking into account the overburden pressure, the modulus of the Breedon gravel was re-estimated to be 60 MN/m^2.

As the principal stress ratio for this layer is relatively high, large shear strains would be expected and hence a value of Poisson's ratio of 0.3 was chosen (Fig. 7.19).

8.3.3 Keuper Marl

The modulus of this layer is governed by the ratio of shear stress to the horizontal stress (Fig. 6.85). In situ the value of horizontal stress would depend on the height of the water table and the value of soil suction. For the purposes of this exercise, the marl is considered to be saturated and the horizontal stress is the same as the overburden pressure (estimated as 10 kN/m^2). An initial estimate of the modulus was made of 60 MN/m^2. The first BISTRO analysis showed that the ratio of the deviator stress to the effective confining stress was 2 or more and hence a value of 25 MN/m^2 was chosen for the modulus (Fig. 6.84)

Three hypothetical stress histories were postulated,

having OCR's of 3, 10 and 160 at a constant effective swelling pressure of 10 kN/m^2 (Fig. 8.3). The OCR of 3 is on the "wet" side, while those of 10 and 160 are on the "dry" side.

Since the modulus of the marl is dependent only on stress level, then the three stress histories will have the same modulus for a given vehicle load but different permanent deformation characteristics.

The Poisson's ratio for this layer was estimated to be 0.4.

8.4 RESILIENT STRAIN CRITERIA

Some pavement design methods (Dormon and Edwards, 1964, Brown, 1974) use limiting values of resilient strain in the asphalt and the subgrade as design criteria. These limiting values have been evaluated for the two pavement structures, and are later compared with the calculated values in the pavement structures.

8.4.1 Tensile Strain in the Bituminous Layer

A fatigue line specifying the maximum allowable strain in the bituminous layer can be determined knowing the percentage volume of binder and the initial ring and ball softening point of the bitumen, using data given by Cooper and Pell (1974).

For the dense bitumen macadam, the values were as follows:

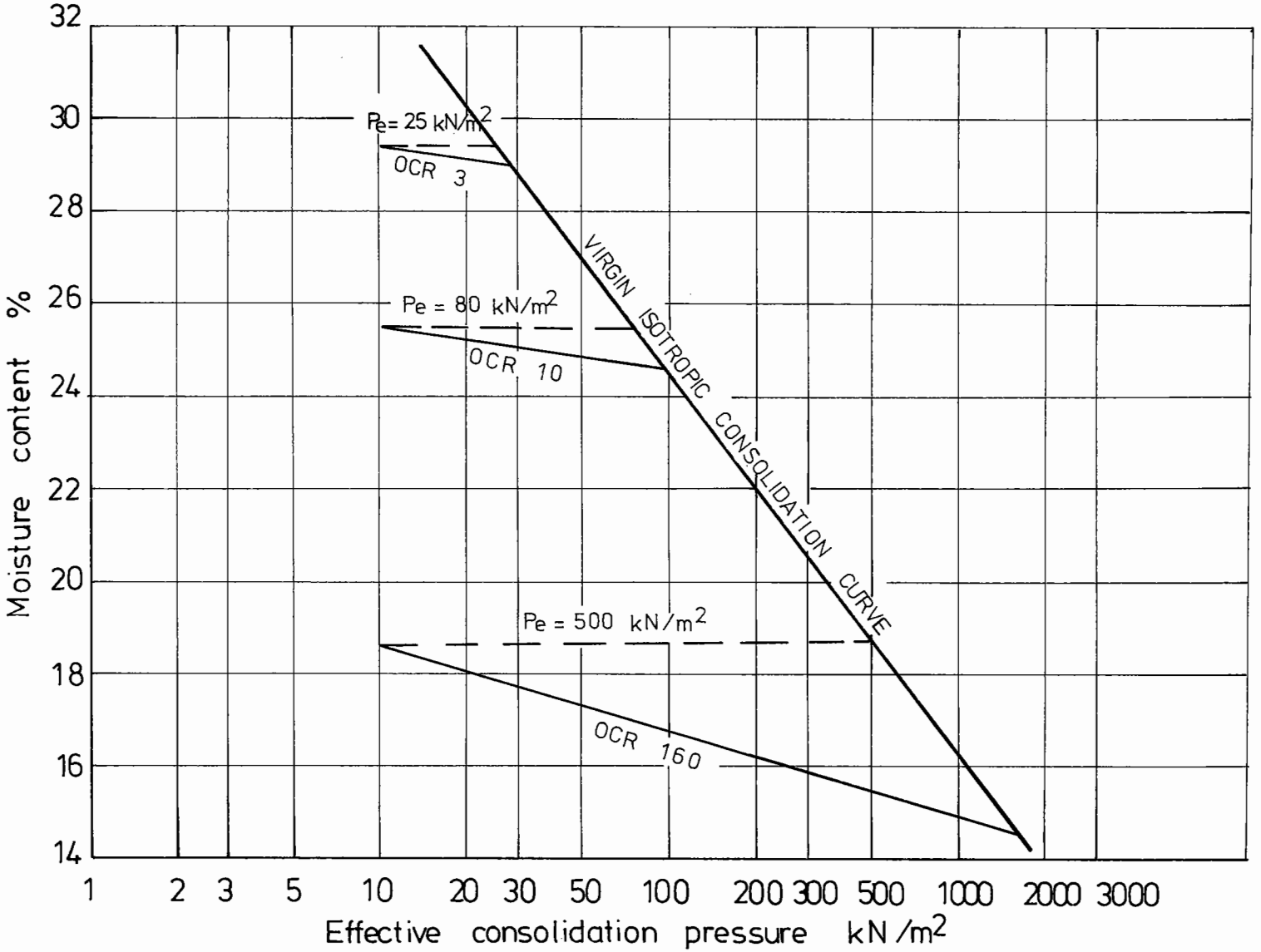

Fig. 8.3 Stress histories chosen for pavement analysis.

10^6 applications: 140 μ strain

10^7 applications: 75 μ strain

8.4.2 Compressive Strain in the Subgrade

The criterion used by Brown (1974) for British roads was adopted. The following allowable resilient strains on the subgrade are given:

10^6 applications: 450 μ strain

10^7 applications: 240 μ strain

8.5 DESIGN PROCEDURE AND EVALUATION

Using Road Note No. 29 pavement structures to be evaluated were designed for 10^6 and 10^7 applications of load and a subgrade CBR of 5%. The depth of the granular layer chosen in both cases was 200 mm. The basecourse and roadbase were combined in one layer which was 150 mm and 250 mm for 10^6 and 10^7 applications respectively.

This procedure does not allow for the effect of temperature or loading time on the asphalt layer, which are considered below in the elastic analysis.

8.5.1 Layered Elastic Analysis

Each thickness of the asphalt layer was considered at three different temperatures, making a total of six pavement systems.

Using the BISTRO programme, analyses were carried out of these pavement systems. The data required was as follows:

(a) Thickness of each layer (except subgrade).

(b) The stiffness of each layer.

(c) The Poisson's ratio of each layer.

The tensile strains at the bottom of the asphalt layer have been given in Table 8.2, together with the compressive strains in the subgrade. Comparison with the allowable values shows that system 1 is slightly under-designed while the strains in system 2 are virtually the same as the allowable values. However, the systems at higher temperatures give strains greatly in excess of the allowable values.

The distribution of the vertical and radial stresses generated by a standard axle load in the unbound layers is given in Figs. 8.4 to 8.9. These show that the radial stresses generated by the wheel load in the granular layers are tensile, but except for systems 5 and 6 these tensile stresses are never greater than the criterion proposed by Brown and Pell (1972) of a half the vertical stress added to the overburden pressure.

The traffic associated lateral stress for marl is very small and hence the confining stress is virtually constant and can be considered as being equal to the overburden pressure, which would be approximately 10 kN/m^2. The value chosen of 25 MN/m^2 for the modulus is, therefore, a reasonable one as the ratio of the deviator stress to the confining pressure is on the whole greater than 1 (see Fig. 6.84).

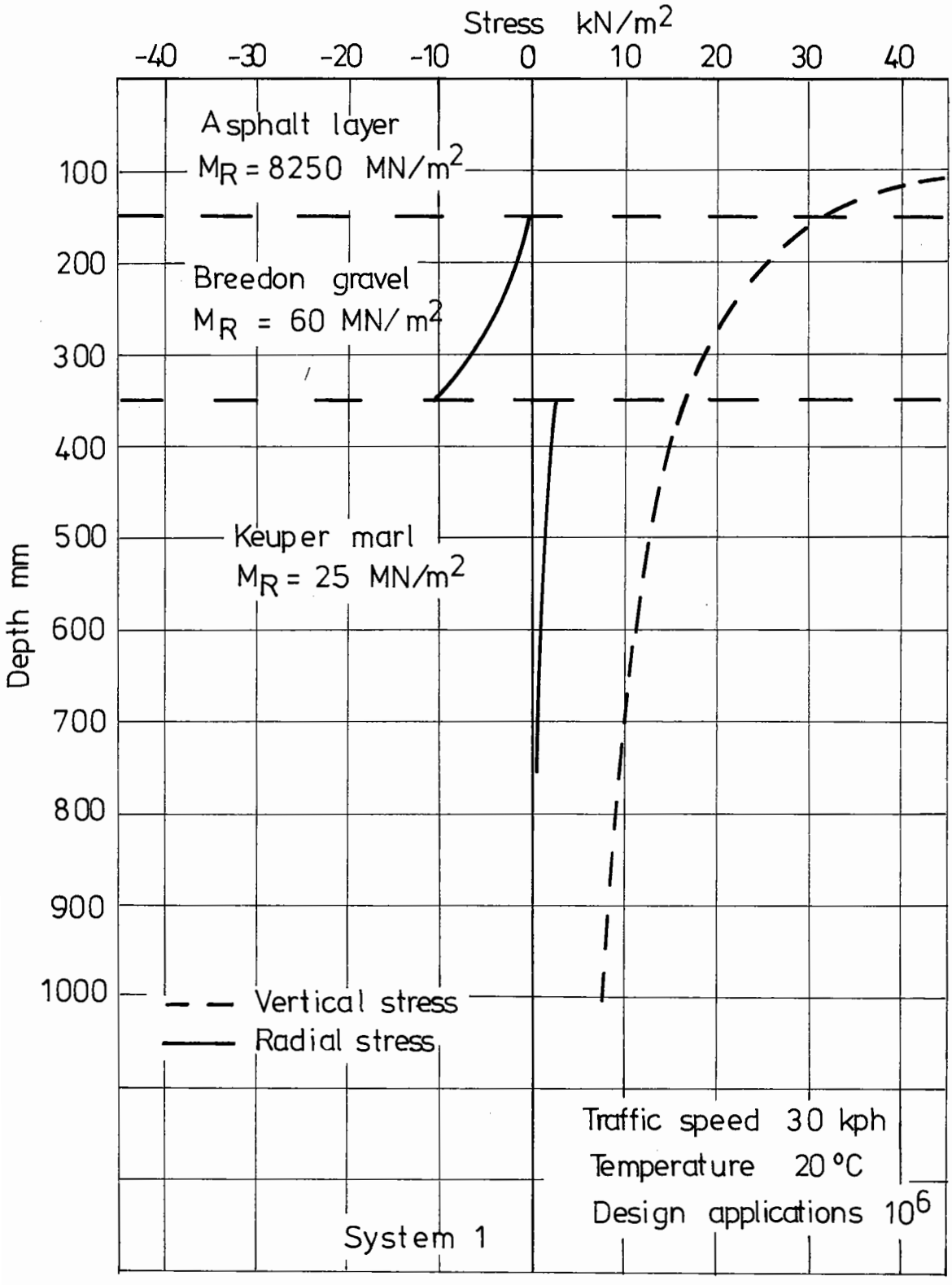

Fig. 8.4 Computed stresses in unbound layers of pavement structure.

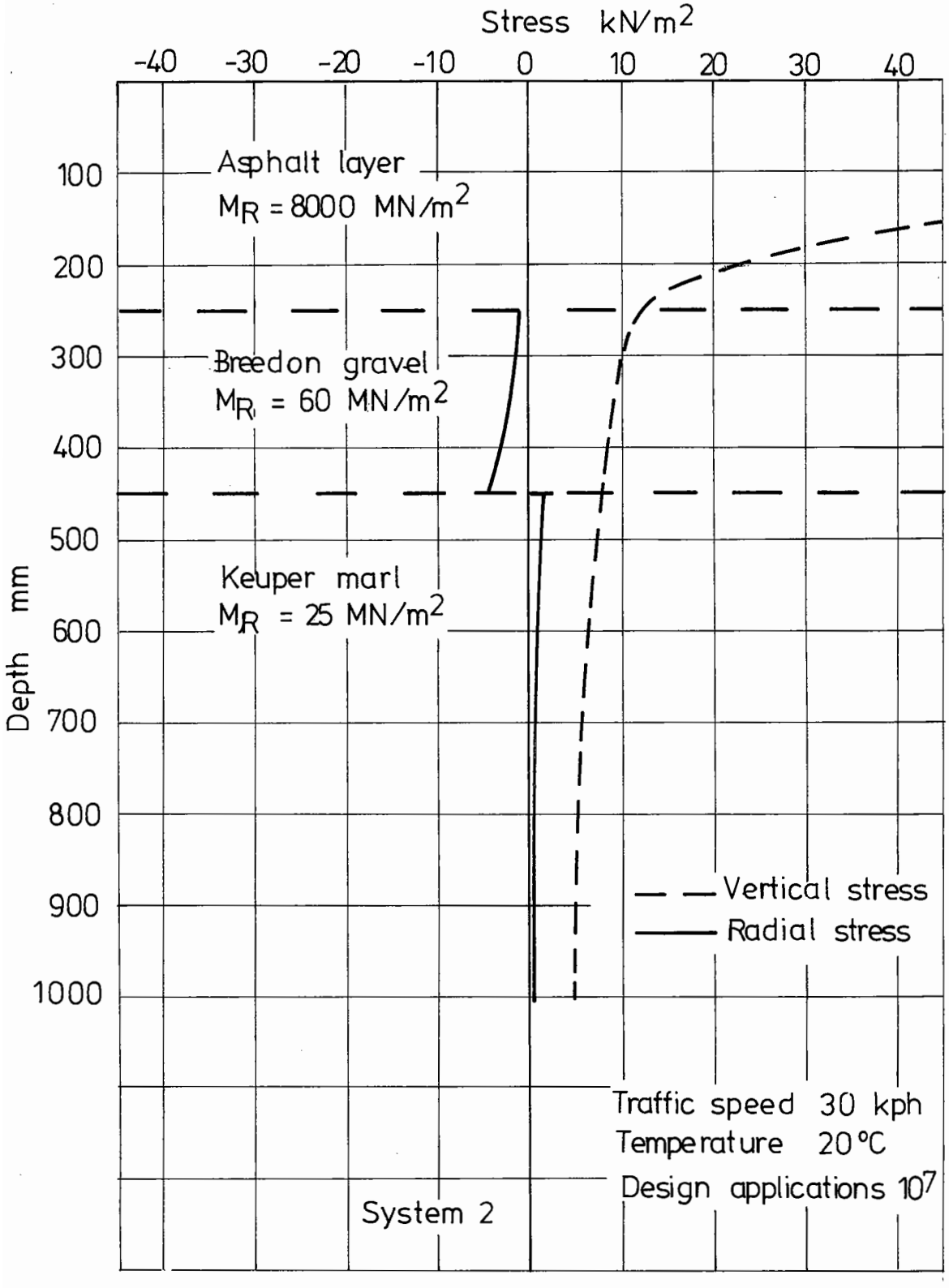

Fig. 8,5 Computed stresses in unbound layers of pavement structure.

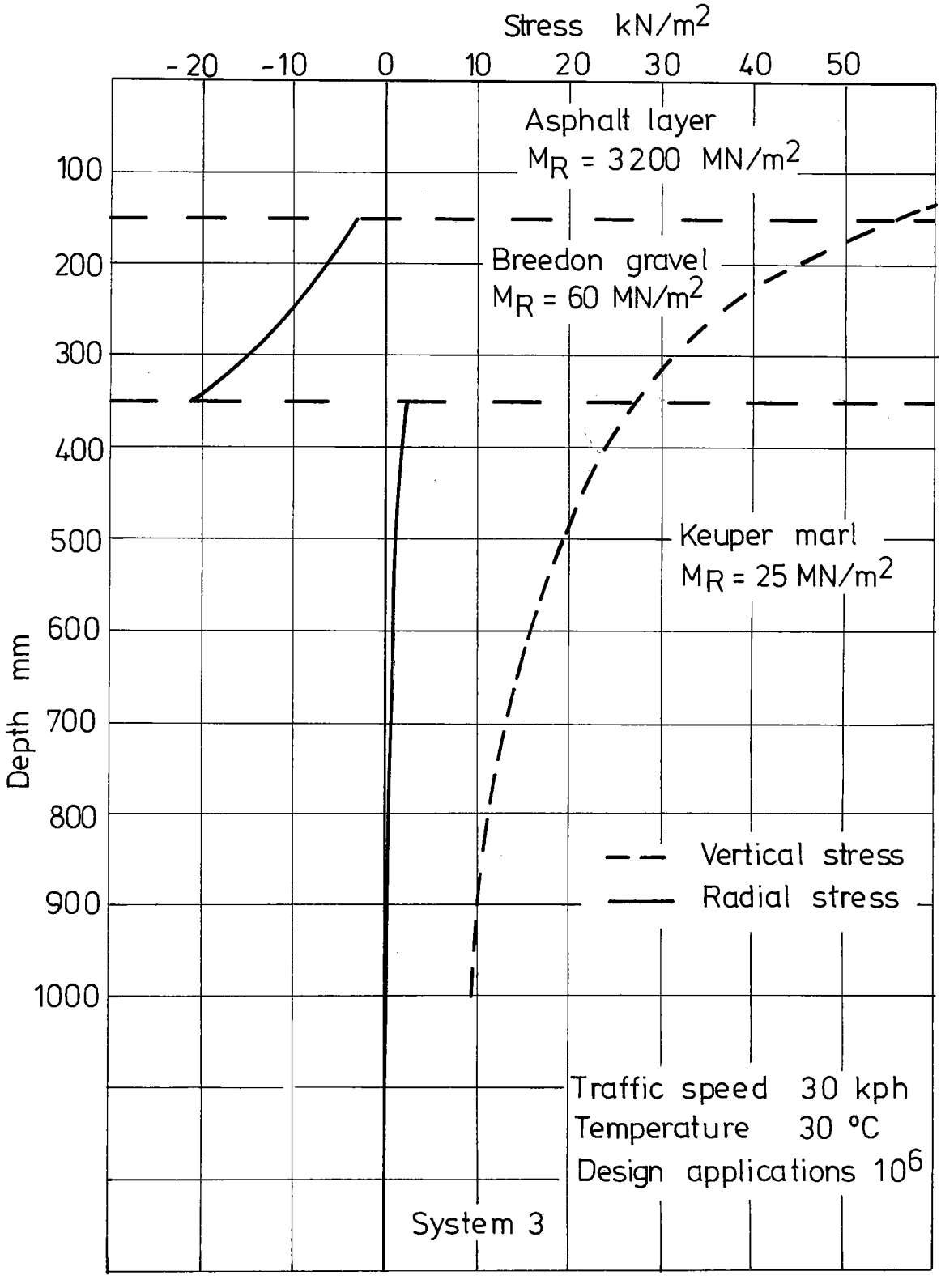

Fig. 8.6 Computed stresses in unbound layers of pavement structure.

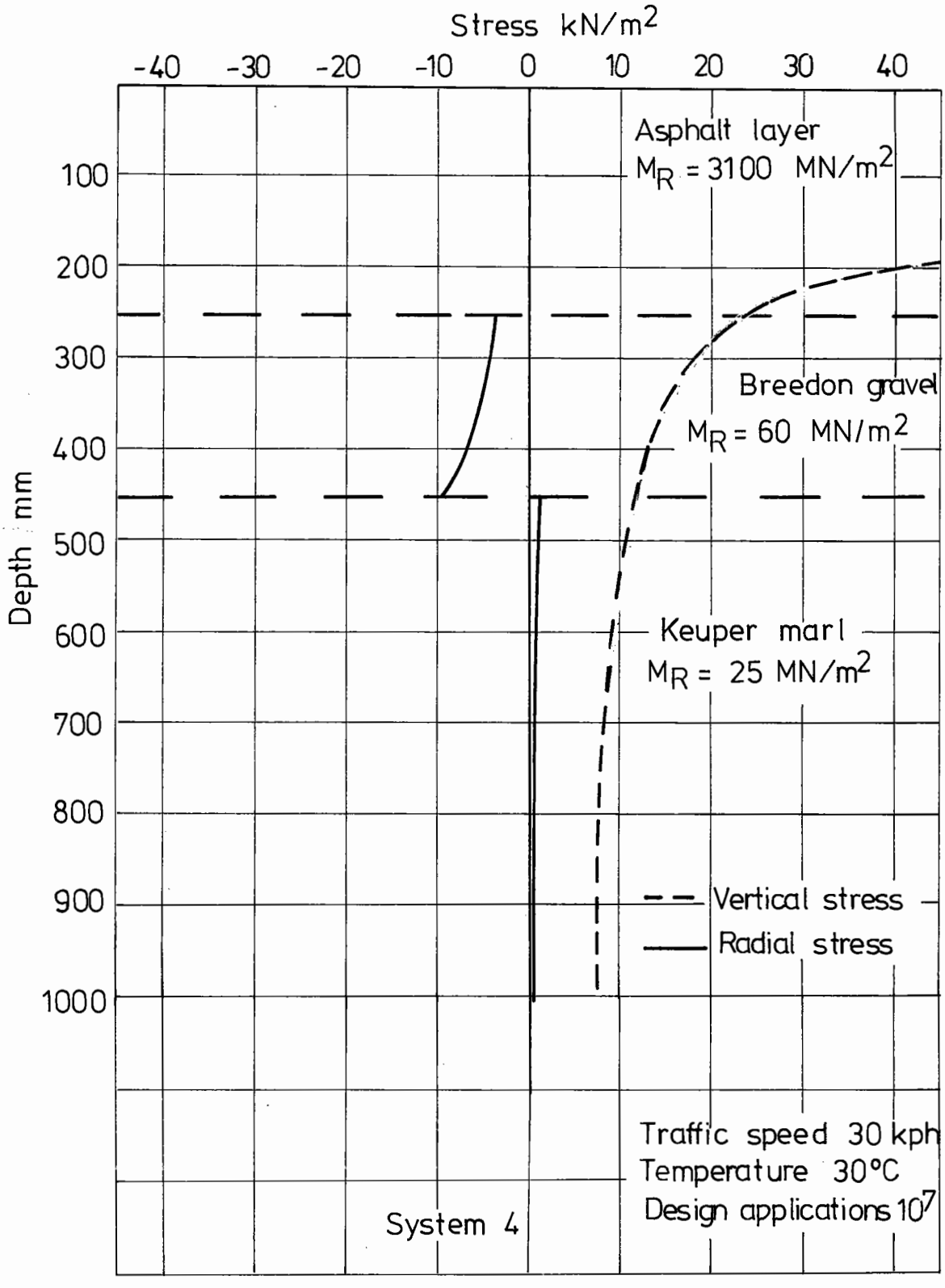

Fig. 8.7 Computed stresses in unbound layers of pavement structure

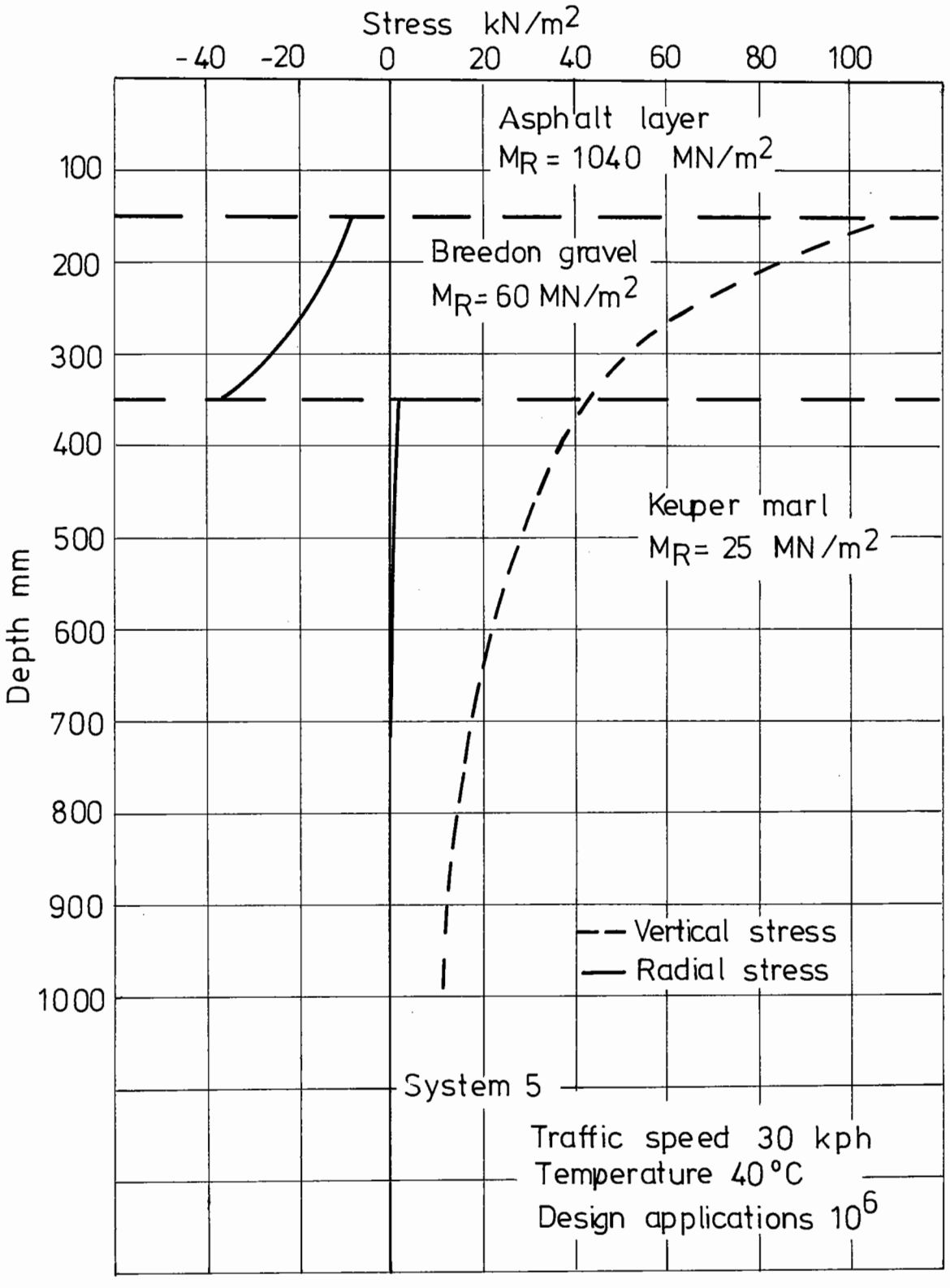

Fig. 8.8 Computed stresses in unbound layers of pavement structure.

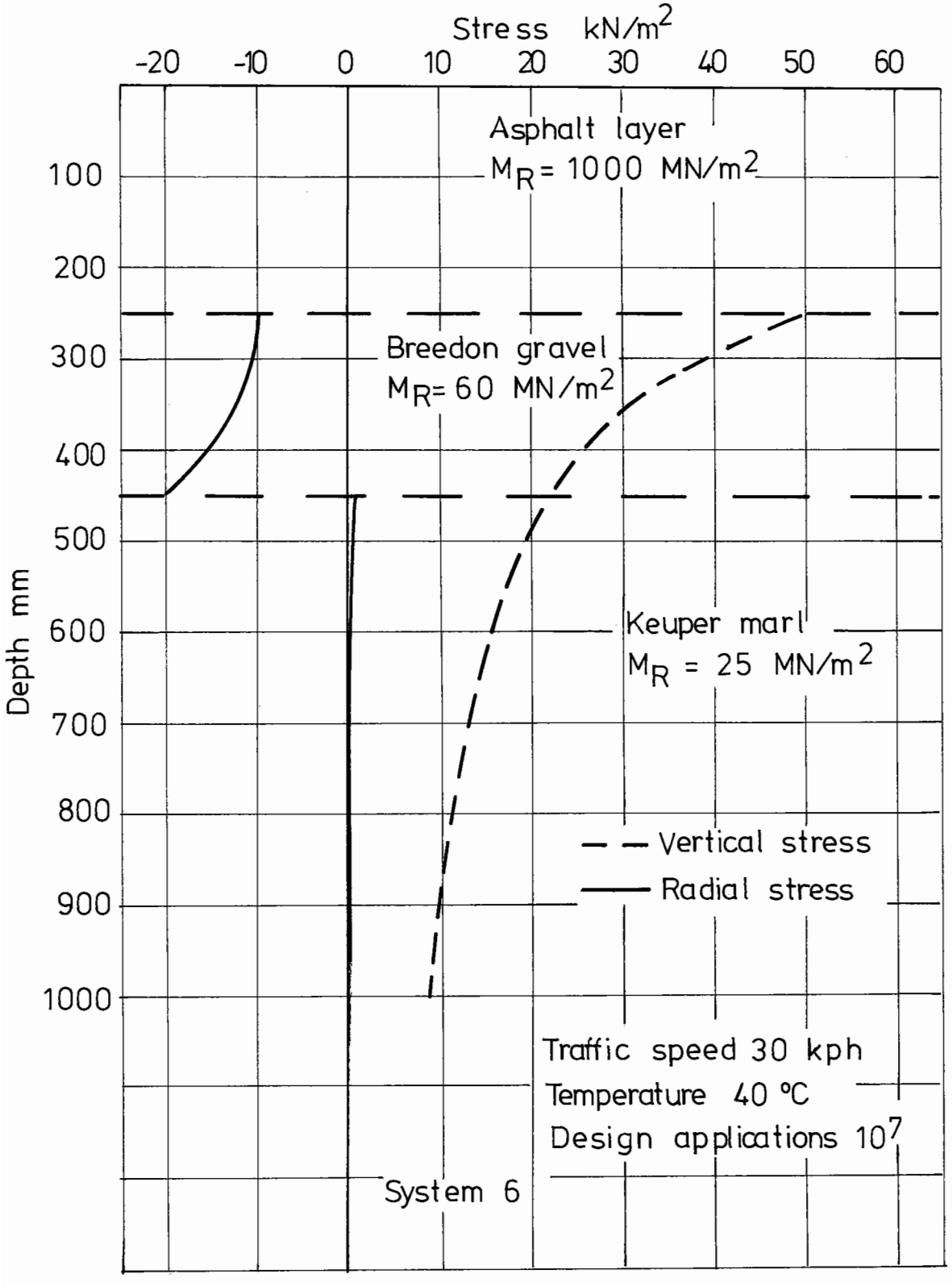

Fig. 8.9 Computed stresses in unbound layers of pavement structure

8.5.2 The Accumulation of Permanent Strain in the Pavement Structure

The permanent strains in the subgrade were computed using equations 6.17 to 6.21. For these it was necessary to know the traffic generated vertical stress, and the equivalent pressure p_e. As the traffic stress varies with depth it was necessary to split the subgrade into sub-layers and consider the mean vertical stress in each of these sub-layers. Table 8.3 lists the stresses in the sub-layers and the resultant deformations. The thickness of sub-layer chosen varied according to the rate of change of stress through the subgrade. The function used for the strain rate was assumed to apply at low stress which may have resulted in a slight overestimate of permanent strain in some cases.

Estimates of permanent strain in the granular layer were made using Fig. 7.10. The lateral stress considered was the approximate net value taking into account the over-burden pressure. These were, however, only approximate as little is known of the effects of tensile stresses in the bottom of this layer. For temperatures of $40^{o}C$ these tensile strains existed throughout the layer and, therefore, no estimate could be made of the permanent strains.

The permanent strains in the bituminous layer were estimated from data given by Snaith (1973). These are also only approximate since no data is available for the behaviour of this particular material under the high

Depth of sub-layer mm	OCR	p_e kN/m²	q kN/m²	$q/\sqrt{p_e}$	ϵ_p%	Sub-layer deformation mm	Total deformation mm
System 1	10^6 applications			20°C			
325	3	25	12.5	2.5	.76	2.47	
325	3	25	9	1.8	.63	2.05	
1000	3	25	4.5	0.9	.50	5.00	9.5
325	10	80	12.5	1.3	.31	1.00	
325	10	80	9	1.0	.23	0.75	
1000	10	80	4.5	0.5	.16	1.6	3.35
325	160	500	12.5	0.56	.17	0.55	
325	160	500	9	0.4	.15	0.49	
1000	160	500	4.5	0.2	.13	1.3	2.34
System 2	10^7 applications			20°C			
275	3	25	6.0	1.2	.79	2.17	
275	3	25	5.0	1.0	.75	2.06	
1000	3	25	2.5	0.5	.66	6.6	10.83
275	10	80	6.0	0.67	.22	0.6	
275	10	80	5.0	0.55	.20	0.55	
1000	10	80	2.5	0.27	.16	1.6	2.75
275	160	500	6.0	0.67	.16	0.44	
275	160	500	5.0	0.22	.16	0.44	
1000	160	500	2.5	0.11	.15	1.5	2.38
System 3	10^6 applications			30°C			
100	3	25	24	4.8	1.36	1.36	
250	3	25	17	3.4	.95	2.37	
300	3	25	11	2.2	.70	2.1	
1000	3	25	4.5	0.9	.5	5.0	10.83
100	10	80	24	2.6	.76	0.76	
250	10	80	17	1.9	.44	1.1	
300	10	80	11	1.2	.27	.81	
1000	10	80	4.5	0.5	.16	1.6	4.27
100	160	500	24	1.07	.25	0.25	
250	160	500	17	0.76	.19	0.475	
300	160	500	11	0.49	.16	0.48	
1000	160	500	4.5	0.2	.13	1.3	2.50

Table 8.3 Permanent Strains in the Subgrade

Depth of sub-layer mm	OCR	p_e kN/m²	q_a kN/m²	$q_a/\sqrt{p_e}$	ε_p%	Sub-layer deformation mm	Total deformation mm
System 4	10^7 applications		30°C				
275	3	25	10	0.2	.97	2.66	
275	3	25	8	1.6	.88	2.42	
1000	3	25	4	0.8	.71	7.1	12.18
275	10	80	10	1.1	.3	0.825	
275	10	80	8	0.89	.26	0.715	
1000	10	80	4	0.44	.18	1.8	3.34
275	160	500	10	0.44	.18	0.49	
275	160	500	8	0.35	.17	0.46	
1000	150	500	4	0.17	.15	1.5	2.45
System 5	10^6 design applications		40°C				
100	3	25	37	7.4	.26	2.6	
250	3	25	25	5	1.43	3.5	
300	3	25	15	3	.86	2.58	
1000	3	25	5	1	.52	5.2	13.88
100	10	80	37	4.1	2.1	2.1	
250	10	80	25	2.7	.83	2.0	
300	10	80	15	1.6	.37	1.1	
1000	10	80	5	0.5	.17	1.7	6.9
100	160	500	37	1.6	.37	0.37	
250	160	500	25	1.1	.25	0.62	
300	160	500	15	0.67	.18	0.54	
1000	160	500	5	0.22	.13	1.3	2.83
System 6	10^7 design applications		40°C				
275	3	25	18	3.6	1.45	3.98	
275	3	25	11	2.2	1.02	2.8	
1000	3	25	5	1	.75	7.5	14.28
275	10	80	18	2	.57	1.56	
275	10	80	11	1.2	.32	0.88	
1000	10	80	5	0.55	.20	2.0	4.44
275	160	500	18	0.8	.24	0.66	
275	160	500	11	0.49	.19	0.52	
1000	160	500	5	0.22	.16	1.6	2.78

Table 8.3 (contd.) Permanent Strains in the Subgrade

Depth of sub-layer mm	OCR	p_e kN/m²	q kN/m²	$q/\sqrt{p_e}$	ϵ_p%	Sub-layer deformation mm	Total deformation mm
System 3	10^5 applications		30°C				
100	3	25	24	4.8	.91	0.91	
250	3	25	17	3.4	.63	1.58	
300	3	25	11	2.2	.47	1.41	
1000	3	25	4.5	0.9	.34	3.4	7.3
100	10	80	24	2.6	.61	0.61	
250	10	80	17	1.9	.35	0.88	
300	10	80	11	1.2	.21	0.63	
1000	10	80	4.5	0.5	.13	1.3	3.4
100	160	500	24	1.07	.20	0.2	
250	160	500	17	0.76	.16	0.4	
300	160	500	11	0.49	.13	0.39	
1000	160	500	4.5	0.2	.11	1.1	2.1
System 4	10^5 applications		30°C				
275	3	25	10	2	.45	1.24	
275	3	25	8	1.6	.40	1.1	
1000	3	25	4	0.8	.33	3.3	5.6
275	10	80	10	1.1	.2	0.55	
275	10	80	8	0.89	.17	0.47	
1000	10	80	4	0.44	.12	1.2	2.22
275	160	500	10	0.44	.13	0.36	
275	160	500	8	0.35	.12	0.33	
1000	160	500	4	0.17	.1	1.0	1.69

Table 8.3 (contd.) Permanent Strains in the Subgrade

Depth of sub-layer mm	OCR	p_e kN/m²	q kN/m²	$q/\sqrt{p_e}$	ε_p%	Sub-layer deformation mm	Total deformation mm
System 5	10,000 applications				40°C		
100	3	25	37	7.4	1.1	1.1	
250	3	25	25	5	.6	1.5	
300	3	25	15	3	.36	1.1	
1000	3	25	5	1	.21	2.1	5.8
100	10	80	37	4.1	1.28	1.28	
250	10	80	25	2.7	.5	1.25	
300	10	80	15	1.6	.23	.69	
1000	10	80	5	0.5	.1	1.0	4.22
100	160	500	37	1.6	.2	0.2	
250	160	500	25	1.1	.15	0.37	
300	160	500	15	0.67	.11	0.33	
1000	160	500	5	0.22	.08	0.8	
System 6	10,000 applications				40°C		
275	3	25	18	3.6	.42	1.15	
275	3	25	11	2.2	.30	0.83	
1000	3	25	5	1.0	.22	2.2	4.18
275	10	80	18	2.0	.29	0.8	
275	10	80	11	1.2	.16	0.44	
1000	10	80	5	0.55	.1	1.0	2.24
275	160	500	18	0.8	.12	0.33	
275	160	500	11	0.49	.09	0.25	
1000	160	500	5	0.22	.08	0.8	1.38

Table 8.3 (contd.) Permanent Strains in the Subgrade

tensile stresses experienced in the lower half of this layer.

A comparison of the deformations accumulated in the individual layers is given in Table 8.4. For all temperatures of the asphalt layer, the contribution of the subgrade is very dependent on the stress history.

Under British climatic conditions one would not expect temperatures of 30°C or 40°C for the design life of a pavement. Computations were, therefore, also made for these temperatures of the deformation accumulated after 10^5 and 10^4 load applications respectively.

The heavily over-consolidated marl, which would be equivalent to an unweathered "cut" situation, suffers small deformations even at relatively high temperatures when the asphalt layer would afford the least protection.

In practice, it is more likely, however, that the geological stress history will have been weathered out of the soil and that it would only be lightly over-consolidated, possibly due to the removal of an overburden. At a temperature of 20°C which is not untypical of temperatures in the asphalt layer under British conditions, then a subgrade of this stress history contributes approximately 50% of the deformation during the design life.

At higher temperatures the asphalt deforms much more while the subgrade deforms by virtually the same amount. Even at very high temperatures of 40°C the increase in deformation of the subgrade over the design life is only 30-40%. One would only expect temperatures of 30°C or

System	Layer	Deformation mm	Total Deformation	No. of Applications	% total deformation p_e=25	% total deformation p_e=80	% total deformation p_e=500
1	DBM	0.86		10^6	5	7	8
1	Breedon Gravel	8		10^6	43	65	71
1	Keuper Marl (p_e=25)	9.5	18.36	10^6	52		
1	K.M. (p_e=80)	3.35	12.21	10^6		27	
1	K.M. (p_e=500)	2.34	11.2	10^6			21
2	DBM	2.76		10^7	13	20	21
2	Breedon Gravel	8		10^7	37	59	60
2	K.M. (p_e=25)	10.83	21.59	10^7	50		
2	K.M. (p_e=80)	2.75	13.51	10^7		20	
2	K.M. (p_e=500)	2.38	13.14	10^7			18
3	DBM	4.37		10^6	17	23	26
3	Breedon Gravel	10		10^6	39	54	59
3	K.M. (p_e=25)	10.8	25.17	10^6	43		
3	K.M. (p_e=80)	4.27	18.64	10^6		23	
3	K.M. (p_e=500)	2.50	16.87	10^6			15
4	DBM	12.84		10^7	36	49	50
4	Breedon Gravel	10		10^7	29	38	40
4	K.M. (p_e=25)	12.18	35.02	10^7	35		
4	K.M. (p_e=80)	3.34	26.18	10^7		13	
4	K.M. (p_e=500)	2.45	25.29	10^7			10

Table 8.4 Permanent Strains in Pavement Layers

System	Layer	Deformation mm	Total Deformation	No. of Applications	% total deformation p_e=25	% total deformation p_e=80	% total deformation p_e=500
5	DBM	30.46		10^6			
5	Breedon Gravel	-		10^6			
5	K.M. (p_e=25)	13.88		10^6			
5	K.M. (p_e=80)	6.9		10^6			
5	K.M. (p_e=500)	2.83		10^6			
6	DBM	77.20		10^7			
6	Breedon Gravel	-		10^7			
6	K.M. (p_e=25)	14.28		10^7			
6	K.M. (p_e=80)	4.44		10^7			
6	K.M. (p_e=500)	2.78		10^7			
3	DBM	3.2		10^5	15	19	21
3	Breedon Gravel	10		10^5	49	60	65
3	K.M. (p_e=25)	7.3	20.5	10^5	36		
3	K.M. (p_e=80)	3.4	16.6	10^5		20	
3	K.M. (p_e=500)	2.1	15.3	10^5			14
4	DBM	5.3		10^5	25	30	31
4	Breedon Gravel	10		10^5	48	57	58
4	K.M. (p_e=25)	5.6	20.9	10^5	27		
4	K.M. (p_e=80)	2.2	17.5	10^5			
4	K.M. (p_e=500)	1.7	17.0	10^5			10

Table 8.4 (contd.) Permanent Strains in Pavement Layers

System	Layer	Deformation mm	Total Deformation	No. of Applications	% total deformation p_e=25	% total deformation p_e=80	% total deformation p_e=500
5	DBM	4.7		10^4			
5	Breedon Gravel	-		10^4			
5	K.M. (p_e=25)	5.8		10^4			
5	K.M. (P_e=80)	4.2		10^4			
5	K.M. (p_e=500)	1.7		10^4			
6	DBM	9.1		10^4			
6	Breedon Gravel	-		10^4			
6	K.M. (p_e=25)	4.2		10^4			
6	K.M. (p_e=80)	2.2		10^4			
6	K.M. (p_e=500)	1.4		10^4			

Table 8.4 (contd.) Permanent Strains in Pavement Layers

40°C during a small proportion of the design life and during these periods it is the deformation of the asphalt which becomes important.

The granular layer used in the hypothetical structure contributes as much as 60% of the total deformation in the pavement. A more accurate evaluation of the behaviour of this material is, however, required, in particular at gradings more typical of those found in a road.

8.5.3 Performance in Terms of Failure Criteria

The term "design life" applied to a road pavement implies a failure condition. Performance criteria have been developed from in-service roads (Croney, 1972). Two criteria can be defined, one corresponding to failure or the state at which major structural repair is required and the second is a critical condition at which overlaying would ensure continued satisfactory performance. The failure criterion for British Pavements is taken as a total deformation of 25 mm (or a rut depth of 20 mm). The critical condition can be taken as a total deformation of 20 mm or a rut depth of 15 mm.

In terms of the design criteria outlined in Section 8.4, pavement system 1 was slightly under-designed while system 2 was virtually correct. Both of these reached a critical total deformation for the poorest subgrade and a temperature of 20°C.

Table 8.4 shows, however, that relatively small numbers of axle loads (10^5) at a higher temperature of 30°C can

bring a pavement to a critical condition if the subgrade has a high moisture content and is lightly over-consolidated.

Failure conditions occur after the design number of applications at a temperature of 30°C. This temperature would not, however, be likely to exist for the design life of a pavement under the conditions of a British climate.

8.6 A STRUCTURAL DESIGN PROCEDURE

Providing an estimate can be made of the traffic loading and temperature spectrum for the design life of the pavement, together with the necessary material characteristics, then a structural design approach for pavements could be adopted, similar to that proposed by Brown and Pell (1972).

The criteria which could be used would be a limiting tensile strain in the base of the asphalt layer (to prevent fatigue cracking) and a limiting permanent deformation of the structure during the design life.

Using an iterative procedure the preliminary designs given in Section 8.5 could be improved according to both engineering and economic criteria.

The engineering criteria for the unbound materials would require simple laboratory repeated load tests to determine their resilient properties and creep tests on the subgrade material to determine its permanent deformation characteristics.

CHAPTER NINE

CONCLUSIONS AND RECOMMENDATIONS FOR FURTHER WORK

9.1 CONCLUSIONS ARISING FROM THE TESTS ON KEUPER MARL

The objectives of the work on this material were to characterise the plastic and elastic properties of an over-consolidated clay subjected to repeated loading and to attempt to relate these properties to a general model of behaviour, while allowing their characterisation whenever possible by simple laboratory tests.

9.1.1 Strain Controlled Tests

(1) There is a steep rise in the pore pressure parameter "A" for the start of all the tests, this rise being the steepest for heavily over-consolidated clays.

(2) If the pore water pressure "u" is normalised with respect to the equivalent pressure p_e, then the equilibrium value of u/p_e decreases as the OCR increases. It is possible to divide the samples tested into two categories, those with OCR's of 10, 20 and 75 are on the "dry" side and those of OCR's of 2 and 4 are on he "wet" side.

the plots of q against p are projected onto a plane by normalising them with respect to p_e, tever the starting point the stress paths all n one point at which q/p_e is equal to 0.45 ls 0.36.

(4) The terminal value of q/p_e is reached at a higher strain as the OCR increases. The value of q_f/p_e = 0.45 is a constant and can be used to calculate the single loading strength for any value of p_e.

(5) Considerable pore pressure gradients exist in lightly over-consolidated samples during strain controlled testing, evidenced by the fact that the equilibrium value of pore water pressure under creep loading is greater for a given value of q than that attained under strain controlled conditions.

9.1.2 Creep and Repeated Loading Tests

The behaviour of clay under these two types of loading has been shown to be very similar, and can be compared in many respects.

9.1.2(a) Pore water pressure

(1) During repeated loading an equilibrium value of pore water pressure is not reached until between 10^5 and 10^6 cycles.

(2) The behaviour of the pore water pressure under creep and repeated loading is very similar although the peak values under creep tend to be higher than under repeated loading.

9.1.2(b) Accumulation of plastic strain

(1) A simple empirical relationship exists during the early stages of a test between the strain accumulated under creep and that accumulated under repeated loading.

For times up to 5000 seconds the strain accumulated under continuous sinusoidal loading is approximately half the value accumulated under a creep load.

(2) For sub-failure stresses the logarithm of the strain rate is directly proportional to the logarithm of time, the slope can be defined as a decay constant and is the same for creep or repeated load tests of the same stress history. For samples on the "dry" side of critical state this decay constant is equal to -1; for the "wet" side it is equal to -0.87.

(3) For a given stress history and a given time, there are unique relationships between the strain rate and the applied stress, depending on whether the stress is static or repeated.

(4) If it is assumed that a repeated stress can be approximated by a finite number of static stress levels, then it is possible to derive a relationship between the strain rate and the deviator stress for the repeated load situation from creep tests. When this process is carried out some measure of agreement is found between individual experimental points and the theoretical line.

(5) Using the relationships between creep and repeated loading it is possible to approximately predict strains accumulated during repeated loading from creep data.

(6) For creep and repeated loading tests it is possible to express the strain rate at a given time in terms of

a function of the deviator stress q and the equivalent pressure p_e. General relationships have been developed for creep and repeated load tests, these depend on whether a sample is on the "wet" or "dry" side of critical state, and take the form:

$$\dot{\epsilon} = e^{\alpha' T^{\lambda}}$$

where $\dot{\epsilon}$ = strain rate

T = time

λ = decay constant

$\alpha' = f(q, p_e)$

By integrating the above relationship between limits, it is possible to predict the accumulated plastic strain.

(7) The ratio of the single loading strength q_f to the equivalent pressure p_e is a constant. The strain rate can, therefore, be expressed as a function of q and q_f. The sample strength is not, however, an independent variable since it depends on the voids ratio of the clay. p_e can be considered as a measure of the voids ratio and is, therefore, a more fundamental parameter than the sample strength.

(8) Rest period loading of lightly over-consolidated samples causes a slight increase in the strain rate and hence the strain accumulated after a given number of cycles. This trend is not, however, evident for the more heavily over-consolidated samples.

9.1.2(c) Recoverable deformation

(1) There is a marked decrease in the resilient modulus with the number of load applications for lightly over-consolidated marl. This decrease becomes less marked as the OCR increases. It is thought that this phenomenon is due to the decrease in effective confining stress during a test.

(2) An equilibrium value of resilient modulus is reached for all OCR's after approximately 10^5 cycles.

(3) The resilient modulus is independent of moisture content and stress history for saturated Keuper marl. There is a hyperbolic relationship between the resilient modulus and the ratio of the deviator stress to the initial effective confining stress.

(4) Two kinds of recoverable deformation are discernable during rest period loading. One is purely elastic and the other is delayed elastic. The largest part of the delayed elastic recovery occurs in less than one second.

(5) A total modulus can be defined by including the delayed elastic component. A comparison of the effect of the application of different numbers of cycles between rest periods showed a marked softening in terms of the total modulus as the number of cycles decreased.

9.2 CONCLUSIONS ARISING FROM THE TESTS ON BREEDON GRAVEL

This material was tested with the objective of determining the effect on the resilient and permanent strain properties of a cyclic confining stress.

9.2.1 Permanent Strain

(1) The total irrecoverable strain under repeated loading is reduced by about 50% at a given level of deviator stress if the load is applied gradually by an increasing load sequence.

(2) There is a single direct relationship between the permanent strain and the deviator stress normalised with respect to the mean level of confining stress for both cyclic and constant confining stresses.

9.2.2 Resilient Properties

(1) Testing samples under increasing sequences of stress does not alter the resilient properties of the material at equilibrium compared with testing individual samples at each level of stress.

(2) For a constant cyclic deviator stress level, it is the mean value of the confining stress which is the determinant of the resilient modulus.

(3) Under a static confining stress the resilient Poisson's ratio varies from less than 0.1 to values in excess of 0.5, and is a function of the principal stress ratio.

(4) For a cyclic confining stress the Poisson's ratio is virtually constant at between 0.2 and 0.1.

(5) The stress paths in the p, q plane for a constant confining stress are a series of parallel lines of slope equal to 3.

(6) Under a cyclic confining stress the slopes of the stress paths vary according to the ratio of q_R to p_R.

(7) The volumetric and shearing components of stress and strain can be considered separately by analyses using octahedral, volumetric and shearing, stresses and strains.

(8) Analysis of the data in terms of volumetric and shear strains shows the behaviour under constant and cyclic confining pressures to be part of a single stress dependent function.

(9) Discontinuities in the stress-strain behaviour occur under conditions of dilation.

(10) The resilient volumetric strain increases as the ratio p_R/p_m increases. It is not, however, affected by the level of the repeated octahedral shear stress, q_R.

(11) As p_R increases, the bulk modulus decreases and as p_m increases, the bulk modulus increases.

(12) The resilient shear strain increases as the ratio q_R/p_m increases, and is independent of the amplitude of the repeated mean normal stress, p_R.

(13) As q_R increases, there is a decrease in the resilient shear modulus and as p_m increases there is a stiffening.

9.3 EQUIPMENT PERFORMANCE

(1) The loading apparatus allowed a flexibility in types of load application which is unique to servo-hydraulic systems. The stability of the applied stresses was not, however, good; it is believed that this was due to a mechanical drift of the null position in the servo valves.

(2) A method was developed of automated data acquisition using a 14 channel F.M. tape recorder. The use of this kind of data acquisition system is justified for large numbers of tests of the same type.

(3) The use of the inductive strain coils allowed the lateral strains under a cyclic cell pressure to be accurately measured. These coils could, in addition, operate in any kind of cell fluid.

9.4 RECOMMENDATIONS FOR FURTHER WORK

9.4.1 Keuper Marl

(1) In order to extend the creep relationship for plastic deformation to partially saturated compacted subgrades, it is recommended that creep and repeated load tests be carried out on this type of material.

(2) Although a qualitative measure of the delayed elastic response of saturated marl has been made, it is recommended that further tests be carried out to quantify this portion of the total elastic deformation.

(3) Further tests at both low and high but sub-failure stresses should be carried out to determine the shape of the ε versus σ function over a larger range. This would be conducive to a more fundamental understanding of the creep properties of this material. To do this would require the development of a triaxial cell with extremely low ram friction and in addition a very stable loading system.

(4) A study of cumulative damage under creep and repeated loading could be carried out using block loading of the different levels of load. This work could lead to the application of random loading to samples which is a model closer to the engineering applications of this type of work.

(5) The use of the inductive strain coils should allow the measurement of lateral strains on samples of saturated marl. This would allow the evaluation of volumetric and shear strains under both repeated and creep loading.

9.4.2 Breedon Gravel

(1) Saturated samples of Breedon gravel could be produced using porous end platens. The sample length would, however, have to be increased because of the end effects involved. The advantages of saturated samples would, however, be that an analysis could be made in terms of effective stresses, as the material has a coarse grading it should be possible to measure dynamic pore pressures.

9.4.3 Equipment

(1) The pore pressure system suffered from problems due to corrosion which were not wholly overcome. A more thorough plating of the system would probably overcome this problem.

(2) A more accurate measurement of vertical strain would be obtained by measurement of deformation directly on the sample. A system using inductive strain coils would allow this to be done.

(3) It is recommended that the electronic servo-control equipment be modified to overcome the drift of the null position of the servo valve.

(4) The variation of both the resilient and permanent deformation of samples is usually examined on a logarithmic time base. A modification of the data recording equipment would allow readings to be taken at logarithmic intervals.

REFERENCES

Ahmed, S.F. and Larew, H.G. (1962), "A study of the repeated load strength modulus of soils", Proc. Int. Conf. on the Struct. Design of Asphalt Pavements, Ann Arbor, Michigan.

Allen, J.J. and Thompson, M.R. (1973), "The effects of non-constant lateral pressures on the resilient response of granular materials", Report, University of Illinois.

Arulanandan, K., Shen, C.K. and Young, R.B. (1971), "Undrained creep behaviour of a coastal organic silty clay", Geotechnique, 21, No. 4, pp. 359-375.

Barden, L. (1969), "Time dependent deformation of normally consolidated clays and peats", Journal of the Soil Mechs. and Found. Eng. Div., ASCE, Vol. 95, No. SM1, pp. 1-31.

Barksdale, R.D. (1972) (1), "Repeated load test evaluation of basecourse materials", GHD Research Project No. 7002, Final Report, Georgia Institute of Technology.

Barksdale, R.D. (1972) (2), "Laboratory evaluation of rutting in basecourse materials", Proc. 3rd Int. Conf. on the Struct. Design of Asphalt Pavements, Vol. 1, London, pp. 161-174.

Barksdale, R.D. and Hicks, R.G. (1973), "Material characterization and layered theory for use in fatigue analyses", Highway Research Board, Special Report No. 140.

Bergan, A.T. and Monismith, C.L. (1973), "Characterization of subgrade soils in cold regions for pavement design purposes", Presented to the Annual Meeting of the Highway Research Board, January.

Biarez, J. (1962), "Contribution a l'étude des propriètés mecaniques des sols et des materiaux pulverents", D.Sci. Thesis, Univ. of Grenoble. (This reference not read.)

Bishop, A.W. and Lovenbury, H.T. (1969), "Creep characteristics of two undisturbed clays", Proc. 7th Int. Cong. on Soil Mechs. and Found. Eng., Mexico, Vol. 1, pp. 29-37.

Bjerrum, L. (1973), "Geotechnical problems involved in foundations of structures in the North Sea", Geotechnique, 23, No. 3, pp. 319-358.

Boyce, J.R., Brown, S.F. and Pell, P.S. (1974), "The behaviour of unbound granular materials under repeated loading", Univ. of Nottingham, Report No. JRB/1, January.

Brown, S.F. (1974) (1), "A simplified fundamental procedure for the design of bituminous pavements", To be published in The Highway Engineer.

Brown, S.F. (1974) (2), Private communication.

Brown, S.F. and Bush, D.I. (1972), "Dynamic response of model pavement structure", Proc. ASCE, Vol. 98, TE4, pp. 1005-1022.

Brown, S.F. and Pell, P.S. (1967), "An experimental investigation of the stresses, strains and deflections in a layered pavement structure subjected to dynamic loads", Proc. 2nd Int. Conf. on the Struct. Design of Asphalt Pavements, Ann Arbor, Michigan, pp. 487-503.

Brown, S.F. and Pell, P.S. (1970), "Developments in the structural design of flexible pavements", Roads and Road Construction, May, pp. 141-156.

Brown, S.F. and Pell, P.S. (1972), "A fundamental structural design procedure for flexible pavements", Proc. 3rd Int. Conf. on the Struct. Design of Asphalt Pavements, Vol. 1, London, pp. 369-381.

Burmister, D.M. (1942), "Laboratory investigation of soils at Flushing Meadow Park", Trans. ASCE, Vol. 107, p. 187.

Burmister, D.M. (1943), "The theory of stresses and displacements in layered systems and applications to the design of airport runways", Proc. Highway Research Board, Vol. 23, pp. 126-149.

Campanella, R.G., Mitchell, J.K. and Singh, A. (1968), "Soil creep as a rate process", Journ. Soil Mechs. and Found. Eng. Div., ASCE, No. SM1, pp. 231-253.

Casagrande, A. (1936), "The determination of the pre-consolidation load and its practical significance", Proc. 1st Int. Conf. Soil Mech. Found. Eng. (Cambridge, Mass.), p. 60.

Chandler, R.J., and Davis, A.G. (1973), "Further work on the engineering properties of Keuper marl", CIRIA Report 47.

Christensen, R.W. and Wu, T.H. (1964), "Analysis of clay deformation as a rate process", Journ. Soil Mech. and Found. Eng. Div., ASCE, Vol. 90, No. SM6, pp. 125-157.

Converse, F.T. (1961), "Stress-deformation relations for soft saturated silt under low frequency oscillating direct shear forces", Symp. on Soil Dynamics, ASTM, STP, No. 305, pp. 15-19.

Cooper, K.E. and Pell, P.S. (1974), "The effect of mix variables on the fatigue strength of bituminous materials", To be published as a TRRL Report.

Cooper, S.W. (1970), "Some shear characteristics of Keuper marl", Ph.D. Thesis, University of Nottingham.

Croney, D. (1972), "Failure criteria for flexible pavements", Proc. 3rd Int. Conf. on the Struct. Design of Asphalt Pavements, Vol. 1, London, pp. 608-612.

Ibid Croney, D. and Bulman, J.N. (1972), "The influence of climatic factors on the structural design of flexible pavements". Vol. 1, pp 67-71.

Cullingford, G., Lashine, A.K.F. and Parr, G.B. (1971), "Servo controlled equipment for dynamic triaxial testing of soils", Geotechnique, Vol. 22, No. 3, Technical Note.

Darter, M.I., Hudson, R.W. and Brown, J.L. (1973), "Statistical variations of flexible pavement properties and their consideration in design", Paper presented at the Annual Meeting of the AAPT.

Dehlen, G.L. (1969), "The effect of non-linear material response on the behaviour of pavements subjected to dynamic loads", Ph.D. Thesis, University of California.

Dehlen, G.L. and Monismith, C.L. (1970), "Effect of non-linear material response on the behaviour of pavements under traffic", Highway Research Record No. 310, pp. 1-16.

Dormon, G.M. and Edwards, J.M. (1964), "Shell 1963 design charts for flexible pavements - an outline of their development", OPD Report No. 232/64M, Shell, London.

Dormon, G.M. and Edwards, J.M. (1967), "Developments in application in practice of a fundamental procedure for the design of flexible pavements", Proc. 2nd Int. Conf. on the Struct. Design of Asphalt Pavements, Ann Arbor, Michigan, pp. 99-108.

Dormon, G.M. and Metcalf, C.T. (1965), "Design curves for flexible pavements based on layered system theory", Highway Research Record, No. 71, pp. 69-84.

Feda, J., Kamenov, B. and Klablena, P. (1973), "Investigation of creep and structure of clayey materials", Proc. 8th Int. Cong. on Soil Mechs. and Found. Eng., Vol. 1.1, pp. 123-128.

Finn, F.N., Nair, K. and Monismith, C.L. (1972), "Applications of theory in the design of asphalt pavements", Proc. 3rd Int. Conf. on the Struct. Design of Asphalt Pavements, Vol. 1, London, pp. 392-409.

Finn, W.D.L. and Shead, D. (1973), "Creep and creep rupture of an undisturbed sensitive clay", Proc. 8th Int. Cong. on Soil Mechs. and Found. Eng., Vol. 1.1, pp. 135-142.

Folque, J. (1965), "Dynamic triaxial tests on compacted unsaturated soils", Proc. 6th Int. Cong. on Soil Mechs. and Found. Eng., pp. 217-220.

Geuze, E.C.W.A. (1963), "The uniqueness of the Mohr-Coulomb concept in shear failure", ASTM, STP, No. 361.

Geuze, E.C.W.A. and Tan, T.K. (1953), "The mechanical behaviour of clays", Proc. 2nd Int. Cong. on Rheology, Oxford, p. 247.

Glasstone, S., Laidler, K. and Eyring, H. (1941), "The theory of rate processes", McGraw-Hill Book Co. Inc., New York.

Glynn, T.E. (1968), "Deformation characteristics of boulder clay subjected to repeated stress applications", Ph.D. thesis, Trinity College, Univ. of Dublin.

Glynn, T.E. and Kirwan, R.W. (1969), "A stress-strain relationship for clays subjected to repeated loading", Proc. 7th Int. Cong. on Soil Mechs. and Found. Eng., Vol. 1, pp. 159-163.

Havens, J.H., Deen, R.C. and Southgate, H.F. (1973), "Pavement design schema", Highway Research Board, Special Report No. 140.

Haynes, J.H. and Yoder, E.J. (1963), "Effects of repeated loading on gravel and crushed stone basecourse materials used in the AASHO road test", Highway Research Record No. 39, pp. 82-97.

Heath, D.L., Shenton, M.J. and Sparrow, R.W. (1972), "Design of conventional rail track foundations", Proc. ICE, Vol. 51, February, pp. 251-267.

Heukelom, W. and Klomp, A.J.G. (1962), "Dynamic testing as a means of controlling pavements during and after construction", Proc. Int. Conf. on the Struct. Design of Asphalt Pavements, Ann Arbor, Michigan.

Hicks, R.G. (1970), "Factors influencing the resilient properties of granular materials", Ph.D. Thesis, University of California.

Hicks, R.G. and Monismith, C.L. (1971), "Factors influencing the resilient response of granular materials", Highway Research Record No. 345, pp. 15-31.

Hicks, R.G. and Monismith, C.L. (1972), "Prediction of the resilient response of pavements containing granular layers using non-linear elastic theory", Proc. 3rd Int. Conf. on the Struct. Design of Asphalt Pavements, Vol. 1, London, pp. 410-430.

Holzer, T.L., Hoeg, K. and Arulandan, K. (1972), "Excess pore pressures during undrained clay creep", Canadian Geot. Journ., Vol. 10, No. 1, pp. 12-24.

Huang, Y.H. (1968), "Stresses and displacements in non-linear soil media", Proc. ASCE, Journ. of Soil Mechs. and Found. Eng. Div., SM1, pp. 1-19.

Humphries, W.K. and Wahls, H.E. (1968), "Stress history effects on dynamic modulus of clay", Proc. ASCE, Journ. of Soil Mechs. and Found. Eng. Div., Vol. 94, No. SM2, pp. 371-389.

Hveem, F.N. (1955), "Pavement deflections and fatigue failures", Highway Research Board Bulletin. No. 114, pp 43-73.

Kallas, B.I. and Riley, J.C. (1967), "Mechanical properties of asphalt pavement materials", Proc. 2nd Int. Conf. on the Struct. Design of Asphalt Pavements, Ann Arbor, Michigan.

Kawakami, F. and Ogawa, M.S. (1963), "Mechanical properties of soils subjected to repeated stress applications", Proc. 2nd Asian Reg. Conf. on Soil Mechs. and Found. Eng., Vol. 1, Paper 1/25.

Kawakami, F. and Ogawa, S. (1965) (1), "Modulus of elasticity and yield stress of compacted soil subjected to repeated stress application", Trans. Japan Soc. of Civ. Engrs, No. 114, pp. 8-16.

Kawakami, F. and Ogawa, S. (1965) (2), "Strength and deformation of compacted soil subjected to repeated stress application", Proc. 6th Int. Cong. on Soil Mechs. and Found. Eng., Vol. 1, pp. 264-269.

Kondner, R.L. (1963), "Hyperbolic stress-strain response: cohesive soils", Proc. ASCE, Vol. 89, No. SM1, pp. 115-143.

Kondner, R.L. and Krizek, R.J. (1964), "Correlation of creep and dynamic response of cohesive soil", Proc. Int. Union of Applied and Theoretical Mechanics, pp. 333-342.

Krizek, R.J. (1971), "Rheologic behaviour of clay soils subjected to dynamic loads", Trans. Soc. of Rheology, Vol. 15, pp. 433-489.

Ibid Krizek, R.J., Achenbach, J.D. and Adeyeri, J.B. (1971), "Hydrorheology of clay soils", 15:4, pp. 771-781.

Lacerda, W.A. and Houston, W.N. (1973), "Stress relaxation in soils", Proc. 8th Int. Cong. on Soil Mechs. and Found. Eng., Vol. 1.1, pp. 221-226.

Larew, A.G. and Leonards, G.A. (1962), "A strength criterion for repeated loads", Proc. Highway Research Board, Vol. 41.

Lashine, A.K.F. (1971), "Some aspects of the behaviour of Keuper marl under repeated loading", Ph.D. Thesis, University of Nottingham.

Lashine, A.K.F. (1973), "Deformation characteristics of a silty clay under repeated loading", Proc. 8th Int. Cong. on Soil Mechs. and Found. Eng., Moscow, Vol. 1, pp. 237-244.

Lashine, A.K.F., Brown, S.F. and Pell, P.S. (1970), "Dynamic properties of soils", Progress Report No. 1, submitted to Koninklijke-Shell Laboratorium, Amsterdam.

Lashine, A.K.F., Brown, S.F. and Pell, P.S. (1971), "Dynamic properties of soils", Progress Report No. 2, submitted to Koninklijke-Shell Laboratorium, Amsterdam.

Lister, N.W. (1972), "The transient and long term performance of pavements in relation to temperature", Proc. 3rd Int. Conf. on the Struct. Design of Asphalt Pavements, London, Vol. 1, pp. 94-100.

Lohnes, R.A., Millar, A. and Hardy, R.L. (1972), "In situ measurement of soil creep", Journ. Soil Mechs. and Found. Eng. Div., ASCE, January, pp. 143-147.

Marek, C.R. and Dempsey, B.J. (1972), "A model utilising climatic factors for determining stresses and deflections in flexible pavement systems", Proc. 3rd Int. Conf. on the Struct. Design of Asphalt Pavements, London, Vol. 1, pp. 101-114.

Mitchell, J.K. (1964), "Shearing resistance of soils as a rate process", Proc. ASCE, Vol. 90, SM1, pp. 29-61.

Mitchell, J.K. and Campanella, R.G. (1964), "Creep studies in saturated clays", ASTM, STP, No. 361.

Moore, W.M., Britton, S.C. and Scrivner, F.H. (1970), "A laboratory study of the relation of stress to strain for a crushed limestone base material", Research Report Number 99-5F, Study 2-8-65-99, Texas Transportation Institute, Texas A & M University.

Morgan, J.R. (1966), "The response of granular materials to repeated loading", Proc. 3rd Conf. Australian Road Research Board, Vol. 3, Part 2, Paper No. 255, pp. 1178-1190.

Murayama, S. (1970), "Dynamic behaviour of clays", Proc. 5th Int. Cong. on Rheology, Tokyo, Vol. 2, pp. 541-558.

Murayama, S. and Shibata, T. (1961), "Rheological properties of clays", Proc. 5th Int. Cong. on Soil Mechs. and Found. Eng., Vol. 1.

Murayama, S. and Shibata, T. (1964), "Flow and stress relaxation in clays", Proc. Symp. on Rheology and Soil Mechanics, Grenoble, pp. 99-129.

Nash, K.L. (1958), "Repeated stresses in soil as the basis for pavement design", Proc. of the Midlands Soil Mechs. and Found. Eng. Society, Vol. 2, Paper No. 9.

Newland, P.L. (1971), "An investigation of the three dimensional creep properties of a clay", Proc. Australia-New Zealand Conf. on Geomechanics, Melbourne, Vol. 1, pp. 132-137.

Parr, G.B. (1972), "Some aspects of the behaviour of London clay under repeated loading", Ph.D. Thesis, University of Nottingham.

Parry, R.H.G. and Amerasinghe, S.F. (1973), "Components of deformation in clays", Proc. Symp. on the Role of Plasticity in Soil Mechanics, Cambridge, pp. 108-127.

Peattie, K.R. (1974), "Introduction to pavement design", Lecture C, Bituminous Materials and Flexible Pavement Design Course, held at University of Nottingham.

Pell, P.S. and Brown, S.F. (1972), "The characteristics of materials for the design of flexible pavement structures", Proc. 3rd Int. Conf. on the Struct. Design of Asphalt Pavements, London, Vol. 1, pp. 326-342.

Peutz, M.G.F., Van Kempen, H.P.M. and Jones, A. (1968), "Layered systems under normal surface loads", Highway Research Record, No. 228, pp. 34-45.

Richards, B.G. (1970), "Effects of environment on pavement design", Proc. Symp. on Soils and Earth Structures in Arid Climates, Adelaide, pp. 20-24.

Richards, B.G. and Gordon, R. (1972), "Prediction of the performance of a flexible pavement on an expansive subgrade", Proc. 3rd Int. Conf. on the Struct. Design of Asphalt Pavements, London, Vol. 1, pp. 133-143.

Road Note No. 29 (1970), "A guide to the structural design of pavements for new roads", TRRL.

Robnett, Q.L. and Thompson, M.R. (1973), "Resilient properties of subgrade soils, Phase 1 - Development of testing procedure", Interim report, Project IHR-603, University of Illinois.

Roscoe, K.H., Schofield, A.N. and Thruairaja, A. (1963), "Yielding of clays in states wetter than critical", Geotechnique, 13, No. 3, pp. 211-240.

Roscoe, K.H., Schofield, A.N. and Wroth, C.P. (1958), "On the yielding of soils", Geotechnique, 8, No. 1, pp. 22-53.

Saito, M. and Uezawa, H. (1961), "Failure of soil due to creep", Proc. 5th Int. Cong. on Soil Mechs. and Found. Eng., Vol. 1, pp. 315-318.

Sangrey, D.A., Henkel, D.J. and Esrig, M.I. (1969), "The effective stress response of a saturated clay soil to repeated loading", Canadian Geotechnical Journal, Vol. VI, No. 3, pp. 241-252.

Schmertmann, J.M. (1955), "The undisturbed consolidation of clay", Trans. ASCE, Vol. 120, p. 1201.

Scott, R.F. (1965), "Principles of soil mechanics", Addison-Wesley Publishing Co. Inc.

Seed, H.B. and Chan, C.K. (1958), "Effect of stress history and frequency of stress application on the deformation of clay subgrades under repeated loading", Proc. Highway Research Board, Vol. 37, pp. 555-575.

Seed, H.B. and Chan, C.K. (1961), "Effect of duration of stress application on soil deformation under repeated loading", Proc. 5th Int. Cong. on Soil Mechs. and Found. Eng., Vol. 1, pp. 341-345.

Seed, H.B. Chan, C.K. and Lee, C.E. (1962), "Resilience characteristics of subgrade soils and their relation to fatigue failures in asphalt pavements", Proc. 2nd Int. Conf. on the Struct. Design of Asphalt Pavements, Ann Arbor, Michigan, pp. 611-636.

Seed, H.B., Chan, C.K. and Monismith, C.L. (1955), "Effects of repeated loading on the strength and deformation of compacted clay", Proc. Highway Research Board, Vol. 34, pp. 541-558.

Seed, H.B. and Fead, J.W.N. (1959), "Apparatus for repeated load tests on soils", ASTM, STP, No. 254.

Seed, H.B. and McNeill, R.L. (1956), "Soil deformation in normal compression and repeated loading tests", Highway Research Board Bulletin No. 141.

Seed, H.B. and McNeill, R.L. (1957), "Soil deformations under repeated stress applications", ASTM, STP, No. 232, pp. 177-196.

Seed, H.B., Mitry, F.G., Monismith, C.L. and Chan, C.K. (1965), "Prediction of pavement deflections from laboratory repeated load tests", Report TE 65-6, Dept. of Civil Engineering, Inst. of Transp. and Traffic Eng., University of California.

Shackel, B. (1972), "The deformation response of a sand-clay subjected to repeated triaxial compressive stress", Proc. Int. Symp. on Strength and Deformation Behaviour of Soils, Bangalore, Vol. 1, p. 145.

Shackel, B. (1973), "Repeated loading of soils - a review", Journ. Australian Road Research Board, Vol. 5, No. 3, pp. 22-49.

Shen, C., Arulandan, K. and Smith, W.S. (1973), "Secondary consolidation and strength of clay", Journ. Soil Mechs. and Found. Eng. Div., ASCE, Vol. 99, No. SM1, pp. 95-110.

Singh, A. and Mitchell, J.K. (1968), "General stress-strain-time function for soils", Proc. ASCE, SM1, pp. 21-46.

Singh, A. and Mitchell, J.K. (1969), "Creep potential and creep rupture of soils", Proc. 7th Int. Cong. on Soil Mechs. and Found. Eng., Vol. 1, pp. 379-384.

Snaith, M.S. (1973), "Deformation characteristics of dense bitumen macadam subjected to dynamic loading", Ph.D. Thesis, University of Nottingham.

Stirling, A.B. and Chadwick, B. (1973), Private communication, TRRL.

Taylor, K.L. (1971), "Finite element analysis of layered road pavements", Ph.D. Thesis, University of Nottingham.

Taylor, P.W. and Bacchus, D.R. (1969), "Dynamic cyclic strain tests on a clay", Proc. 7th Int. Cong. on Soil Mechs. and Found. Eng., Vol. 1, pp. 401-410.

Ter-Stepanian, G., Meschaian, S.R. and Galstian, R.R. (1973), "Investigation of creep of clay soils at shear", Proc. 8th Int. Cong. on Soil Mechs. and Found. Eng., Vol. 1.2, pp. 433-438.

Thrower, E.N., Lister, N.W. and Potter, J.F. (1972), "Experimental and theoretical studies of pavement behaviour under vehicular loading in relation to elastic theory", Proc. 3rd Int. Conf. on the Struct. Design of Asphalt Pavements, London, Vol. 1, pp. 521-535.

Walker, L.K. (1969), "Undrained creep in a sensitive clay", Geotechnique, Vol. 19, pp. 515-529.

Waters, J.M. and Shenton, M.J. (1968), "Track foundation design", The Railway Gazette, 4th October.

Williams, G.T. (1963), "Stress/strain relationships of granular soils", Report R1297, Thornton Research Centre, Shell Research Ltd.

Wroth, C.P. and Loudon, P.A. (1967), "The correlation of strains with a family of triaxial tests on overconsolidated samples of kaolin", Proc. Geotechnical Conf., Oslo, pp. 159-166.

APPENDIX A

DESIGN OF PORE WATER PRESSURE AND CELL PRESSURE TRANSDUCERS

A.1 DIAPHRAGM DESIGN

It was decided to standardise the type of diaphragm used in both pore water pressure and cell pressure transducers. A stainless steel diaphragm 0.635 mm thick, rigidly clamped at a radius of 10.7 mm, was chosen. Two criteria were considered:

(a) Volume change - this must be a minimum in order to maintain the compliance of the pore pressure system at a minimum.

(b) Elastic limit - in order that no drift should occur in the transducers, the diaphragms should not be loaded past their elastic limit.

A.1.1 Volume Change

For a rigidly edge-supported diaphragm, the deformation y is given by Timoshenko (1952) as:

$$y = \frac{p}{64D}(a^2-x^2)^2$$

where $D = \frac{Et^3}{12(1-\nu^3)}$

E = Young's modulus (21.4×10^7 kN/m^2 for stainless steel)

ν = Poisson's ratio (0.283)

a = radius

t = thickness

p = pressure

The volume displacement V is given by:

$$V = \int_o^a 2\pi xy\,dx$$

$$= \frac{\pi p}{32D} \int_o^a x(a^2-x^2)\,dx$$

$$V = \frac{2\pi p a^6 (1-\nu^2)}{33Et^3}$$

If the limit for distortion is taken as the minimum value noted in previous work (Parr, 1972), then $V_{max} = 4.76 \times 10^{-3}$ mm^3 per kN/m^2. Then, for p = 1 kN/m^2, a = 10.7 mm, t = .635 mm then V = 4.72×10^{-3} mm^3 per kN/m^2. This is an acceptable value.

A.1.2 Elastic Limit

The maximum radial stress for a rigidly edge-supported diaphragm is given by Roarke (1964) as:

$$\sigma_{ra} = \frac{3pa^2}{4\pi t^2}$$

For stainless steel, the yield stress is 3.7×10^5 kN/m^2, taking the elastic limit as 3.0×10^5 and assuming this most not be exceeded by p = 1100 kN/m^2, then the minimum thickness must be:

$$t = 0.28 \text{ mm}$$

this criterion is satisfied.

A.2 STRAIN GAUGE DESIGN

The diaphragms were gauged with Redshaw 20 mm diaphragm gauges. These had a full wheatstone bridge configuration having a nominal arm resistance of 220 Ω. The applied bridge voltage was 6 volts and the current through the arms was, therefore, 13 mA. This is small enough to allow heat dissipation, prevent oxidation of the gauge and give long term stability.

A.3 PORE WATER PRESSURE TRANSDUCER

The assembled pore water pressure transducer is shown in Fig. A.1, and in cross section in Fig. A.2. By making sure that all the connections were tightly bedded onto flat surfaces, a continuous passage from the ceramic probe to the diaphragm without air traps was ensured. In this way, the compliance was reduced to 5×10^{-6} $cm^3/kN/m^2$. This compares very well with the value already calculated above.

The calibrations for each transducer are given in Table A.1.

A.4 CELL PRESSURE TRANSDUCER

The cell pressure transducer was manufactured from brass hexagonal bar in two halves. A standard strain gauged stainless steel diaphragm as described above was clamped between the two halves using six 2 BA bolts.

The cable entry was sealed using a 5/32 enots fitting. The base of the transducer was threaded to allow it to be

screwed onto the valves on top of the triaxial cells. A bleed was let into this bottom chamber to allow the transducer to be de-aired.

The calibrated outputs of the two transducers are given in Table A.2.

Cell Base No.	Output mV/kN/m^2
1	8.66
2	6.4
3	5.02
4	7.21
5	6.0
6	7.84

Table A.1 Calibrations of Pore Water Pressure Transducers

Rig. No.	Output mV/kN/m^2
1	5.95
2	5.82

Table A.2 Calibration of Cell Pressure Transducers

APPENDIX B

LATERAL STRAIN MEASUREMENT

B.1 INTRODUCTION

In order to be able to evaluate material behaviour under a cyclic confining pressure it is necessary to measure both the vertical and lateral strains. The vertical strain was measured using a conventional LVDT arrangement on the loading ram. For the purposes of lateral strain measurement on a granular material the use of LVDT's is unpracticable. In addition, the use of water as a confining fluid made their use difficult. A decision was made, therefore, to use inductive strain coils which do not depend on a very accurate location on the soil sample and in addition allow the use of water as a confining fluid.

B.2 DESCRIPTION OF INDUCTIVE COIL STRAIN MEASURING SYSTEM

The strain coil system consists of two components, (a) a pair of sensors and (b) an external instrument package. The sensors, each of which is a disc shaped coil, are placed in near parallel and co-axial alignment. The sensors used were 25 mm in diameter. The separation of the sensors is related to the eletro-magnetic coupling between the two. By means of an inductance bridge an output voltage as a function of strain may be obtained since a change in spacing from the initial spacing produces a bridge unbalance.

The coils can operate at any spacing between 1 and 4 times their diameter. The effects of rotational or

transverse movement are negligible.

The geometry of the samples did not allow direct measurement of strain across the centre section of the sample, since to do this it was necessary to generate a flux field which was cut by the movement of the end platen, thus causing wild fluctuations in the output.

A system of measurement was, therefore, devised whereby a coil which was attached to the sample was coupled with a stationary coil mounted outside the cell wall (Fig. B.1). It was found during routine calibration tests that there was considerable lateral translation of the sample and hence it was necessary to have a balancing pair of coils on the opposite side of the sample (Fig. 4.6). By connecting the inner coils on the sample in parallel and doing the same with the two outside coils any lateral translation automatically cancelled itself out.

The steel bands used to reinforce the perspex cell walls were removed as they were in the flux field. It was found that the presence of the cell top clamping rods at each side had no effect on the output.

The water in the cell was found to have no effect on the sensitivity of the coils (Table B.1). This was verified by carrying out calibrations with the coils clamped to a perspex dummy specimen, with and without water in the triaxial cell.

B.3 SETTING UP PROCEDURE

After the Breedon gravel samples were placed on the

Movement of coil thou"	Water in triaxial cell		Air in triaxial cell	
	Output Volts (increasing)	Output Volts (decreasing)	Output Volts (increasing)	Output Volts (decreasing)
0	0.00	0.01	0.00	0.07
1	0.46	0.50	0.38	0.55
2	0.89	0.98	0.84	1.03
3	1.4	1.41	1.29	1.53
4	1.91	1.93	1.78	2.05
5	2.41	2.36	2.24	2.53
6	2.83	2.89	2.80	2.96
7	3.38	3.41	3.32	3.48
8	3.89	3.92	3.87	3.97
9	4.41	4.46	4.44	4.52
10	4.90	4.96	5.04	4.98
20	9.91	9.99	9.95	9.95
30	13.12		12.11	

Table B.1 Calibration of Strain Coils with and without Water - Using a Perspex Dummy Specimen

cell base two perspex threaded coil holders were attached directly onto the specimen diametrically opposte each other, and held lightly in position by rubber bands. The holders were shaped to a 101 mm radius to fit the sample and covered a surface area of approximately 1000 sq.mm. The filter paper drains were then put in position and a latex membrane was carefully placed over the sample. The membrane was punctured to allow the threaded portion of the holder to protrude. The membrane was then sealed by being clamped with a rubber "O" ring. The strain coils were then attached to the holders. The external coils were mounted to allow adjustment both vertically and horizontally. These were then accurately lined up with the coils attached to the sample. The cell top was placed in position and the cell filled with water. This done the coils were calibrated by using the micrometer adjustments on the external coils. For testing purposes, the coils were maintained at a separation of two diameters. The coil separation was adjusted for each reading by moving the external coils in unison until an approximately zero output was obtained from the inductive bridge. This procedure allowed the coils to be used at their maximum sensitivity for resilient purposes, while the range of permanent strain was limited only by the travel of the micrometer.

B.4 PERFORMANCE EVALUATION

Readings were taken using a u.v. recorder. This gave a band of noise equivalent to 2.5 microns at the systems

maximum sensitivity. It was possible to resolve strain readings to 5 microstrain, a typical resilient strain reading would be of the order of 100 microstrain. Calibrations before and after tests gave repeatable results.

APPENDIX C

EQUIPMENT CALIBRATION

C.1 DISPLACEMENT CALIBRATION

The LVDT's were calibrated using a micrometer device. The input voltage was set so that the sensitivities were 300 mV/mm.

As all LVDT readings for vertical displacement were taken on the triaxial cell loading ram instead of on the sample, it was necessary to correct for the displacement of the loading system.

A dummy aluminium specimen was set up in the triaxial cell with lubricated membranes on the end platens. This was then loaded vertically both statically and dynamically and the output from the LVDT measured. The results given in Tables C.1 and C.2 are the mean values of four tests. The corrections necessary to the LVDT output were as follows:

Static: 0.122 mV/kN/m^2

Dynamic: 0.0106 mV/kN/m^2

Repeated load tests at various frequencies between 1 and 10 Hz with the dummy specimen showed no appreciable frequency effect.

C.2 STRESS CALIBRATION

The load cells on each rig were calibrated using accurate weights and the bridge supply voltage was adjusted such that the sensitivities were exactly 10 mV/kN/m^2.

A thermistor device coupled to the LVDT was used to increase the load on a sample as the area of the sample increased, hence maintaining a constant stress. The calibration readings for this stress control system are given in Table C.3.

Deviator Stress kN/m^2	LVDT Output mV
0	0
50	6
100	12
200	25
300	37
400	50
500	60
600	73

Table C.1 Static Deformation of System

Deviator Stress kN/m^2	LVDT Output mV
0- 80	0-16
0-220	0-28
0-350	0-40
0-465	0-50
0-680	0-73
0-810	0-84

Table C.2 Dynamic Deformation of System

Movement of LVDT mm	Stress control voltage output volts	Theoretical voltage output volts
0	1.0	1.0
2.5	1.015	1.026
5.0	1.040	1.053
7.5	1.063	1.081
10.0	1.100	1.111
12.5	1.140	1.143
15.0	1.172	1.176
17.5	1.214	1.212
20.0	1.252	1.250
22.5	1.280	1.290
25.0	1.328	1.333

Table C.3 Stress Control Calibration

APPENDIX D

DATA ACQUISITION AND ANALYSIS FACILITIES

D.1 INTRODUCTION

An automatic data recording facility was developed to take advantage of a high speed Analogue to Digital (A/D) converter linked to a 16K PDP11 computer. This appendix contains a detailed description of these facilities, together with Fortran software developed for use with this computer installation.

Data collection and processing is shown in block diagram form in Fig. D.1.

D.2 TAPE RECORDER AND DIGITAL SEQUENTIAL PROGRAMMER (DSP)

The automated acqusition of data from the testing rigs was carried out using a 14 channel F.M. tape recorder (Fig. D.2). This was sufficient to record two tests running concurrently.

Eleven channels were used for recording the output from the two rigs (Table D.1). In order to be able to record the complete range of LVDT output and at the same time record resilient deflections with accuracy, it was necessary to split the output of the LVDT into two components. The signal was fed through a high pass filter for one channel (thus eliminating the D.C. component) and for the other it was fed effectively through an amplifier with unity gain.

A digital sequential programmer was incorporated into a remote control unit to operate the tape recorder (Figs.

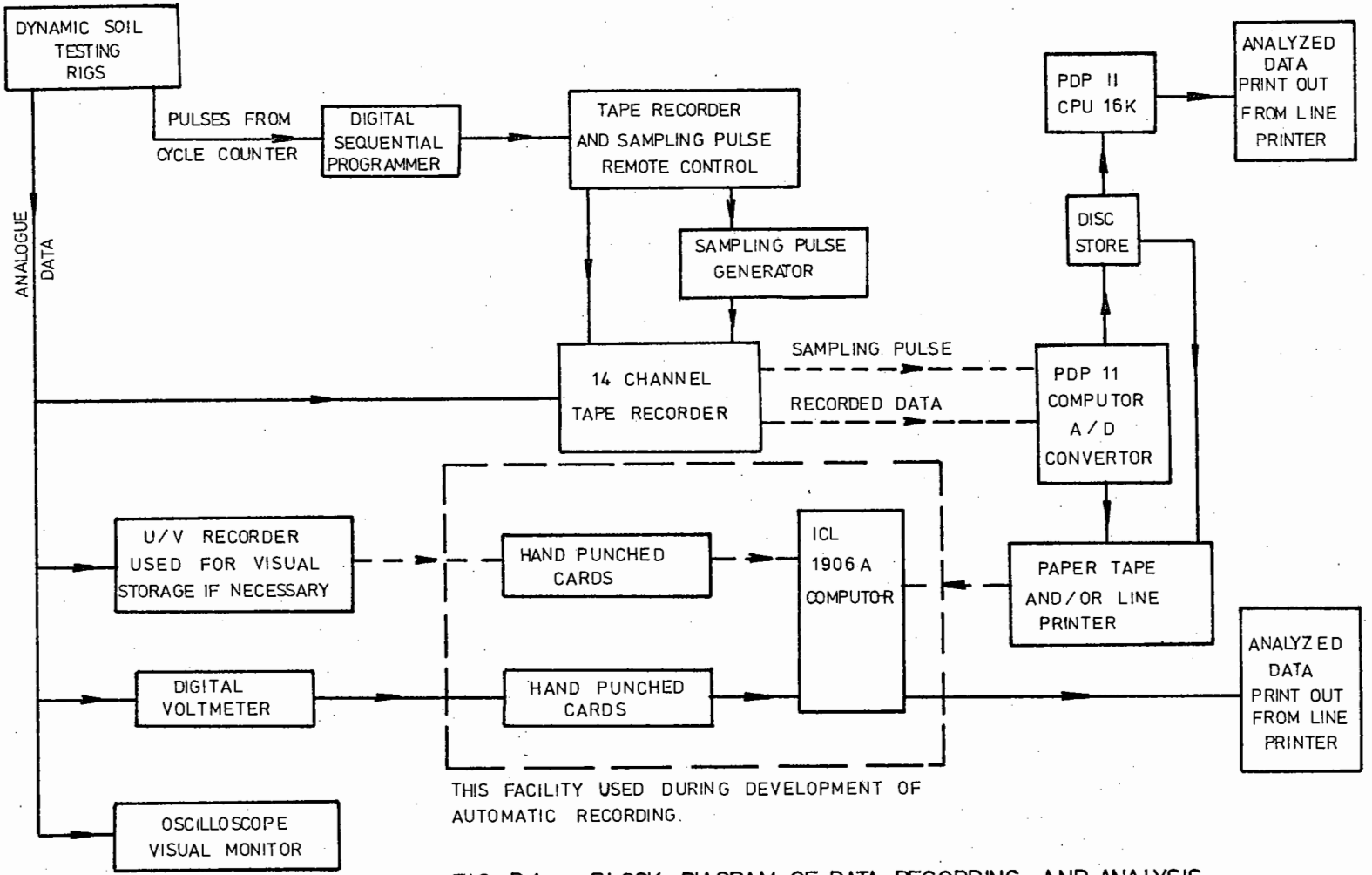

FIG. D.1 BLOCK DIAGRAM OF DATA RECORDING AND ANALYSIS.

F.M. Recorder Channel	Signal	Rig
1	Load	1
2	Cell Pressure	1
3	LVDT x 1	1
4	Pore Water Pressure	1
5	Load	2
6	Cell Pressure	2
7	LVDT x 1	2
8	Pore Water Pressure	2
9	LVDT (Filtered)	1
10	LVDT (Filtered)	2
14	Sampling Pulse and Voice	-

Table D.1 Arrangement of Channels on Tape Recorder

D.3 and D.4). This allows tests to be recorded at regular intervals over the full 24 hour period. The programmer can be set to sample data at intervals of from 10 to 100,000 cycles.

There are five preselections on the programmer each of which can be set to initiate an operation after a set number of signal pulses (or cycles). The operations which are controlled are as follows:

(1) RUN — Starts tape drive.

(2) RUN/RECORD — Starts recording data.

(3) STPG ON — Sampling trigger pulse generator on.

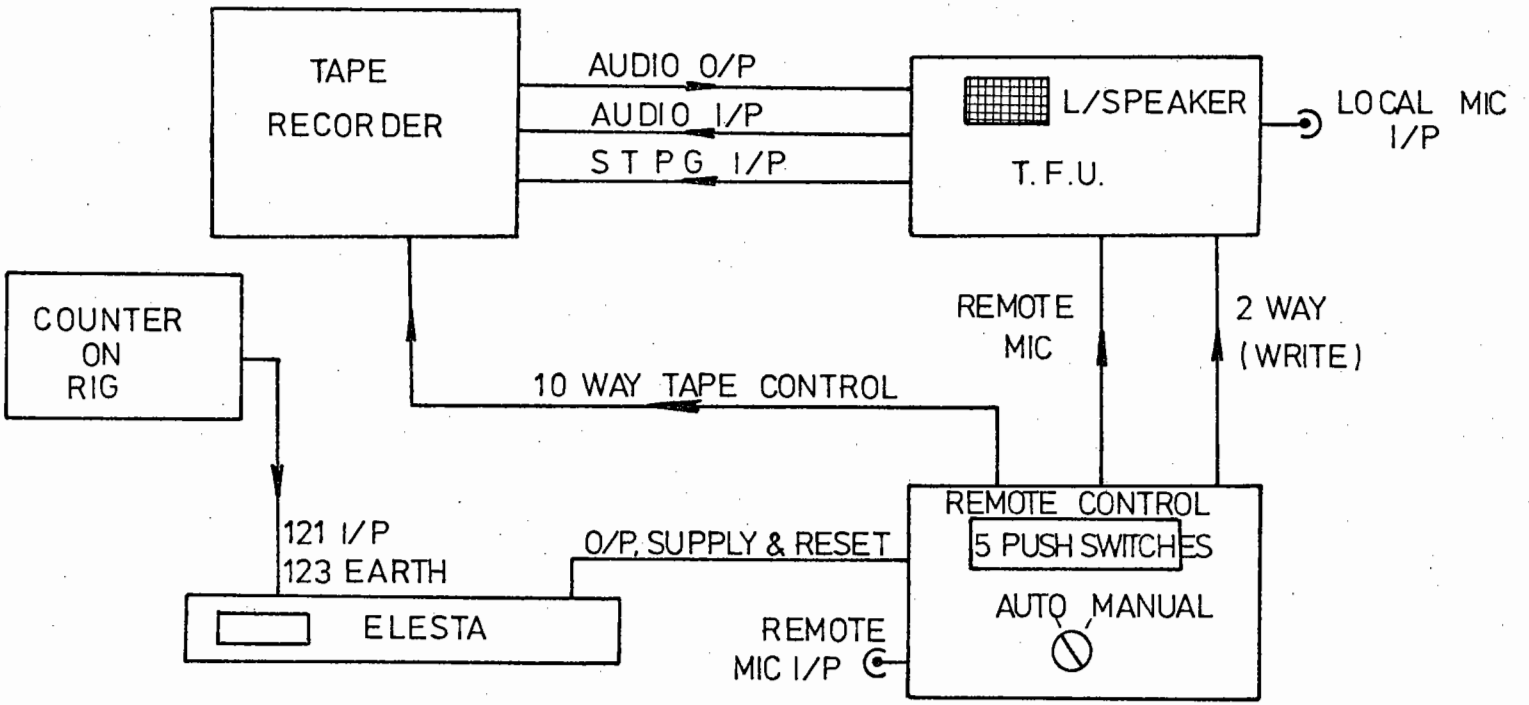

FIG. D.3. Block diagram of tape control system.

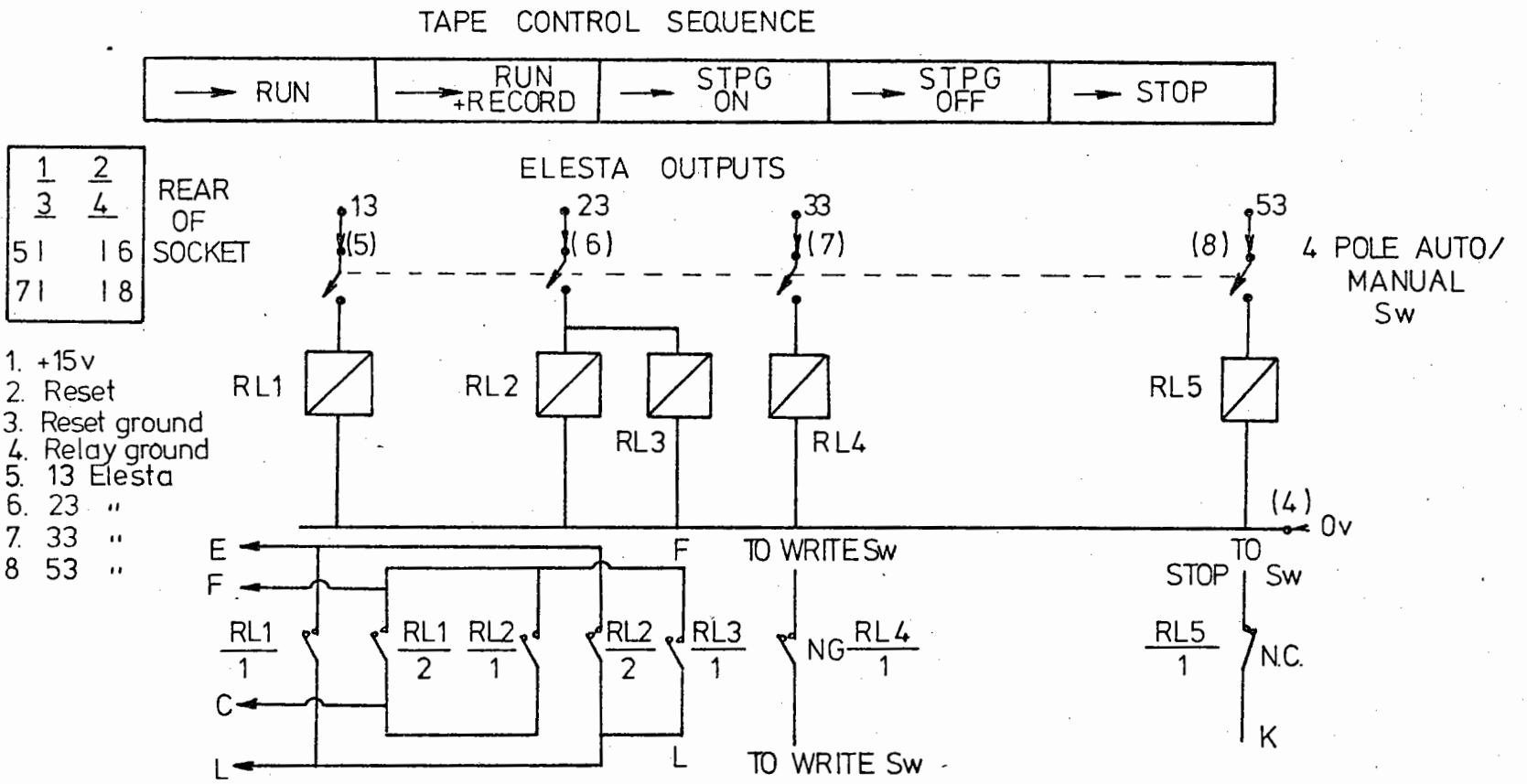

FIG. D.4 Tape facilities unit (remote)

(4) STPG OFF — Sampling trigger pulse generator off.

(5) STOP — Stops tape drive.

The sampling pulse is required by the A/D converter to initiate multiplexed sampling of the data channels which are being fed in. The pulse frequency can be set at 15, 30, 75, 150, 300 or 750 Hz. In practice for creep, strain controlled and repeated load tests carried out at 1 Hz, the pulse was set at 75 Hz. For tests performed at 10 Hz, the pulse was set at 750 Hz. These settings allowed the collection of 75 readings per second or per cycle.

D.3 THE COMPUTER INSTALLATION

The computer installation used was a DEC PDP11/15 16K computer. The peripherals attached to this computer were a teletype console, a high speed tape reader and punch, a line printer, a disc drive, and a high speed A/D converter (Fig. D.5).

The software for the operating system is contained on the disc. This software allows for the editing, compiling and linking of Fortran programmes. In addition, software is available allowing easy transfer of files between peripherals.

Fig. D.6 shows the F.M. tape recorder used to replay the data through the A/D converter. A program "A5SHOT" described below was written which, provided recording had been carried out in a regular fashion, allowed data to be automatically stored on the disc for further analysis at a

later stage. Data was replayed from 5 channels simultaneously for repeated load tests (4 channels for creep and strain controlled tests).

As soon as all the data from a particular test was stored on the disc, it was then analysed using another Fortran programme "DYNLOD", again described at the end of this appendix.

A linear relationship was assumed between the voltage output from the rigs and the digital values stored on the disc. This relationship was expressed in the form:

$$V = aN + b$$

where V = volts o/p

N = digital values stored by A/D converter

a = constant

b = constant

The values of "a" and "b" for each channel are given in Table D.2.

Channel	a	b
1	0.003244	0.104
2	0.003698	-0.119
3	0.002351	-0.048
4	0.002300	0.008
5	0.003198	0.156
6	0.003613	-0.053
7	0.002365	-0.040
8	0.002312	-0.050
9	0.00705	-0.008
10	0.00701	-0.015

Table D.2 Calibration Constants for Tape Recorded Data

D.4 PROGRAMMES USED FOR DATA ANALYSIS

A5 SHOT

This programme was used to store data on disc from the magnetic tape using the A/D converter. An assembly language subroutine is used to enable data to be converted at a very high speed (Middleton, 1974). Care had to be taken when using this programme that the amount of data to be converted was not larger than the file to which it was to be allocated, because under certain circumstances, it was possible to overwrite the disc operating system. The reason for this was that much of the protection had been removed to increase the speed of transfer to data. A listing of the programme is given below.

CREEP

This programme analyses data recorded and stored on disc from creep and strain controlled tests. It contains an averaging routine to reduce the stored data which is then processed and printed out on the line printer.

DYNLOD

This programme was used for the reduction and analysis of data stored on disc from dynamic tests. Because of the limitations of core storage, it was necessary to write this programme using overlay techniques. To do this, the part of the core reserved for programmes is split into two sections. The top section contains the resident programme which is made as small as possible and remains in the core while the programme is being run. To the resident

programme are linked other programmes which are stored on disc. These programmes or overlays are called from the disc as required and stored in the core below the resident programme.

As each overlay is called, it overwrites any overlay which has been previously used. The overlays are written and compiled as separate programmes and then linked to the main programme. The programme path is shown in Fig. D.8, and a full listing is also given below with some explanatory notes. In addition, the operating procedure for linking overlays is given overleaf.

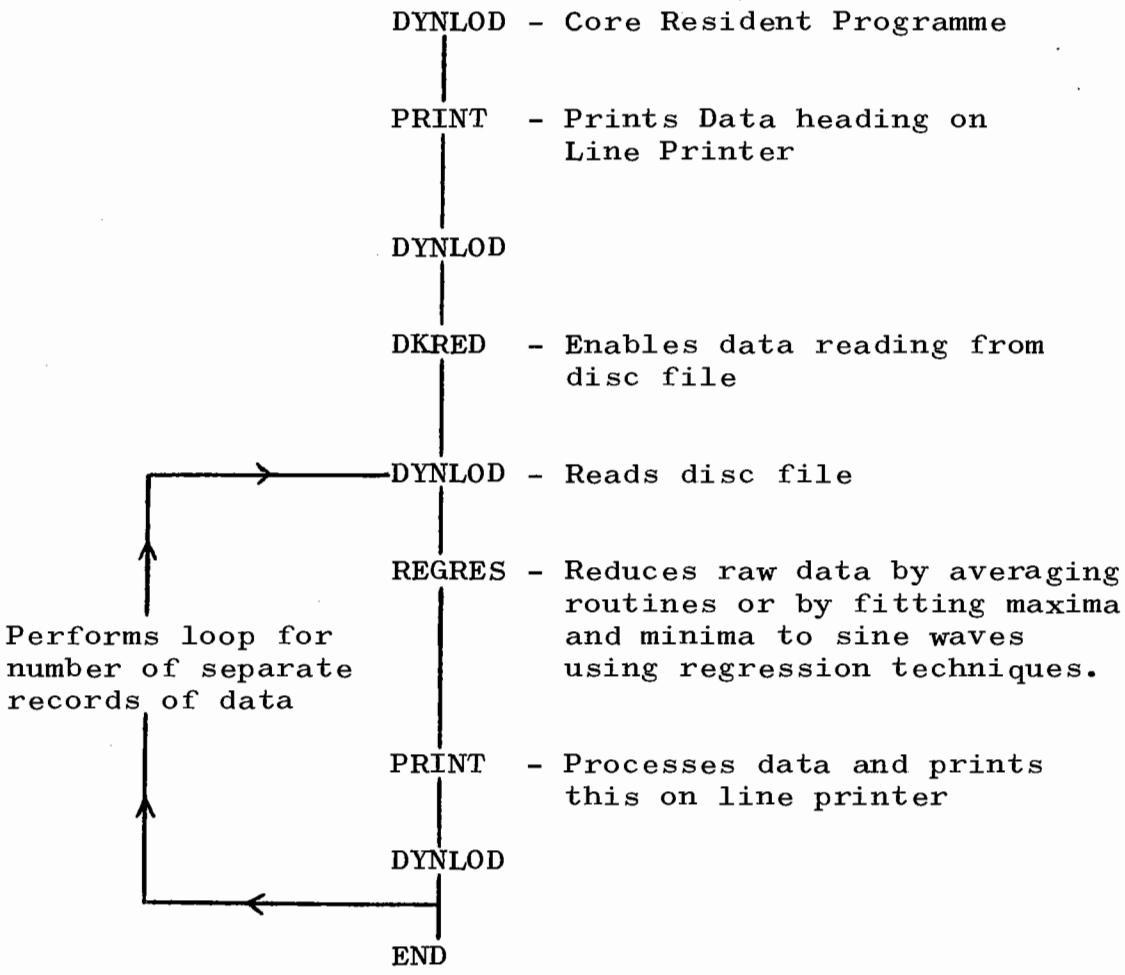

Fig. D.7 Programme path for analysis of repeated load data stored on disc

OPERATING PROCEDURE FOR LINKING OVERLAYS

```
LINK-11  V007A

PASS 1
#DYNLOD,LP:,DK:DYNLOD<DYNLOD,ENDFL,EAELIB[1,1]/L/U/E

PASS 2
```

Address of low limit of DYNLOD obtained from load map: 070072

```
LINK-11  V007A

PASS 1
#PRINT<DYNLOD.STB,PRINT/T:070070,EAELIB[1,1]/L/U/E

TRANSFER ADDRESS: 061044
LOW LIMIT: 061044
HIGH LIMIT: 070070

PASS 2
```

High limit of overlay in core set just below resident programme at 070070

```
LINK-11  V007A

PASS 1
#DKRED<DYNLOD.STB,DKRED/T:070070,DEFIN,EAELIB[1,1]/L/U/D

TRANSFER ADDRESS: 066512
LOW LIMIT: 066512
HIGH LIMIT: 070070

PASS 2
```

```
LINK-11  V007A

PASS 1
#REGRES<DYNLOD.STB,REGRES/CC/T:070070,EAELIB[1,1]/L/U/E

TRANSFER ADDRESS: 056552
LOW LIMIT: 056552
HIGH LIMIT: 070070

PASS 2
```

```
LINK-11  V007A

PASS 1
#↑C
.KI
```

```
C       ASSHOT

C***    PROGRAM TO DO A TO D CONVERSION AND STORE                    D9
C***    DATA ON DISC
C
        COMMON /GRP1/NPTS,NCHNL,NCYC,IDA,NBLK,IND,
        1GAIN,RSTAT,PTCNT,CYCNT
        INTEGER GAIN,RSTAT,PTCNT,CYCNT
1       WRITE(6,100)
100     FORMAT(/,' RECORDS= I4',/)
        READ(6,200)NCYC
200     FORMAT(I4)
        NPTS=256
        NCHNL=5
        ANCHNL=NCHNL                          )
        SIZE=NPTS*ANCHNL*NCYC                 ) size of storage check
        IF(SIZE-384000.)3,3,2                 )
2       WRITE(6,101)
101     FORMAT(//' DATA SPACE REQUESTED IS TOO LARGE',
        1/' MAXIMUM NO OF DATA POINTS IS 26112'/)
        GOTO 1
3       CONTINUE
8       GAIN=16
15      CALL IOC
C
C       DO A TO D CONVERSION AND STORE RESULTS ON DISC
C
        WRITE(6,201)
201     FORMAT(/' TYPE CO TO CONTINUE',/)
        PAUSE
        CALL AD6                              AD6 is an assembly
        NCNT=0                                language subroutine for
16      CONTINUE                              A/D conversion
        CALL NEWCYC
        NCNT=NCNT+1
        IF(NCNT-NCYC)17,18,18
17      IF(RSTAT)19,19,18
19      TIM=0
191     TIM=TIM+1                             )
        IF(TIM.LT.12000.)GOTO 191             ) Timing loop
        WRITE(6,300)NCNT
300     FORMAT(/' NUMBER OF RECORDS STORED',/
        2,I5,/)
        GOTO 16
18      CONTINUE
        GO TO(10,11,12,13,14)RSTAT
10      WRITE(6,210)
        GO TO 21
11      WRITE(6,211)
        GO TO 20
12      WRITE(6,212)
        GO TO 20
13      WRITE(6,213)
        GO TO 20
14      WRITE(6,215)
20      WRITE(6,214)CYCNT,PTCNT
21      CONTINUE
210     FORMAT(//' ALL DATA CONVERTED',/)
211     FORMAT(//' TIME OUT IN ADC LOOP',/)
212     FORMAT(//' TIMING ERROR IN CONVERTER',
        1/' PROBABLE CAUSE OF ERROR DATA TOO FAST',/)
213     FORMAT(//' DISC TRANSFER  NOT COMPLETE BEFORE NEW CYCLE',/)
214     FORMAT(/' NO. OF CYCLES CAPTURED',I5,
        1/' NO. OF POINTS CAPTURED',I5,
        2//' TYPE CO TO CONTINUE',//)
215     FORMAT(//,' ADC STATUS NOT CLEAN AT START OF ADC',//)

        END
```

```
C       CREEP
C       PROGRAMME FOR CREEP TESTS ON CLAY
C       THIS PROGRAMME ANALYSES DATA STORED ON DISC
C       FROM MAGNETIC TAPE
        DIMENSION IDAT(10),AMEAN(10),KDAT(4,256)
        WRITE(6,100)
100     FORMAT(//,' TYPE TEST NO.,  RIG NO.,  NO. OF RECORDS,
       1 CYCLE INTERVAL',',//,'  PWP NO.,
      1PWP INIT,  LVDT INIT ',//)
        NSECS=0
       READ(6,101)NTST,NCH,NRIN,INSECS,NP,IPWPI,LVDT
        WRITE(5,103)NTST
103     FORMAT(I4)
101     FORMAT(7I4)
102     FORMAT(//,'  NSECS  DEVIATOR     STRAIN      PWP       DE
       1LTAPWP        A     EFFCELL      CELL ',//)
        WRITE(5,102)
C       TO READ DISC FILE
        M=256
        L=1024
        CALL SETFIL(3,'ADCDAT.    ',-1,'DK ',0,10256,155,0)
        CALL DEFIN (3,NRIN,L,U,NREC)
        NREC=1
        DO 5 N=1,NRIN
        READ(3'NREC)((KDAT(J,K),J=1,4),K=1,256)
       DO 4 J=1,10                          )
       AMEAN(J)=0                           )
4      CONTINUE                             )
       DO 3 J=1,4                           )   Averaging Routine
       DO 2 K=1,M                           )
       AMEAN(J)=KDAT(J,K)+AMEAN(J)          )
2      CONTINUE
       AMEAN(J)=AMEAN(J)/M
3      CONTINUE
        GOTO(6,7),NCH
6       SIG3=(3.698*AMEAN(2)-119.)/6.72
        DEV=(0.3244*AMEAN(1)+10.4)*((101.6-((2.351*AMEAN(3)-48.
       1)/300))/101.6)-0.0352*SIG3
       STR=((2.351*AMEAN(3)-48.)-.122*DEV)/3048
8       PWP=(2.300*AMEAN(4)+8.)
        GOTO 10
7      SIG3=(3.613*AMEAN(2)-53.)/6.14
       STR=((2.365*AMEAN(3)-40.)-.122*DEV)/3048
       DEV=(0.3244*AMEAN(1)+10.4)*((101.6-((2.365*AMEAN(3)-40.
      1)/300))/101.6)-0.0352*SIG3
9       PWP=(2.312*AMEAN(4)-50.)
C       INSERT APPROPRIATE CALIBRATION BELOW
C       MILLIVOLTS/KN/METRE SQUARED
10      IF(NP.EQ.1)PWP1=PWP/8.66
       IF(NP.EQ.2)PWP1=PWP/6.4
```

```
C       DYNLOD
C       RESIDENT PROGRAMME FOR ANALYSIS OF REPEATED
C       LOADING DATA STORED ON DISC
C       5 CHANNEL VERSION
        DIMENSION KDAT(5,256),DAT(10)
        COMMON/B1/KDAT,J,K/B2/AMAX,AMIN/B5/DAT
       1/B6/JUMP,NRIN,STRB,Q2,NCH,INSECS,NP,IPWPI,LVDT,N,NREC
        DATA A2,B2/'YES','NO'/
        GOTO 51
        WRITE(5,50)F                    )
50      FORMAT(F10.0)                   )
        WRITE(6,300)                    )  Dummy format statements used
300     FORMAT(//,'  ',/)                )  to load line printer driver
        WRITE(6,101)A,I                 )  routines into resident
101     FORMAT(A3,I4)                   )  programme
51      CONTINUE                        )
        STRB=0
        JUMP=1
        CALL LINK('PRINT.LDA')
        CALL LINK('DKRED.LDA')
        NREC=1
        DO 3 N=1,NRIN
        READ(3'NREC)((KDAT(J,K),J=1,5),K=1,256)
        CALL LINK('REGRES,LDA')
        JUMP=-1
        CALL LINK('PRINT.LDA')
3       CONTINUE
        CALL ENDFL(3)
        END
```

The above programme is the core resident programme. Linked to it are a series of overlays which are all called via the resident programme using the 'CALL LINK' statement. The listings for the overlays are given below.

```
C       OVERLAY  'PRINT'                          Linked to DYNLOD
C       THIS OVERLAY PRINTS OUT  PROCESSED DATA
        DIMENSION DAT(10)
        COMMON/B5/DAT/B6/JUMP,NRIN,STRB,Q2
        1,NCH,INSECS,NP,IPWPI,LVDT,N,NREC
        DATA A2,B2/'YES','NO '/
        IF(JUMP.EQ.-1)GOTO 2
        WRITE(6,100)
100     FORMAT(//,' IS THERE PWP MEASUREMENT',/)
        READ(6,101)Q1
101     FORMAT(A3)
        IF(Q1.EQ.B2)GOTO 1
        Q2=-1
        WRITE(6,102)
102     FORMAT(//,' TYPE TEST NO., RIG NO., NO. OF RECORDS,
        1CYCLE INTERVAL,',/,' PWP NO., PWP INIT,LVDT INIT IN I4',/)
        READ(6,103)NTST,NCH,NRIN,INSECS,NP,IPWPI,LVDT
103     FORMAT(7I4)
        WRITE(5,109)NTST
109     FORMAT(I4)
        WRITE(5,99)
99      FORMAT(//,' CYCLES   DEVIATOR      STRRAT    ELSTR   PERMSTR
        1      MR     SIG3       EFFC          A        PWP     DELPWP
        2  CRITP',/)
        GOTO 2
1       WRITE(6,104)
        Q2=1
106     FORMAT(//,' CYCLES   DEVIATOR    STRRAT    ELSTR
        1  PERMSTR         MR        SIG3 ',/)
        READ(6,105)NTST,NCH,NRIN,INSECS,LVDT
105     FORMAT(5I4)
104     FORMAT(//,' TYPE TEST NO., RIG NO., NO. OF RECORDS,
        1CYCLE INTERVAL, LVDT INIT ',/)
        WRITE(5,109)NTST
        WRITE(5,106)
2       CONTINUE
        IF(JUMP.EQ.1)GOTO 10
        GOTO(6,7),NCH
6       SIG3=(3.698*DAT(3)-119.)/5.95
        DEV=(0.3244*(DAT(1)-DAT(2)))*((101.6-
        1((2.351*DAT(5)-48.)/300.))/101.6)
        STR=((2.351*DAT(5)-48.)-0.122*(0.3244*DAT(1)+10.4))/30480.
        PWP=(2.300*DAT(7)+8.)
        RSTR=((0.705*(DAT(9)-DAT(10)))
        1-(0.01059*DEV))/30480.
        GOTO 8
7       SIG3=(3.613*DAT(3)-53.)/5.82
        STR=((2.365*DAT(5)-40.)-0.122*(0.3198*DAT(1)+15.6))/30480.
        DEV=(0.3198*(DAT(1)-DAT(2)))*((101.6-((2.365
        1*DAT(5)-40.)/300.)))/101.6)
        RSTR=((0.701*(DAT(9)-DAT(10)))-(0.01059*DEV))/30480.
        PWP=(2.312*DAT(7)-50.)
8       IF(NP.EQ.1)PWP1=PWP/8.66
        IF(NP.EQ.2)PWP1=PWP/6.4
        IF(NP.EQ.3)PWP1=PWP/5.02
        IF(NP.EQ.4)PWP1=PWP/7.21
        IF(NP.EQ.5)PWP1=PWP/6.
        IF(NP.EQ.6)PWP1=PWP/7.84
        CYC=INSECS*N
C       STRAINRATE  MICROSTRAIN/CYCLE
        STRRAT=((STR-STRB)/INSECS)*1000000.
        STRB=STR
```

PRINT (CONTD.)

```
C       RESILIENT MODULUS MN/METRE SQUARED
        RM=DEV/(RSTR*1000.)
        EFFC=(SIG3-PWP1)
        P=(DEV+3*EFFC)/3
C       RESILIENT MICROSTRAIN
        RSTR=RSTR*1000000.
        STR1=STR*100
        IF(Q2.GT.0)GOTO 9
        DELPWP=(PWP-IPWPI)/(PWP/PWP1)
        A=DELPWP/DEV
        WRITE(5,107) CYC,DEV,STRRAT,RSTR,STR1,
       1RM,SIG3,EFFC,A,PWP1,DELPWP,P
107     FORMAT(F8.0,11F10.3)
        GOTO 10
9       WRITE(5,108)CYC,DEV,STRRAT,RSTR,STR1,RM,SIG3
108     FORMAT(F9.0,6F10.3)
10      CONTINUE
        CALL RETURN
        END
```

```
C       DKRED                                          Linked to DYNLOD
C       OVERLAY TO READ DISC FILE
        DIMENSION KDAT(5,256),DAT(10)
        COMMON/B1/KDAT,J,K/B2/AMAX,AMIN/B5/DAT
       1/B6/JUMP,NRIN,STRB,Q2,NCH,INSECS,NP,IPWPI,LVDT,N,NREC
        M=256
        L=128
        CALL SETFIL(3,'ADCDAT.    ',-1,'DK ',0,10256,155,0)
        CALL DEFIN (3,NRIN,L,U,NREC)
        CALL RETURN
        END
```

The above programme called 'DKRED' defines the name of the file on which the data has been stored 'ADCDAT', the area of the disc where it may be found and the amount of store to be accessed.

Linked to DYNLOD

```
C       REGRES
C       LINEAR REGRESSION OVERLAY
        DIMENSION DAT(10),KDAT(5,256)
        COMMON/B1/KDAT,J,K/B2/AMAX,AMIN/B5/DAT
        DO 4 J=1,5,2
        CALL LINREG
        J1=2*J-1
        J2=2*J
        DAT(J1)=AMAX
        DAT(J2)=AMIN
4       CONTINUE
        DAT(3)=0
        DAT(7)=0
        DO 5 K=1,256
        DAT(3)=KDAT(2,K)+DAT(3)
        DAT(7)=KDAT(4,K)+DAT(7)
5       CONTINUE
        DAT(7)=DAT(7)/256
        DAT(3)=DAT(3)/256
        DAT(4)=0
        CALL RETURN
        END
        SUBROUTINE LINREG
        DIMENSION KDAT(5,256),IDAT1(250),IDAT2(250)
        COMMON/B1/KDAT,J,K/B2/AMAX,AMIN/B3/TOT
        L=0
        M=0
        K=1
        CALL TOTAL
        IF(K+3.EQ.256)GOTO 100
        TOT1=TOT
98      CALL TOTAL
        IF(K+3.EQ.256)GOTO 100
        TOT2=TOT
        IF(TOT1-TOT2)3,98,4
C       3,98,4 MAX,UNDECIDED,MIN
C       LOOK FOR MAXIMUM SET
3       TOT1=TOT2
97      CALL TOTAL
        IF(K+3.EQ.256)GOTO 100
        TOT2=TOT
        IF(TOT1-TOT2)3,97,6
6       NOISE=0
        K1=K-8
        K2=K-1
        DO 7 K=K1,K2
        L=L+1
        IF(KDAT(J,K).GT.1000)NOISE=1
        IF(KDAT(J,K).LT.-1000)NOISE=1
        IDAT1(L)=KDAT(J,K)
7       CONTINUE
        K=K2+1
        IF(NOISE.EQ.1)L=L-8
        GOTO 4
```

This subroutine looks for maximum and minimum sets of data readings and stores them.

Check for transients in data readings

REGRES (CONTD.)

```
C       LOOK FOR MINIMUM SET
4       TOT1=TOT2
96      CALL TOTAL
        IF(K+3.EQ.256)GOTO 100
        TOT2=TOT
        IF(TOT1-TOT2)9,96,4
9       NOISE=0
        K1=K-8
        K2=K-1
        DO 10 K=K1,K2
        M=M+1
        IF(KDAT(J,K).GT.1000)NOISE=1
        IF(KDAT(J,K).LT.-1000)NOISE=1
        IDAT2(M)=KDAT(J,K)
10      CONTINUE
        K=K2+1
        IF(NOISE.EQ.1)M=M-8
        GOTO3
C       EVALUATION OF MAX AND MIN
100     CALL MAXMIN(IDAT1,L,AMAX)
        CALL MAXMIN(IDAT2,M,AMIN)
        RETURN
        END
        SUBROUTINE TOTAL
        DIMENSION KDAT(5,256)
        COMMON/B1/KDAT,J,K/B3/TOT
99      NOISE=0
        TOT=0
        K1=K
        K2=K+7
        DO 1 K=K1,K2
        IF(KDAT(J,K).GT.1000)NOISE=1
        IF(KDAT(J,K).LT.-1000)NOISE=1
        TOT=TOT+KDAT(J,K)
1       CONTINUE
        TOT=TOT/8
        K=K2-3
        IF(K+3.EQ.256)GOTO 2
        IF(NOISE.EQ.1)GOTO 99
2       CONTINUE
        RETURN
        END
        SUBROUTINE MAXMIN(IDAT,N,AM)
        DIMENSION IDAT(250)
        AM=0
        N4=0
        N1=N/8
        DO 1 I=1,N1
        N2=(8*I)-7
        N3=N2+7
        X=0
        Y=0
        XY=0
        X2Y=0
        DO 2 N=N2,N3
        X=X+1
        Y=Y+IDAT(N)
        XY=XY+(X*IDAT(N))
        X2Y=X2Y+(X*X*IDAT(N))
```

This subroutine adds sets of data for the purposes of comparison to ascertain maxima or minima.

This subroutine fits a second order curve to the maximum or minimum sets of points and computes the maximum or minimum value of this curve.

REGRES (CONTD.)

```
2       CONTINUE
        ALPHA=8.*XY-36.*Y
        DELTA=8.*X2Y-Y*204.
        B=((ALPHA/3024.)-(DELTA/28560.))/0.005229
        A=(ALPHA-(336.*B))/3024.
        C=Y/8.-A*25.5-B*4.5
        IF(-B/(2*A))3,5,4
4       IF(9+B/(2*A))3,5,5
3       N4=N4+1
        GOTO 1
5       AM=(B*B)/(4*A)-(B*B)/(2*A)+C+AM
1       CONTINUE
        IF(N1-N4)7,6,7
6       AM=0
        GOTO 8
7       AM=AM/(N1-N4)
8       RETURN
        END
```

APPENDIX E

ESTIMATION OF PRECONSOLIDATION PRESSURE AND IN SITU CONSOLIDATION CURVE

There are three methods of estimating the in situ virgin consolidation curve. The starting point for all of these methods is the use of the oedometer test or confined compression test.

A sample of the soil is compressed one dimensionally, while drainage is allowed from each end. The volume change is measured for each pressure increment and the void ratio is plotted against the log of the pressure.

The void ratio:

$$e = \frac{V_V}{V_S} = \frac{\text{Volume of voids}}{\text{Volume of soil solids}}$$

is directly related to the moisture content for a saturated soil by the relationship:

$$e = m\, G_S$$

where m = moisture content

G_S = specific gravity of soil solids

From the void ratio-log (pressure) curve obtained in the laboratory, there are the following methods of estimating the preconsolidation pressure and the in situ consolidation curve:

(1) Casagrande (1936) suggested the following procedure. The point of minimum curvature T, as illustrated in

Fig. E.1, is estimated. A line is drawn parallel to the pressure axis and another line is drawn tangential to T. The angle between these two lines is bisected and a third line drawn. The intersection of this line with the back projection of the straight line portion of the virgin consolidation curve gives the value of the pre-consolidation pressure.

(2) Burmister (1942, 1951) proposed an alternative procedure whereby, as soon as the straight line portion of the e versus log p curve is approached, the sample is rebounded (Fig. E.2) and then reloaded. The triangle (shown shaded) formed by the rebound and reloading curve is then shifted up onto the first loading curve. The preconsolidation pressure p_c is defined by the intersection of the apex of the triangle with the straight line portion of the curve.

(3) The third procedure was proposed by Schmertmann (1955) and is illustrated in Fig. E.3. The loading rebound and reloading procedure is the same as in Burmister's procedure. From the point (e_o, p_o) a line is drawn parallel to the mean slope of the rebound curve. A point on this line is selected as the assumed value of p_c and a line is drawn from this point to intersect the laboratory curve at $0.42\ e_o$. The assumed virgin curve is plotted against log (pressure). This procedure is repeated for several assumed positions of p_c and the position

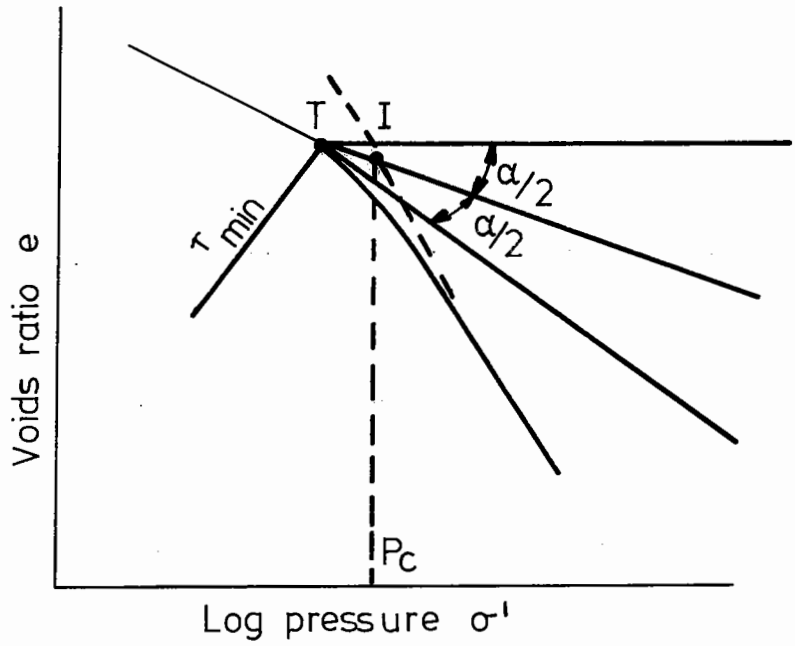

Fig. E.1. Estimation of Preconsolidation Pressure (Casagrande)

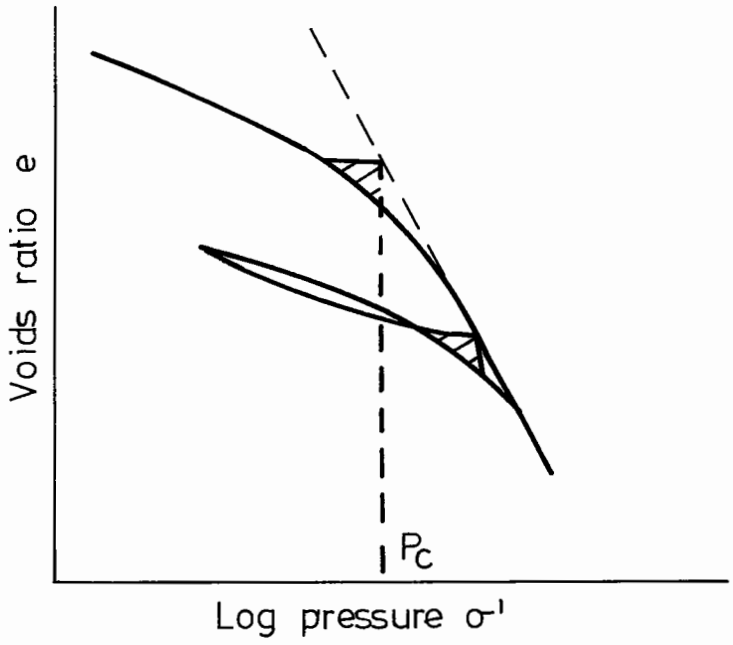

FigE.2 Estimation of Preconsolidation Pressure (Burmister)

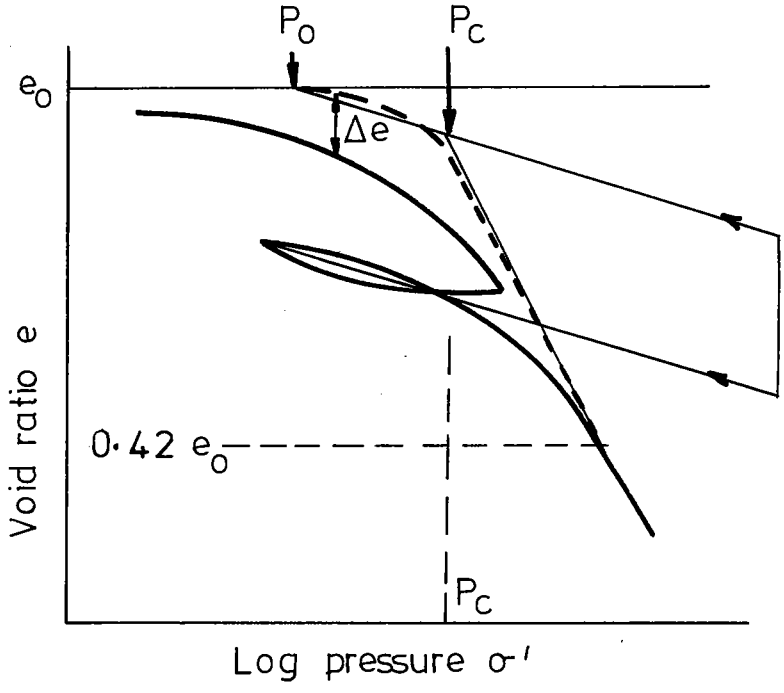

Fig.E.3 Estimation of Preconsolidation Pressure (Schmertmann)

to produce the most symmetrical curve of Δe versus log (pressure) is selected.

REFERENCES TO APPENDICES

Burmister, D.M. (1942), "Laboratory investigation of soils at Flushing Meadow Park", Trans. ASCE, Vol. 107, p. 187.

Burmister, D.M. (1951), "The application of controlled test methods in consolidation testing", Symp. on Consolidation Testing of Soils, ASTM, STP, No. 126, p. 83.

Casagrande, A. (1936), "The determination of the pre-consolidation load and its practical significance", Proc. 1st Int. Conf. Soil Mech. and Found. Eng. (Cambridge, Mass.), p. 60.

Middleton, V. (1974), "General purpose ADC package for a university environment", DEC Users Society, European Convention, Zurich.

Parr, G.B. (1972), "Some aspects of the behaviour of London clay under repeated loading", Ph.D. Thesis, University of Nottingham.

Roarke, R.J. (1964), "Formulae for stress and strain", McGraw-Hill.

Schmertmann, J.M. (1955), "The undisturbed consolidation of clay", Trans. ASCE, Vol. 120, p. 1201.

Timoshenko, S. (1952), "Strength of materials, Part II", Van Nostrand, 2nd ed.